Dissertation zur Erlangung des Doktorgrades

der Fakultät für Chemie und Pharmazie

der Ludwig-Maximilians-Universität München

Imidazolidine-4-thiones

as Prebiotic Organocatalysts

Molecular Evolution on the Early Earth

Anna Carla Closs

aus

Frankenthal, Deutschland

2021

Dissertation eingereicht am   07.06.2021

1. Gutachterin / 1. Gutachter: Prof. Dr. Oliver Trapp

2. Gutachterin / 2. Gutachter: Prof. Dr. Paul Knochel

Mündliche Prüfung am   20.07.2021

II

Abstract

Despite all thorough interdisciplinary endeavours to explore the origin of life, a holistic scenario for the emergence of organic complexity from the abiotic feedstock is still missing. This thesis is focussing on utilising the powerful approach of organocatalysis to simultaneously enable versatile modifications of simple molecular structures as well as a propagation of chirality along the chemical pathway towards our homochiral biosystem.

Imidazolidine-4-thiones were discovered as a class of promising prebiotic organocatalysts: (1) A highly plausible existence of these heterocycles was shown under realistic conditions of the early Earth. The desired catalysts were obtained either by defined reactions starting from aminonitriles or from one-pot mixtures starting from carbonyl compounds, cyanide, ammonia, and hydrogen sulphide. This way, a library of various organocatalysts was synthesised. Numerous series of experiments under different reaction conditions confirmed the robustness of the system. Starting from prebiotically realistic mixtures of carbonyl compounds, clear preferences for certain species depending on the reaction media were revealed, suggesting a possible mode of selection. The observed crystallisation of single molecules as conglomerates also offers the potential for spontaneous resolution and thus initial symmetry breaking. (2) The catalytic activity of imidazolidine-4-thiones was demonstrated by their successful application in the challenging α-alkylation of aldehydes which enabled this transformation in a prebiotic environment for the first time. Comparison of different imidazolidine-4-thiones revealed superior activities and enantioselectivities of the preferentially formed structures and isomers. While the initially designed system still utilised the combination with photoredox activation, further in-depth studies showed catalytic conversion even under exclusion of light. Since this transformation has generally not been feasible without light before, detailed mechanistic studies were performed. These demonstrated the interplay of all three reactive centres of the organocatalysts used, culminating in the proposal of a new reaction mechanism. (3) With this functionalisation of aldehydes, the imidazolidine-4-thiones were able to modify their own building blocks. The successful incorporation of this extended feedstock into the catalyst structure led to the formation of second generation catalysts. In addition, the ability to dynamically exchange incorporated carbonyl compounds with the surrounding reservoir enabled ongoing (self-)variation of

its own structure even in the absence of the other reactants. In combination with the repetitive production and selection of individual species shown, this mutation mechanism allows adaptation to the continuously changing environment on the early Earth and thus represents a first form of evolution on the molecular level.

Kurzzusammenfassung

Trotz der intensiven interdisziplinären Bemühungen den Ursprung des Lebens zu erforschen, fehlt weiterhin ein ganzheitliches Szenario für die Entstehung organischer Komplexität aus abiotischem Ausgangsmaterial. Diese Arbeit setzt den Fokus auf den Einsatz von Organokatalyse, um sowohl vielseitige Modifikationen einfacher molekularer Strukturen als auch einen nachhaltigen Transfer von Chiralität entlang des chemischen Weges zu unserem homochiralen Biosystem zu ermöglichen.

Hierbei wurden Imidazolidin-4-thione als eine Klasse vielversprechender präbiotischer Organokatalysatoren entdeckt: (1) Zunächst wurde die höchst plausible Existenz dieser Heterozyklen unter realistischen Bedingungen der frühen Erde gezeigt. Die gewünschten Katalysatoren wurden entweder durch definierte Reaktionen auf der Basis von Aminonitrilen oder aus One-Pot-Gemischen ausgehend von Carbonylverbindungen, Cyanid, Ammoniak und Schwefelwasserstoff erhalten. Auf diese Weise konnte eine Bibliothek an zahlreichen Organokatalysatoren synthetisiert werden. Zahlreiche Ansätze unter verschiedenen Reaktionsbedingungen bestätigten die Robustheit des Systems. Ausgehend von präbiotisch realistischen Gemischen von Carbonylverbindungen zeigten sich deutliche Präferenzen für bestimmte Spezies in Abhängigkeit vom Reaktionsmedium, was auf einen möglichen Selektionsmodus hindeutet. Die beobachtete Kristallisation von einzelnen Molekülen als Konglomerate bietet zudem das Potential für eine spontane Racematspaltung und damit für einen ersten Symmetriebruch. (2) Die katalytische Aktivität von Imidazolidin-4-thionen wurde durch deren erfolgreiche Anwendung in der schwer zugänglichen α-Alkylierung von Aldehyden demonstriert. Somit wurde diese Transformation erstmals in einer präbiotischen Umgebung ermöglicht. Hierbei zeigten die bevorzugt gebildeten Imidazolidin-4-thione erhöhte Aktivität und Enantioselektivität. Während im zuerst entworfenen katalytischen System noch die Kombination mit Photoredox-Aktivierung genutzt wurde, zeigten vertiefende Untersuchungen eine katalytische Umsetzung auch unter Lichtausschluss. Da diese Reaktion ohne Licht bisher generell nicht möglich war, wurden detaillierte mechanistische Studien durchgeführt. Diese deckten ein Zusammenspiel aller drei reaktiven Zentren der eingesetzten Organokatalysatoren auf, auf dessen Grundlage ein neuer Reaktionsmechanismus formuliert wurde. (3) Durch diese Funktionalisierung von

Aldehyden waren die Imidazolidin-4-thione in der Lage, ihre eigenen Bausteine zu modifizieren. Der erfolgreiche Einbau dieses erweiterten Ausgangsmaterials in die Katalysatorstruktur führte zur Bildung von Katalysatoren der zweiten Generation. Zudem ermöglichte die Fähigkeit, eingebaute Carbonylverbindungen dynamisch mit dem umliegenden Reservoir auszutauschen, eine kontinuierliche (Selbst-)Variation der eigenen Struktur auch in Abwesenheit der übrigen Reaktanden. In Kombination mit der gezeigten repetitiven Produktion und Selektion einzelner Verbindungen erlaubt dieser Mutationsmechanismus die Anpassung an die sich ständig verändernde Umgebung auf der frühen Erde und stellt damit eine erste Form der Evolution auf molekularer Ebene dar.

Scientific Contributions

During the time of this dissertation, scientific contributions in the form of publications, talks, and poster presentations were made, with parts being represented in this thesis.

Publications

M. Siebert, R. Sure, P. Deglmann, <u>A. C. Closs</u>, F. Lucas, O. Trapp, *J. Org. Chem.* **2020**, *85*, 8553-8562.

    Mechanistic Investigation into the Acetate-Initiated Catalytic Trimerization of Aliphatic Isocyanates: A Bicyclic Ride.

<u>A. C. Closs</u>, E. Fuks, M. Bechtel, O. Trapp, *Chem. Eur. J.* **2020**, *26*, 10702-10706.

    Prebiotically Plausible Organocatalysts Enabling a Selective Photoredox α-Alkylation of Aldehydes on the Early Earth.

<u>A. C. Closs</u>, O. Trapp, *Angew. Chem.* submitted manuscript.

    Molecular Evolution of a Prebiotic Organocatalyst.

Talks

<u>A. C. Closs</u>, O. Trapp, *Gordon Research Seminar Origin of Life*, Galveston (Texas, USA), January 2020.

    Prebiotically plausible organocatalysts enabling the α-alkylation of aldehydes on the Early Earth.

<u>A. C. Closs</u>, O. Trapp, *Heidelberg Initiative for the Origins of Life (HIFOL) Colloquia*, München (Germany), June 2021.

    Molecular Evolution of Prebiotically Plausible Organocatalysts.

Poster Presentations

<u>A. C. Closs</u>, E. Fuks, O. Trapp, *Molecular Origins of Life CAS Conference*, München (Germany), October 2018.

    Investigation of a prebiotically plausible organocatalyst for photochemical alkylations.

<u>A. C. Closs</u>, E. Fuks, O. Trapp, *Science of Early Life Conference*, Kloster Seeon (Germany), November 2019.

    Selective Formation of Organocatalysts on the Early Earth.

<u>A. C. Closs</u>, O. Trapp, *Gordon Research Conference Origin of Life*, Galveston (Texas, USA), January 2020.

    Prebiotically plausible organocatalysts enabling the α-alkylation of aldehydes on the Early Earth.

List of Abbreviations

A	adenine
Ala	alanine
bpy	2,2′-bipyridine
°C	degree Celsius
C	cytosine
CPL	circular polarized light
d	day(s)
DABCO	1,4-diazabicyclo[2.2.2]octane
DMAP	4-dimethylaminopyridine
DNA	deoxyribonucleic acid
EDA	electron donor-acceptor
ee	enantiomeric excess
ESI	electrospray ionisation
Et	ethyl
EtOAc	ethyl acetate
G	guanine
GC	gas chromatography
Glu	glutamic acid
h	hour(s)
HPLC	high performance liquid chromatography
HRMS	high resolution mass spectrometry
iPr	isopropyl
Iva	isovaline
MHz	megahertz
min	minute(s)
MS	mass spectrometry
Me	methyl
NMR	nuclear magnetic resonance
Ph	phenyl
Pr	propyl

Pro	proline
RNA	ribonucleic acid
SET	single electron transfer
SIPF	salt induced peptide formation
T	thymine
*t*Bu	*tert*-butyl
U	uracile
UV	ultra violet
Val	valine

Table of Contents

1 Introduction

Vielleicht lernen wir erst dann was Leben ist, wenn wir verstehen wie es begonnen hat.

– Ernst Peter Fischer in Erwin Schrödinger: Was ist Leben? –

One of the most fundamental but at the same time least understood phenomena dates back around 4 billion years: the emergence of life. The central question about the origins of mankind is not only driven by the scientific and philosophical curiosity but by any considerations of current and future extraterrestrial or artificial life.

Even though a broad-based, interdisciplinary research community has taken on this task, the small amount of survived, unchanged relicts from such a distant past prevents the full clarification of the chain of events that led to life's origin. What conditions prevailed on the early Earth? How did the simple abiotic mixture evolve into these highly complex and versatile living organisms of our biosystem? And what made this transformation so selective to result in a homochiral world? The process that actually took place can never be discovered, but it can be re-invented.[1] By applying the knowledge of modern synthetic chemistry to prebiotic theories, plausible reaction pathways from simple inorganic matter to the essential building blocks of life can be developed. For this purpose, a variety of scenarios that cover a wide range of temperatures, reaction atmospheres and energy sources are provided by geologists and astrophysicists. What initially appears to be a great deal of synthetic flexibility harbours the biggest challenge. Most pathways are designed separately and fulfil the requirements of distinct prebiotic environments. These often comprise conflicting presumptions and constraints, making them incompatible. Yet, it is the interaction of all biomolecules that gives rise to our self-sustaining system, defined life.

Given the high complexity of self-replication and information storage enabled by peptides, RNA, and DNA in modern life, it is reasonable to speculate that simpler mechanisms have preceded them. A prebiotic system that is able to transfer information as well as dynamically adapt to its ever-changing environment could represent a primitive analogue of Darwinian evolution and thus an important part in the origin of life.

2 Theoretical Background

2.1 Early Earth's Environment

When the Earth condensed out of our sun's nebula 4.54 billion years ago (Ga), it represented an unhostile habitat of around 2000 K.[2] Sedimentary records of this time up to the first evidences for life attributed to carbon isotope ratios (3.8 Ga)[3] and microfossils (3.5 Ga)[4] are rare. This makes it not only difficult to narrow down the time frame for the origin of life but also to gain information about the preceding conditions. Especially until 3.8 Ga, a period of heavy bombardments probably changed the early Earth's environment repeatedly and it is questionable if already formed life could have survived these large impacts. Despite the missing rocky records, geological estimations as well as chemical and biological requirements for prebiotic and biotic systems deliver boundary conditions for the early Earth environment during the origin of life. One important prerequisite for life is the existence of liquid water. After moon formation, the Earth must have cooled down below the boiling point of water to form a continental crust and hydrosphere. Detrital zircons ($ZrSiO_4$) of Western Australia indicate liquid water as early as 4.4 Ga.[5] Opposing this assumption is the fact that the activity of the young sun must have been much lower with only 70 % of our current luminosity, which would have resulted in temperatures far below freezing and thus an overall surface glaciation.
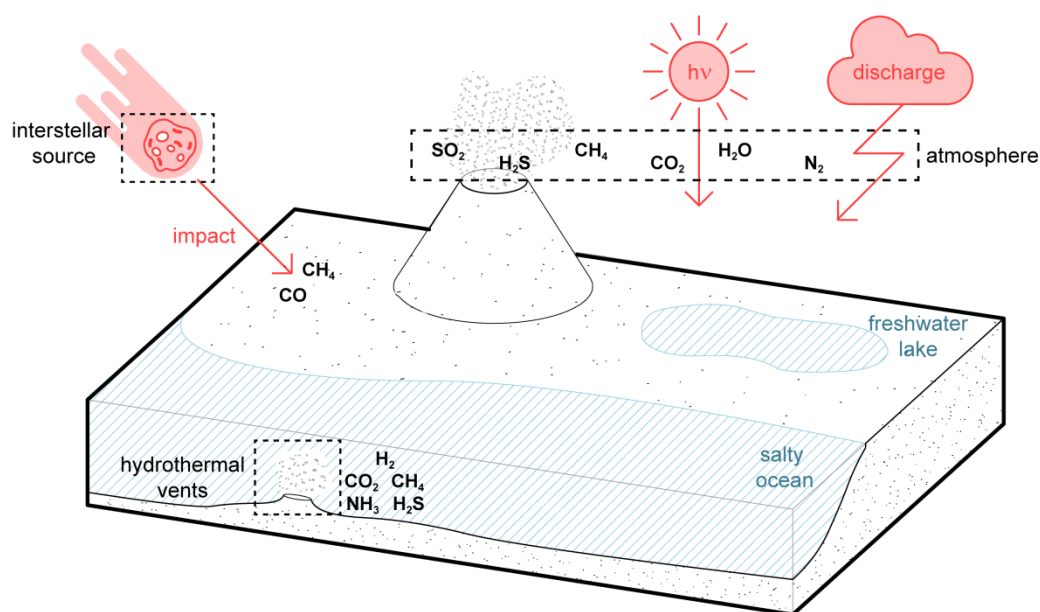
Figure 2.1: Schematic illustration of plausible reaction sites on the early Earth. Potential energy sources are depicted in red, and the reaction sites discussed in this work are framed with dashed lines.

To offset this lack of radiation, an atmospheric greenhouse effect of CO_2 is often hypothesised,[6] but the prevalent gas compositions are still under debate. It is generally assumed that free oxygen was absent until 2.0 Ga and if the atmosphere was defined by outgassing mechanisms of the Earth's mantle, it would have been fairly neutral, dominated by CO_2, N_2, and H_2O (Figure 2.1).[7-8] Especially in proximity to volcanic activity, sulphur gases like H_2S and SO_2 are highly plausible.[9] Prebiotic organic compounds, however, are much more readily produced in a reductive environment with significant abundances of CO, H_2, CH_4, and NH_3.[10-11] The latter two unfortunately suffer from photo instability and quickly decompose under UV irradiation.[6,12] In turn, methane photolysis is reported to have the power of shielding ammonia enough to be present and contribute significantly to the greenhouse warming and maintain a surface temperature above 0 °C.[13] Also chemical equilibrium calculations on thermal outgassing of chondritic material predict an early presence of the desired reducing gases.[14] Another explanation for reducing conditions is given with an atmosphere generated by impact degassing instead of mantle outgassing, which would provide (at least long-lived transient) CO- and CH_4-rich atmospheres and with them abundant chemical energy as well as HCN and NH_3.[15]

Another possibility is to abandon the atmosphere as place of the first formation of organic molecules. The theory of (Pseudo-)Panspermia even shifts the origin of life to outer space followed by its transport to Earth via meteoritic impacts. This is supported by the discovery of various small organic compounds on carbonaceous chondrites, including aliphatic and aromatic hydrocarbons, carbonyl compounds, alcohols, amines, amides, nitrogen heterocycles, and even nucleobases and amino acids.[16-19] Also the interstellar space provides a variety of prebiotically relevant molecules.[20] Although these asteroidal fragments are considered to resemble compositions only slightly altered from that of the sun and also criticisms such as low elemental concentrations and questionable chances of survival in space or on impact with the Earth were countered with theoretic calculations, this scenario is not solving the puzzle. It only transfers the location for the emergence of life. However, meteoritic transport of small organic abiotic compounds might still have initiated subsequent processes on Earth by additionally providing a source of high impact energies.

The hydrosphere represents a third potential production site for biotic matter. In this context, both Darwin's warm freshwater pond and the salty ocean resulting from concentrated outgassed volatiles are discussed.[15,21-22] Particular significance is attributed to hydrothermal vents.[23-24] In these deep sea geysers, superheated water erupts into the cold surroundings leading to mineral precipitation and highly interesting thermal and chemical gradients. In close vicinity to the volcanic activity these vents are mainly formed from iron and manganese sulphides and provide temperatures of around 400 °C, acidic media with a pH of 2 to 3, as well as high concentrations of CO_2, NH_3, CH_4, and H_2S (black smokers).[23-25] In further distance, white smokers are formed from deposits of barium, calcium, and silicon sulphates, carbonates, and hydroxides. The prevailing conditions are driven by serpentinisation and are much colder (40-90 °C) and basic (pH 9-10) but still reducing with the presence of CH_4 and H_2.[23,26-27] The high concentrations of prebiotic precursors in the proximity of mineral catalysts under a diverse set of reaction conditions and continuous energy supply represent promising scenarios for the chemical and biological processes of life. Still nowadays, hydrothermal vents harbour rich and unique ecosystems.[23] The drawbacks of aqueous reaction sites are the instability of biologically relevant molecules to hydrolysis and the often occurring condensation reactions which are thermodynamically unfavourable in this medium. Therefore, wet-and-dry cycles as a consequence of evaporation or day-and-night periods as well as completely solvent free systems dominated by mechanical influences of erosion, tectonics, and meteoritic impacts are discussed.

Concluding, a wide range of conditions has been proposed as prebiotically plausible so far with significant differences depending on the respective reaction environment. As high dilution of the reactants is a general issue, the prebiotic feedstock should, at best, be concentrated in one place and react via simple and robust self-assembly. Due to its abundance, transformations in water are highly likely, or at least resistance towards aqueous conditions seems to be a plausible constraint on the evolutionary path. Energy can be provided by thermal and mechanical sources, redox-, pH- and concentration-gradients, solar irradiation or electrical discharges. Minerals, acids, bases, and porous surfaces are available for (catalytic) activation and temperatures can vary from below freezing up to several hundred degrees Celsius.

2.2 Emergence of Organic Complexity

The evolution of prebiotic inorganic matter into the key organic molecules that our modern biosystem is based on represents a fundamental question in the origin of life. To reinvent this step, the prebiotic chemist can only help himself to a very limited toolbox, restricted by the conditions presented above. As possible carbon nutrients, carbon dioxide, carbon monoxide, methane, and hydrogen cyanide are discussed in the literature with particular emphasis on the latter. HCN is ubiquitous in the interstellar space, has been detected in volcanic gases and hydrothermal vents[28] and can be produced by electric discharges or meteoritic impact shocks in a CO or CO_2 containing atmosphere.[29-31] Moreover, this highly reactive molecule already showed its potential as central molecule by being implemented in prebiotic pathways towards amino acids, nucleobases, as well as sugar and lipid precursors (see the following).[32-33] In addition, small carbonyl compounds can directly be used as feedstock components. Although their formation already represents a first step towards organic matter, their prebiotic existence is considered very probable. They are likely intermediates in high energy atmospheric reactions and both aldehydes and ketones can be found on precometary ice analogues and carbonaceous chondrites with a predominance of low carbon number carbonyls and formaldehyde, acetaldehyde and acetone showing the highest abundance.[34-36]

2.2.1 Top-down Approach

In a top-down approach, scientists take the important biomolecules of life and try to realise their formation out of this simple prebiotic feedstock. Over the last years, various synthetic routes within the constraints of the early Earth environment have been proposed.

Amino acids and Peptides

The prebiotic presence of α-amino acids is one of the least doubted. This class of molecules and their derivatives have been widely detected on meteorites[18,37-39] and in experiments mimicking the early Earth.[40-43] Their formation could be explained by the simple Strecker reaction of aldehydes with hydrogen cyanide and ammonia via α-amino nitriles (Scheme 2.1).[44] Also, preformation of the carbonyl compound and the use of NH_3 could be surpassed by direct hydrolysis of HCN oligomers.[45-47] The subsequent polymerisation to peptides remains a bigger challenge. As this peptide bond formation is

a condensation reaction, it is thermodynamically unfavourable in aqueous media. To enable the oligomerisation, different coupling reagents were studied. In the prebiotic context, polyphosphates, nucleotides, cyanamides, cyanates, and imidazole, were proposed as suitable candidates.[48-50]
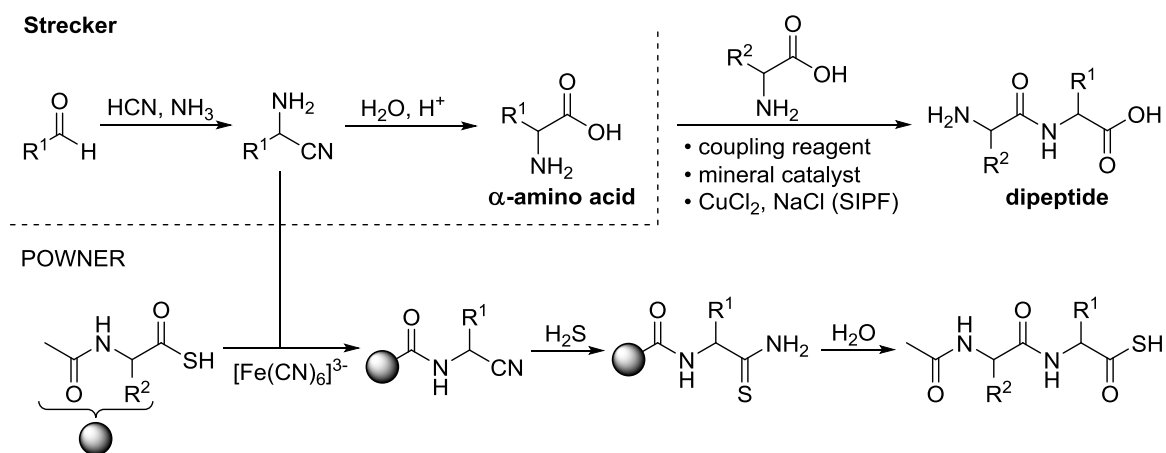
Scheme 2.1: Prebiotically plausible formation of amino acids via Strecker reaction and different mechanisms for peptide formation.

Further, polymerization in the presence of mineral surfaces as well as metal catalysts in concentrated aqueous salt solutions, the salt induced peptide formation (SIPF), led to the formation of short peptides.[51-53] Another possibility is the polymerisation of activated amino acid derivatives instead of the unreactive acid. POWNER presented a coupling strategy of α-amino nitriles (Scheme 2.1, bottom).[54] Activated by *N*-acylation, the aminonitrile undergoes thiolysis with H_2S to the thioamide, followed by hydrolysis to the α-amido thioacid which subsequently ligates with the next α-amino nitrile in the presence of ferricyanide. In some of these mechanisms, yields could be improved by evaporation in wet-and-dry cycles, and first preferences were observed for the condensation of α- over β- or γ-amino acids.[54-56] Still, only short oligomers were formed and no selective incorporation of the 20 proteinogenic monomers was obtained, let alone a preferential coupling of the biotic L-enantiomer.

Sugars

The most prominent source for sugars on the early Earth has been the Formose reaction, first presented by BUTLEROW in 1861.[57] In the presence of an alkaline earth hydroxide catalyst, formaldehyde oligomerises in aqueous solution into a broad network of aldoses and ketoses, dominated by (retro-)aldol reactions and isomerisation (Scheme 2.2). The

challenging step is the initial dimerization to glycolaldehyde that requires an Umpolung. It can be achieved photochemically or by adding catalysts, including saccharides like glycolaldehyde itself. The main drawback of this process is its uncontrollable course into a complex product mixture with various side-products and eventually water insoluble tar. Instead, selectivity in the formation of certain sugars, e.g. glyceraldehyde and ribose for nucleoside synthesis, is desired.

Formose
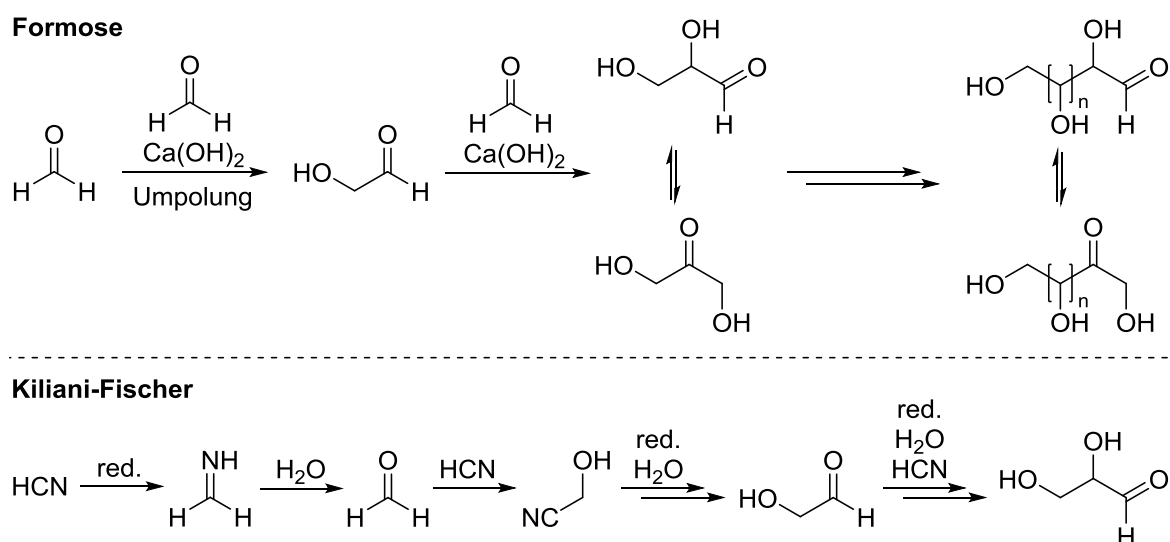
Kiliani-Fischer

Scheme 2.2: Prebiotically plausible formation of sugars via Formose reaction or Kiliani-Fischer type synthesis. In the latter, "red." refers to the reduction with H_2S and UV irradiation, catalysed by light induced copper (I) cyanide oxidation.

Another pathway starting from hydrogen cyanide was presented by SUTHERLAND. Photoredox Kiliani-Fischer type reaction with hydrogen sulphide as reductant selectively converted HCN via formaldehyde to glycolaldehyde and glyceraldehyde accelerated by copper(I)/(II) redox cycling.[58]

Nucleobases, Nucleosides and Nucleotides

Besides their detection on meteorites and in electric discharge experiments,[17,59] various pathways for the formation of pyrimidines from cyanoacetylene and canonical purines from hydrogen cyanide were reported.[60-62] The subsequent coupling with D-ribose to RNA-nuleosides turned out to be more difficult, especially regarding regioselectivity and desired furanose formation. SUTHERLAND surpassed this last sugar-nucleobase linking step by connecting glyceraldehyde with 2-aminooxazole to the pentose aminooxazoline (Scheme 2.3, top).[63] Following reaction with cyanoacetylene builds up the pyrimidine structure of cytosine. The corresponding uracil nucleosides can only be accessed by

partial hydrolysis of cytidine under UV irradiation accompanied by destructive photochemistry. This sequential procedure was further improved to a possible one-pot sugar mixture by addition of 2-aminothiazole that resulted in selective aminal crystallisation of the needed glycolaldehyde and glyceraldehyde.[64] Exchanging 2-aminooxazole with 2-thiooxazole enabled the formation of both pyrimidine and 8-oxo-purine nucleosides.[65] The canonical purine RNA-nucleosides have previously been accessed by a different pathway of CARELL condensing formamidopyrimidine (FaPy) intermediates with D-ribose (Scheme 2.3, middle).[66] Recently, TRAPP accomplished the formation of the respective DNA nucleosides with high regio- and stereoselectivity.[67] The canonical nucleobases were converted with acetaldehyde to the vinyl species which then reacted with D-glyceraldehyde or formaldehyde to form the deoxyribonucleosides (Scheme 2.3, bottom).
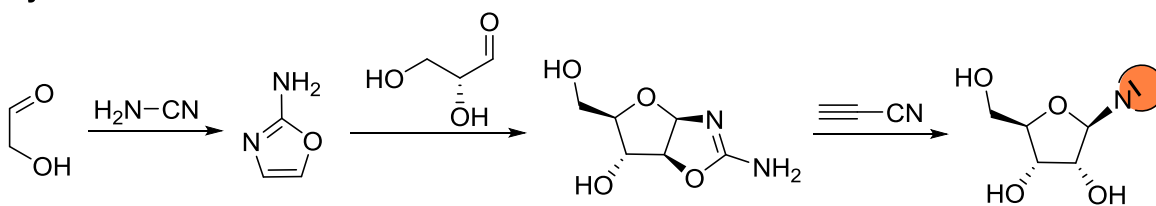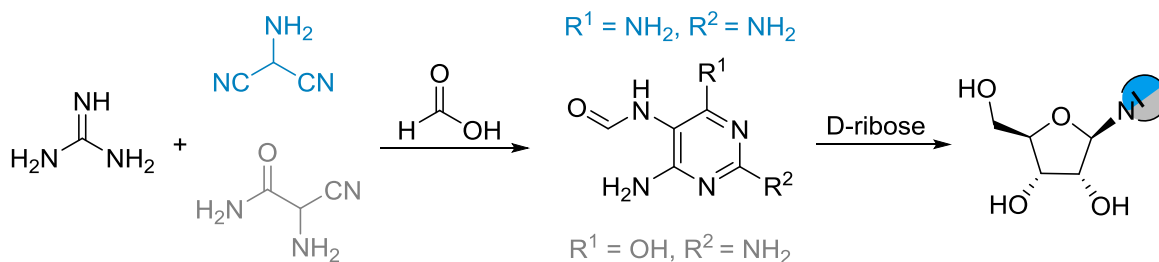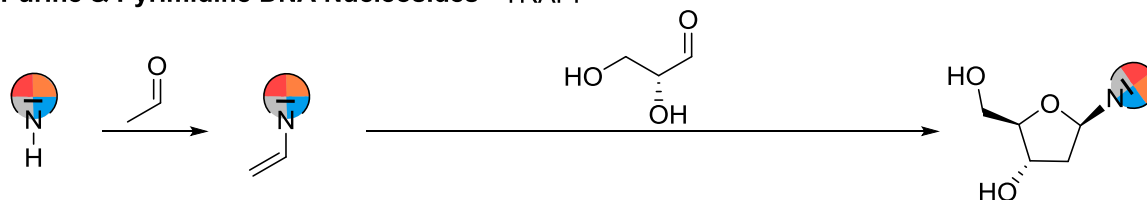
Scheme 2.3: Prebiotically plausible formation of RNA and DNA nucleosides. The coloured *N*-heterocycles refer to the respective nucleobases with orange = C, red = T, blue = A, grey = G. U is not shown, but could be formed by subsequent photochemical hydrolysis of C in the upper pathway.

The phosphorylation to enable polymerization to RNA/DNA strands would be the following necessary step. KRISHNAMURTHY demonstrated that diamidophosphate (DAP)

is capable of not only phosphorylating nucleosides but also amino acids and lipid precursors under aqueous conditions.[68]

All these successful syntheses of essential biomolecules in prebiotically plausible scenarios represent great achievements in the context of explaining their initial formation. However, these pathways are often considered separately which leads to challenges regarding their compatibility. In fact, it is the interconnection of building blocks that could have been a decisive factor in the selective emergence of life.[69-70] To take these factors into account, a more holistic and cooperative approach of systems chemistry gained increasing attention. As already mentioned for the phosphorylation reaction, prebiotic scenarios are sought that could provide the reactants as well as conditions for the emergence of all relevant building blocks of life. One example is the proposed cyanosulphidic protometabolism.[70-71] Following the potential of HCN as versatile carbon and nitrogen source, this molecule can be converted into precursors of ribonucleotides, peptides and lipids by the reactions mentioned above. The comprehensive network operates with similar chemistry of reductive HCN homologation and is driven by UV photoredox reactions and H_2S as reductant.

2.2.2 Bottom-up Approach

Placing the focus only on the successors of billion years of biological evolution might overlook molecules that pre- or co-existed and thus played an important role on the pre-Darwinian Earth. A bottom-up approach investigates the structures that naturally arise from the heterogeneous prebiotic feedstock, including prebiotic but non-biological (by)products. Instead of directed synthesis, analysing these reactant mixtures could lead to unique structures with unexpected but relevant function.

An early representation of this approach is the prominent MILLER-UREY-experiment. Assuming a reducing atmosphere of CH_4, H_2, NH_3, and H_2O at that time, this gas mixture was enclosed and treated with electric discharges to imitate lightning.[41-42,72] The resulting product mixture was condensed and accumulated in the boiling water flask, revealing the formation of amino acids, hydroxy acids, short aliphatic acids, urea and amines. This setup was modified multiple times in the following years providing these compounds as well as an extended scope under various conditions.[40,59,73-74]

Another example focuses on the environment of volcanic hydrothermal systems. Herein, WÄCHTERSHÄUSER explored the transformations of the prevalent C1-compounds CO_2, CO, COS, HCN, as well as CH_3CN in the presence of volcanic gases as well as iron, cobalt, and nickel salts at temperatures above 100 °C.[75] Under basic conditions, successful carbon fixation was observed with the formation of amino acids, hydroxy acids, and their derivatives from cyanide.

As can be observed in these two prebiotic scenarios as well as on meteoritic samples, the existence of α-hydroxy acids on an early Earth seems to be highly likely. Therefore, these compounds have been studied regarding their potential to assist or imitate biological mechanisms. Indeed, their easy polymerisation by simple drying of monomeric mixtures revealed promising properties. For example, these polyesters formed membraneless microdroplets that were capable of compartmentalisation.[76] As plausible pre-existing analogues of our lipid bilayers, these cell-like structures could provide concentration and protection of primitive prebiotic molecules to enhance chemical reactions. Further, copolymerization with α-amino acids enabled the formation of protopeptides, called depsipeptides, by lowering the activation entropies for amide bond formation.[77-78] Subsequent ester-amide exchange reactions led to an enrichment of amino acids over time and thus an efficient pathway to pure peptides that are not easily accessible otherwise.

The potential of mediated transformations relates not only to non-biological molecules but can also be found within biotic monomers and polymers themselves.[69] And the general power of molecular interaction is not restricted on facilitating the formation of complex organic compounds but can also have played a role in the emergence of homochirality.

2.3 Emergence of Homochirality

In contrast to the ongoing progress in introducing molecular complexity and variety into a prebiotic environment, scientists still face a puzzle regarding the emergence of homochirality. Our living organisms are almost exclusively built from L-amino acids and D-sugars, resulting in important properties as enzyme functions or the stability of our predominant DNA double helix. After million years of evolution, the mechanisms of intermolecular recognition and replication maintain this single-handedness as it is simply the only way that biomolecules function within our system. However, there is no chemical reason why the exact mirror image – formed from D-amino acids and L-sugars – would not work as well. Starting from a presumably racemic prebiotic mixture, two questions arise. Was the initial preference for one enantiomer over the other just a random coincidence or the result of a primordial template? And how could this distortion not only be sustained but amplified into the homochiral world which we live in.

2.3.1 Potential Causes for Symmetry Breaking

The imbalance between two enantiomeric molecules is referred to as symmetry breaking. Only a few theories suggest that life originated in a racemic environment and that chirality occurred at a later stage of evolution. In these cases, the prevailing of one enantiomer is justified with higher biological efficiency, evolutionary advantages, or simply by chance.[79] These biogenic scenarios do not find much support. Instead, various proposals have been made for potential symmetry breaking processes prior to life's origin (Figure 2.2).[80]
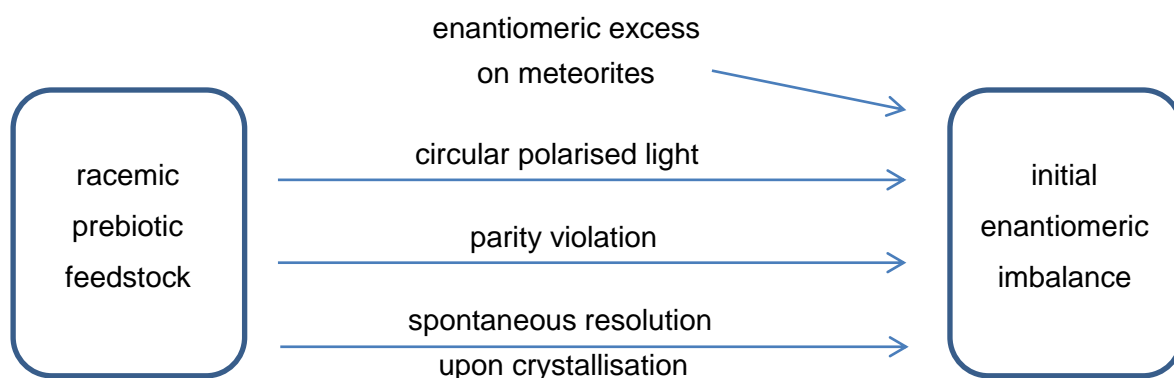
Figure 2.2: Processes that could have caused initial enantiomeric imbalance on the early Earth.

As already mentioned above as possible source for first organic material, carbonaceous chondrites are widely discussed as carrier of enantiomeric excess (*ee*) to the early Earth. Apart from the variety of organic matter found on the Murchison meteorite, α-methyl amino acids – isovaline, α-methyl norvaline, α-methyl valine, α-methyl isoleucine – have been detected with a favoured L-configuration of up to 15 %.[19,81-82] As these molecules are unknown in terrestrial matter and stable to chemical racemization due to the α-methyl group, the contamination on Earth as source for the small excesses can be nearly excluded. The ^{15}N enrichment of the Murchison amino acids relative to their terrestrial representative supported this assumption.[37] Further studies showed that they can be transformed to proteinogenic α-amino acids by decarboxylative transamination reactions with α-keto acids under chirality transfer or even amplification.[83-84] Although this could be the reason for an enantiomeric imbalance with a predominance of L-amino acids on the primitive earth, this theory does not explain its origin in outer space.

One explanation is based on the discovery of parity violation in the nuclear β-decay in 1957. As a consequence, there is a small energy difference between two enantiomers, stabilizing one with respect to the other. Especially as calculations indicated that L-amino acids and D-sugars would be favoured, this hypothesis raised its potential for prebiotic symmetry breaking.[85-88] However, the estimated energy differences due to this electromagnetic interaction are minimal and thus not yet observed experimentally. Estimates range from $10^{-14} – 10^{-13}$ J/mol, which corresponds to an *ee* value of approximately 10^{-15} %.[86,89-90] Whether such small intrinsic excesses are sufficient to initiate biological homochirality is questionable and still the subject of scientific debate.

Another hypothesis ascribes the emergence of chirality to the external influence of circular polarised light (CPL) in space. Because of the circular dichroism, asymmetric molecules react differently when exposed to CPL, which can lead to preferential synthesis or destruction. The latter is extensively studied since the successful asymmetric photodegradation of ethyl-α-bromopropionate in 1929, resulting in a change in optical rotation of 0.1°.[91] Recent reports have transferred this approach to prebiotically plausible solid-state amino acids, yielding an enantiomeric excess of 2.6 % for L-leucine und up to 4.2 % for L-alanine.[92-93] To gain an enrichment of L-amino acids by photolysis, right-handed CPL at wavelengths between 200 – 230 nm without subsequent exposure to

unpolarised UV light is required. Various possible astronomical sources for UV circular polarised light were proposed, including synchrotron radiation from supernovae, magnetic white dwarfs, polars, and reflection nebulae in some regions of star formation.[94-95] However, they either lack a sufficient amount of UV CPL or, if they show circular polarization of up to 50 %, the probability of having interacted with organic molecules in a molecular cloud is rather low.[95]

The most plausible and effective mechanism yet discovered is the spontaneous resolution upon crystallisation of conglomerates out of racemic solutions.[80] Unlike racemic compounds, each enantiomer of a conglomerate crystallises separately, which can lead to one being preferred while the other remains in solution.[96-97] As already shown by PASTEUR in 1848 with the resolution of sodium ammonium tartrate, an enantiomeric separation can be achieved without any optically active auxiliary agent.[98] This resolution happens randomly, but can lead to an irreversible imbalance by various scenarios. The remaining solution could rapidly equilibrate during the crystallisation process, resulting in a continuous conversion of one enantiomer into the other until the entire racemate has crystallised as single enantiomer. The enantiomer remaining in solution could also undergo further reaction or the solid and liquid phases get separated. In a prebiotic scenario, the latter could be realised by any slow moving water, weather or periodic wet-and-dry cycles. Unfortunately, this phenomenon is rather rare and nearly all natural amino acids except asparagine and threonine crystallise as racemates under moderate temperatures.[96,99-100] An approach to still achieve the crystallisation behaviour of conglomerates is the addition of porous material and in some cases the use of different salts or acetylated, benzoylated, and tosylated derivatives.[96]

None of these mechanisms can be confirmed with certainty, but neither can be eliminated from the list of potential reasons for an initial enantiomeric imbalance on the early Earth. Regardless of how the first symmetry breaking occurred, the second unresolved question directly follows. How could the small enantiomeric excesses be amplified over time resulting in a universal impact and eventually homochirality?

2.3.2 Amplification of the Initial Imbalance

As already indicated in the previous section for the crystallisation of conglomerates, irreversibility of enantiomeric excess formation is strongly connected with "far-from-equilibrium" processes. If reverse reactions or mechanisms are kinetically avoided, enantioselectivity can not only arise but also be amplified. For this behaviour both chemical and physical models have been proposed.[101]

In 1953, FRANK presented a mathematical model that tried to explain the emergence of homochirality with an autocatalytic reaction mechanism.[102] He suggested that one product enantiomer could catalyse its own production from an unlimited substrate pool while inhibiting the formation of its mirror image. In addition, heterochiral dimers would lead to catalyst deactivation. In this way, at an equimolar presence of D- and L-catalysts, both become deactivated. However, as soon as a small imbalance occurs, the respective excess maintains its self-replication capacity resulting in an amplification of the initial ratio. Starting from a small initial enantiomeric excess, the associated loss of the majority of catalyst molecules to deactivated heterodimers has to be considered.

A first non-linearity between the enantiomeric excesses of product and applied catalyst was observed by KAGAN more than 30 years later for asymmetric oxidations and aldolisation reactions.[103] Still, it was not the product that served as the catalyst. This missing part and thus an actual asymmetric autocatalysis was achieved by SOAI in 1995. In the alkylation of pyrimidyl aldehydes with dialkylzincs, the reaction rate was not only accelerated by catalytic amounts of the product but the enantiomeric excess of the yielded alcohol exceeded the *ee* of the initially employed one. Within only four catalytic cycles, the *ee* value of the alcohol increased from 2 % to 88 % (Scheme 2.4).[104]
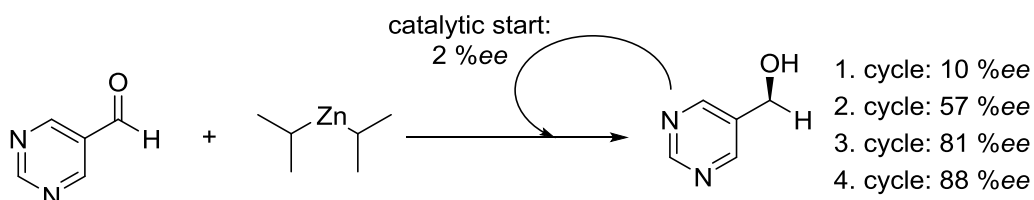
Scheme 2.4: Asymmetric autocatalytic SOAI reaction of pyrimidine-5-carbaldehyde with diisopropylzinc catalysed by the product pyrimidyl alcohol with a starting *ee* of 2 %.

Following studies by the same group presented further improvements of the catalytic system, eventually amplifying a miniscule enantiomeric excess of 0.00005 % to over

99.5 %*ee* after only three cycles.[105] In addition to reaching a range of enantiomeric imbalance that might be plausible in a prebiotic scenario, they were also able to show that the initial symmetry breaking could not only be induced by the enantiomerically enriched alcohol catalyst but also by circular polarised light, quartz minerals, chiral organic crystals, amino acids, or even by the small mirror image difference of ^{12}C/^{13}C carbon isotope chirality.[106-109] Although the experimental conditions of the SOAI reaction are not compatible with an early Earth environment, it demonstrates that asymmetric autocatalysis could be capable of transforming a miniscule enantiomeric excess into homochirality. Recently, autocatalysis and *ee* amplification was observed in a completely metal-free organic reaction.[110] This chemical transformation is more likely to withstand aerobic and aqueous surroundings and thus reinforces the idea that this concept may have had prebiotic significance.

Analogous physical out-of-equilibrium autocatalytic processes were observed during the crystallisation of conglomerates. As already mentioned above, conglomerates form separate, enantiopure L- and D-crystals. Having the same physical properties, including solubility, a mixture of these two crystals will always equilibrate to an equal amount of L- and D-molecules in the solution. If a non-racemic crystal mixture is dissolved, the enantiomeric excess in the liquid phase ($ee = 0$) and solid phase ($ee \neq 0$) will differ and phase partitioning could lead to an enantioenrichment in the solid phase. During the crystallisation of conglomerates, usually equal amounts of both enantiomeric crystals are formed (Figure 2.3 A).
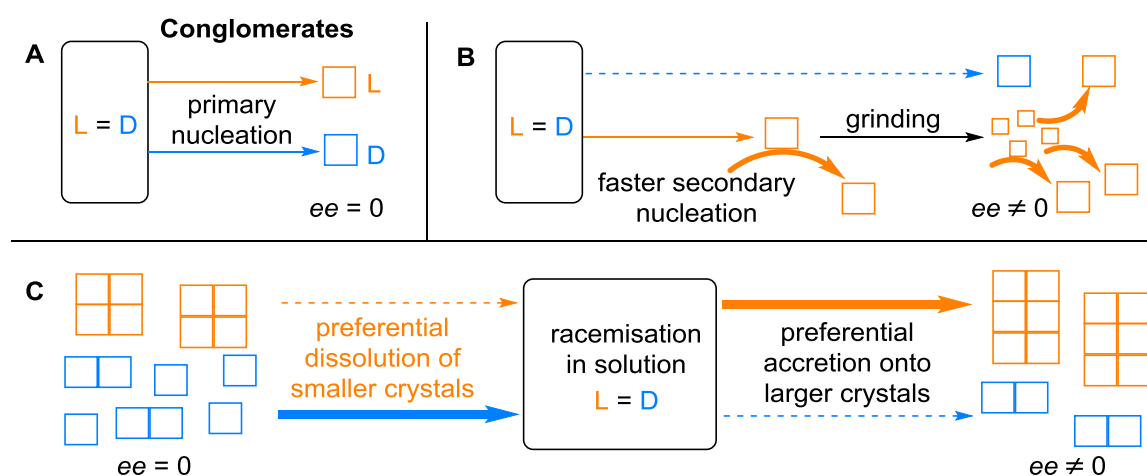
Figure 2.3: Theoretical mechanisms for *ee*-amplification in the solid phase (squares) of conglomerates. A: primary nucleation to a racemic solid phase. B: autocatalytic secondary nucleation in vicinity to the "mother nucleus". C: preferential dissolution/accretion behaviour depending on the crystal size.

16

However, examples were reported, in which molecules crystallised with nearly single chirality. In 1990, KONDEPUDI showed that rapid stirring upon the chiral crystallisation of the achiral sodium chlorate ($NaClO_3$) in water resulted in the predominance of one enantiomorph crystal with an optical purity greater than 99 % (with random handedness in repeated experiments).[111] This was explained by the fact that secondary nucleation is much faster than primary nucleation, resembling a chiral autocatalytic process (Figure 2.3 B). The rapid stirring breaks the "mother nucleus" into thousands of new nuclei of the same handedness, which subsequently catalyse secondary nucleation fast enough to deplete the solute below the threshold for spontaneous primary nucleation. Thus, crystallisation of the second enantiomer is suppressed obtaining homochirality.[111-112] Another study of the $NaClO_3$ system by VIEDMA in 2005 revealed the possible emergence of single chirality even starting from an equilibrated racemic crystal mixture (Figure 2.3 C).[113] Simply adding glass beads to the gently stirred saturated solution led to the complete conversion of one solid enantiomer to the other over time (again with random handedness in repeated experiments). Continual abrasion by the glass beads produced smaller crystals that according to the Gibbs-Thomson rule dissolve faster than larger ones. As a consequence, the solution is slightly supersaturated with achiral $NaClO_3$ that re-accretes to any of the solid enantiomers, but with preference to the larger crystals (Ostwald ripening). If there is a random predominance in the handedness of the larger crystals, they will grow on the expense of smaller ones up to the sole presence of the respective enantiomer. This concept was based on $NaClO_3$, an achiral solution phase molecule, which has the ability to add to either solid enantiomer. However, it was already successfully transferred to intrinsically chiral amino acids and their derivatives by making use of solution phase racemisation.[114-115] Stirring a saturated aspartic acid solution in acetic acid with an *ee* below 10 % and catalytic amounts of salicylaldehyde, a single chiral solid state was obtained after six days at 160 °C. The mechanical energy necessary for these mechanisms could be found in any prebiotic running water over sand or pebbles.

In contrast to the enrichment of solid enantiomers in the case of conglomerates, phase separation of racemic compounds can lead to enantiomeric excesses in solution. This phenomenon was already described as prebiotically relevant in 1969 by MOROWITZ and is based on the fact that many molecules are more soluble as pure enantiomers than their

racemic crystals.[116-117] Starting with a small excess of L-amino acid in pure water, the final ratio can be determined by the following equation:

$$[\text{L}]/[\text{D}] = S_\text{L}^2/S_\text{DL} \qquad [1]$$

with S_L being the solubility of L and S_DL the solubility product of a racemic crystal of DL. If the solubility of the enantiopure crystal is twice that of the racemic solid, an enantiomeric excess of 16/1 would result in the solution. The only requirement for this amplification process is that the amount of water is small enough that both the racemic and the homochiral crystal are dissolved to saturation. Considering the omnipresence of water on early Earth, this scenario could be realised through evaporation cycles or very short water exposure periods representing rain drops falling on these mixtures. Although the theoretical values predicted by the above equation were not fully reached in the subsequent experimental studies, drastic increases up to >99 %*ee* from small initial enantiomeric fluctuations were observed for amino acids,[83,118-119] ribonucleosides[120] and sugars.[121]

Although asymmetric autocatalytic chemical reactions have not been observed in a prebiotically plausible transformation so far and the concept of singular chirality formation during crystallisation and dissolution is only theoretically realised in early Earth scenarios, all these autocatalytic mechanisms demonstrate that complete optical purity of a molecule could evolve from even the smallest enantiomeric imbalance. Assuming a successful initial symmetry breaking followed by amplification, the final or intervening step toward universal homochirality would be the transfer of chirality onto further molecules.

2.3.3 Transfer of Chirality

Regardless of which compounds developed first chiral imbalances, this information must have been passed on to propagate to single chirality. It is not clear whether amino acids, sugars or completely different molecules initialised this pathway, but finding a connection between them is more likely than that both homochiral biomolecules were independently subject to a random symmetry breakage.

One plausible mechanism was already mentioned above for the transformation of the meteoritic L-α-methylated amino acids into L-biological amino acids by direct

decarboxylative transamination of α-keto acids. The prebiotic existence of the latter could be explained by oxidation of α-hydroxy acids, found on meteorites.[122-123] In a first study, enantiopure α-methylated valine converted pyruvate into alanine and phenylpyruvate to phenylalanine with a maximum product *ee* of up to 9.5 %.[124] However, the stereoconfiguration was reversed which would result in a predominant existence of D-amino acids on the early Earth. Two years later, it was reported that the correct L-form could be synthesised by catalysing this reaction with copper.[83] In doing so, L-phenylalanine was obtained in 37 %*ee*, L-alanine in 20 %*ee*, and L-valine in 23 %*ee*.

Following on from this, a transfer of enantiomeric excess from the proteinogenic amino acids to glyceraldehyde in the natural D-configuration was reported.[125-126] Adding different L-amino acids to the reaction mixture of SUTHERLAND's pathway towards pyrimidine nucleosides (see Section 2.2.1) yielded the D-aminooxazoline precursor with an excess of up to 58 %*ee*. Only histidine led to a preferred formation of the unnatural L-product. This chirality transfer occurred via kinetic resolution of the racemic feedstock molecule glyceraldehyde. The L-amino acid selectively reacts with 2-aminooxazole and the unnatural L-sugar in a side-reaction, leaving D-glyceraldehyde in solution for further conversion into the desired D-RNA precursors. Over time, an enantioenrichment of D-glyceraldehyde of greater than 90 %*ee* was observed in the reaction mixture. This chiral selectivity of amino acid-sugar interaction also worked vice versa. The L-L (D-D) combination reacted ca. 2.5 times faster than the hetero combination and as long as one of them was present in nonracemic form, resolution of the racemic molecule occurred.

According to these two mechanisms, an exemplary pathway is conceivable that starts with an imbalance in meteoritic L-α-methylated amino acids that transfer chirality to natural amino acids which in turn pass the information on to glyceraldehyde to build up the respective nucleosides. At every stage, the enantiomeric excesses could be amplified by the processes described in Section 2.3.2. Although this pathway could be compatible with early Earth scenarios and the chiral connection between L-amino acids and D-sugars is of high prebiotic interest, it is so far based on very distinct stepwise transformations that need high concentrations of the transfer agents. Therefore, a more holistic approach to propagate chirality with only small amounts of simple chiral molecules would be a successful application of these compounds as asymmetric organocatalysts.

2.4 Organocatalysis

The field of asymmetric catalysis has long been dominated by metal and biocatalysts. It is only since the turn of the millennium that small purely organic molecules have increasingly become established as powerful alternatives for transition metal complexes and enzymes. These catalysts bear the advantages of easy low cost synthesis, moisture and oxygen stability, as well as low toxicity and are not only implemented in transformations that have to meet these criteria but also in reactions that have not been feasible otherwise. Although the potential of organocatalysis has only recently been recognised, the first report dates back to 1860 when LIEBIG presented the synthesis of oxamide from dicyan and water catalysed by acetaldehyde (Scheme 2.5).[127]
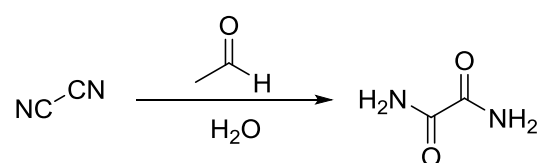
Scheme 2.5: Reaction of dicyan and water to oxamide as first reported organocatalytic synthesis.

More than 100 years later, the next milestone was set with the discovery of the first highly enantioselective organocatalytic process, the Hajos-Parrish-Eder-Sauer-Wiechert reaction (Scheme 2.6).[128-131] This asymmetric L-proline catalysed intramolecular aldol reaction inspired not only the later thorough investigations on this amino acid, but also the general emergence of the broad field of nitrogen and in particular secondary amine catalysis.
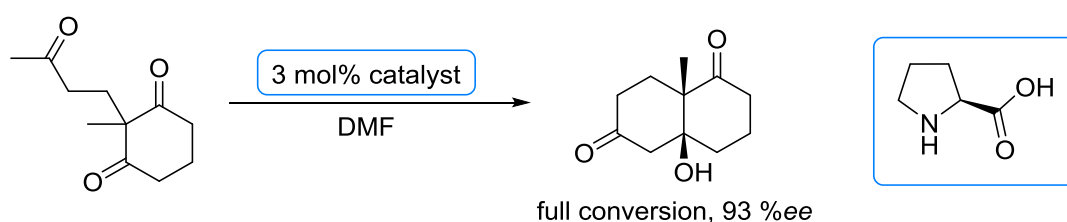
Scheme 2.6: Proline catalysed intramolecular aldol reaction (Hajos-Parrish-Eder-Sauer-Wiechert) as first reported asymmetric organocatalytic synthesis.

Depending on the activation behaviour, the catalysts can be classified as Lewis acids/bases or Brønsted acids/bases. Overall, secondary amines dominate organocatalytic transformations.[132]

The vast amount of organocatalytic reactions as well as the respective organocatalysts are extensively discussed and reported in numerous reviews[132-140] and will not be the focus of this thesis. The following Figure 2.4 only presents the most prominent enamine, iminium

and non-covalent H-bonding activation with an established corresponding catalyst and an excerpt of their catalysed reactions. It is worth mentioning that the catalyst is not limited to only one type of activation. Instead, different mechanisms can be used for different transformations or even combinations of them within one catalytic application.

Enamine Catalysis	Iminium Catalysis	H-bonding Catalysis
(Cross-)Aldol	Friedel-Crafts	Strecker
Mannich	Diels-Alder	Mannich
Michael	Hydride reduction	Biginelli
Intramolecular α-alkylation	Conjugate amination	Reductive amination
Knoevenagel	Mukaiyama-Michael	
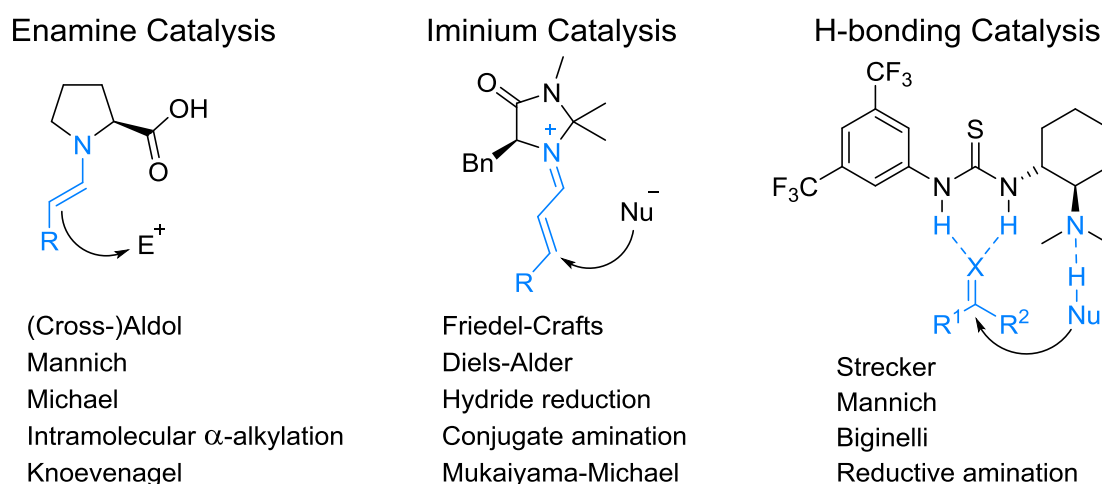
Figure 2.4: Examples of transformations feasible through enamine, iminium and H-bonding organocatalysis with a prominent catalyst representative in their respective activation mode and typically catalysed reaction.

2.4.1 Prebiotic Organocatalysis

Considering the variety of chemical transformations feasible via organocatalysis, this approach could have played a key role in the emergence of molecular complexity on the early Earth. The demands on reaction conditions can be brought in line with aqueous and oxygenated environments and the low substrate-specificity compared to enzyme catalysis can account for a broad applicability. Simultaneously, single enantiomeric excesses could be transferred to different molecules, ensuring the propagation of chirality. In this context, prebiotic research in particular focuses on the synthesis of the essential homochiral biomolecules: amino acids and sugars. A prebiotic asymmetric Strecker reaction to build up the former has not been discovered yet, but asymmetric aldol condensations yielding the latter are extensively studied. So far, almost exclusively amino acids have been considered as prebiotically promising catalysts. They not only show catalytic activity in modern organic chemistry but are also highly discussed as (meteoritic) sources of initial enantiomeric imbalances (see Section 2.3.1) and would thus provide a link between the biotic L-amino acids and D-sugars. The most efficient and versatile representative is L-proline, which has shown to provide high enantioselectivities in aldol condensations

including the dimerisation of protected glycolaldehyde to tetroses.[141-142] However, all these reactions were carried out in organic solvents and its catalytic activity drastically diminished in the presence of water, ubiquitous in prebiotic environments.[143] Moreover, proline has not been detected in meteorites and only scarcely in experiments mimicking the early Earth.[144-146] But above all, the proteinogenic L-proline catalysed the formation of the undesired, abiotic L-sugars.[121,141-142]

Surprisingly, experimental findings indicated the opposite for the prebiotically more plausible primary amino acids. PIZZARELLO and WEBER were the first to demonstrate that both L-alanine and L-isovaline are able to catalyse the aldol condensation of glycolaldehyde to tetroses in aqueous triethylammonium acetate buffer (pH 5.4), resulting in a preferred formation of D-threose (Scheme 2.7).[143]

		Threose	Erythrose
TEAA buffer pH 5.4, 50 °C	L-Ala	7 %*ee* **D**	
	L-Iva	11 %*ee* **D**	
	L-Pro	—	—
	L-Ala-L-Ala		33 %*ee* **D**
	L-Val-L-Val		75 %*ee* **D**
NaAc buffer pH 4.9, 25 °C	L-Val-L-Val		82 %*ee* **D**
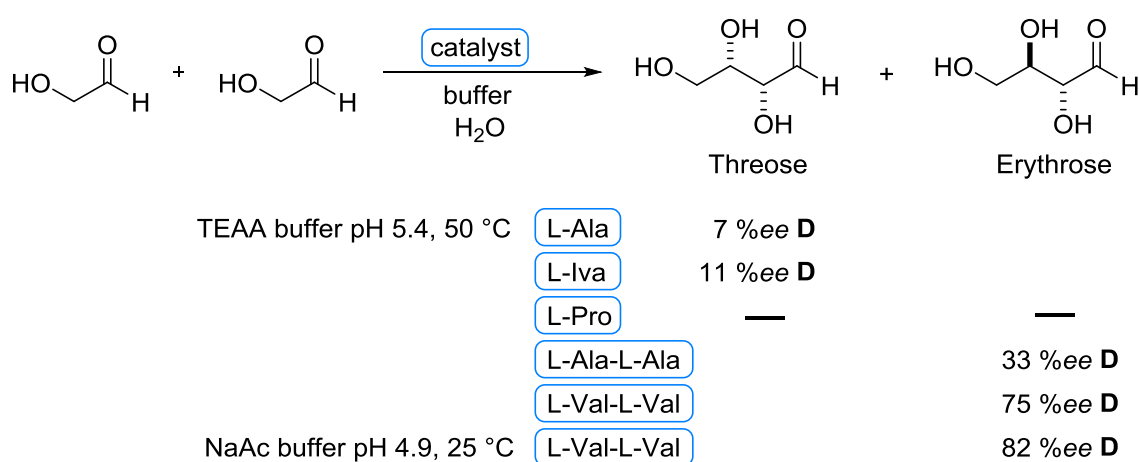
Scheme 2.7: Aldol reaction of glycolaldehyde catalysed by amino acids and dipeptides.[143,147] Only the enantiomeric excess of the preferentially formed diastereomer is presented. TEAA = triethylammonium acetate, NaAc = sodium acetate.

Depending on the applied catalyst *ee*, the sugar was obtained with an enantiomeric excess of up to 11 % (L-isovaline 100 %*ee*) and asymmetric effects were still observed at *ee* levels found in meteorites. The use of proline under these conditions did not show any product formation. They further reported a significant increase in enantioselectivity upon using various homochiral L-dipeptide catalysts. In this study, however, D-erythrose was predominantly formed with a maximum of 82 %*ee* for L-Val-L-Val.[147] The selectivity for this diastereomer was also observed by CLARKE during the investigations on amino acid esters as catalysts for the formation of C4-sugars from glycolaldehyde under aqueous conditions.[148-149] Here, esters of L-alanine, L-leucine, and L-valine yielded D-tetroses, whereas L-proline esters led to product formation but with a dominance of the L-sugar.

The same trend was reported by BRESLOW for the amino acid catalysed reaction of glycolaldehyde and formaldehyde to the C3-sugar glyceraldehyde in pure water (Scheme 2.8).[121] All prebiotically plausible primary amino acid catalysts resulted in small to medium excesses of the D-sugar. In contrast, L-proline did show activity for the opposite L-enantiomer. Thorough investigations on the reaction conditions, however, revealed that the product configuration could be reversed by performing the catalysis under more basic conditions.[125,150] Starting at pH 6.6 and above, L-proline catalysed the formation of the desired natural D-glyceraldehyde. Vice versa, L-glyceraldehyde was formed from the primary L-amino acids.

	catalyst	D-Glyceraldehyde	L-Glyceraldehyde
pH 2.9-4.2[a]	L-Glu	35 %ee	
	L-Pro		20 %ee
pH 6.6-7.6[b]	L-Glu		4 %ee
	L-Pro	2 %ee	
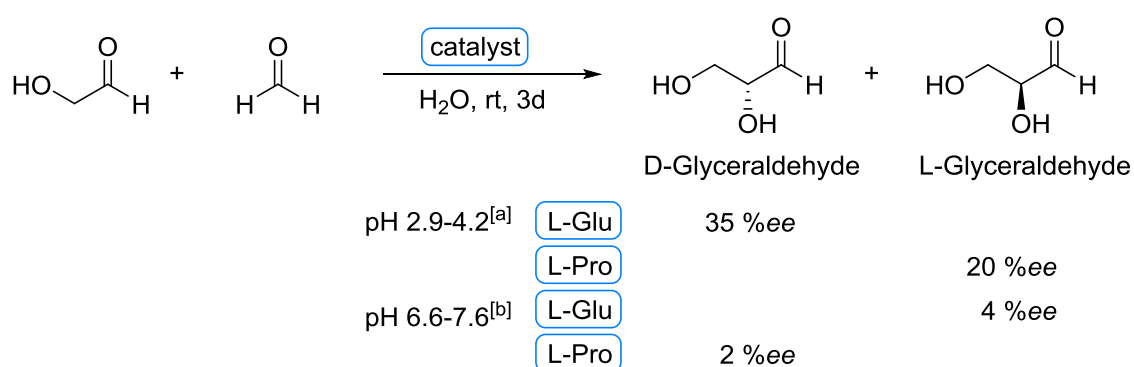
Scheme 2.8: Aldol reaction of glycolaldehyde with formaldehyde catalysed by amino acids at different pH-values.[150] [a] pH-value that resulted in water without the addition of any acid/base, [b] pH-value adjusted with the addition of NaHCO$_3$.

This pH sensitivity demonstrates how the surrounding environment of such reactions on the early Earth might have had an impact on the stereochemical outcome. Assuming a more likely existence of primary L-amino acids, the prebiotic media appear to have been rather acidic in order to favour the catalysed formation of D-sugars.

All these studies demonstrate that organocatalytic asymmetric aldol condensations are highly plausible on a primordial Earth and that the concept of prebiotic organocatalysis has in general great potential to explain the origin of molecular chirality and complexity. To increase the plausibility of this theory, further functionalisations have to be realised. One important transformation is the alkylation of small aldehydes. This elongation reaction would not only provide new prebiotically accessible molecular structures but also increase the insolubility in water, a property much needed for cellular-like compartmentalisation.

2.4.2 Organocatalytic α-Alkylation

The intermolecular organocatalytic α-alkylation of simple aldehydes has not only been an unsolved challenge in prebiotic chemistry, but also considered the Holy Grail in modern chemistry for many years. The difficulties to control this reaction are attributed to various competing side-reactions, including self-condensation of the aldehyde species, Cannizzaro or Tishchenko reactions (based on disproportionation), and *N-* or *O*-alkylations of the respective catalyst. STORK already recognised, with the reaction bearing his name, that the formation of enamines is advantageous for the predominant carbon alkylation of carbonyl compounds.[151] Despite this stoichiometric application and the success of enamine catalysis in various other transformations, an enamine catalysed alkylation was not succeeded for years. In 2004, LIST achieved a first breakthrough with an intramolecular approach (Scheme 2.9).[152] By using proline or proline derivatives as catalysts and one equivalent of base, halo-aldehydes were converted into the respective carbocycles with excellent yields and enantioselectivities.
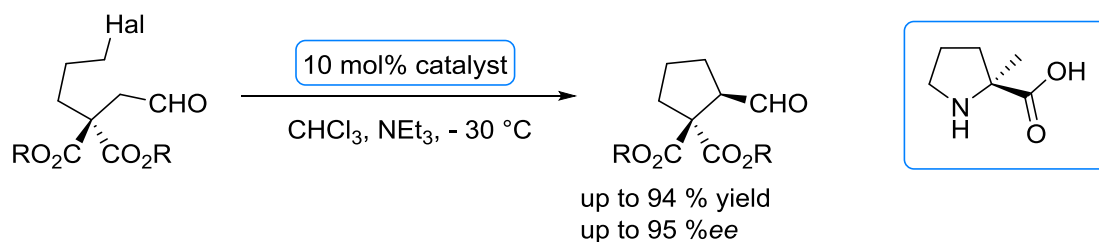
Scheme 2.9: Organocatalytic intramolecular α-alkylation of halo-aldehydes with proline derivatives.

The corresponding intermolecular reaction, however, only led to deactivation of the catalyst due to *N*-alkylation. This next step was accomplished four years later by MACMILLAN with merging amine catalysis and organometallic photoredox catalysis (Scheme 2.10).[153] Here, the activation occurs through single-electron SOMO (singly occupied molecular orbital) catalysis resulting from two interlocking catalytic cycles: after photoexcitation, a ruthenium photosensitiser generates highly electrophilic alkyl radicals via reduction of alkyl bromides, and simultaneously an electron-rich chiral enamine is formed from the condensation of an amine catalyst with the aldehyde. The first connection of the two cycles appears when the excited $*Ru(bpy)_3^{2+}$ (bpy = 2,2′-bipyridine) accepts a single electron (SET) from a sacrificial quantity of initially formed enamine to become the strong reducing agent $Ru(bpy)_3^+$. From the first catalytic cycle on, this SET goes hand in hand with the oxidation of the coupled α-amino radical to the iminium ion

that subsequently hydrolyses to provide the α-alkylated aldehyde and recover the amine catalyst. High yields and enantioselectivities were obtained for various aliphatic aldehydes using different alkyl bromides with electron withdrawing groups (EWG).

Photoredox Organocatalytic Alkylation of Aldehydes

Scheme 2.10: Photoredox organocatalytic α-alkylation of aldehydes. Left: mechanism of the interconnection of photoredox-catalysis (yellow) and organocatalysis (blue). Right: exemplary product scope and similarities of the mechanism to the process of photosynthesis.

This procedure has further been extended to α-perfluoroalkylation,[154] α-cyanomethylation,[155] and α-benzylation[156] as well as to the use of different transition metal complexes,[154,156-157] semiconductors,[158-159] organic dyes,[160] electron donor-acceptor

(EDA) complexes[161-162] or even the transiently generated enamines themselves[163] as photosensitisers. Although this process cannot be regarded as purely organocatalytic, the needed photoexcitation does not exclude its prebiotic relevance. On the contrary, this interlocked combination is reminiscent to the conversion of solar energy to chemical energy in photosynthesis (Scheme 2.10, bottom right). Given its importance in nature, a similar preceding mechanism on the early Earth is not unlikely, especially considering the large impact of solar irradiation.

Besides the combined photoredox approach, a completely organocatalytic α-alkylation of aldehydes was performed in high yields and moderate to high enantioselectivities by intercepting the enamine with highly stabilised carbocations in an S_N1-type reaction instead of using alkyl radicals.

S_N1-type Organocatalytic Alkylation of Aldehydes

COZZI 2009
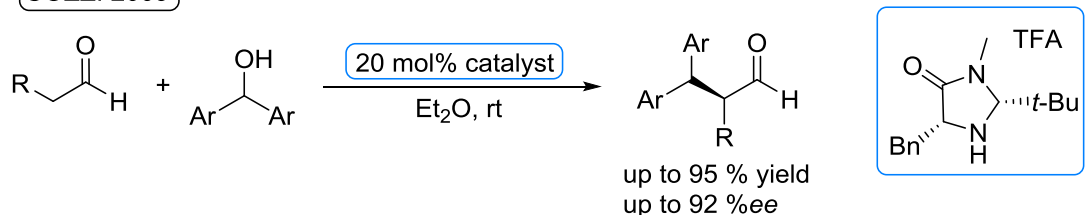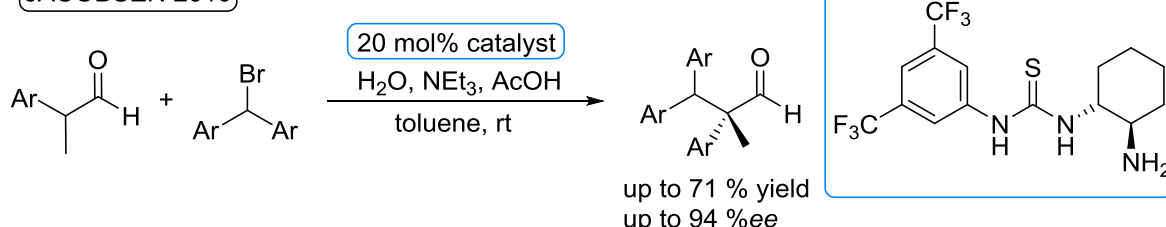
S_N2-type Organocatalytic Alkylation of Aldehydes

PALOMO 2011
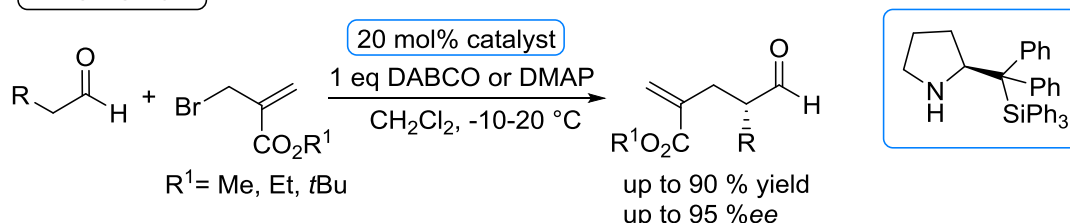
Scheme 2.11: Organocatalytic alkylation of aldehydes with diaryl alcohols or halides via S_N1-type reaction or with electron-deficient allylic bromides and DABCO or DMAP as activating agent via S_N2-type reaction.

Whereas PETRINI and MELCHIORRE used L-proline as catalyst and 3-(1-arylsulfonylalkyl)-indoles as electrophilic precursors,[164-165] COZZI and JACOBSEN applied diaryl alcohols[166] or

halides[167] together with the MacMillan imidazolidinone or (thio)urea derivatives, respectively (Scheme 2.11, top and middle). To promote the carbocation formation, the former two needed potassium fluoride supported on basic alumina, but the latter reported the addition of acids as crucial step. Finally, an S_N2 type addition-elimination route via enamine-catalysis was discovered by PALOMO also for the intermolecular alkylation (Scheme 2.11, bottom).[168] Here, the allylic bromides as alkylating agents had to be activated as ammonium salts by adding equimolar amounts of DABCO (1,4-diazabicyclo[2.2.2]octane) or DMAP (4-dimethylaminopyridine). The bases had to provide the right balance of nucleophilicity and nucleofugacity, as well as low basicity to prevent racemisation of the aldehyde.

These studies show that the experimental realisation of theoretically simple transformations is not always trivial and that already small deviations in scope or conditions demand a new and explicitly designed system. Despite all these achievements, a general organocatalytic method for the alkylation of aldehydes with simple alkyl halides still needs to be discovered for both modern and prebiotic chemistry.

2.5 Imidazolidine-4-thiones

The first report on imidazolidine-4-thiones is dated back almost 100 years. In the course of studying the influence of hydrogen sulphide on aminonitriles in ethanolic ammonia, GATEWOOD and JOHNSON observed different reaction behaviour depending on the nitrile applied. While amino acetonitrile (R^1, R^2 = H) was converted into a dithiopiperazine and the aminonitrile of acetaldehyde (R^1 = H, R^2 = CH$_3$) predominantly formed dipropionitrile amine, the interaction of H$_2$S with the aminonitrile of acetone (R^1, R^2 = CH$_3$) yielded a well-defined crystalline substance that they assigned to the imidazolidine-4-thione structure (Scheme 2.12).[169]
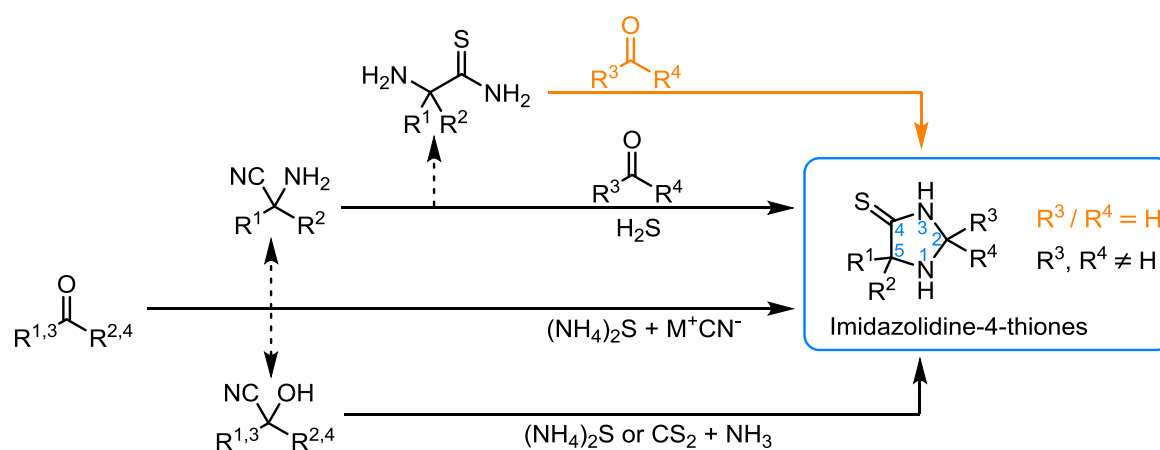
Scheme 2.12: Synthetic pathways to imidazolidine-4-thiones. Highlighted in orange is the only pathway that allowed for the condensation with aldehydes instead of ketones.

The formation of this structural motif was extended to asymmetrically substituted heterocycles in 1949 by treating α-aminonitriles with various ketones in ethereal solutions saturated with H$_2$S and catalytic amounts of pyridine.[170] In addition, α-aminothioamides were identified as highly likely intermediates. Due to the drawbacks of the susceptible equilibrium of aminonitrile formation, this procedure has been steadily improved. Stepwise addition of the ring closing ketone to the crude aminonitrile mixture four hours after the addition of H$_2$S increased the yields. This especially avoided the previous high losses during aminonitrile isolation.[171] Instead of aminonitriles, also cyanohydrins could be converted into imidazolidine-4-thiones via reaction with either ammonium sulphide or carbon disulphide together with ammonium hydroxide.[172-174] This approach was further simplified by circumventing the preliminary cyanohydrin or aminonitrile synthesis and directly treating the respective ketone with a cyanide salt in aqueous ammonium sulphide solution.[173,175] Both these reaction pathways have drawbacks in terms of broad

applicability. While symmetrically substituted imidazolidine-4-thiones can be synthesised from ketones easily, the combination of different side-chains is difficult and aldehydes can mostly not be implemented as condensation compounds.[169-170,173] Only starting directly from α-aminothioamides enabled the reaction with aldehydes and thus the formation of 2,5,5-trisubstituted species.[171] However, the selective synthesis of α-aminothioamides from aldehydes or straight chain ketones in turn often required multiple steps and protection of the α-amine. Finally, the (N3)-methylated derivatives can be synthesised from their oxygen analogous MacMillan imidazolidinones via thionation with P_4S_{10}.[176] Although this method is more cumbersome, it bears the advantage of direct access to enantioenriched compounds. Otherwise, stereoinformation could only be introduced at ring position 5 by starting from chiral α-aminothioamides.[177]

Reactivity of imidazolidine-4-thiones

Imidazolidine-4-thiones have been tested towards oxidation, reduction, hydrolysis, as well as various functionalisations (Figure 2.5).
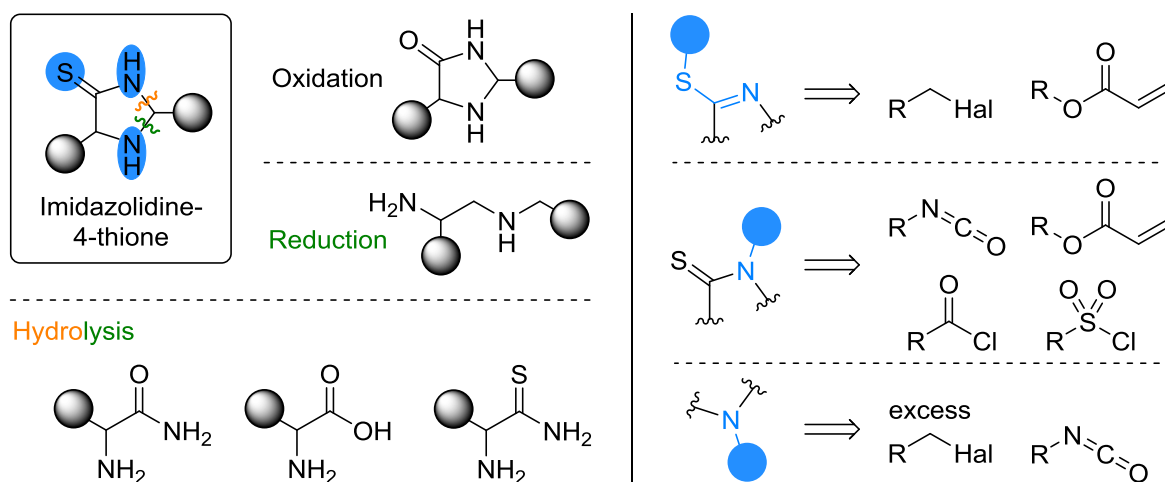
Figure 2.5: Reactivity of imidazolidine-4-thiones. Left: observed products resulting from oxidation, reduction, and hydrolysis. Right: observed reaction centres for the functionalisations with the respective reactants.

Oxidation with hydrogen peroxide or potassium permanganate yielded imidazolidine-4-ones. Upon reduction with lithium aluminium hydride ring opening occurred next to the amine (Figure 2.5, green wavy line), resulting in the respective diamine.[178] The ring structure is also not stable against hydrolysis, leading first to ring opening next to the amide followed by hydrolysis of the resulting imine under release of the carbonyl species (Figure 2.5, yellow and green wavy line). Depending on the reaction conditions, α-amino acid amides, α-amino acids, or α-aminothioamides were detected.[179-180]

The imidazolidine-4-thiones have three potential nucleophilic reaction centres for functionalisation, namely the thioamide sulphur and nitrogen, and the amine nitrogen (Figure 2.5, blue). With alkyl halides in basic media, the primary substitution took place at the sulphur atom of the thioamide, followed by the amine in case of an alkyl halide excess.[177,181-183] Using acrylates instead shifted the alkylation towards the thioamide nitrogen with an *N/S*-adduct ratio being dependent on the acrylate as well as the imidazolidine-4-thione residues.[183] Predominant alkylation on the thioamide *N* was also achieved by converting the imidazolidine-4-thione to the *N*-sodium species prior to the addition of alkyl halides. This pre-activation as well as the presence of weaker bases also led to thioamide *N*-acyl and *N*-arylsulfonyl derivatives from the respective acid chlorides.[184] The dynamic reaction behaviour of imidazolidine-4-thiones is also noticeable in the interaction with isocyanates. In the presence of a strong base they are reported to add to the thioamide nitrogen, whereas formation of the urea derivative with the amine was observed without a base.[184-185]

Applications of imidazolidine-4-thiones and their derivatives

Imidazolidine-4-thiones and their derivatives were mainly studied for industrial applications. Their *N*-carbamoyl derivatives have been found to stabilise polyolefins towards deterioration due to UV exposure or heat without affecting the respective colour properties. The latter is of particular interest for coatings such as paints and lacquers.[185] Furthermore, alkylated imidazolidine-4-thiones are utilised as oil-soluble, metal- and phosphorus-free additives for lubricants. Unlike the state-of-the-art zinc dialkyldithiophosphates, no ash residue is produced and the efficiency of catalytic converters is not affected.[183,186]

Over the last 10 years, however, imidazolidine-4-thiones have also aroused academic interest for their use as potential organocatalysts. Their *N*3-methylated derivatives have high structural similarities to the widely used MacMillan imidazolidinones, raising the potential for an analogous catalytic reactivity. Due to the higher C-N rotating barrier in thioamides compared to amides,[187-188] a more rigid ring structure and thus even better stereoselectivity was anticipated.[176] This hypothesis was tested in the asymmetric Friedel-Crafts alkylation of pyrroles and indoles with α,β-unsaturated aldehydes and the asymmetric oxyamination of aldehydes (Scheme 2.13, top and middle).[176,189-190] All

corresponding products were obtained with comparable yields and enantioselectivities to the MacMillan catalysts and for indoles the stereoselectivity was even increased.

Friedel-Crafts alkylation - SU 2010/12

up to 85 %
up to 98 %*ee*

up to 88 %
up to 96 %*ee*
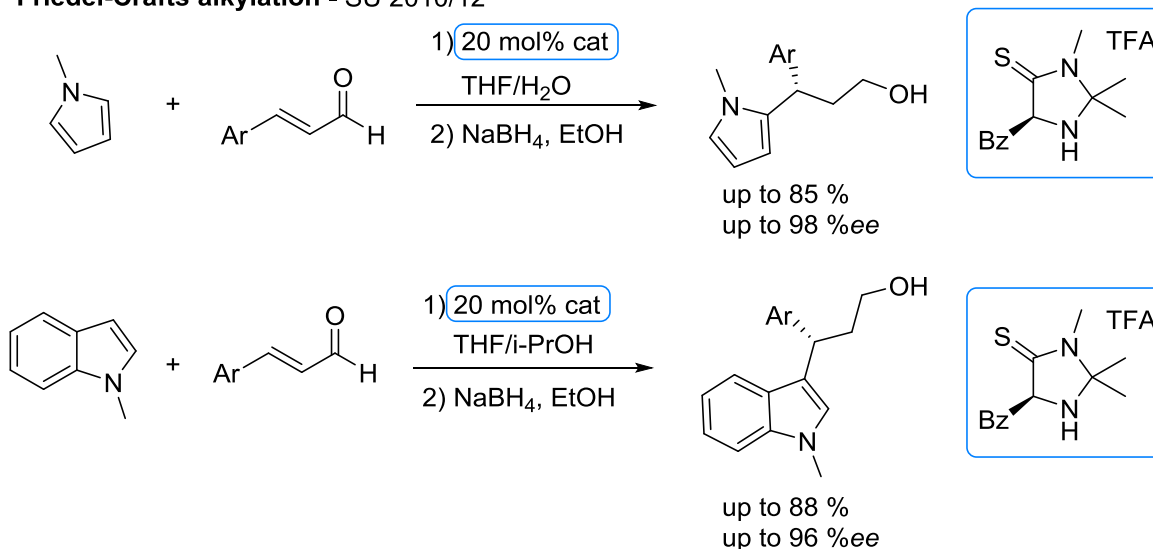
Oxyamination - SU 2014

up to 89 %
up to 90 %*ee*
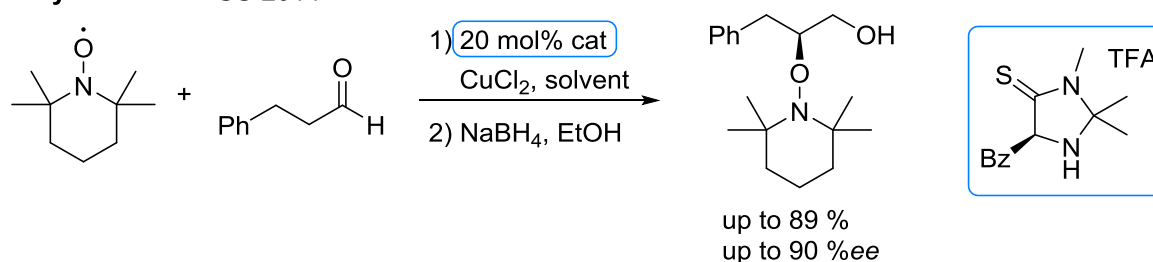
Henry reaction - SEDLAK 2016/17

up to 99 %
up to 98 %*ee*

R^1 = H, Me
R^2 = - , Bz, resin
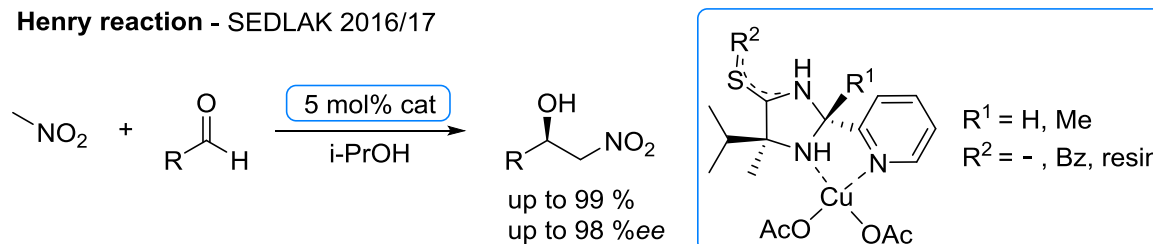
Scheme 2.13: Transformations catalysed by imidazolidine-4-thiones and their derivatives.

But also the non-methylated pure imidazolidine-4-thiones were used as organocatalysts. Their copper (II) complexes showed high catalytic activity and moderate to good enantioselectivity in the asymmetric Henry-reaction of nitromethane with aldehydes (Scheme 2.13, bottom).[177,181] The *trans*-substitution of the residues led to superior results and the formation of the *R*-product. Further, the free thioamide group enabled anchoring to a polymeric resin via the sulphur atom. This modification simplifies separation and recycling highly desired for ecological and economic aspects. Alkylation as well as

immobilisation to a resin at the thioamide sulphur did not affect the reactivity and enantioselectivity in the Henry reaction.[177,181] In contrast to the previous transformations, this catalysis is not based on enamine formation but on metal coordination of both reactants to the chiral copper species. The few reports show that the amine functionality of the imidazolidine-4-thione skeleton can be used for organocatalytic activation. However, mainly alkylated derivatives have been employed so far.

Imidazolidine-4-thiones as intermediates towards activated amino acids

Besides the presented applications in modern academia and industry, PAVENTI and EDWARD have brought the basic structure into a first discussion about a prebiotic relevance, namely as intermediates on the reaction pathway to α-aminothioamides.[180] The latter are discussed as activated peptide precursors that could enable the challenging polymerisation step that is not feasible with the unreactive α-amino acids (see Section 2.2.1). However, a direct synthesis of α-aminothioamides by treating α-aminonitriles with hydrogen sulphide was often not successful. Thus, acetone was added to this mixture to selectively form an imidazolidine-4-thione that can subsequently be converted into the α-aminothioamide by acid hydrolysis and release of the ketone (Scheme 2.14).
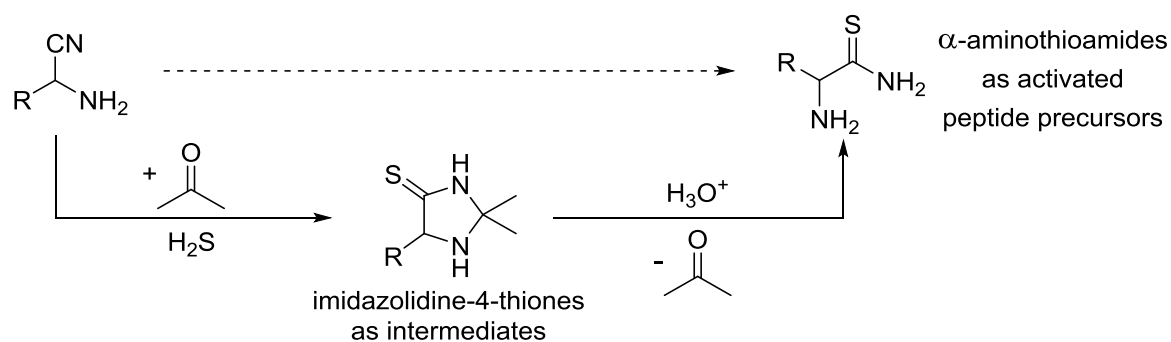
Scheme 2.14: Potential prebiotic relevance of imidazolidine-4-thiones as intermediates towards activated α-aminothioamides. The dashed arrow illustrates the inaccessible direct formation of α-aminothioamides.

In this way, the corresponding thioamides of nine proteinogenic amino acids were accessed.

3 Objectives

Despite numerous successes in finding plausible scenarios for the emergence of essential biomolecules under prebiotic conditions, the underlying pathways are rarely compatible. The connecting link between these building blocks of life could be provided by organocatalysis. With the advantages of broad applicability as well as water and oxygen tolerance, this concept would be a powerful tool in building up complexity while transferring chirality with only small amounts of catalysts. In contrast to the rapidly growing field of organocatalysis in modern chemistry, its transfer to the prebiotic context has barely been explored. So far, mainly amino acids were studied and the transformations were limited to aldol reactions.

Therefore, this thesis aims to extend this promising approach with regard to both prebiotically plausible catalysts and feasible functionalisations. In search for a suitable organocatalyst, the focus was not limited to current biomolecules. Even though they prevailed as the basis of life after four billion years of evolution, they are not necessarily its sole initiator. Further small organic structures might have preceded or coexisted, playing a crucial part in the transition from abiotic to biotic matter. Considering the available feedstock on the primitive Earth as well as the catalytic activity of secondary amines, imidazolidine-4-thiones were identified as promising candidates and thus designated as the foundation of this work (Figure 3.1).
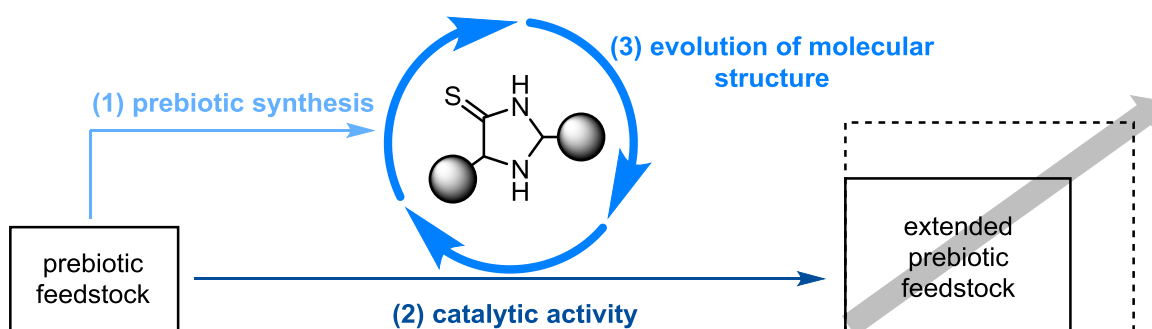
Figure 3.1: Introduction of imidazolidine-4-thiones as a prebiotically plausible class of organocatalysts to enable the emergence of complexity towards life. The intended aims to verify this theory are shown in blue.

In support of the objective of finding a prebiotically plausible organocatalytic system that enables increasing complexity towards the origin of life, the following points shall be addressed:

(1) For a plausible existence of imidazolidine-4-thiones on the early Earth, their formation shall not only depend on but also withstand prebiotic conditions. Thus, various structures shall be accessible by robust self-assembly out of a one-pot mixture. Starting from a broad pool of reactants, a selective preference for certain structural variants or isomers is to be examined.

(2) The synthesised imidazolidine-4-thiones shall be investigated for their catalytic activity. Preferably, the so far unfeasible (asymmetric) α-alkylation of small aldehydes shall be enabled under prebiotic conditions. Differences in the reactivity within the catalyst library are to be explored.

(3) In view of an ever-expanding reservoir of prebiotic molecules over time, a possible adaptation of the imidazolidine-4-thiones to their environment shall be investigated. In combination with a selective preference for certain structures, the dynamic variation of their own skeleton would take the process of evolution from the biological to the molecular level.

4 Results and Discussion

The choice of investigating imidazolidine-4-thiones as plausible and efficient prebiotic organocatalysts was based on various factors. As cyclic secondary amines, they possess the catalytic active site of prominent modern representatives and the possibility of introducing sterically demanding side-chains seemed to be advantageous for desired asymmetric catalysis. Further, structural similarities to the MacMillan imidazolidinone catalysts promised comparable versatile activity, especially with respect to transformations other than aldol reactions, which has already been demonstrated in a few examples for the thioamide *N*-methylated derivatives (see Section 2.5). The presence of two additional potential reactive centres in the pure imidazolidine-4-thione structure – the thioamide sulphur and nitrogen – could even extend its catalytic abilities. Moreover, the synthetic pathway to MacMillan imidazolidinones (and the sulphur analogues formed from them) is not conceivable in an early Earth scenario. Although starting from proteinogenic amino acids, the following amidation as well as acidic refluxing conditions or Lewis acids used for the crucial ring formation are not prebiotically plausible (Scheme 4.1).
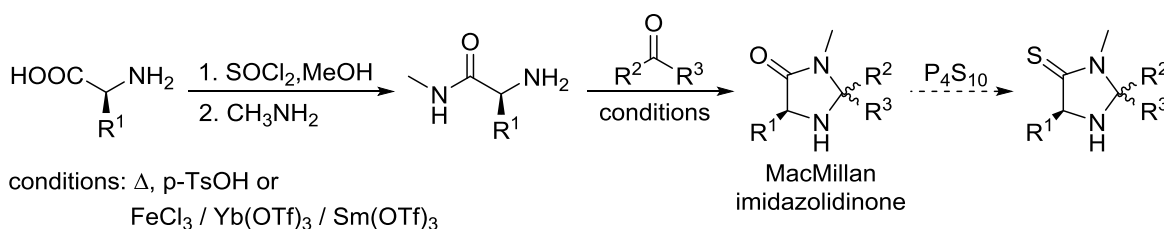
Scheme 4.1: Synthetic procedure for the MacMillan imidazolidinones and corresponding *S*-analoga.

On the contrary, introduction of the thioamide facilitates ring closure and enables a synthesis from simple building blocks (see Section 2.5).

To verify the plausible existence of imidazolidine-4-thiones on the early Earth, a broad variety should be synthesised under prebiotic conditions. This would further build up a foundation for subsequent investigations on their selective formation and catalytic activity.

4.1 Synthesis of Imidazolidine-4-thiones

As presented in Section 2.5, different routes towards imidazolidine-4-thiones **3** had been reported and this thesis was oriented towards the synthesis from α-aminonitriles **2** and ketones. The formation of α-aminonitriles **2** according to the first step of the Strecker reaction is highly plausible in a prebiotic scenario as the existence of all their building blocks – hydrogen cyanide, ammonia and aldehydes/ketones – is widely accepted. Also their hydrolysis products – α-amino acids – were detected in meteorites and experiments mimicking the early Earth.[18,28,34-36,42,191] In addition, only hydrogen sulphide is needed, which can be traced back to volcanic activity both on the Earth's surface and in hydrothermal vents.[23-24,26,192-193] In their procedure, PAVENTI and EDWARD observed an immediate precipitation of **3** after mixing the two reactants in the presence of hydrogen sulphide.[180]

4.1.1 Creation of an Imidazolidine-4-thione Library

To build up an imidazolidine-4-thione library of structural variants, various α-aminonitriles **2** were synthesised. The small aldehydes, acetaldehyde **1a**, propionaldehyde **1b**, butyraldehyde **1c** and isobutyraldehyde **1d**, as well as acetone **1f** were chosen because they were found on meteorites.[34-35] Benzaldehyde **1e** and butanone **1g** were added to allow a later investigation of the steric influence on the formation as well as catalytic activity and selectivity of the resulting imidazolidine-4-thiones. In an established two-phase procedure, the aldehydes and ketones **1a-g** were treated with potassium cyanide and ammonium chloride in a mixture of concentrated aqueous ammonia and tetrahydrofuran before being converted into the hydrochloride salts of the respective α-aminonitriles **2a-g** in overall yields between 35 and 58 % (Scheme 4.2).

2a-HCl: 29 % **2b-HCl**: 48 % **2c-HCl**: 35 % **2d-HCl**: 51 % **2e-HCl**: 44 % **2f-HCl**: 53 % **2g-HCl**: 58 %
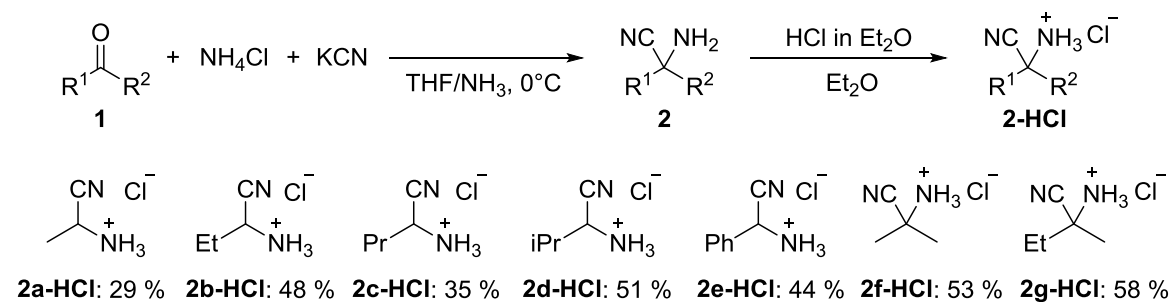
Scheme 4.2: Synthesis of α-aminonitriles **2**. The given yields refer to the isolated corresponding hydrochloride salts after precipitation with HCl in ether.

Next, the received α-aminonitriles had to be transformed into imidazolidine-4-thiones **3**. The reported procedure was slightly modified by reducing the time of hydrogen sulphide treatment and omitting ethanol as solvent, as both changes had no influence on the product yields but led to saving of resources and a reaction performance under completely prebiotic conditions. First, all α-aminonitriles **2a-g** were reacted with acetone **1f** and butanone **1g** in concentrated aqueous ammonia in the presence of hydrogen sulphide and potassium hydroxide (Scheme 4.3).
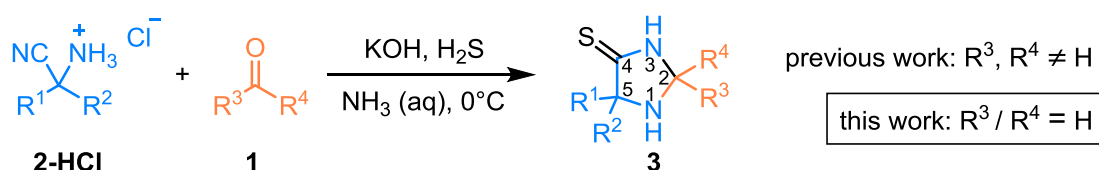
Scheme 4.3: Synthesis of imidazolidine-4-thiones **3**. In the product structure, atom numbering for the ring atoms is shown.

All corresponding imidazolidine-4-thiones **3** (R^3, $R^4 \neq H$) were successfully formed in good yields, reproducing the previous results as well as extending them in case of butanone. Up to this point, this transformation was claimed not feasible when exchanging the ketone with an aldehyde ($R^3 / R^4 = H$) based on their higher reactivity towards hydrogen sulphide leading to linear or cyclic polythianes.[170,173,180] This replacement, however, would not only increase the number of accessible imidazolidine-4-thiones **3** without extending the reactant feedstock but also include aldehydes as a prebiotically more abundant class of molecules. Further, one stereocentre and thus the chirality of **3** would be guaranteed. To investigate the claimed hypothesis, 2-cyanopropan-2-aminium chloride **2f** was reacted with propionaldehyde **1b** according to the above mentioned procedure. Surprisingly, the desired imidazolidine-4-thione **3fb** already started precipitating during hydrogen sulphide addition, leading to a final yield of 50 %. The reaction was applied to all combinations of α-aminonitriles **2a-g** and aldehydes **1a-e** forming various imidazolidine-4-thiones (including $R^3 / R^4 = H$) in yields of up to 76 %.[194] Thereby, even the smallest and most reactive aldehyde used, acetaldehyde **1a**, was inserted into the imidazolidine-4-thione skeleton resulting in an extensive library of a total number of 37 isolated structural variants (Table 4.1). Only the incorporation of benzaldehyde **1e** turned out to be more challenging (products not formed are displayed in grey). Whereas the corresponding aminonitrile **2e** at least successfully reacted with the ketones **1f** and **1g**, no imidazolidine-4-thione with a phenyl residue in ring position 2 (**3xe**) could be isolated or identified with

NMR spectroscopy. Only MS and HPLC-MS analysis of the reaction mixture indicated their formation.

Table 4.1: Library of synthesised imidazolidine-4-thiones **3** with corresponding isolated yields. Molecules depicted in grey could not be isolated nor detected with NMR spectroscopy. [a] no separation of **3fg** and **3gf** was achieved with column chromatography.

	2a	2b	2c	2d	2e	2f	2g
1a	3aa: 72 %	3ba: 65 %	3ca: 32 %	3da: 51 %	3ea: –	3fa: 59 %	3ga: 80 %
1b	3ab: 54 %	3bb: 76 %	3cb: 48 %	3db: 72 %	3eb: –	3fb: 50 %	3gb: 4 %
1c	3ac: 12 %	3bc: 32 %	3cc: 44 %	3dc: 48 %	3ec: –	3fc: 31 %	3gc: –
1d	3ad: 44 %	3bd: 20 %	3cd: 24 %	3dd: 32 %	3ed: –	3fd: 18 %	3gd: 12 %
1e	3ae: –	3be: –	3ce: –	3de: –	3ee: –	3fe: –	3ge: –
1f	3af: 24 %	3bf: 28 %	3cf: 37 %	3df: 43 %	3ef: 83 %	3ff: 50 %	3gf: [a]
1g	3ag: 3 %	3bg: 55 %	3cg: 70 %	3dg: 65 %	3eg: 43 %	3fg: [a]	3gg: 71 %

In any reaction, in which the secondary aminonitriles **2f** and **2g** were employed, also the imidazolidine-4-thiones with the corresponding residues in ring position 2 (**3ff**, **3gg**) were observed. Since **1f** and **1g** were not added, they must have formed in-situ through reversible formation of the aminonitrile (for more details on this phenomenon see Section 4.2.1). While these side-products could be easily separated with column chromatography, the reaction of **2f** with **1g** also yielded the oppositely substituted **3gf**, which could not be separated from the desired **3fg**. The same observation was made for the reaction of **2g** and **1f** and thus neither **3gf** nor **3fg** were isolated purely. Finally, structures with sterically demanding side-chains were formed with diastereomeric ratios of up to 75:25 (**3dd**) with an excess for the *trans*-isomer. This was attributed to less steric hindering of the residues in ring position 2 and 5 compared to the *cis*-isomer as the ratio increased with increased alkyl chain length or branching.

This simple two-step procedure only needs aldehydes or ketones as organic feedstock, a cyanide and ammonia source as well as hydrogen sulphide and is performed in aqueous solution at 0 °C. Thus, all reaction components and conditions are compatible with the environment of the early Earth, which makes the existence of imidazolidine-4-thiones **3** highly probable.

4.1.2 One-Pot Synthesis of Imidazolidine-4-thiones

Since both reaction steps for the imidazolidine-4-thione formation can be performed in concentrated aqueous ammonia at 0 °C and involve the same class of organic reactants, the intuitive idea was to reduce them to an even more realistic one-pot synthesis. Aside from short-term or seasonal variations and concentration gradients, the prebiotic feedstock and environment is most likely not changing in between reaction steps. Thus, a plausible formation scenario should be robust in the presence of all influencing reactants and exclude the need for sequential additions or removals. The intermediate step of α-aminonitrile precipitation as hydrochloride salts can be omitted as it only provides higher stability for storage reasons. To simplify the analysis of the expected complex product mixture, the carbonyl compound was initially reacted with only one of the two reactants – KCN and H_2S. The choice fell on eliminating KCN, as leaving out H_2S would only result in the mixture of aminonitrile formation.

Reaction of Aldehydes with H₂S in Ammonia

In a first approach, acetaldehyde **1a**, propionaldehyde **1b** and isobutyraldehyde **1d** were each reacted with hydrogen sulphide in concentrated aqueous ammonia. Instead of a complex reaction mixture, GC-MS analysis and NMR spectroscopy revealed the selective formation of the triethylated dithiazinanes **4a** and **4b** in the case of **1a** and **1b**. As by-products only small amounts of dialkylated trithiolane **6a**, **6b** and propenylpropanimine **5b** in the case of propionaldehyde were detected (Scheme 4.4).
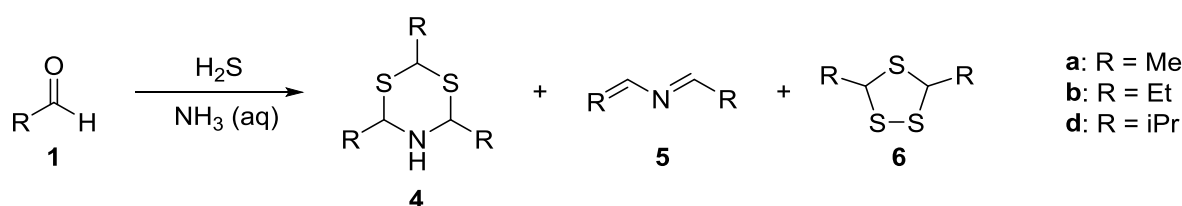
Scheme 4.4: Products detected with GC-MS in the reaction of aldehydes **1** with hydrogen sulphide in concentrated aqueous ammonia after 20 h.

The lack of formation of **5a** can be justified by the low stabilisation of this structure compared to **5b**. This assumption is strengthened by the fact that in the reaction of isobutyraldehyde **1d**, the even better stabilised analogue **5d** is the major product after 24 h, accompanied by **4d** and minor amounts of **6d**. Trialkylated dithiazinanes **4** are nowadays used as additives in food chemistry due to their characteristic odors (e.g. onion and bacon) and are naturally formed from degradation of sulphur-containing amino acids.[195-196] As mentioned above, it was postulated that the formation of imidazolidine-4-thiones from α-aminonitriles and aldehydes was not possible and attributed to a competitive, faster reaction of the latter with H₂S. Here, this exact transformation occurs. Therefore, to gain a better understanding of the reaction course and rate, the conversion of propionaldehyde with H₂S in ammonia was studied by mass spectrometry at different time intervals (Figure 4.1). The formation of dithiazinane **4b** (m/z 206.1032) and propenylpropanimine **5b** (m/z 98.0967) was already seen immediately after the start of the reaction. Additionally, propanimine **7b** (m/z 58.0651), the intermediate **8b** (m/z 132.0841), and the triethylated thiadiazinane **9b** (m/z 189.1416) were present. The latter almost completely disappeared within the first hour, whereas the peak of **4b** clearly gained in intensity and is the only clear signal after 2 h. Accordingly, thiadiazinane **9b** represents the kinetic product and dithiazinane **4b** the thermodynamic product. Trithiolane **6b** or other heterocycles containing only sulphur cannot be detected via ESI-MS due to their

poor ionisation and their presence can thus not be ruled out. The gas chromatogram after 20 h, however, indicates that they only remain in minor amounts at the end of the reaction.
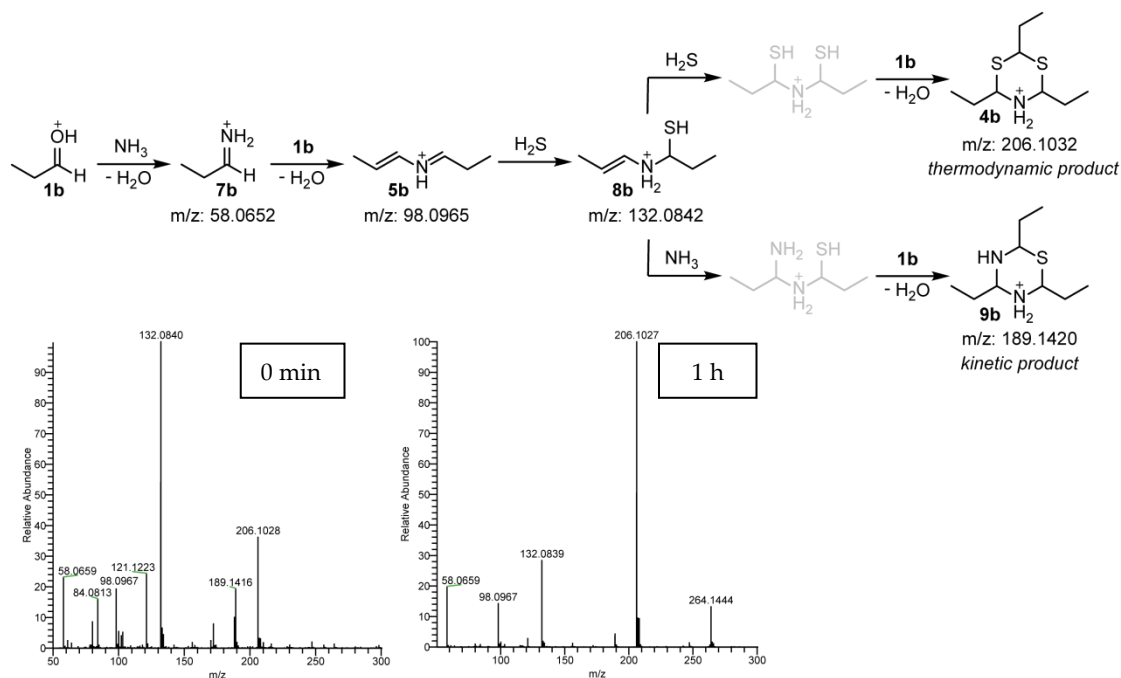
Figure 4.1: Reaction of propionaldehyde **1b** with H$_2$S in concentrated aqueous ammonia. Top: reaction pathway derived from structures observed with HR-MS. Experiments indicated reaction equilibria for all reaction steps, but the corresponding arrows were omitted for clarity. Molecules depicted in grey were not found but added as plausible intermediates. Bottom: exemplary HR mass spectra of the samples taken directly after mixing the reactants (left) and after 1 h (right). Peaks at m/z 84.0813 and 121.1223 were also detected in the blank measurements and thus not part of the samples.

Finally, the experiment was repeated with equimolar amounts of **1a** and **1b** to account for the expected simultaneous presence of multiple aldehydes on the early Earth. GC analysis revealed that all possible structural variants of **4** were formed in a statistical distribution without any selectivity for a single species (Figure 4.2).
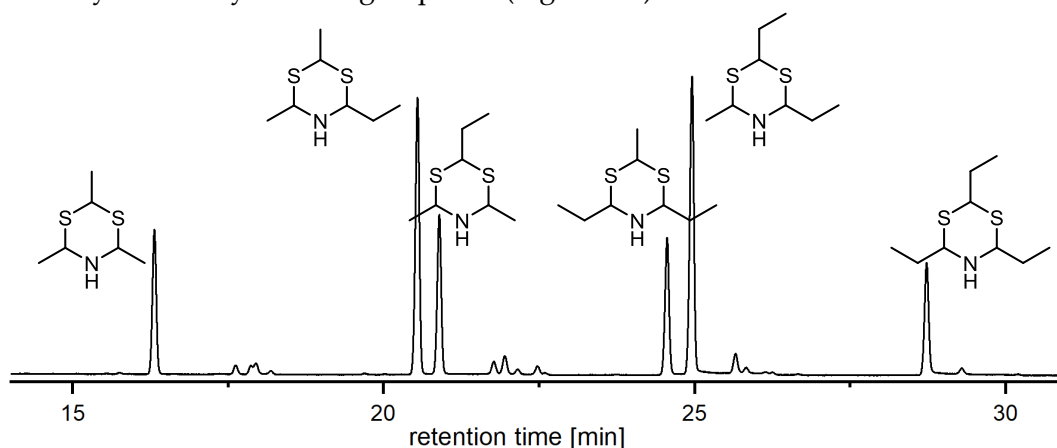
Figure 4.2: Gas chromatogram of the product mixture formed in the reaction of equimolar amounts of acetaldehyde **1a** and propionaldehyde **1b** with H$_2$S in concentrated aqueous ammonia. Peak assignment to the six differently substituted dithiazinanes was possible due to characteristic EI-MS-fragmentation.

The limited number of compounds formed in this procedure motivated the assumption of a manageable analysis also for the full one-pot mixture of carbonyl compound, KCN, H_2S and NH_3.

One-Pot Reaction of Aldehyde, KCN and H_2S in Ammonia

In a first attempt, propionaldehyde **1b** was mixed equimolar with all reagents of the two-step procedure - KCN, NH_4Cl, KOH - in concentrated aqueous ammonia before H_2S was added at 0 °C. As expected, initial experiments showed that the addition of ammonium chloride and potassium hydroxide could be omitted, reducing the investigated mixture to **1b**, KCN, and H_2S in ammonia (Scheme 4.5, A).
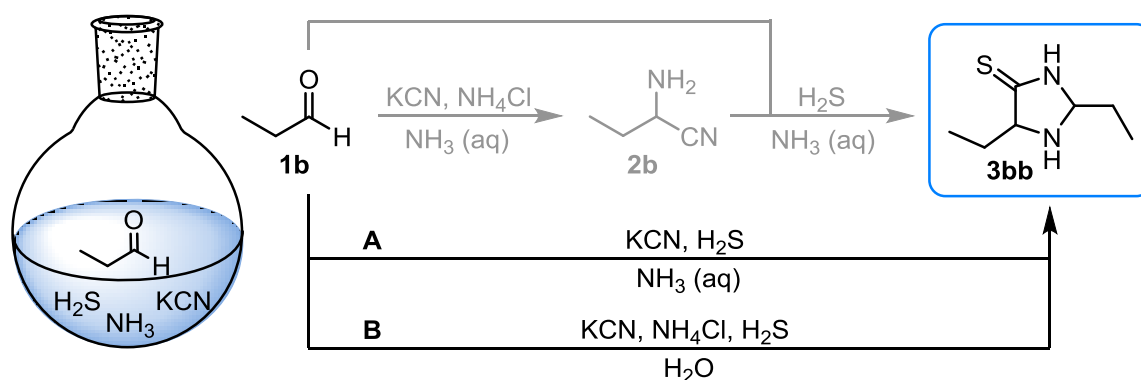
Scheme 4.5: One-pot synthesis of imidazolidine-4-thione **3bb**. **A**: Reaction of an equimolar mixture of propionaldehyde **1b** and potassium cyanide in concentrated aqueous ammonia in the presence of hydrogen sulphide. **B**: Reaction of an equimolar mixture of propionaldehyde **1b**, potassium cyanide, and ammonium chloride in water in the presence of hydrogen sulphide.

After 24 h, imidazolidine-4-thione 3bb was isolated in 6 % yield. In expectation of a complex mixture of by-products, mass spectrometry was chosen as the appropriate method for direct and comprehensive qualitative analysis. Samples were taken after distinct time periods, diluted with acetonitrile and directly injected into the mass spectrometer (Figure 4.3).

Already the first sample, taken after 30 min, showed formation of the desired imidazolidine-4-thione **3bb** (*m/z* 159.0950), which was further observed in all following samples. Also, the amidine **10b** (*m/z* 102.1029) and thioamide **11b** (*m/z* 119.0640) were detected throughout the experiment. The initially most prominent peak (*m/z* 206.1031) can be assigned to the previously observed triethylated dithiazinane **4b**. Its presence, however, decreased over the course of the reaction until it completely disappeared after 4 h. Thus, the above hypothesis of a competing faster reaction of the aldehyde with H_2S

can be partially confirmed, as it occurs in the beginning but does not prevent the ultimate formation of imidazolidine-4-thiones **3**. In a similar manner, the initially detected nitrogen analogue imidazolidine-4-imine **12b** (*m/z* 142.1338) is consumed after 24 h.
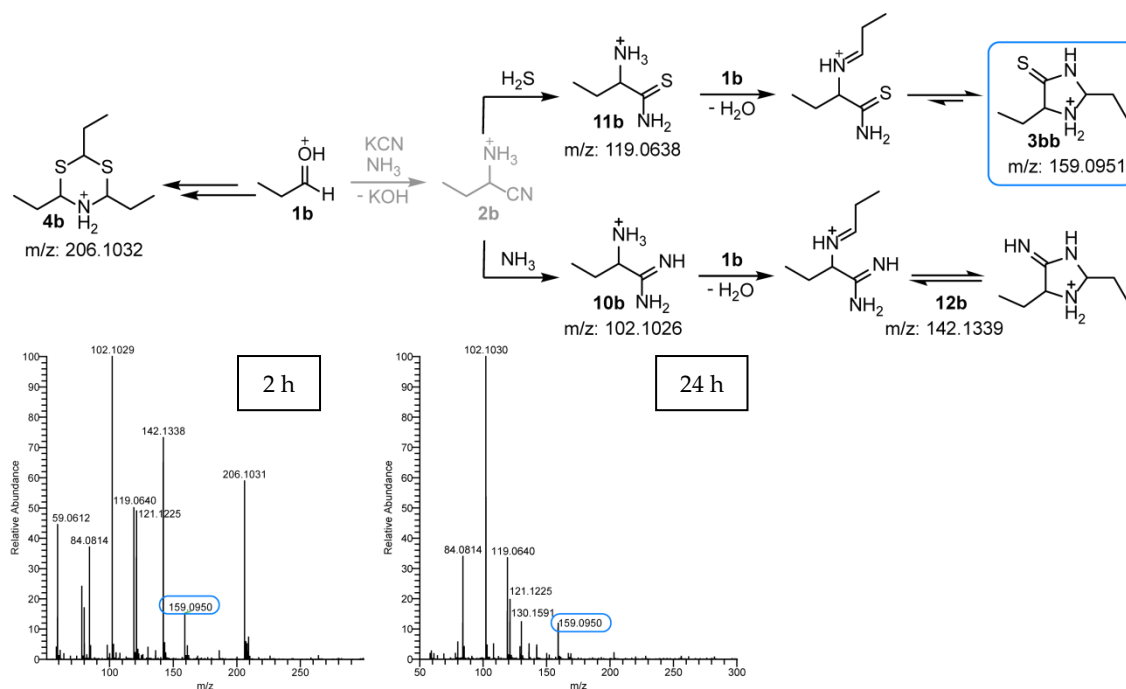
Figure 4.3: One-pot reaction of propionaldehyde **1b** with KCN, NH₄Cl and H₂S in concentrated aqueous ammonia. Top: reaction pathway derived from structures observed with HR-MS. Experiments indicated reaction equilibria for all reaction steps, but the corresponding arrows were omitted for clarity. Molecules depicted in grey were not found but added as plausible intermediates. Bottom: exemplary HR mass spectra of the samples taken after 2 h (left) and 24 h (right). The peaks that refer to the desired imidazolidine-4-thione **3bb** are framed in blue. Peaks at *m/z* 84.0814 and 121.1225 were also detected in the blank measurements and thus not part of the samples.

Using acetone **1f** as carbonyl compound instead of aldehyde **1b** also gave the respective imidazolidine-4-thione **3ff** after 24 h. However, the formation was much slower and not observed within the first 4 h. Further, detected side-products were limited to the nitrogen analogous imidazolidine-4-imine **12f**.

To further study the reagent's influences on imidazolidine-4-thione formation, the reactions of both propionaldehyde **1b** and acetone **1f** were transferred to pure water – along with the addition of ammonium chloride – and the ratios of reactants were varied. In all experiments, formation of the respective imidazolidine-4-thione was observed, proving its robustness against various changes in the environment. Only the nature and distribution of by-products differed. When performing the reaction of **1b** with KCN, H₂S, and NH₄Cl in water, the proportion of dithiazinane **4b** decreased and nitrogen rich

structures **10b** and **12b** were not detected at all, due to the reduced amount of ammonia present (Figure 4.4).
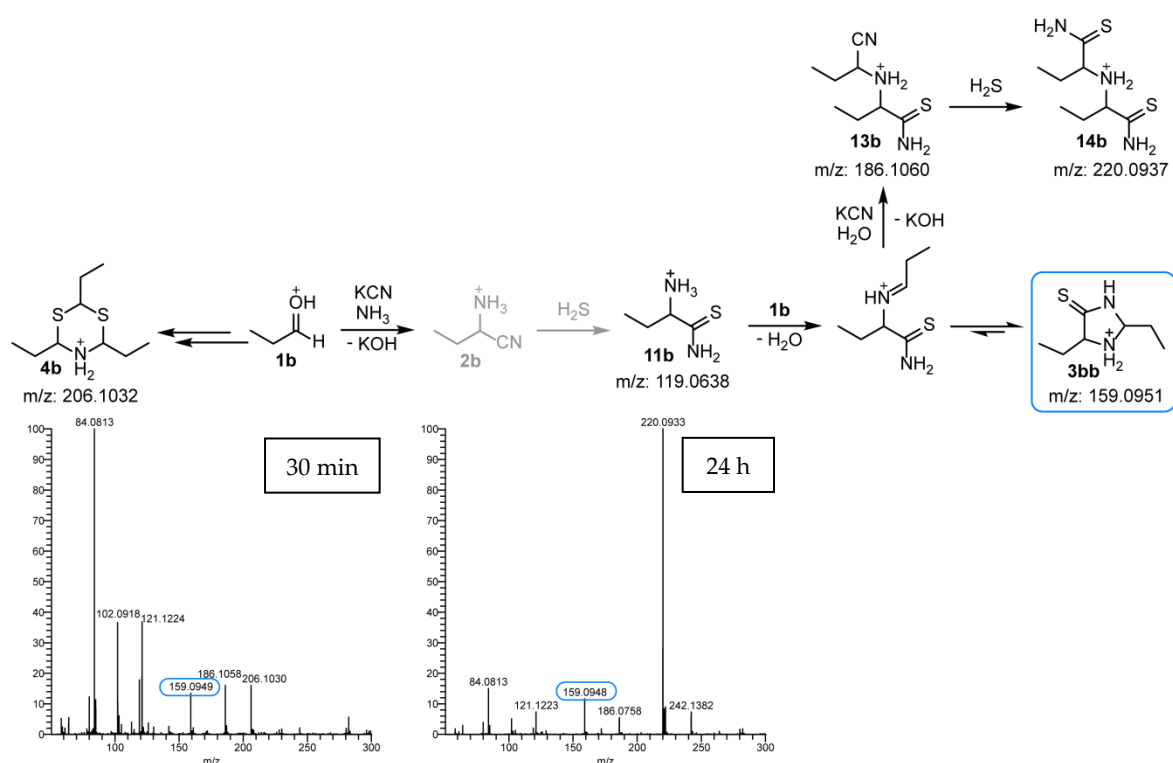
Figure 4.4: One-pot reaction of propionaldehyde **1b** with KCN, NH₄Cl and H₂S in water. Top: reaction pathway derived from structures observed with HR-MS. Experiments indicated reaction equilibria for all reaction steps, but the appropriate arrows were omitted for clarity. Molecules depicted in grey were not found but added as plausible intermediates. Bottom: exemplary HR mass spectra of the samples taken after 30 min (left) and 24 h (right). The peaks that refer to the desired imidazolidine-4-thione **3bb** are framed in blue. Peaks at *m/z* 84.0813, 102.0918, and 121.1224 were also detected in the blank measurements and thus not part of the samples.

Instead, dithioamide **14b** (*m/z* 220.0933) and its precursor **13b** (*m/z* 186.1058) are formed as main by-products. The former can be assigned to the highest peak after 24 h and precipitates out of the reaction solution after several days. Smaller quantities of **13b** and **14b** were also discovered in later samples of the respective reaction in ammonia. For the reaction of acetone in water, **13f** and minor amounts of **14f** were the only observed compounds besides the imidazolidine-4-thione **3ff**. Comparing the two reaction media, water led to less by-products and a more selective formation of the imidazolidine-4-thione. This was also seen based on a 19 % isolated yield of **3bb** in water compared to 6 % in ammonia (the yield of the two-step procedure was 76 %). Applying different ratios of carbonyl to KCN to ammonia had the following effects: 1) higher amounts of ammonia led to an expected favourable formation of nitrogen rich compounds **10** and **12** and 2) an excess of aldehyde led to a predominance of dithiazinanes **4**.

4.1.3 Overview of Intermediates and Side-products

Summarising the previous analyses, the one pot approach gives rise to the following reaction network of intermediates and side-products (Scheme 4.6). Reacting equimolar amounts of carbonyl **1**, ammonium chloride**,** and potassium cyanide with hydrogen sulphide in water favoured the selective formation of imidazolidine-4-thiones **3** (blue). If a ketone is applied under these conditions, only **13** and **14** were detected as additional products (purple). For aldehydes, the competing but reversible pathways framed in yellow dominate the initial phase. Increasing the amount of ammonia increased the presence of the nitrogen analogous **10** and **12** for both aldehydes and ketones (red).
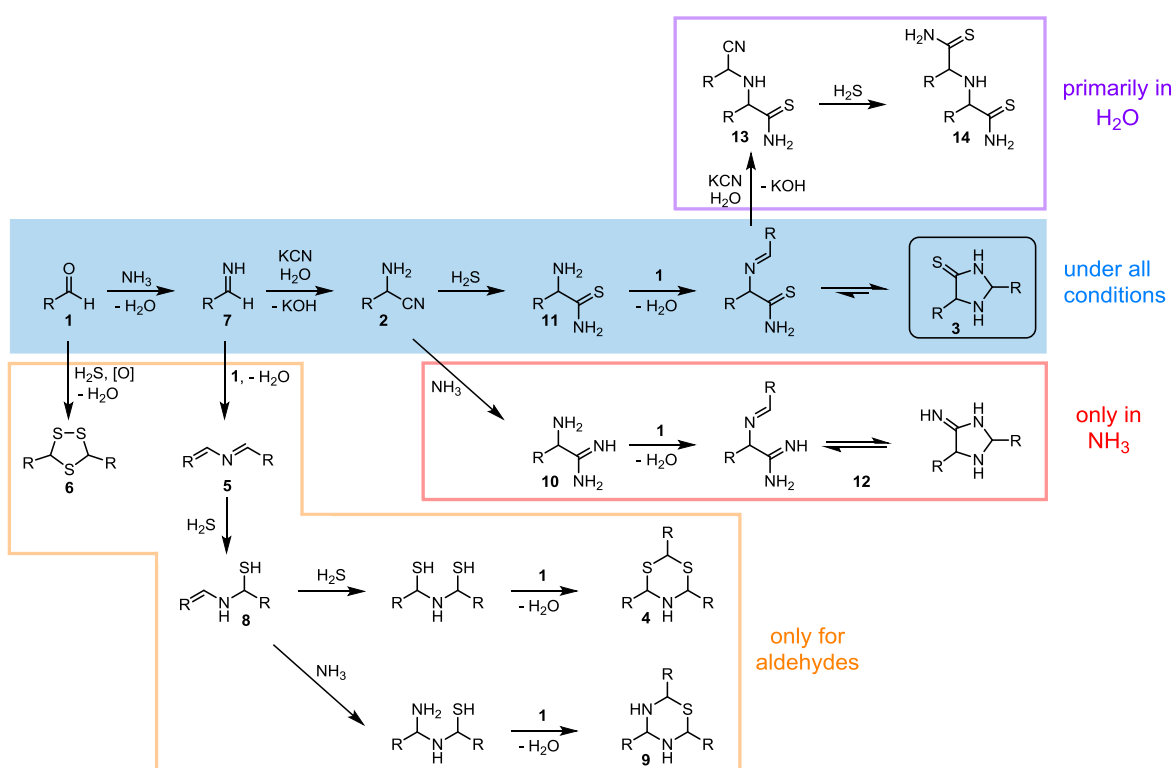
Scheme 4.6: Overview of the reaction network forming in the one-pot reaction of a carbonyl compound with hydrogen sulphide, a cyanide, and an ammonia source in aqueous media.

Nevertheless, imidazolidine-4-thiones were obtained in all experiments involving an aldehyde or ketone, KCN, H₂S, and a source of ammonia in different reactant ratios. Considering the highly plausible existence of all these simple compounds on an early Earth, especially in any location of volcanic activity, the continuous self-assembly of imidazolidine-4-thiones is not only possible but very likely.

4.2 Dynamics of Imidazolidine-4-thione Formation

The presented studies on the synthesis of imidazolidine-4-thiones **3** revealed various competing side-reactions that were based on reversible equilibria. But also the synthetic pathway to imidazolidine-4-thiones themselves turned out to be highly dynamic.

4.2.1 Susceptible Aminonitrile Equilibrium

During the second step of the directed two-step procedure to imidazolidine-4-thiones **3** in ammonia, in some cases not only the expected product (blue-orange), but also the inverse (orange-blue) and both symmetrically substituted structures (blue-blue, orange-orange) were obtained (Figure 4.5) in different ratios.[194]
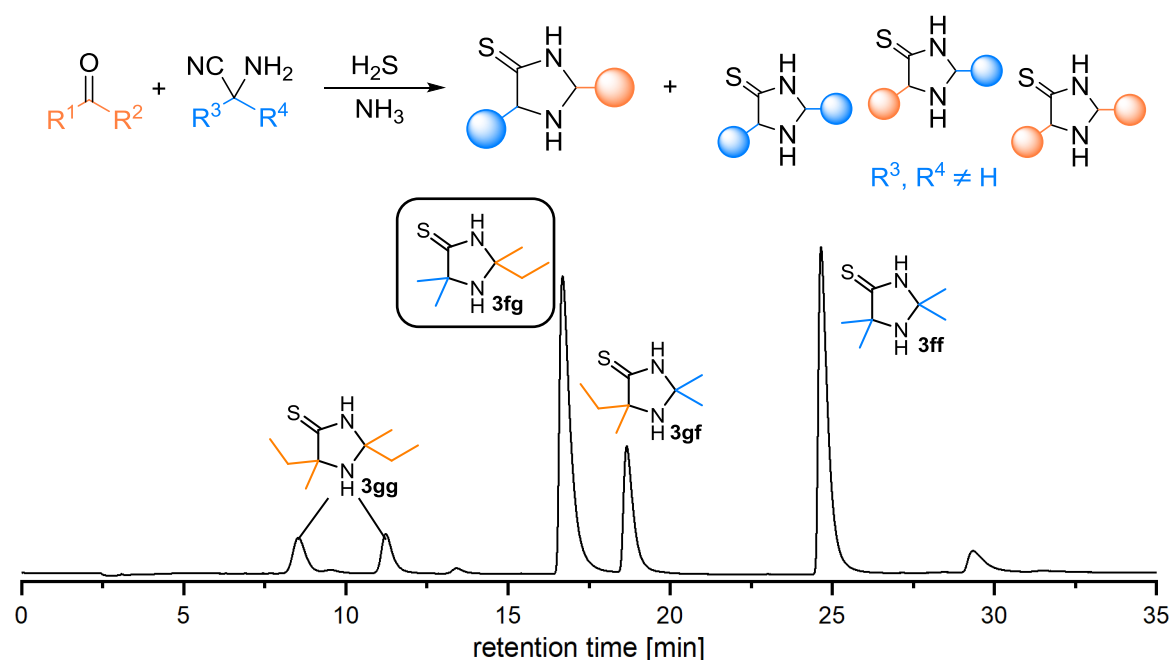
Figure 4.5: Expected imidazolidine-4-thione **3** as well as inverse and symmetrically substituted molecules detected in the reaction of secondary aminonitriles with aldehydes or ketones in concentrated aqueous ammonia. Top: schematic overview. Bottom: HPLC chromatogram of the products formed from the reaction of **2f** with **1g**; the expected imidazolidine-4-thione **3fg** is framed.

This phenomenon was already observed when applying the α-aminonitrile of acetone[180] and it was now confirmed that it only occurs for secondary α-aminonitriles. The behaviour can be explained by a lower stability of the latter under the prevailing conditions leading to partial decomposition into its building blocks. The resulting ketone can now also act as the carbonyl substrate (blue side-chain at ring position 2) and the released cyanide can be intercepted by the initial carbonyl compound to form the respective α-aminonitrile reactant (orange side-chain at ring position 5). The final product composition was always dominated by the imidazolidine-4-thiones arising from the

applied aminonitrile. This supports the mentioned mechanism and indicates that as soon as the heterocycle is formed, no significant amount of back-reaction occurs that would result in an equal product distribution predetermined by thermodynamics and independent of using the reactant as carbonyl or aminonitrile building block.

4.2.2 Carbonyl Exchange at Ring Position 2

In contrast to the high stability of imidazolidine-4-thiones **3** in ammonia, the skeleton appeared to be highly dynamic in water. Stirring any variant of **3** in the presence of additional carbonyl compounds, the side-chain at ring position 2 was partially exchanged, releasing the initial carbonyl moiety and replacing it with those in solution (Figure 4.6).
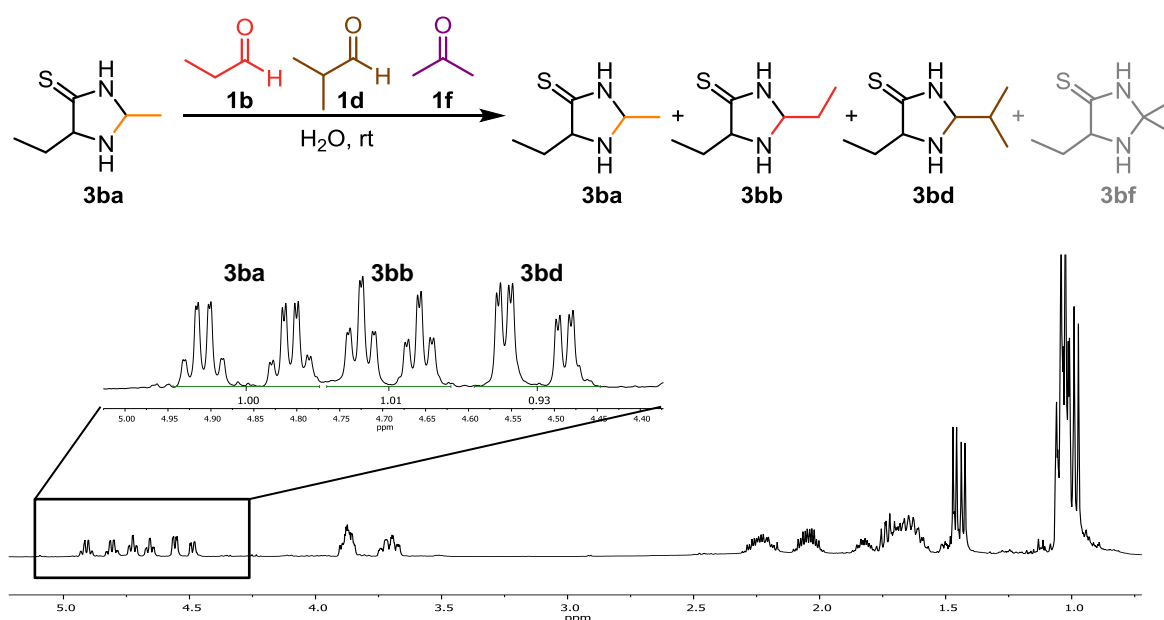
Figure 4.6: Dynamic exchange of the carbonyl residue at ring position 2 of imidazolidine-4-thiones **3** in water. ^{1}H-NMR spectrum of the product mixture that results from stirring an equimolar mixture of **3ba** and carbonyls **1b**, **1d**, and **1f**. Outlined on the left is the enlarged area of the respective protons at ring position 2 to illustrate the 1:1:1 product ratio. **3bf**, depicted in grey, is not formed.

However, there was one important exception: acetone **1f** was released but never inserted into the imidazolidine-4-thione structure. Over time, the dimethyl substituent of acetone could thus be replaced by a single alkyl residue of an aldehyde, which creates a chiral centre and ensures the chirality of the catalyst regardless of its remaining structure.

To further determine the required conditions for this dynamic behaviour, the influence of the pH was studied between pH 7.0 and 12.0. Under aqueous reaction conditions carbonyl exchange was observed up to pH 10.0. In more alkaline ranges as well as in acetonitrile, the heterocycle was stable. In all cases of exchange, the product distribution resembled the

equimolar ratio of the reactant mixture of imidazolidine-4-thione and carbonyls (Figure 4.6). Increasing the amount of carbonyl compound also raised the amount of its incorporation to the same extent. No variation at ring position 5 or other side-products that would indicate further decomposition were observed by NMR spectroscopic analysis. The imidazolidine-4-thione **3** is hydrolysed to the respective α-aminothioamide **11**, followed by immediate condensation with a different carbonyl compound **1** and cyclisation.

As presented in Section 2.5, an irreversible hydrolysis of imidazolidine-4-thiones **3** has been observed with strongly acidic reagents, a reversible interconversion under mild and aqueous conditions, however, was unknown so far. It is exactly the latter dynamic behaviour that would be a powerful property in the context of the early Earth. In this environment, a constant simultaneous presence of various reactants cannot be guaranteed over a long period of time or spatial distance. Thus, a temporary drying up of only one of the sources would stop the ongoing production. With this exchange mechanism, imidazolidine-4-thiones could adapt to temporal, local or evolutionary changes in the carbonyl pool by incorporating the present substrates even in the absence of ammonia, cyanide and hydrogen sulphide. Moreover, the absence of acetone insertion provides a powerful mode of selection towards chiral molecules.

4.3 Selectivity of Imidazolidine-4-thione Formation

Motivated by the observed preferences in the formation of imidazolidine-4-thiones **3** for the *trans*-isomers (see Section 4.1.1) as well as the absence of acetone **1f** incorporation via the dynamic carbonyl exchange (see Section 4.2.2), the formation selectivity was studied in detail. On the early Earth the simultaneous existence of multiple aldehydes and ketones is highly likely so that the investigation of mixtures thereof represents a more realistic scenario and a preference for distinct species would allow for their enrichment in the broad prebiotic pool. Considering the continuous increase of available molecules, this could reduce complexity and build the foundation of directed natural evolution. As the first step towards imidazolidine-4-thiones **3** is the conversion of carbonyls **1** into α-aminonitriles **2** – regardless whether performed explicitly or in-situ – a first approach focused on the selectivity of their formation.

4.3.1 Selectivity of Aminonitrile Formation

First, a suitable analytical method had to be found to separate all potentially forming α-aminonitriles **2**.

Analytics of α-aminonitriles

For common UV- or fluorescence-detection in HPLC, the analytes have to contain a chromophore. As only the aromatic residue of **2e** fulfils this requirement, derivatization prior to the analysis is necessary. One of the few known procedures of converting an amine into a detectable compound is its reaction with *o*-phthalaldehyde (OPA) and 3-mercaptopropionic acid as thiol to form isoindol-derivatives. However, this method only led to multiple peaks resulting from the instability of the OPA-reagent that could not be assigned to the aminonitrile. This behaviour is reported in literature and makes sensitivity and reproducibility difficult.[197] A promising alternative was offered by capillary electrophoresis (CE) that detects the analytes' conductivity after being separated according to their ionic mobility. Due to the missing pK_a values of the aminonitriles, a suitable buffer system to guarantee ionic state as well as separation had to be found by trial and error. The use of 2 M acetic acid provided the most intense peaks and enabled the separation of all species as long as they differed in number of carbon atoms.

Mixture of α-aminonitriles

Due to insufficient separation of all possible aminonitriles, different combinations of aldehydes and ketones were reacted with an undersupply of KCN and NH_4Cl. After precipitation as HCl-salts, the resulting mixtures were analysed with CE (Figure 4.7).
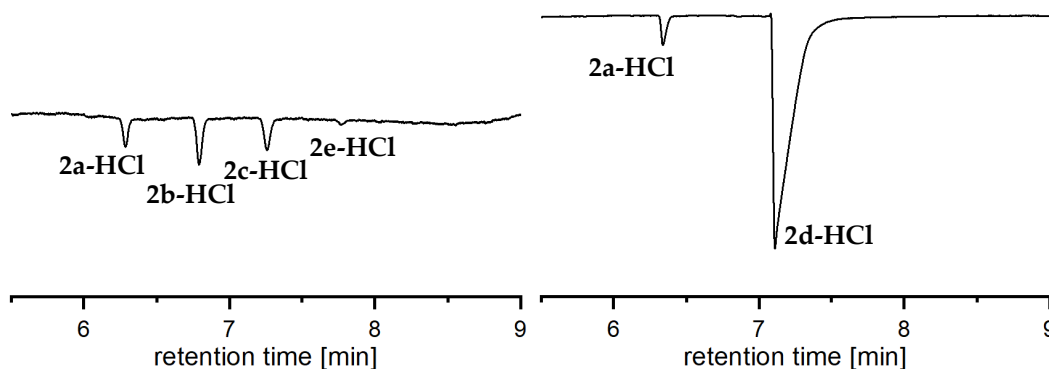
Figure 4.7: CE electropherograms of the HCl-salts of α-aminonitriles **2** forming from a mixture of aldehydes and ketones **1**. Left: products formed from a mixture of acetaldehyde **1a**, propionaldehyde **1b**, butyraldehyde **1c**, and benzaldehyde **1e**. Right: products formed from a mixture of acetaldehyde **1a**, isobutyraldehyde **1d**, and acetone **1f** (not detected).

Despite the lack of easy quantification, following qualitative conclusions were drawn:

1) the aminonitrile of benzaldehyde **2e** is hardly formed out of any carbonyl mixture,

2) all linear aldehydes are converted without significant preference for one species, but

3) aminonitrile **2d** resulting from the branched isobutyraldehyde is formed with high selectivity and completely prevents the conversion of acetone **1f** into **2f**.

The last hypothesis was additionally confirmed by analysing a simplified mixture of acetaldehyde **1a**, isobutyraldehyde **1d** and acetone **1f** that enabled peak separation in ¹H NMR spectra and thus quantification (Figure 4.8).
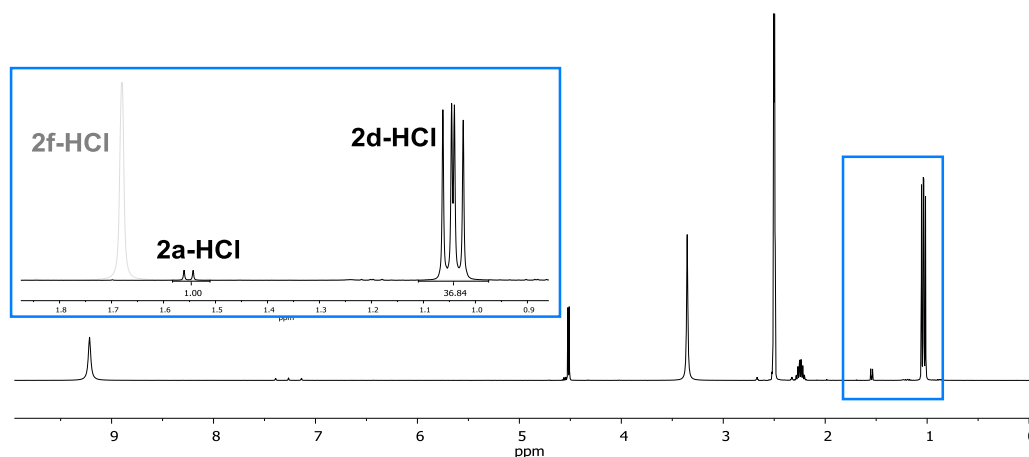
Figure 4.8: ¹H-NMR spectrum in DMSO-d_6 of aminonitriles resulting from the mixture of acetaldehyde **1a**, isobutyraldehyde **1d**, and acetone **1f**. Outlined in blue is an enlarged area to illustrate the ratio of the CH_3 group(s) of **2a-HCl** and **2d-HCl** as well as the missing CH_3 signal of **2f-HCl** superimposed in grey.

After precipitation as HCl-salts, a product ratio of 1:19:0 between **2a-HCl:2d-HCl:2f-HCl** was detected.

4.3.2 Selectivity of Imidazolidine-4-thione Formation

The number of potentially forming imidazolidine-4-thiones **3** out of a carbonyl mixture is higher than for the aminonitriles **2**, as every reactant can be incorporated at both 2- and 5-position of the heterocycle. The simplified mixture of **1a**, **1d**, and **1f** could already result in nine different species of **3**, which were not separable by NMR spectroscopy. Therefore, another method of analysis with sufficient separation had to be found which, at best, does not require additional steps of derivatisation to omit further influences on the product distribution.

Analytics of imidazolidine-4-thiones

Analysis with HPLC provides various parameters to adjust for peak separation as well as the possibility of direct relative quantification. Coupling to mass spectrometry (MS) further facilitates molecule identification. The C-S double bond of the imidazolidine-4-thiones **3** showed an absorption maximum at 270 nm which not only made derivatisation unnecessary but also differentiated from the absorbance of side-products. Initial screening of conditions for the separation of reference compounds showed that modifications in ring position 2 (resulting from one aminonitrile and several carbonyl compounds) led to bigger differences in retention time than in ring position 5 (resulting from several aminonitriles and one carbonyl). For each carbonyl **1**, a different gradient elution of *n*-hexane/isopropanol was developed to successfully achieve baseline separation.

One aminonitrile, several carbonyls

To reduce the complexity of the arising imidazolidine-4-thione mixture, the selectivity was first studied by starting at the stage of α-aminonitriles **2**. As better separation was obtained for the combinations resulting from one aminonitrile and several carbonyl compounds, and the selectivity of α-aminonitrile **2** formation was already studied separately, this set of reactants was chosen. Each aminonitrile **2a-g** was reacted with all aldehydes **1a-e** and hydrogen sulphide in ammonia for 24 h, followed by the usual extraction work-up and direct analysis with HPLC-MS without further purification. In a second approach, the same experiments were repeated with adding the ketones **1f-g**. In every case, all possible structural variants of imidazolidine-4-thiones **3** were formed.
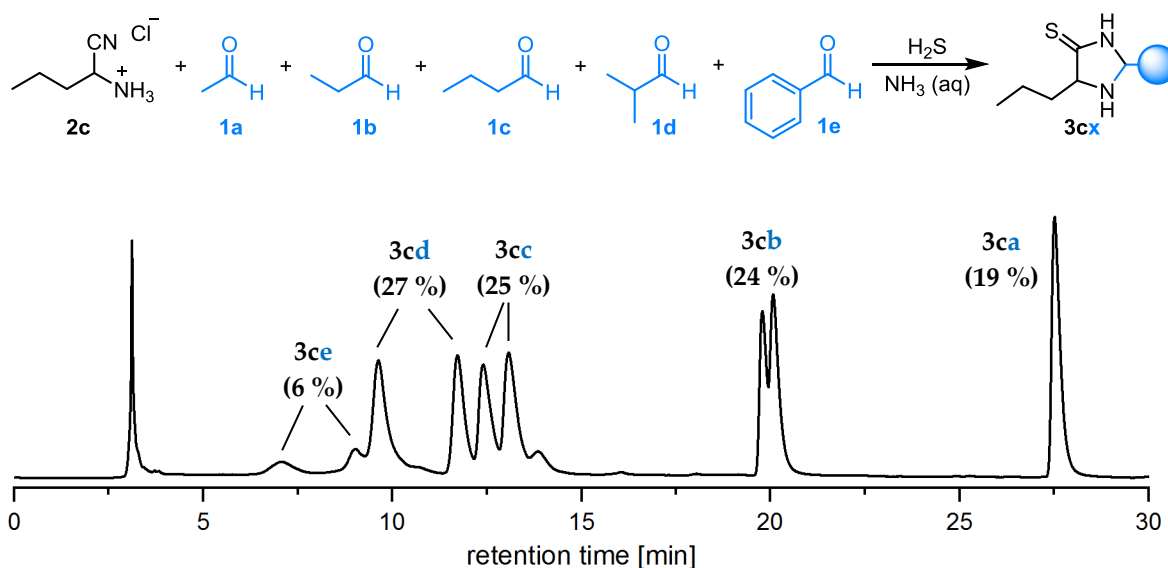
Figure 4.9: Selectivity of the reaction of **2c** with an equimolar mixture of aldehydes **1a-e**. HPLC separation and relative ratio of the imidazolidine-4-thiones **3** in the product mixture determined by peak integration.

Regarding a selective preference for certain carbonyls, the following statements were made: For all aminonitriles, the reaction with benzaldehyde **1e** hardly occurred, which is consistent with the unsuccessful attempts of synthesising each of the respective imidazolidine-4-thiones **3xe** (see Section 4.1.1). For the primary α-aminonitriles **2a-e**, the distribution of the product mixture was rather uniform, and no expected preferential incorporation of the more reactive smaller aldehydes was observed (Figure 4.9). On the contrary, for the smaller primary aminonitriles the combination with **1a** or **1b** was less favoured than with the larger **1c** or **1d**. For the larger aminonitriles, a small preference for the reaction with ketones could be derived.
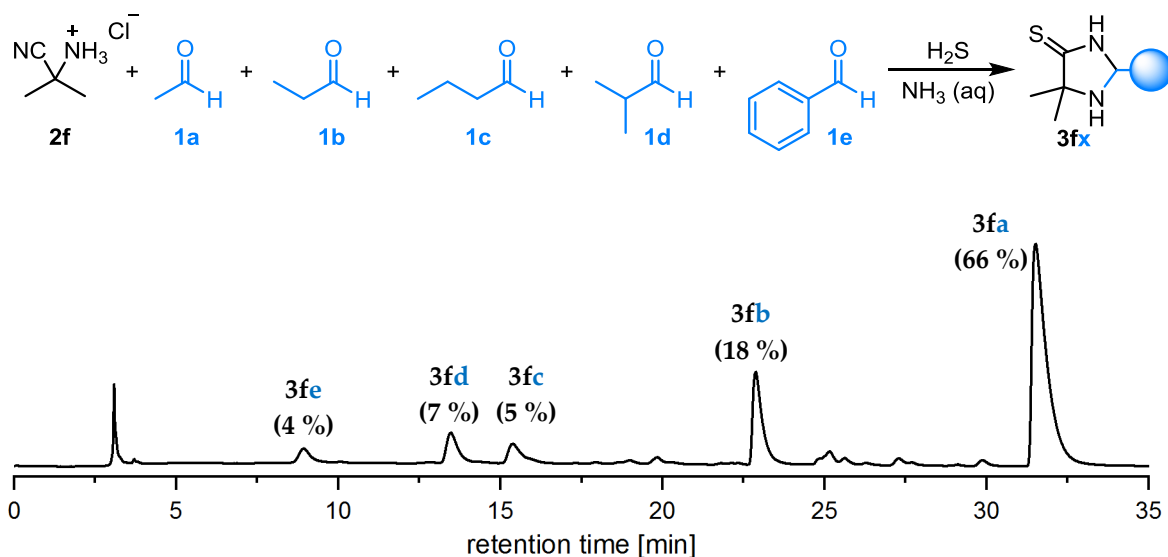
Figure 4.10: Selectivity of the reaction of **2f** with an equimolar mixture of aldehydes **1a-e**. HPLC separation and relative ratio of the imidazolidine-4-thiones **3** in the product mixture determined by peak integration.

When applying the secondary α-aminonitriles **2f** and **2g**, however, a significant selectivity was obtained. For both aminonitriles, with or without the addition of ketones, the combination with acetaldehyde **1a** was strongly favoured (Figure 4.10).

Several aminonitriles, one carbonyl

Next, the reactant mixture was reversed to study the incorporation selectivity of one aminonitrile over the other. Acetaldehyde **1a** and acetone **1f** were each reacted with several primary α-aminonitriles **2a,b,d** and hydrogen sulphide in concentrated aqueous ammonia for 24 h, followed by the usual extraction work-up and direct analysis with HPLC-MS without further purification. Here, the aminonitrile of butyraldehyde **2c** and benzaldehyde **2e** were left out due to the resulting insufficient HPLC separation. In a second approach, the same experiments were repeated with the addition of the secondary aminonitrile of acetone **2f**. The primary aminonitriles were represented in the product imidazolidine-4-thione mixture according to their size with a decreasing proportion from larger to smaller residues (Figure 4.11, **3da** > **3ba** > **3aa**).
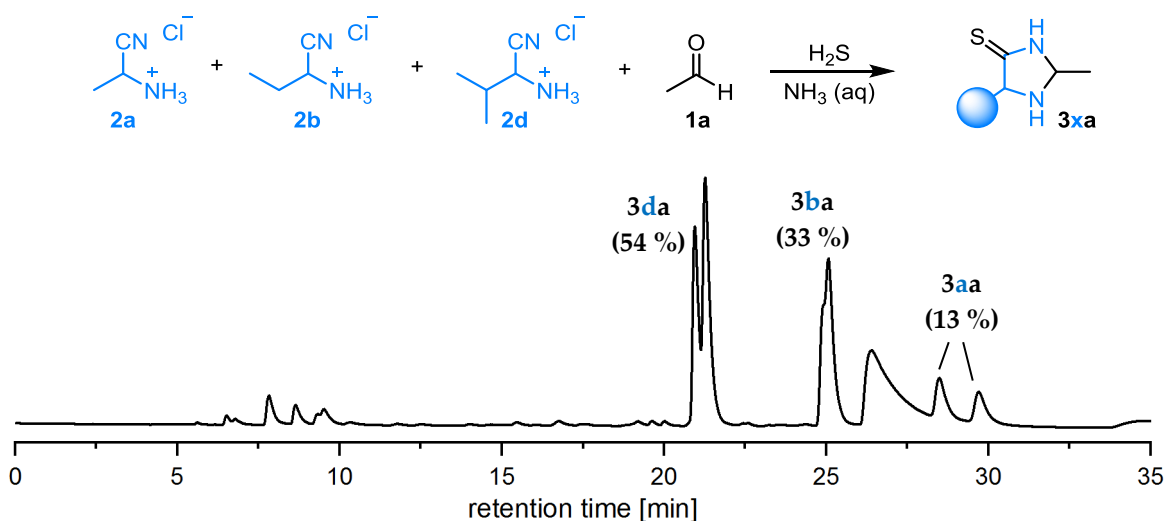
Figure 4.11: Selectivity of the reaction of **1a** with an equimolar mixture of aminonitriles **2a,b,d**. HPLC separation and relative ratio of the imidazolidine-4-thiones **3** in the product mixture determined by peak integration. The broad peak at 47 min does not belong to an imidazolidine-4-thione.

Thereby, the aminonitrile of isobutyraldehyde **2d** would not only preferentially form out of a carbonyl mixture as shown in Section 4.3.1 but also favourably react further with any carbonyl. As a result, the isopropyl residue in ring position 5 should be highly dominant. Adding the secondary aminonitrile **2f**, however, again drastically influenced the selectivity (Figure 4.12).
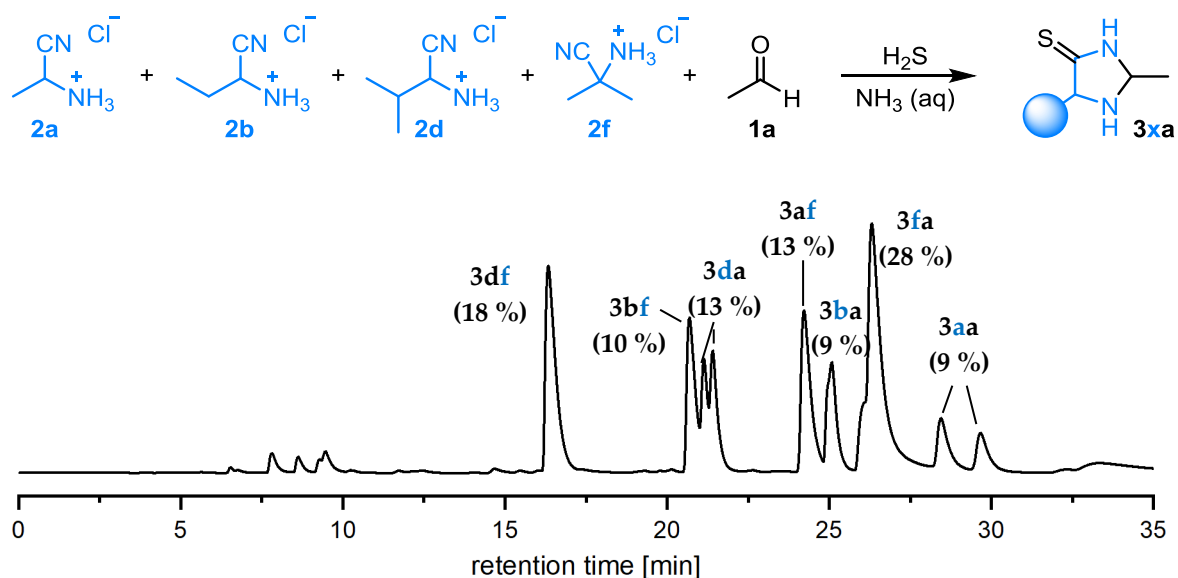
Figure 4.12: Selectivity of the reaction of **1a** with an equimolar mixture of aminonitriles **2a,b,d,f**. HPLC separation and relative ratio of the imidazolidine-4-thiones **3** in the product mixture determined by peak integration.

First, a significant preference was obtained for the reaction of acetaldehyde **1a** with **2f** to form **3fa**. Second, the next most abundant imidazolidine-4-thiones also incorporated acetone but in ring position 2. Resulting from degradation of the instable **2f** (see Section 4.2.1), acetone **1f** was present in solution to react with the aminonitriles. Because of the formation of acetone **1f** in any reaction with **2f**, analysing the same reaction with **1f** instead of acetaldehyde **1a** only changed the proportion of products.

Overall selectivity of the two-step-procedure

The above results indicated that for the second step of imidazolidine-4-thione synthesis – the reaction of an α-aminonitrile **2** with a carbonyl **1** – acetone is preferentially incorporated into the imidazolidine-4-thione skeleton. However, it was also observed that the respective aminonitrile is not formed at all in the presence of competing aldehydes and is thus at least not thermodynamically favoured. To also take into account the influence of this first step of aminonitrile **2** formation, the next approach started at the level of carbonyls **1**. An excess of aldehydes **1a,b,d** was reacted with KCN and NH_4Cl for 1.5 h, followed by the usual workup for the synthesis of single aminonitriles. Instead of precipitation as hydrogen chloride salts to eliminate by-products, the resulting product mixture was directly treated with an excess of the same carbonyls **1a,b,d** and H_2S for 12 h (Figure 4.13, A).
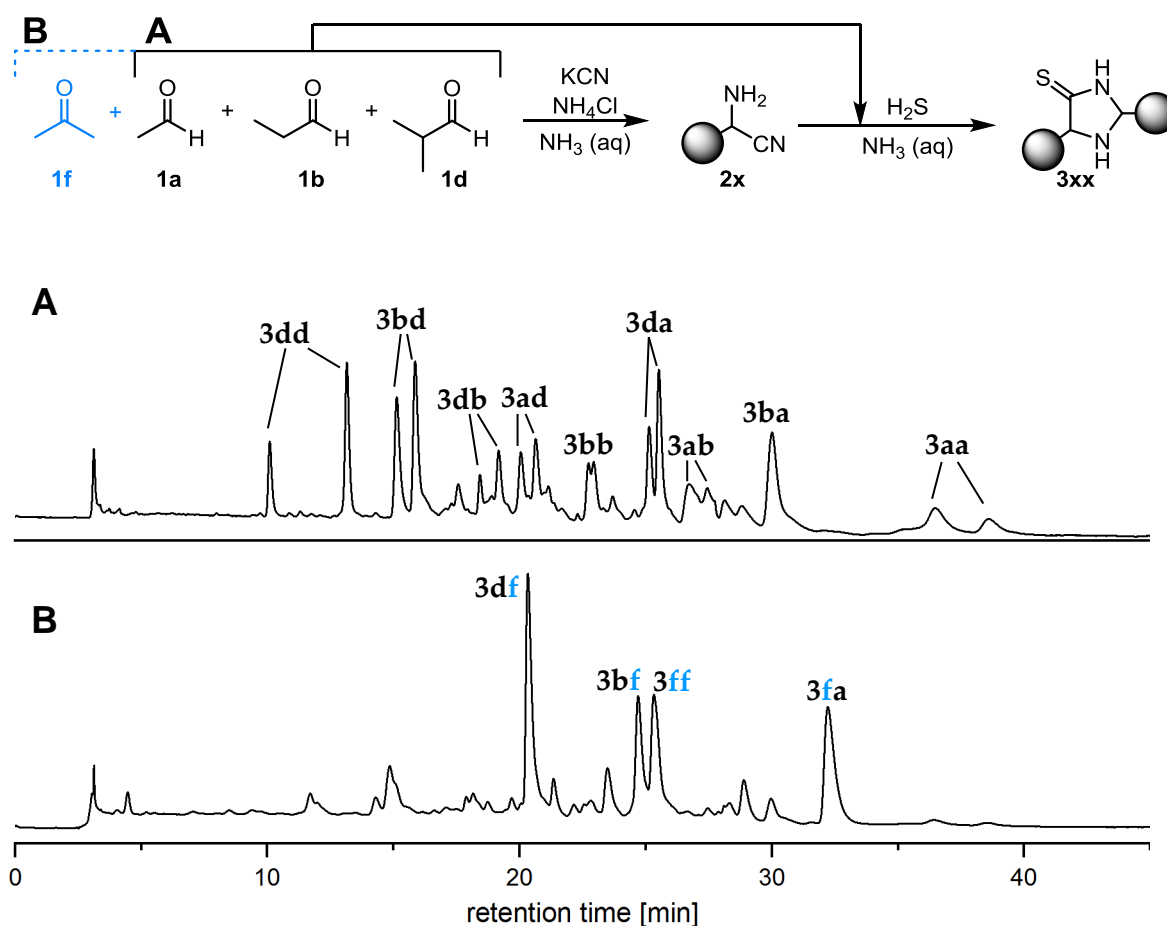
Figure 4.13: Selectivity of the two-step formation of imidazolidine-4-thiones **3** in concentrated aqueous ammonia without aminonitrile **2** purification in between. HPLC separation of the imidazolidine-4-thiones **3** in the respective product mixture. **A**: an equimolar mixture of aldehydes **1a**, **1b**, and **1d** was applied in both reaction steps. **B**: an equimolar mixture of aldehydes **1a**, **1b**, and **1d** as well as acetone **1f** was applied in both reaction steps.

Then, the experiment was repeated with adding acetone **1f** to the aldehyde mixture in both reaction steps (Figure 4.13, B). Although no baseline separation for exact quantification of all product imidazolidine-4-thiones **3** was achieved, qualitative conclusions could be drawn. If only aldehydes were present, all possible structural combinations of **3** were formed. However, as soon as acetone **1f** was present, the distribution changed significantly. Instead of a more complex mixture with all additional imidazolidine-4-thiones that incorporate acetone, the number of arising species decreased. Selectively, four molecules prevailed and all of them contained at least one acetone building block. Thus, the results of the preliminary studies were verified in terms of selective acetone **1f** insertion at both ring positions as well as a clear preference for the combination with acetaldehyde **1a** to form **3fa**.

By variation of the applied carbonyls, consistent observations could be made and are summarised in Scheme 4.7. In all experiments, imidazolidine-4-thiones formed from acetone **1f** were favoured.
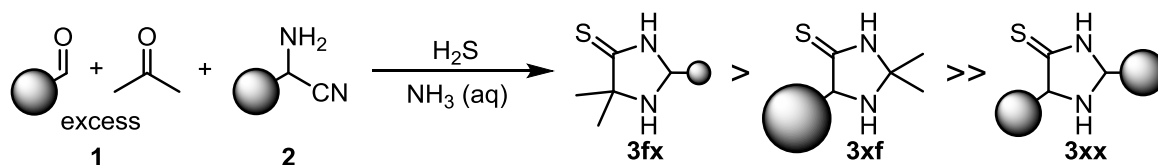
Scheme 4.7: Selectivity of imidazolidine-4-thione **3** formation out of carbonyl **1** and aminonitrile **2** mixtures. The size of the ball illustrates the size of the aldehyde carbon chain.

Further, the ketone **1f** preferentially reacted with the largest possible α-aminonitrile. When reacting as its corresponding secondary aminonitrile **2f**, however, the combination with the smallest possible aldehyde dominated, resulting in **3fa** being the preferentially formed imidazolidine-4-thione in all mixtures. Here, the second step – reaction of α-aminonitrile **2** with carbonyl compound **1** – turned out to be decisive for the resulting imidazolidine-4-thione **3** distribution. When an equimolar mixture of **2a**, **2b**, **2d**, and **2f** was applied instead of the crude aminonitrile mixture formed in the first reaction step, the product composition resembled the one of Figure 4.13, B.

4.3.3 One-Pot Selectivity in Ammonia and Water

Finally, to imitate prebiotic conditions, the overall selectivity in a one-pot mixture of several carbonyls was investigated. The above findings indicated that the selectivity of the two-step imidazolidine-4-thione **3** formation in ammonia mainly refers to the existence of acetone and only to a minor extent to the size of the aldehyde. Reducing the one-pot carbonyl mixture to acetaldehyde **1a**, the sterically more demanding isobutyraldehyde **1d**, and acetone **1f** should therefore be sufficient to make general statements about more complex compositions while still allowing for peak separation necessary for quantification. The observed preferential incorporation of acetone into the imidazolidine-4-thione **3** skeleton in ammonia contradicted the selective decrease of acetone containing structures detected for the dynamic exchange in water (Section 4.2.2). Thus, both reaction media were studied for the one-pot formation of **3** as promising mode of different selection.
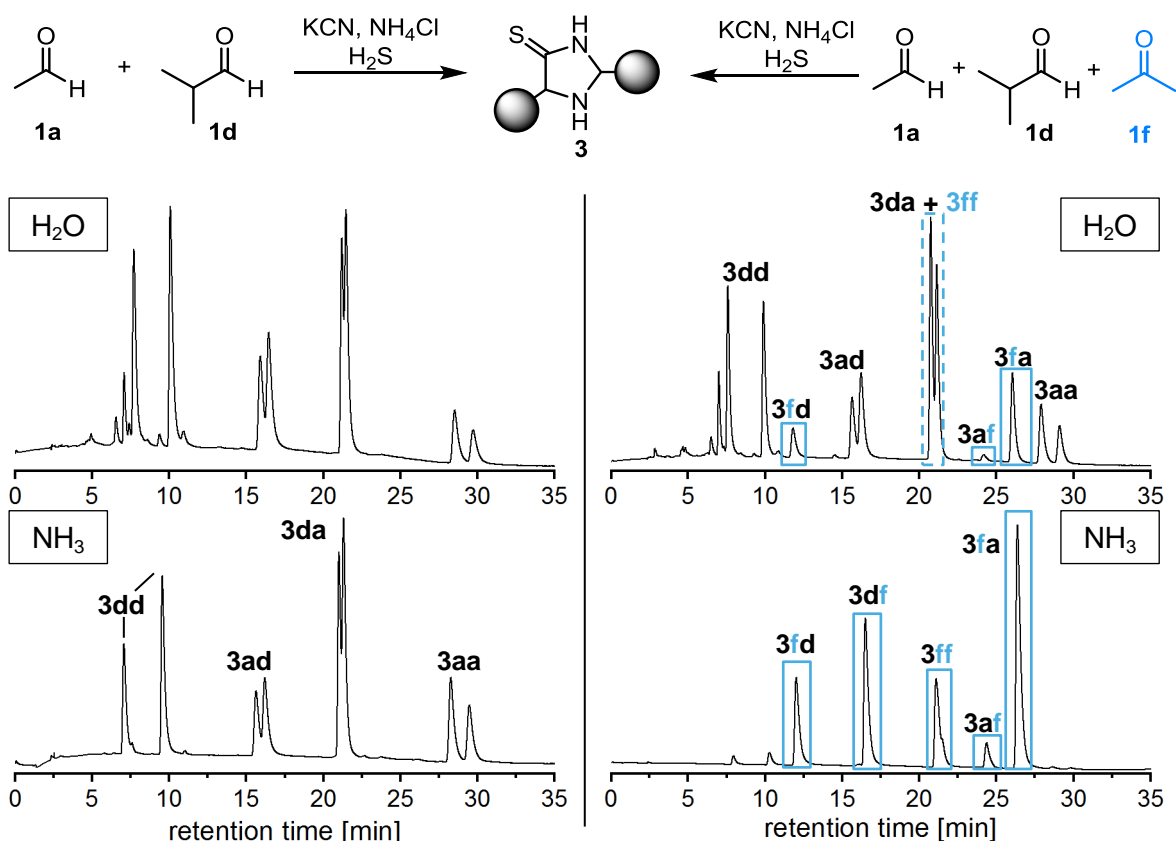
Figure 4.14: Comparison of the one-pot formation of imidazolidine-4-thiones **3** in different media. HPLC chromatograms of the mixture formed from a carbonyl mixture without (left) and with acetone **1f** (right) in water (top) and concentrated aqueous ammonia (bottom). Acetone **1f** containing structures are highlighted in blue.

57

In a first approach, only two aldehydes **1a** and **1d** were reacted with potassium cyanide, ammonium chloride, and hydrogen sulphide in water and ammonia for 12 hours. The resulting products did not differ for the two reaction media (Figure 4.14, left). Adding acetone **1f**, however, changed the product distribution in different ways (Figure 4.14, right). For the reaction in ammonia, a selective incorporation of acetone **1f** was observed that resembled the above results of the two-step procedure. In water, the corresponding imidazolidine-4-thiones **3xf/3fx** were also formed but did not dominate the product mixture. On the contrary, the formation of **3df** was not detected at all.

This strong and opposing influence of the solvent would be a powerful mode of selection and thus initiated a more detailed investigation on the present imidazolidine-4-thiones **3** over time. Samples were taken directly after hydrogen sulphide addition as well as different time periods and the relative proportion of each imidazolidine-4-thione was determined by integration of the corresponding HPLC peaks. Comparison of the different product distributions over time revealed a different course of selectivity for ammonia and water (Figure 4.15).

In ammonia, acetone containing structures dominated the set of compounds from the very beginning. The favoured formation of **3fa** and **3df** was consistent with the conclusions of Section 4.3.2: if acetone reacted as carbonyl (ring position 2), the combination with the largest aminonitrile **2d** was preferred, and if its aminonitrile **2f** was incorporated, it mainly reacted with the smallest aldehyde **1a**. This resulted in **3fa** as the most pronounced product with a share of over 50 %. Initially, the homo-substituted imidazolidine-4-thiones of acetaldehyde **3aa** and isobutyraldehyde **3dd** were also formed but successively degraded over time. Counterintuitively, this selective prevalence of acetone **1f** can be explained by its lower reactivity compared to aldehydes. In the presence of ammonia and basic conditions, the latter are consumed by faster side-reactions, resulting for example in the identified dithiazinanes **4**, which are not formed from acetone. The ketone remains in solution with an excess and can be incorporated into the imidazolidine-4-thione structure at both ring positions 2 and 5.
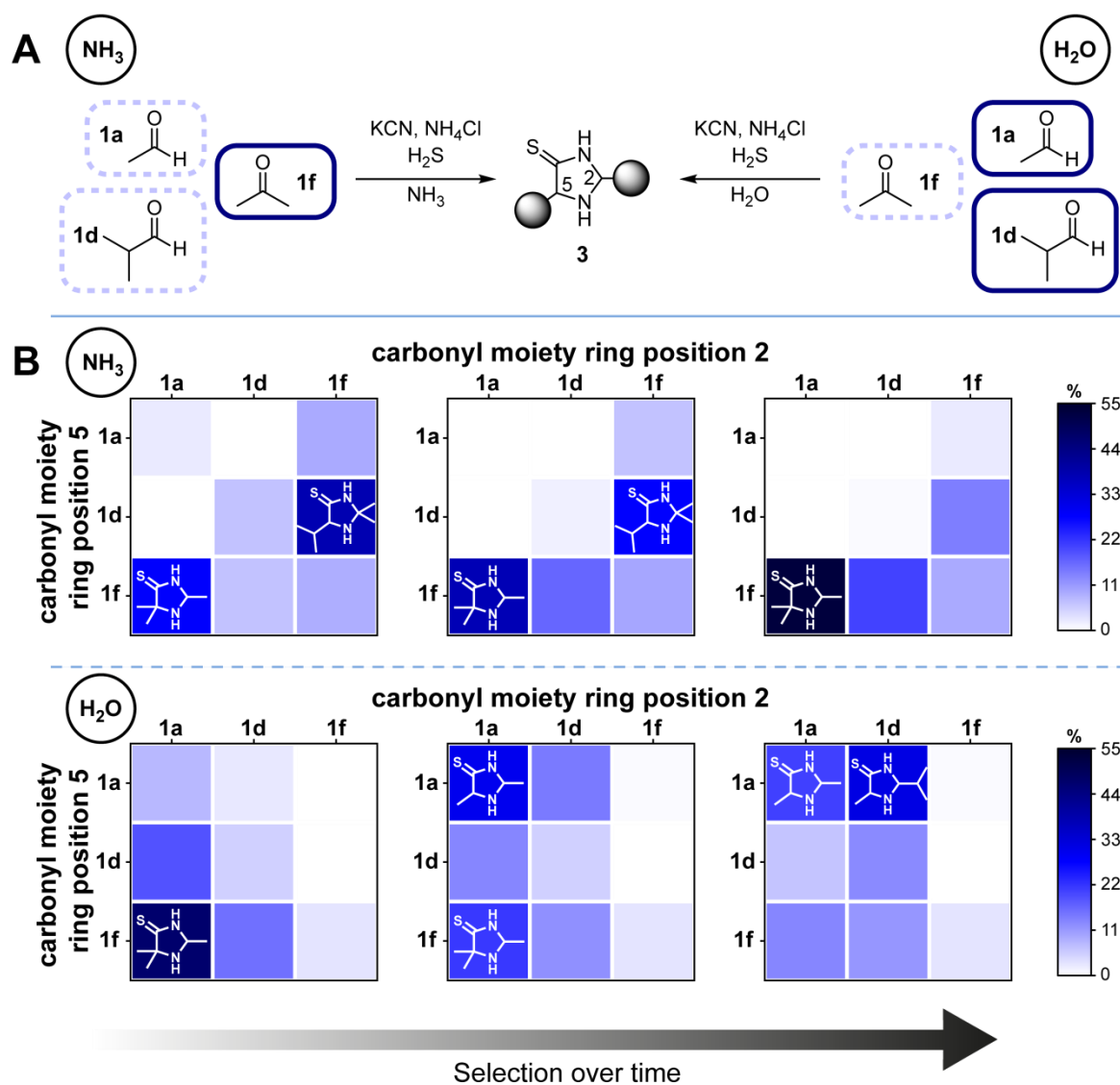
Figure 4.15: Selectivity of the one-pot formation of imidazolidine-4-thiones **3** in water and concentrated aqueous ammonia. **A**: Schematic formation of catalysts **3** depending on the reaction medium. Preferentially incorporated carbonyl components **1** are highlighted (left = $NH_{3(aq)}$; right = H_2O). **B:** Change of selectivity in catalyst **3** formation with increasing reaction progress after 0 min, 30 min, and 4 h (top = $NH_{3(aq)}$; bottom = H_2O). The colour code indicates the relative ratio determined by HPLC-MS.

In contrast to the observation of increasing selectivity in ammonia, ongoing reaction in water led to a growing uniform distribution. The lower pH and absence of ammonia caused less side-reactions and thus had a positive effect on the present amount of aldehydes in solution. Directly after mixing the reactants, the imidazolidine-4-thiones formed from the secondary aminonitrile of acetone **2f** dominated. This result contradicted our investigations on the selectivity of α-aminonitrile formation which showed no acetone conversion in the presence of acetaldehyde **1a** and isobutyraldehyde **1d**. However, the preferred formation of the corresponding imidazolidine-4-thiones can be explained by a faster following cyclisation reaction of **2f**. According to the Thorpe-Ingold effect, the quaternary carbon accelerates ring formation. The share of the carbonyl moiety in ring

position 2 reflected the reactivity and steric hindering of the intermediary formed imine with a decreasing selectivity going from acetaldehyde **1a** to isobutyraldehyde **1d** to acetone **1f**. For all aminonitriles, the latter was hardly incorporated at all. Over time, this kinetically induced distribution changed due to the dynamic carbonyl exchange in ring position 2 (see Section 4.2.2). The proportion of inserted isobutyraldehyde **1d** increased whereas acetone **1f** could not be included via this mechanism and remained in solution. The equal availability of all reactants resulted in a uniform distribution dictated by thermodynamics. As the equilibrium ratio of the product's carbonyl moieties reflected approximately the ratio of applied aldehydes, the energetic influence of the right side-chain is only small. The slight predominance of **3ad** over **3aa** and **3dd** over **3da** could also be explained by a reduced presence of acetaldehyde **1a** in solution due to its higher volatility as well as higher reactivity towards side-reactions.

Concluding, the imidazolidine-4-thiones form out of carbonyl mixtures with distinct selectivities for certain species depending on the reaction environment. Instead of converting a single reactant, these mixtures are more plausible reflections of the prebiotic soup. In ammonia, acetone is preferentially converted and especially the combination with acetaldehyde forming **3fa** dominates. In water, the imidazolidine-4-thione composition equalises over time with the exception of missing acetone incorporation at ring position 2. Thus, the surrounding conditions – for example local pH differences or the amount of ammonia present – would influence the composition of structural variants. Since imidazolidine-4-thiones can continuously form as well as dynamically interconvert between species, a changing environment results in a changing compound distribution and can thus be used as a mode of selection.

4.4 Crystallisation as Conglomerate

The previous sections demonstrated that imidazolidine-4-thiones not only readily assembled out of a prebiotically abundant feedstock but that distinct structural variants and diastereomers were favoured depending on the reaction conditions. However, all species were formed as racemic mixtures. Considering the potential organocatalytic function of imidazolidine-4-thiones on the early Earth, it would be of particular interest if they were present with enantiomeric enrichments. Thereby, they could simultaneously enable the formation of inaccessible higher complex molecules and transfer stereoinformation to spread and amplify these enrichments towards homochirality.

Throughout the crystallisation studies out of the respective racemic solutions, several imidazolidine-4-thiones **3** as well as the amine-methylated derivative of **3ff** were obtained as single crystals. Remarkably, an enantiomerically pure crystal was observed for **3ba** (Figure 4.16).
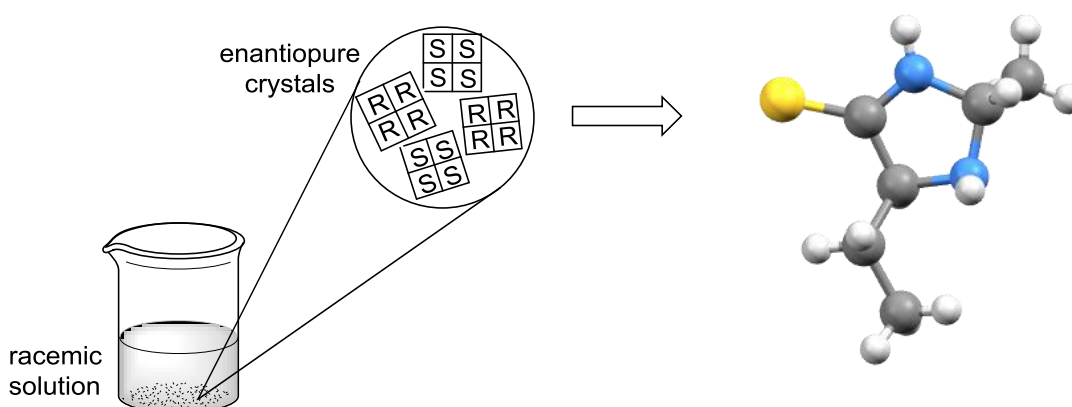
Figure 4.16: Enantiopure crystallisation of **3ba** out of a racemic solution (conglomerate).

To determine this characteristic, the measured space group and the Flack parameter have to be taken into account. For a chiral crystal structure, the former does not need to be chiral itself but must belong to one of the 65 SOHNCKE space groups that only contain symmetry operations of the first kind (e.g. rotations and translations that relate congruent objects).[198] Then, the Flack parameter must either be nearly 0 (the modelled enantiomer refers to the correct absolute configuration) or nearly 1 (the inverted enantiomer is present). Intermediate values imply mixtures and twinning with racemic crystals having a value close to 0.5.[199]

In contrast to the crystallisation as racemic compound, which is by far the most common process, the formation of such a conglomerate can result in spontaneous resolution. As described in detail in Section 2.3.1, this phenomenon is widely proposed as a promising mechanism for the emergence of initial symmetry breaking on the early Earth. If the imidazolidine-4-thione **3ba** acts as an enantioselective organocatalyst, this enantiomeric imbalance is not limited to this molecule class but can be transferred and potentially amplified. In the context of homochirality, this pathway would represent a powerful extension to the pure crystallisation hypothesis.

4.5 Catalytic Activity

To investigate the potential of imidazolidine-4-thiones **3** as powerful tools in the emergence of life, we sought for a catalytic activity in the α-alkylation of small aldehydes. This transformation is not only challenging in modern chemistry but was also unfeasible in prebiotic scenarios. Though, it would be essential in enlarging and functionalising the initial molecular structures to broaden the prebiotic pool as well as provide water insoluble compounds for compartmentalisation.

4.5.1 Photoredox Organocatalytic α-Alkylation of Aldehydes

Due to the structural similarities to the MacMillan imidazolidinone catalyst, its established photoredox α-cyanomethylation[155] was chosen as promising starting point and studied in collaboration with E. FUKS.[194] The high abundance of solar irradiation provides an energy source for such photo-induced reactions as well as a plausible atmospheric existence of the reactant 2-bromoacetonitrile **15** used in this process by radical recombination of interstellar bromine and acetonitrile.[20,200] Further, hydrolysis of the product's nitrile group would result in prebiotically relevant functionalities. However, the MacMillan system is based on long chain aldehydes, DMSO as solvent, 2,6-lutidine as base, and $Ru(bpy)_3Cl_2$ as photosensitiser, which are not compatible with the early Earth. E. FUKS was able to adapt this catalytic procedure to prebiotically plausible reaction conditions (Scheme 4.8).[201]
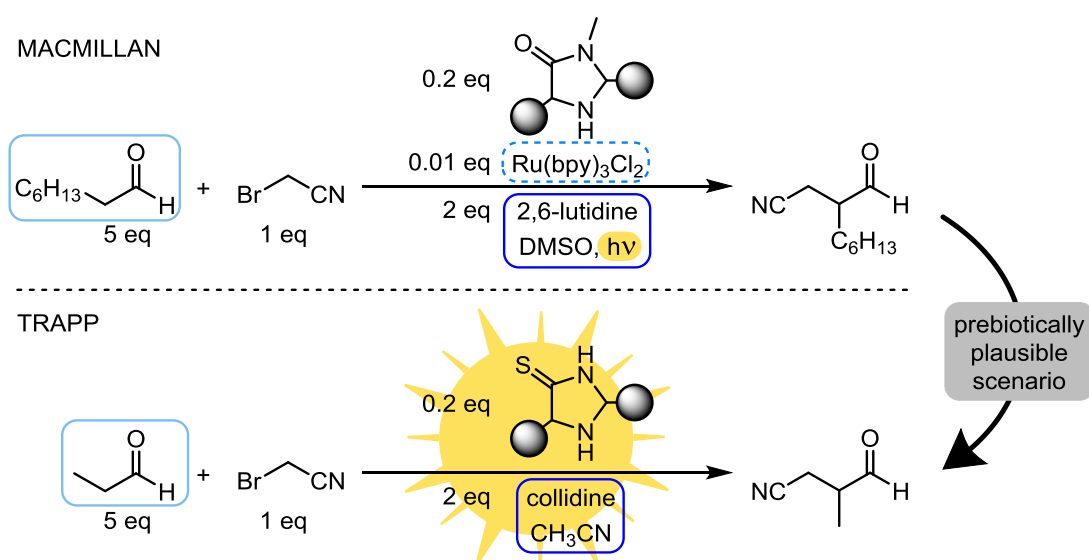
Scheme 4.8: Photoredox organocatalytic α-cyanomethylation of aldehydes. Top: established procedure by MACMILLAN, bottom: prebiotically plausible procedure adapted by E. FUKS in her parallel thesis.[201] Outlined reactants and reagents on top were exchanged by the outlined compounds in the same colour on the bottom or completely excluded (dashed).

Surprisingly, performing the reaction without any photosensitiser had no negative effect on the product yields and thus eliminates a reagent as well as the drawbacks of metal complexes in terms of water sensitivity. Instead of octanal, the smaller propionaldehyde **1b** could also be converted into the respective alkylated product and DMSO as solvent could be replaced by acetonitrile or by simply performing the reaction in an excess of aldehyde. Exchanging 2,6-lutidine as base turned out to be more difficult and was only succeeded with structurally related 2,4,6-trimethylpyridine **16** (collidine) and 2-methylquinoline, whereby steric shielding of the aromatic nitrogen atom was decisive. These compounds have been found on the Murchison meteorite and could be formed by Fischer-Tropsch type synthesis from aldehydes and ammonia or photochemically from benzene and naphthalene derivatives in interstellar ices.[202-203] The developed conditions with collidine **16** in acetonitrile not only enabled the alkylation reaction in an early Earth scenario but also increased product formation compared to the established system of 2,6-lutidine and DMSO. Now, only a prebiotically plausible alternative for the MacMillan catalyst was missing, which was provided by this thesis. Satisfyingly, initial application of imidazolidine-4-thione **3ff** demonstrated successful formation of cyanomethylated propionaldehyde **1b'** in 76 % yield, thus even exceeding the activity of the MacMillan imidazolidinone.[194] Unlike the latter catalyst, the imidazolidine-4-thiones did not require inert reaction conditions to provide maximum activity, proving its robustness towards the existence of oxygen.

Structural influences on activity and enantioselectivity

To test the influence of structural differences on the product formation, various of the synthesised imidazolidine-4-thiones **3** were applied and compared by E. FUKS (Scheme 4.9).[194,201] For all organocatalysts the desired cyanomethylated propionaldehyde **1b'** was observed and the highest yields were reached with **3fa** and the achiral catalyst **3ff**. This leads to the assumption that dimethylation at ring position 5 is beneficial for the catalytic activity. Intriguingly, these two most active catalysts are also the ones which were preferentially formed out of the diverse one-pot carbonyl mixture in ammonia (see Section 4.3.3). Also, the favoured *anti*-substituted isomer of **3ba** led to higher yields compared to its *syn*-analogue. This correlation between the formation ratio of

imidazolidine-4-thiones and their catalytic activity represents a potential selection mode for early evolutionary processes on a molecular level.
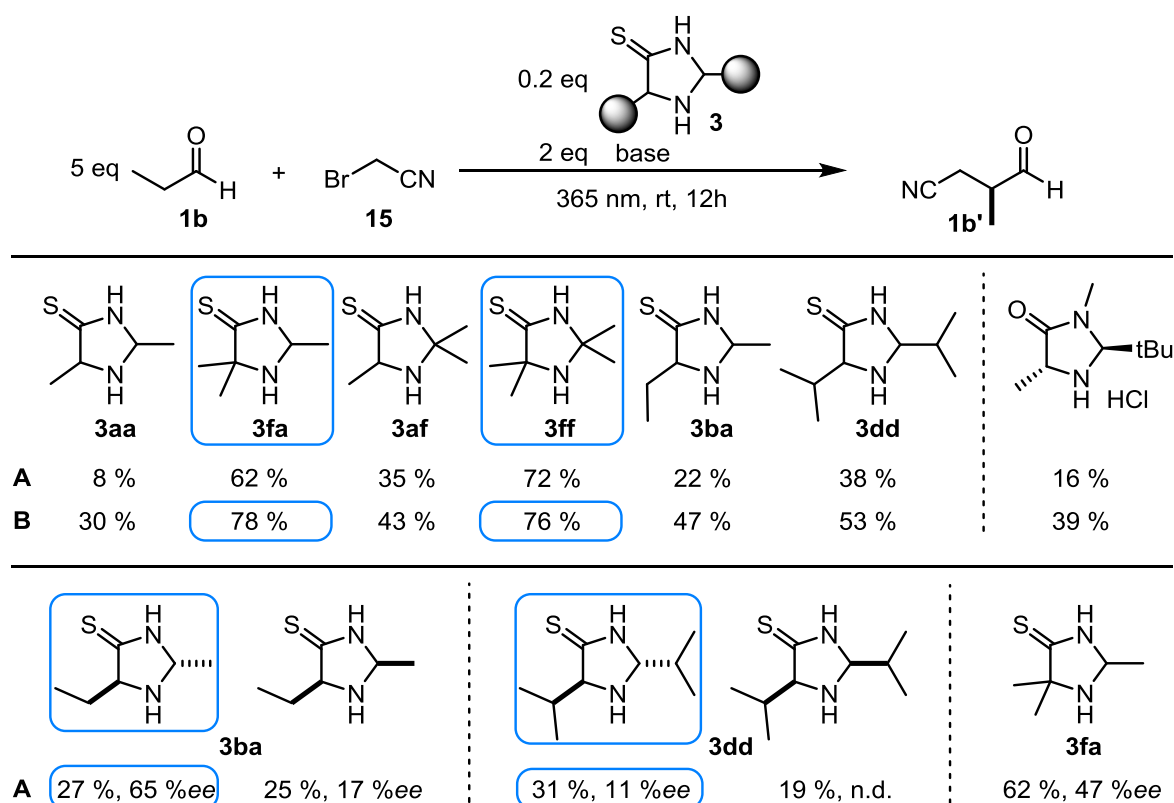
Scheme 4.9: Product yields and enantioselectivities obtained by E. FUKS in the photoredox organocatalytic α-cyanomethylation of propionaldehyde **1b** under aerobic conditions. **A**: The reaction was performed in DMSO with 2,6-lutidine as base. **B**: The reaction was performed in acetonitrile with collidine **16** as base. Yields were determined by ^{1}H NMR analysis of the crude reaction mixture and the enantiomeric excess (*ee*) was determined by enantioselective GC analysis of the corresponding alcohol. Molecules and percentages outlined in blue refer to the preferentially formed imidazolidine-4-thiones and isomers in ammonia as well as the highest yields/enantioselectivities, respectively.

Motivated by the discovered enantiopure crystallisation of **3ba** (see Section 4.4), the potential of imidazolidine-4-thione organocatalysts was also investigated in terms of chirality transfer. Therefore, the enantiomers of the most active chiral catalyst **3fa**, the conglomerate **3ba**, and the sterically most demanding imidazolidine-4-thione **3dd** were separated by chiral preparative HPLC. For the latter two, an enantiomer of each diastereomer was isolated. The observed superiority of the respective *anti*-isomer regarding its catalytic activity turned out to be even more pronounced for its enantioselectivity. In case of the conglomerate catalyst **3ba**, **1b'** was obtained with an enantiomeric excess of 65 % compared to 17 %. Surprisingly, introducing sterically more demanding side-chains decreased the resulting product *ee*. Thus, the imidazolidine-4-

thiones formed from the prebiotically more abundant smaller carbonyl compounds are not only sufficient to transfer chirality but even more selective.

This organocatalytic photoredox approach gave first proof of the prebiotically plausible catalytic activity of imidazolidine-4-thiones. Thereby, these structures enabled the α-alkylation of aldehydes, a transformation that has so far not been feasible in an early Earth scenario.

4.5.2 Organocatalytic α-Alkylation of Aldehydes in the Dark

So far, the intermolecular organocatalytic α-alkylation of aldehydes with an alkylating halide was not possible via simple S_N2 reaction and, instead, dominated by coupling with photoredox chemistry that activates the alkylating halide as radical (Figure 4.17, left). Also the catalytic procedure described above can be assigned to this type of photo-initiated radical mechanism.
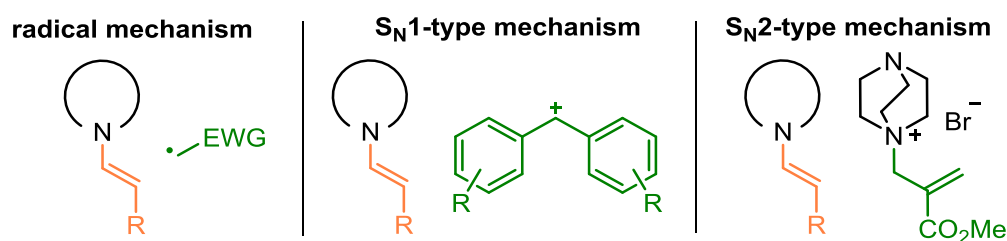
Figure 4.17: Known activation modes for a successful organocatalytic α-alkylation of aldehydes. Orange: activation of the aldehyde, green: activation of the respective alkylating agent.

Besides that, stabilised diaryl carbocations allowed for S_N1-type reactions[166-167] (Figure 4.17, middle) and one publication demonstrated a possible activation of the alkylating halide as ammonium salt of DABCO or DMAP leading to an S_N2-type addition-elimination mechanism (Figure 4.17, right).[168] In all cases, the reacting aldehyde is catalytically activated as enamine by a secondary amine (see Section 2.4.2 for more details).

Surprisingly, a significant formation of the product aldehyde **1b'** was observed when catalysing the reaction with **3ff** at 40 °C in the absence of light (Figure 4.18). This approach was taken to mimic the increased temperature resulting from irradiation. Repeated experiments in brown glass or covered in aluminium foil verified product formation in the dark. Therefore, this catalytic reaction is not initiated by light and has to proceed via a completely different mechanism.
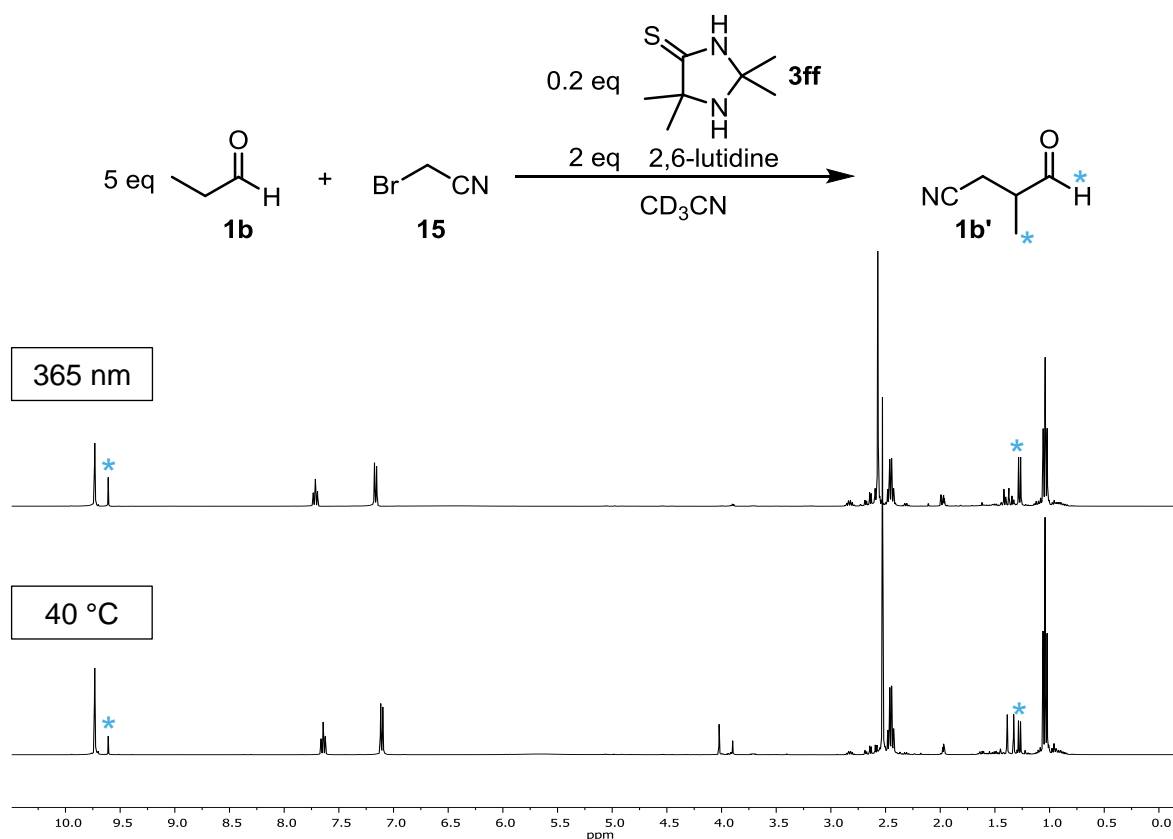
Figure 4.18: ^{1}H NMR spectra of the crude reaction mixture of the cyanomethylation of propionaldehyde **1b** with bromoacetonitrile **15**. Top: under irradiation with 365 nm. Bottom: without light at 40 °C. The aldehyde as well as methyl signals of the product aldehyde are highlighted in blue.

Without radical activation or plausible carbocation stabilisation of bromoacetonitrile **15**, especially the activation of the alkylating agent in the dark reaction raised questions and represents an unknown direct access to alkylated aldehydes without the need for additional reagents. Thus, the underlying mechanism was studied in detail with in-situ ^{1}H NMR spectrometry.

Analysis of the reaction mixture of propionaldehyde **1b**, bromoacetonitrile **15**, 2,6-lutidine and catalytic amounts of **3ff** at 40 °C after certain time periods revealed a 30-minute delay in product formation (Figure 4.19, left). Interestingly, in this initial stage the signals of **3ff** decreased significantly (Figure 4.19, right). Concomitant, two new species were formed and could be identified as the *S*-cyanomethylated imidazolidine-4-thione derivative **3ff-CN** and the respective enamine **3ff-CN-En**. Selective alkylation at the sulphur atom can be detected effectively by the missing CH$_2$-coupling to the carbon atom in ring position 2 in the HMBC spectrum (which is clearly visible for both *N*-alkylations) as well as a distinct upfield shift of the thiocarbonyl carbon in the ^{13}C NMR spectrum.
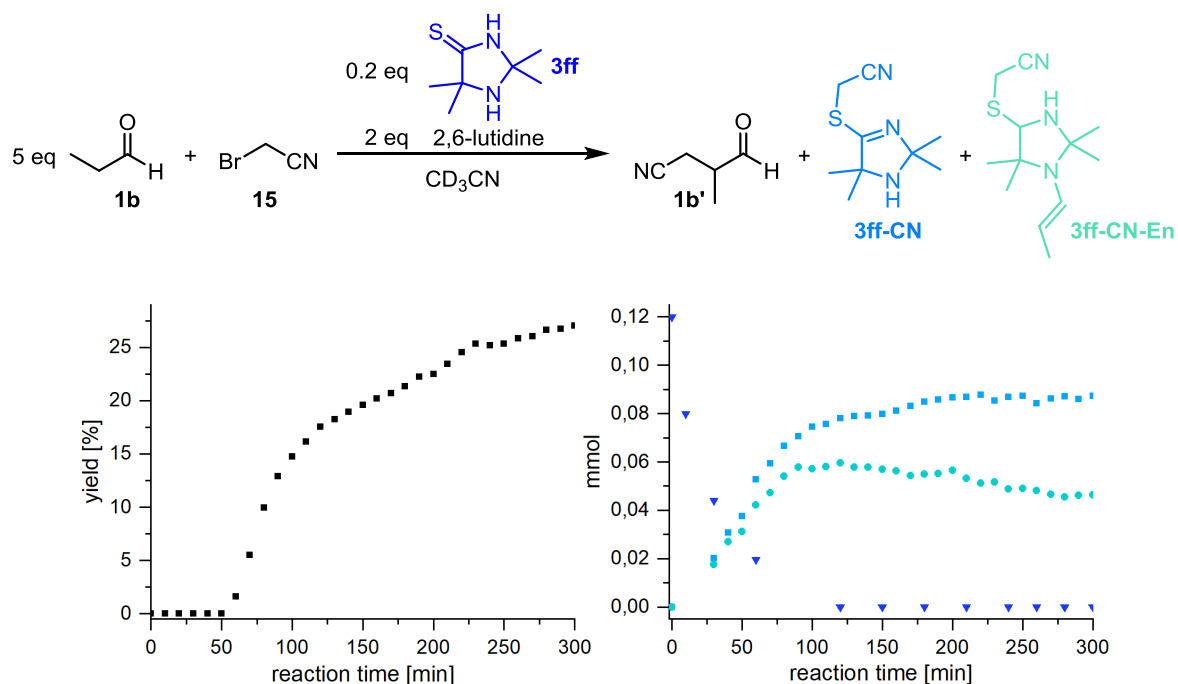
Figure 4.19: In-situ ¹H NMR analysis of the reaction progress of the α-alkylation of propionaldehyde **1b**, catalysed by **3ff**. Left: time-dependent product **1b′** formation. Right: time-dependent decrease of imidazolidine-4-thione **3ff** (triangle) and simultaneous increase of **3ff-CN** (square) and **3ff-CN-En** (circle).

These observations led to the initial conclusions that the imidazolidine-4-thione **3ff** is not only necessary for enamine formation but also to activate bromoacetonitrile **15** by previous nucleophilic attack of the thioamide-sulphur. To verify these hypotheses, different imidazolidine-4-thione derivatives with selective protection of proposed catalytically relevant sites were synthesised (Scheme 4.10).
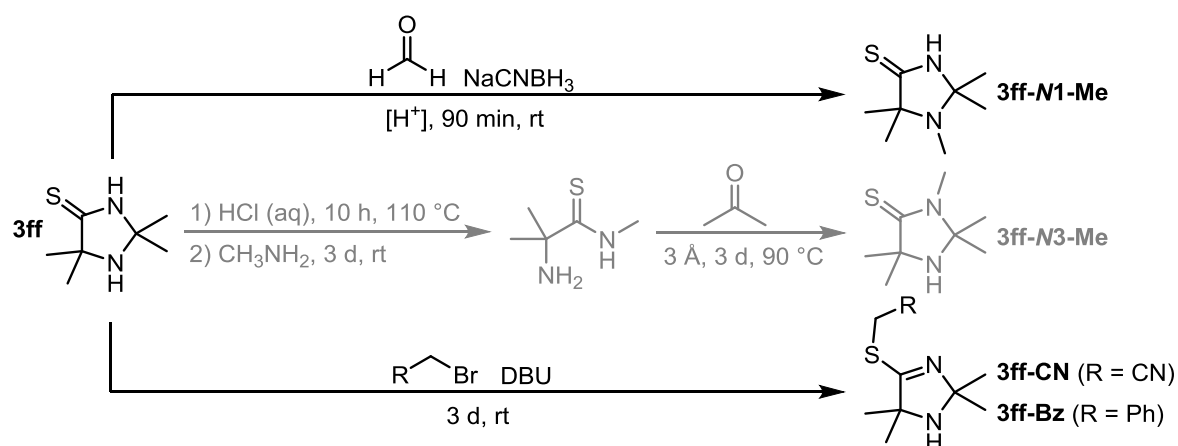
Scheme 4.10: Synthetic pathways to imidazolidine-4-thione derivatives. The synthesis of **3ff-N3-Me**, depicted in grey, was designed and performed by M. Ebeling.

Depending on the success of the α-cyanomethylation of propionaldehyde **1b** catalysed with these derivatives, an influence of the respective functionality on the catalytic activity was derived (Table 4.2).

Table 4.2: Yield and observed intermediates for the organocatalytic α-cyanomethylation of propionaldehyde **1b** at 40 °C using different derivatives of imidazolidine-4-thione **3ff** as catalyst. Yields refer to ^{1}H NMR yields of **1b'** after 3 h and after 24 h for no yield. Molecules depicted in grey were not observed. [a] without the addition of **15**, [b] 0.1 eq of each catalyst.

Entry	Catalyst	Yield	Observed Intermediates
1	**3ff**	25 %	**3ff-CN** **3ff-CN-En**
2	**3ff-N1-Me**	—	**3ff-CN-N1-Me**
3	**3ff-N3-Me**	—	**3ff-N3-Me-En**
4[a]	**3ff-CN** +	—	**3ff-CN-En** traces
5	**3ff-Bz**	35 %	**3ff-Bz-En** **3ff-CN**
6[b]	**3ff-N1-Me** + **3ff-N3-Me**	—	**3ff-CN-N1-Me** **3ff-N3-Me-En**

First, the amine was methylated by Eschweiler-Clarke reductive amination using formaldehyde to yield **3ff-*N*1-Me**. As byproduct, small amounts of **3ff-*N*1-Me-*N*3-CH₂OH,** additionally hydroxymethylated at the thioamide-nitrogen, were formed and separated by preparative HPLC for purification. As expected, applying this amine-alkylated derivative in the catalysis did not lead to product formation which indicates the necessary participation of the enamine. Next, the structure with an *N*-methylated thioamide **3ff-*N*3-Me** was tested. This molecule was synthesised by M. EBELING of our group by acid promoted ring opening of **3ff**, treatment with methyl amine and subsequent cyclisation with acetone. Again, the cyanomethylated propionaldehyde **1b'** was not observed in the respective catalysis. The tertiary thioamide hinders *S*-alkylation which would thus strengthen the initial theory of bromoacetonitrile **15** activation by the thioamide sulphur. For further verification of the role of **3ff-CN** as activated alkylating agent, the cyanomethylated imidazolidine-4-thione intermediate was isolated and applied as catalyst in a reaction without additional bromoacetonitrile **15** but with equimolar amounts of a lutidine salt, which would have accompanied the in-situ formation of **3ff-CN** in the original catalysis mixture. However, this approach did not yield any product and thus contradicts the proposed mechanism of an *S*-activated bromoacetonitrile **15**. The observation of the respective enamine **3ff-CN-En** reinforces the refutation. Following the hypothesised two modes of activation – enamine formation and thioalkylation – this species alone would have been sufficient for product formation. Further contradicting results were provided by using the *S*-benzylated derivative **3ff-Bz**. Considering an activation via the thioamide sulphur, the respective catalysis should either yield the benzylated propionaldehyde or no product at all. However, the cyanomethylated propionaldehyde **1b'** was formed with an even higher yield. Monitoring this reaction with in-situ ¹H NMR spectroscopy revealed the corresponding enamine **3ff-Bz-En** as only additional imidazolidine-4-thione derivative to emerge. The reversibility of *S*-alkylation under the catalysis conditions and thus the exchange of the benzylated with the cyanomethylated species would have been a final possibility for the initially proposed mechanism, but the necessary **3ff-CN** was not observed at all throughout the experiment.

New plausible mechanism

Summarising the above results, enamine formation is necessary for a successful catalysis. Further, *S*-alkylation appears to be a crucial step, but not as activation of the alkylating halide. This leads to the sensible conclusion that the initial cyanomethylation of the imidazolidine-4-thione **3ff** is, instead, the activation of the catalyst (Scheme 4.11).
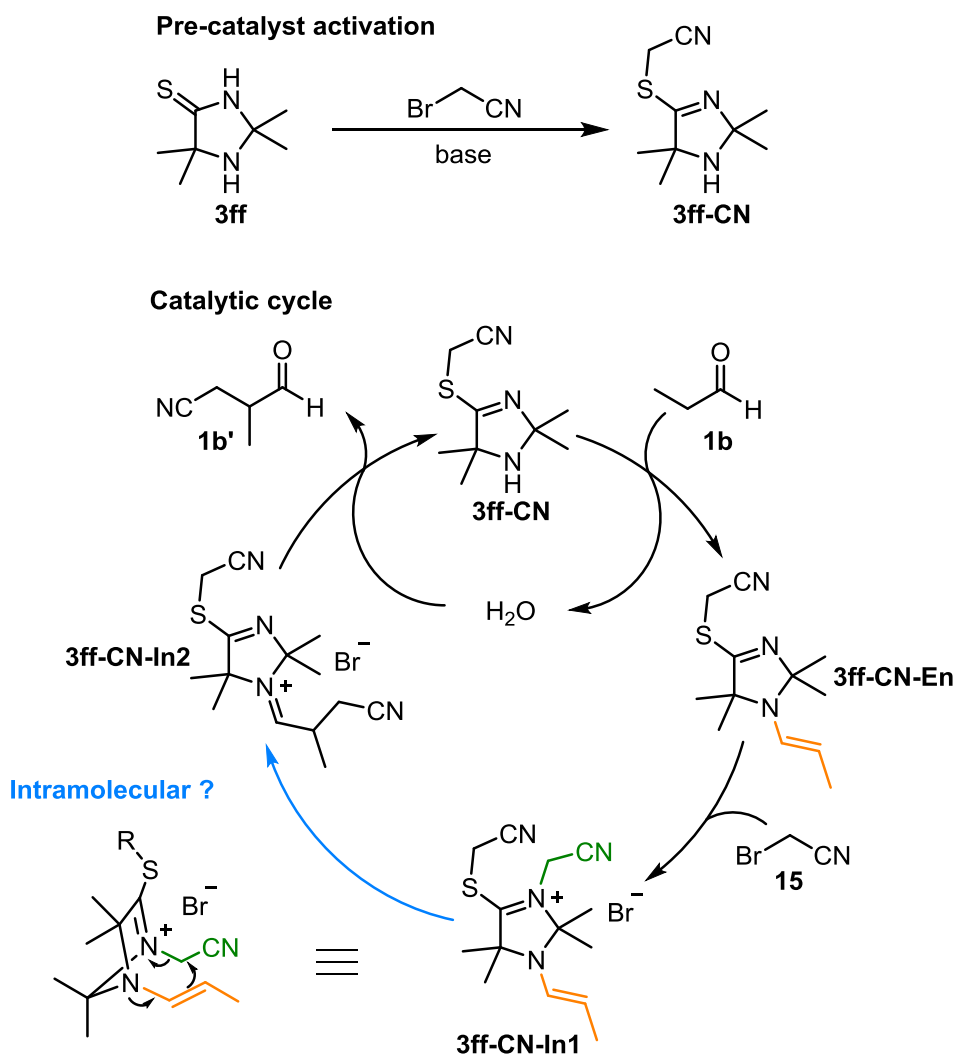
Scheme 4.11: Proposed mechanism of the cyanomethylation of propionaldehyde **1b** with bromoacetonitrile **15** catalysed by imidazolidine-4-thione **3ff**.

3ff is only the pre-catalyst that is converted into the actual catalyst **3ff-CN**, a transformation that explains the observed induction period of product formation. The high stability of the isolated **3ff-CN** as well as its existence also at the end of the catalysis supports its role as catalyst rather than intermediate. Comparing the structural properties of pre-catalyst **3ff** and catalyst **3ff-CN**, the activation of bromoacetonitrile **15** was now derived as ammonium salt activation, similar to the one reported for the use of DABCO and DMAP.[168] The possibility of 2,6-lutidine forming the activated ammonium salt was

ruled out by successful catalysis using K_2CO_3 as base as well as unsuccessful product formation upon employment of the *N*-cyanomethylated 2,6-lutidine salt as only alkylating reagent. Instead of needing an additional reagent, the active imidazolidine-4-thione catalyst **3ff-CN**, activated by the reactant itself, is able to activate both propionaldehyde **1b** and bromoacetonitrile **15**.

The proposed catalytic cycle starts with the formation of the enamine **3ff-CN-En** followed by the addition of a second molecule of bromoacetonitrile **15** to form the ammonium salt intermediate **3ff-CN-In1** (Scheme 4.11). After nucleophilic attack of the enamine, iminium ion **3ff-CN-In2** forms and is hydrolysed to catalyst **3ff-CN** upon release of the cyanomethylated propionaldehyde **1b'**. Although the two ionic structures were not observed in ^{1}H NMR spectra due to fast ongoing reaction, the corresponding mass was detected by Orbitrap high resolution mass analysis. However, as their exact masses are identical, no assignment to one of these species was possible. This proposed mechanism would also explain why the yield was higher when the benzylated imidazolidine-4-thione **3ff-Bz** was used. This structure is already activated and can start the catalytic cycle. The original catalyst **3ff** consumes bromoacetonitrile **15** during pre-activation and thus reduces its availability for the catalytic alkylation. The question that remains is whether the nucleophilic attack of the enamine happens inter- or intramolecular. The latter mechanism is strengthened by the favoured six-membered transition state present in the ammonium salt intermediate (Scheme 4.11). Further, performing the catalysis with a mixture of the amine-methylated and thioamide-*N*-methylated imidazolidine-4-thione derivatives **3ff-*N*1-Me** and **3ff-*N*3-Me** did not lead to product formation (Table 4.2, Entry 6). Yet, *S*-alkylation of **3ff-*N*1-Me** occurred and the enamine of **3ff-*N*3-Me** was formed. Neglecting the influence of different substitutions on the enamine and ammonium salt reactivity, an intermolecular reaction step would still yield the alkylated propionaldehyde **1b'**. To further support the higher probability of the intramolecular mechanism, quantum chemical calculations on the transition states are currently performed.

Structural influences on activity

In the photoredox activated catalysis (Section 4.5.1), the use of different imidazolidine-4-thiones revealed different activities and enantioselectivities. Thus, the structural influences were also investigated for the discovered purely organocatalytic α-alkylation. In addition, a successful application of a chiral imidazolidine-4-thione would enable a potential chirality transfer. As structural variants, the most active chiral catalyst of the photoredox approach **3fa**, the oppositely substituted **3af**, as well as the compound with the sterically most demanding residues **3dd** were tested (Table 4.3). Besides 40 °C, the catalysis was additionally performed at room temperature. Also at the lower temperature, **1b′** was formed but more slowly.

Table 4.3: Yields and enantioselectivities for different imidazolidine-4-thione catalysts **3** in the organocatalytic α-cyanomethylation of propionaldehyde **1b**. A solid line refers to no product formation and a blank entry to no performed experiment.
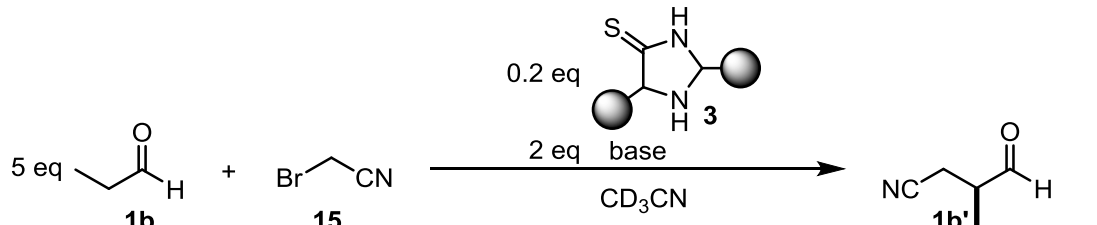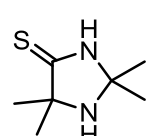
	3ff	**3fa**	**3af**	**3dd**	**3fa**
6 h, 40 °C	26 %	13 %	—	—	30 %*ee*
24 h, 40 °C	19 %	16 %	—	—	
6 h, rt	11 %	13 %			60 %*ee*
24 h, rt	13 %	15 %			

The trimethylated **3fa** was less active than the tetramethylated **3ff** but still led to product formation at both temperatures. Since this catalyst has the benefit of being chiral, the two enantiomers were separated by chiral preparative HPLC to investigate the enantioselectivity of the α-alkylation in the dark. Following the same procedure of the light-induced approach, the product aldehyde was reduced to the alcohol to allow for sufficient chiral GC separation. At 40 °C, an *ee* of 30 % was obtained, which was lower than the 47 % in the photoalkylation. This was attributed to the sensitivity of **1b′** to racemisation due to the increased temperature. Indeed, performing the experiment at

room temperature doubled the *ee* to 60 %. The now higher enantioselectivity compared to the radical mechanism could be a further indication for an intramolecular C-C bond forming step. Surprisingly, no product formation was observed for **3af** and **3dd**. These imidazolidine-4-thiones also gave lower yields than **3fa** and **3ff** in the photo-induced alkylation but still yielded the desired product (Scheme 4.9). By comparing the structures of active and inactive imidazolidine-4-thiones, a quaternary carbon in ring position 5 seemed to be a prerequisite for successful catalysis. To gain further insight into the different reaction behaviours, the intermediates in the reaction mixture of the inactive imidazolidine-4-thione **3af** were investigated as comparison to those already discovered for the active catalyst **3ff**. For better stability of the intermediary formed derivatives, the reaction mixtures of **3af** and **3ff** were analysed at room temperature instead of 40 °C. The only observable difference with both ^{1}H NMR spectroscopy and Orbitrap-MS was the significantly higher amount of enamine species present for **3af** (Figure 4.20).
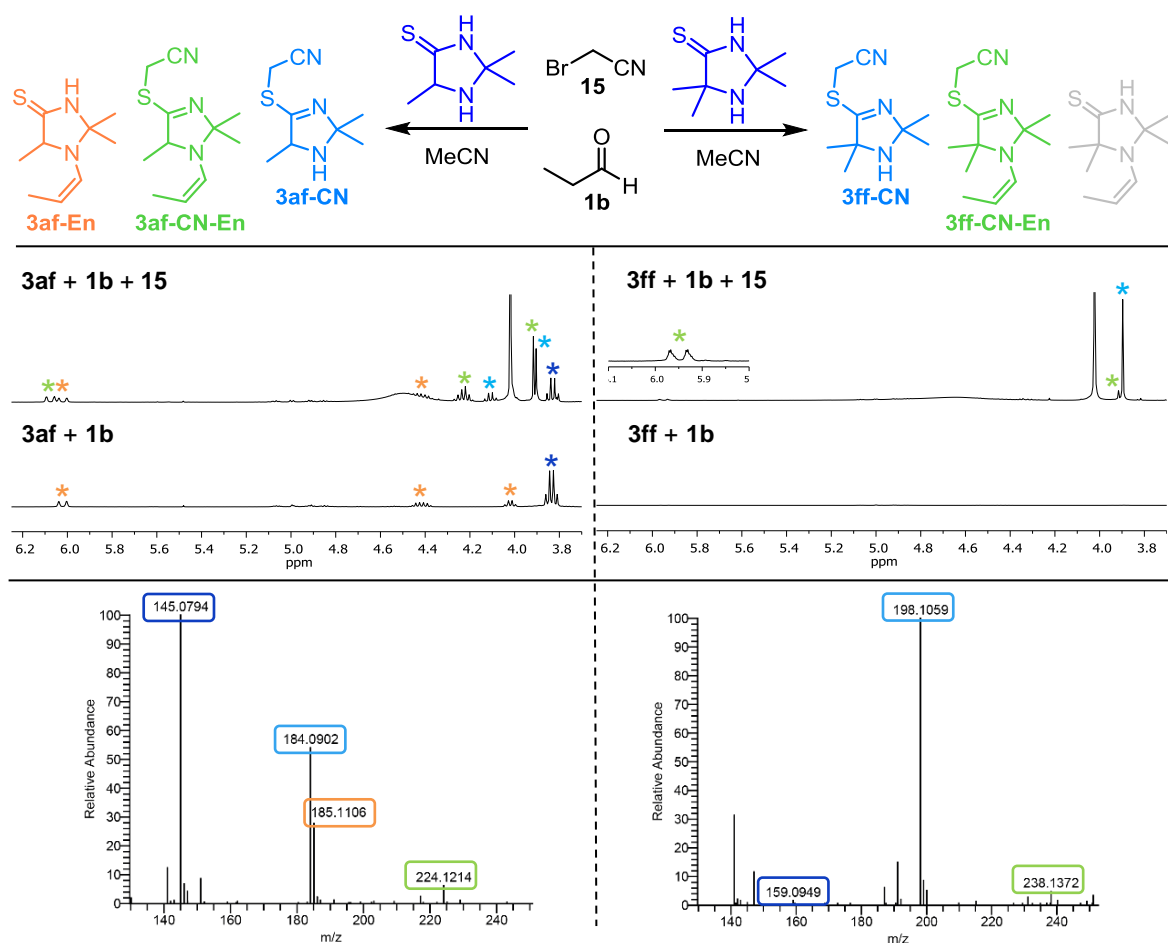
Figure 4.20: Imidazolidine-4-thione derivatives observed in the reaction mixture of **3af** (left) or **3ff** (right) with propionaldehyde **1b** and bromoacetonitrile **15** at room temperature. Middle: excerpt of the ^{1}H NMR spectra obtained 2 h after adding only **1b** and 5 h after adding **1b** and **15**. Bottom: mass spectra of the full reactant mixture obtained after 3 h.

This not only refers to the enamine of the *S*-alkylated species **3af-CN-En**, but also to the respective derivative of the imidazolidine-4-thione **3af-En**. The latter was not detectable for the active catalyst **3ff** at all. This indicates that a too stable enamine is not favourable, an observation which is consistent with recent reports on secondary amine catalysts that were deactivated by aldol reaction products.[204] In case of the tetramethylated imidazolidine-4-thione **3ff** the steric hindrance might promote the leaving tendency and thus accelerate product formation. This could also explain the significantly higher reaction rate of **3ff** compared to all other imidazolidine-4-thione catalysts, that was observed in our previous photoredox alkylation.[194]

While the steric influence on the enamine stabilities can explain the superior activity of the tetramethylated **3ff**, it would not cause the large differences between both trimethylated species **3fa** and **3af**. One explanation for this could be provided by different stabilities of the imidazolidine-4-thiones themselves throughout the catalysis. Here, hydrolysis of the heterocycle was shown to be possible under milder conditions if ring position 5 was not dialkylated. This exactly refers to the species **3af** and **3dd** with lower (photo-induced reaction) or no catalytic activity (dark reaction) in the studied α-alkylation.[179-180] The observation was explained with a corresponding better puckering of the ring since breaking of the *C*2-*N*3 bond is stereoelectronically facilitated if it is located as closely as possible antiperiplanar to the free electron pair of the amine. Indeed, no imidazolidine-4-thiones or their derivatives were clearly detected in the catalysis mixture of **3af** and **3dd** after 3 h at 40 °C with ^{1}H NMR or MS analysis. As the dark reaction requires the initial induction phase of pre-catalyst activation, simultaneous hydrolysis within this period of time consumes the needed heterocycle. If hydrolysis is too fast, no catalyst is left in the solution. In the photoredox approach, product **1b′** is formed from the beginning. Thus, the faster hydrolysis of monoalkylated imidazolidine-4-thiones in ring position 5, **3af** and **3dd**, led to reduced yields but still product formation.

Besides their successful application in a photoredox organocatalytic approach that is based on enamine catalysis, imidazolidine-4-thiones were now shown to enable the cyanomethylation of aldehydes without light. A completely new mechanism was proposed that makes use of the additional thioamide functionality to activate the alkylating halide after being previously activated by this reactant itself. Although photo-

induced processes on the early Earth can be explained with sun irradiation, this dark reaction excludes the necessity for alkylated pyridines as bases and generally extends the robustness and accessibility of prebiotic alkylations. Moreover, this catalytic transformation also provides a previously unknown pathway for modern chemistry with a reduced number of reagents required.

4.5.3 Nucleophilicity of Imidazolidine-4-thiones

For a better understanding of the reactivities of imidazolidine-4-thiones **3**, their nucleophilicities were investigated. Thereby, the differences between structural variants as well as in terms of the different reactive sites within one compound could be revealed. For this, the kinetics of their reaction with reference electrophiles had to be determined. The needed electrophiles and technical setup as well as valuable know-how and support was provided by the group of A. OFIAL. According to the linear free energy relationship [2], the nucleophile-specific parameters N and s_N can be calculated from experimentally determined second-order rate constants k_2 for their reactions with electrophiles of known electrophilic reactivity E.

$$\log k_2 (20\ °C) = s_N (N + E) \qquad [2]$$

As reaction partners, the four benzhydrylium ions **dma**, **morph**, **mfa**, and **pfa** were chosen since they had proven suitable in a recent study on the structurally related imidazolidinones (Scheme 4.12).[205-206] If the reference compounds are not electrophilic enough, no reaction occurs and if they are too electrophilic, the rate constants are determined by the rates of diffusion.
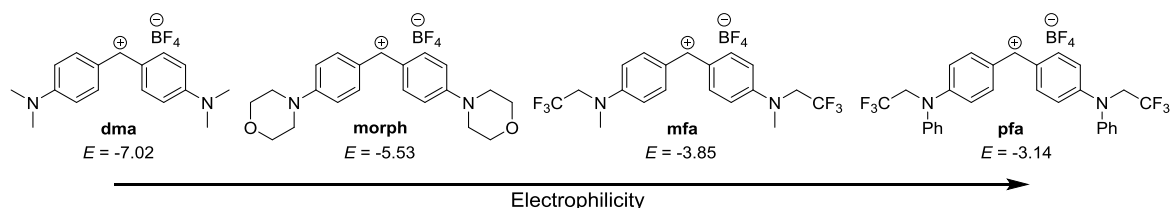
Scheme 4.12: Overview of the benzhydrylium salts used as reference electrophiles for the nucleophilicity determination of **3**. Electrophilicity parameters E were taken from the freely accessible database.[207]

The above investigation on the organocatalytic alkylation of propionaldehyde revealed that imidazolidine-4-thiones **3** possess a competing nucleophilic reaction centre to the amine: the thioamide sulphur. To ensure which nucleophilicities are going to be determined in the following kinetic measurements, a product study preceded

(Scheme 4.13). In an NMR experiment the benzhydrylium ion was treated with two equivalents of **3af** and quantitatively yielded the *S*-alkylated species. Thus, nucleophilic attack initially occurs by the sulphur atom of the thioamide and the obtained kinetics will refer to the *S*-nucleophilicity of the imidazolidine-4-thiones.
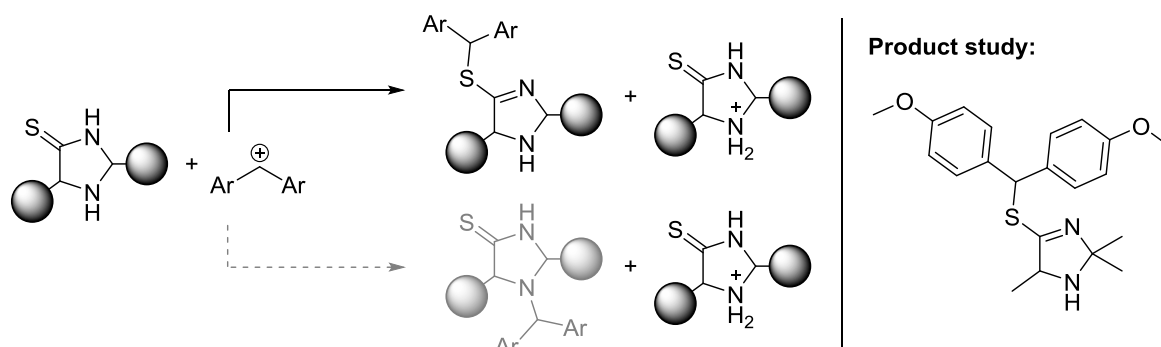
Scheme 4.13: Nucleophilic substitution reaction of **3** with benzhydrylium ions. Left: Proposed potential substitution centres of **3** and the corresponding resulting products. Right: Product of the reaction of **3af** with a benzhydrylium chloride, identified by NMR spectroscopy.

All reactions were performed in acetonitrile at 20 °C using an at least 10-fold excess of imidazolidine-4-thione to electrophile to achieve pseudo-first-order kinetics. With a stopped-flow technique the bond formation was monitored photometrically by following the decay of the coloured cationic electrophile (Figure 4.21, left). From the mono-exponential decay of the electrophile absorption, first-order rate constants k_{obs} (s^{-1}) can be obtained by least-squares fitting of the single-exponential function $A_t = A_0 \exp(-k_{obs}t) + C$ to the time-dependent absorbance A_t. Linear correlation of the first-order rate constant k_{obs} with the initial concentration of imidazolidine-4-thione **3** enables the determination of the second-order rate constant k_2 from the respective slope (Figure 4.21, middle).
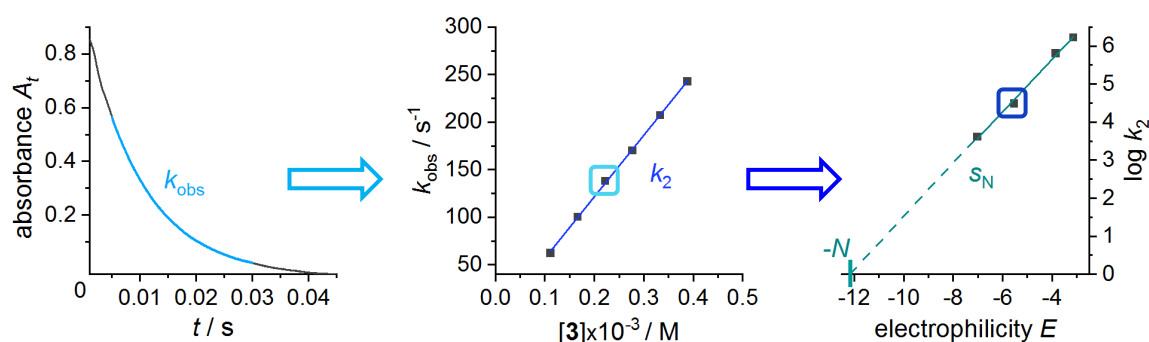
Figure 4.21: General workflow of the kinetic method to determine the nucleophilicity. Left: Determination of pseudo-first-order rate constant k_{obs}. Middle: Determination of second-order rate constant k_2. Right: Determination of nucleophilic parameters s_N and N.

By plotting the k_2 values for the reactions of **3** with all four electrophiles versus the corresponding electrophilicity parameters E, the nucleophilicity parameters can now be

derived (Figure 4.21, right). Based on equation [2], the slope of the linear correlation refers to the nucleophile-specific parameter s_N and from the intercept with the abscissa, the nucleophilicity N can be calculated.

However, initial studies on the reaction of imidazolidine-4-thione **3fa** with **mfa** revealed no linear increase of k_{obs} with **3fa** concentration (Figure 4.22 a).
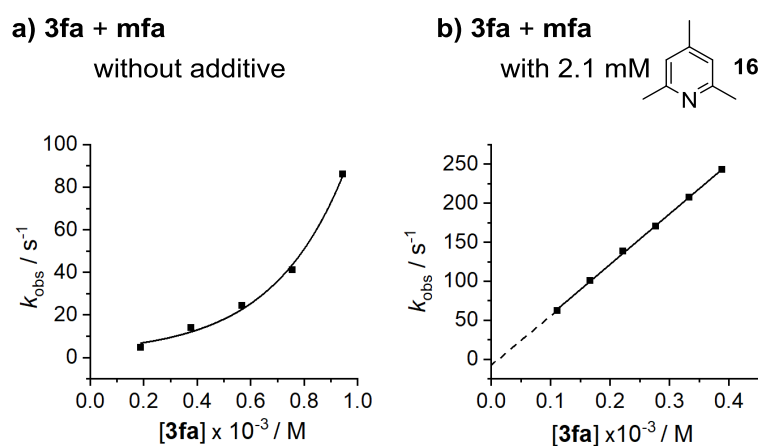
Figure 4.22: Effect of adding alkylated pyridine bases to achieve second-order kinetics. Comparison of the reaction of **3fa** with a) **mfa** (1.37 x 10^{-5} M) without additive and b) **mfa** (9.45 x 10^{-6} M) with **16**.

This higher order in imidazolidine-4-thione can occur if the deprotonation step is rate determining and has already been observed for various nucleophiles.[205] If deprotonation of the cation generated in the first step is slower than the back reaction, the deprotonation and not the nucleophilic attack is rate-determining. To shift the equilibrium to the product side, AN *et al*. added alkylated pyridine bases.[205] Also in the case of the imidazolidine-4-thiones, adding either collidine **16** or 2,6-di-*tert*-butyl-4-methyl-pyridine **17** led to a linear correlation and thus second-order kinetics (Figure 4.22 b). The derived second-order rate constants k_2 for the reactions of **3fa** with all four electrophiles were plotted versus the corresponding electrophilicity parameters E and showed a linear correlation (Figure 4.23).
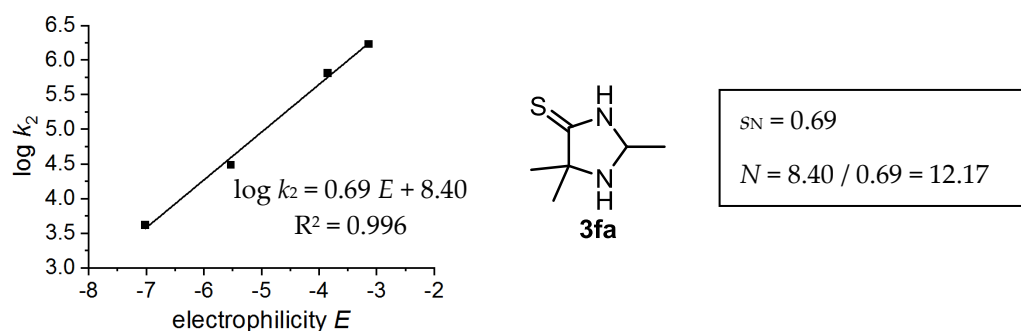
Figure 4.23: Determination of nucleophilic parameters of **3fa**. Plot of log k_2 versus E of the corresponding reference electrophiles in acetonitrile at 20 °C and derivation of the resulting parameters s_N and N.

The kinetic measurements were repeated for the reversed substituted imidazolidine-4-thione **3af**, the achiral **3ff**, as well as both diastereomers of **3dd** with **dma**, **morph**, and **mfa**. The resulting second-order rate constants k_2 as well as nucleophilic parameters are presented in Table 4.4.

Table 4.4: Obtained second order rate constants and nucleophilicities of imidazolidine-4-thiones **3** in acetonitrile at 20 °C. The corresponding nucleophilic centre is highlighted in blue.

		3fa	3af	3ff	trans-3dd	cis-3dd	3fa-Bz	3ff-Bz	3ff-N3-Me
k_2 $(M^{-1}s^{-1})$	dma	4.14×10^3	3.81×10^3	1.98×10^3	1.76×10^3	1.35×10^3		kinetics could not be determined	
	morph	3.07×10^4	3.49×10^4	3.27×10^4	2.60×10^4	2.41×10^4	2.00×10^3		
	mfa	6.46×10^5	5.17×10^5	7.33×10^5	5.49×10^5	4.43×10^5	3.41×10^4		
	pfa	1.69×10^6					1.34×10^5		
N		12.17	12.39	11.11	10.98	11.03	9.67		
s_N		0.69	0.67	0.81	0.81	0.79	0.78		

The similarity of the obtained N values indicated a low influence of the alkyl residues, which also supports the assumption of a reaction at the sulphur atom. The shielding of the amine is drastically changed by the different vicinal substituents and would thus affect its nucleophilic reactivity more strongly. Especially substituents on both faces of the ring would have a significant impact. AN *et al.* showed that *trans*-substituted imidazolidinones are 20 times less reactive than their *cis*-isomers. Further, dimethylation at one carbon next to the secondary amine reduced the nucleophilicity by two orders of magnitude.[205] The nucleophilic reactivity of the secondary amine in catalyst **3ff** is thus expected to be much lower compared to the other imidazolidine-4-thiones. To determine these values, the kinetics of the benzylated derivatives **3ff-Bz** and **3fa-Bz,** as well as the thioamide-*N*-methylated species **3ff-N3-Me** were measured to prevent the reaction at the sulphur and instead enable the nucleophilic attack by the amine functional group. As expected, the nucleophilicity of the thioamide-protected imidazolidine-4-thione **3fa-Bz** (the amine functionality) was lower compared to **3fa** (the thioamide sulphur). The reactions of **3ff-Bz** and **3ff-N3-Me** did not follow second-order kinetics. Even the most reactive electrophile **pfa** was barely consumed and the equilibrium could not be shifted significantly with increasing base concentration. The high steric shielding from both sides of the ring as well as both sides of the amine does not provide enough space for a stable bond formation with the sterically demanding benzhydrylium ions. For successful nucleophilicity

determination of these imidazolidine-4-thione derivatives, other types of electrophiles with comparable reactivity could be studied. Also for the determination of the amine-nucleophilicity of non-alkylated imidazolidine-4-thiones, the carbocation methodology could be replaced with different electrophiles.

Concluding, the second-order rate constants k_2 indicate that the nucleophilic reactivity of the amine in **3** is at least one order of magnitude lower than of the thioamide sulphur, which explains the observed initial *S*-cyanomethylation during pre-catalyst activation in the investigated alkylation of propionaldehyde (Section 4.5.2). This characteristic is of particular interest as alkylation of the amine is often observed as deactivation mechanism of secondary amine catalysts in attempts to achieve organocatalytic α-alkylation. In imidazolidine-4-thiones, the competing *S*-alkylation allows for a free amine for enamine formation. Further, the nucleophilicity of both reactive centres is higher than for the MacMillan imidazolidinones but lower than for most of the pyrrolidines (Figure 4.24). Since the latter are highly active catalysts for aldol reactions, a comparable reactivity would consume the reactant aldehyde in this competing reaction and prevent alkylation or other functionalisation.
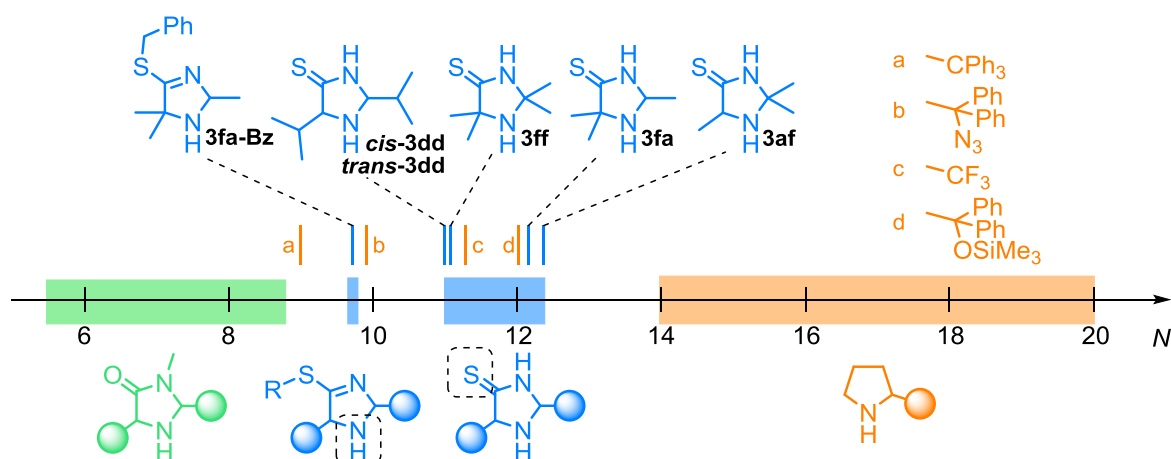
Figure 4.24: Nucleophilicity ranges of imidazolidinones (green), imidazolidine-4-thiones (blue), and pyrrolidines (orange).

The nucleophilicity of imidazolidine-4-thiones thus balances the reactivities of both these classes of established organocatalysts. This area seems to be beneficial for catalysing the alkylation of aldehydes which might also be the case for further transformations.

4.6 Evolution on the Molecular Level

Our current living biosystem is the result of ever-changing organisms over the past million years. This process is driven by the natural selection of species that are able to better adapt to their surroundings leading to a survival advantage known as Darwinian evolution. The underlying mutations happen at the level of genes that encode the different biological traits and inherit them to future generations. Considering the high complexity of these mechanisms, an identical process is not conceivable on the primitive Earth. However, a much simpler preceding analogue could have existed to explain the stepwise evolution of abiotic to biotic matter. In view of the experimental findings in this work, the dynamic imidazolidine-4-thione organocatalysts seems promising in representing a first form of evolution on the molecular level.[208]

Repetitive production as preceding reproduction

The mechanism of reproduction and inheritance as characteristic of Darwinian evolution requires processes too complex for the prebiotic feedstock. The possibility of repetitive production over a long time period under various conditions would be a sufficient alternative to guarantee an evolutionary behaviour. As presented in Section 4.1.2, imidazolidine-4-thiones readily assemble out of carbonyl compounds in the presence of ammonia, cyanide and hydrogen sulphide over a range of conditions. These are all prebiotically abundant molecules which makes the ongoing production of these organocatalysts on the early Earth very likely.

Molecular mutation by variation of the building blocks

The synthesised library of imidazolidine-4-thiones (Table 4.1) demonstrates that this class of molecules can form from a variety of carbonyl compounds. A change in prevailing aldehydes or ketones thus automatically leads to a structural mutation of the catalyst by incorporation of the carbonyls present. Moreover, the reactant pool is not only influenced by temporal or local differences due to external impacts but can be varied by the imidazolidine-4-thiones themselves. As shown in Section 4.5, they are capable of catalysing the α-cyanomethylation of aldehydes with and without the presence of light, thereby modifying their own building blocks into new starting material. As the catalytic abilities of these organocatalysts are most likely not limited to the transformations presented in this work, further functionalisation reactions and thus self-induced

mutations are conceivable. To test the proposed possibility of building a second generation of imidazolidine-4-thiones out of their self-modified building blocks, the cyanomethylated propionaldehyde **1b'** should get incorporated into the catalyst skeleton (Scheme 4.14). Due to the low isolable yield of **1b'**, the aldehyde was first reacted with the secondary aminonitrile **2f** to omit the additional step of aminonitrile formation. However, no imidazolidine-4-thione **3fb'** formation was detected by NMR spectroscopy or mass spectrometry. In a second approach, **1b'** was first successfully converted into the respective α-aminonitrile **2b'** by treatment with potassium cyanide and ammonium chloride in ammonia. Subsequent reaction with acetone **1f** and hydrogen sulphide in ammonia yielded the desired heterocycle **3b'f**, a 2nd generation catalyst.[208] Even though the yield was only 3 %, it represented a proof of concept.
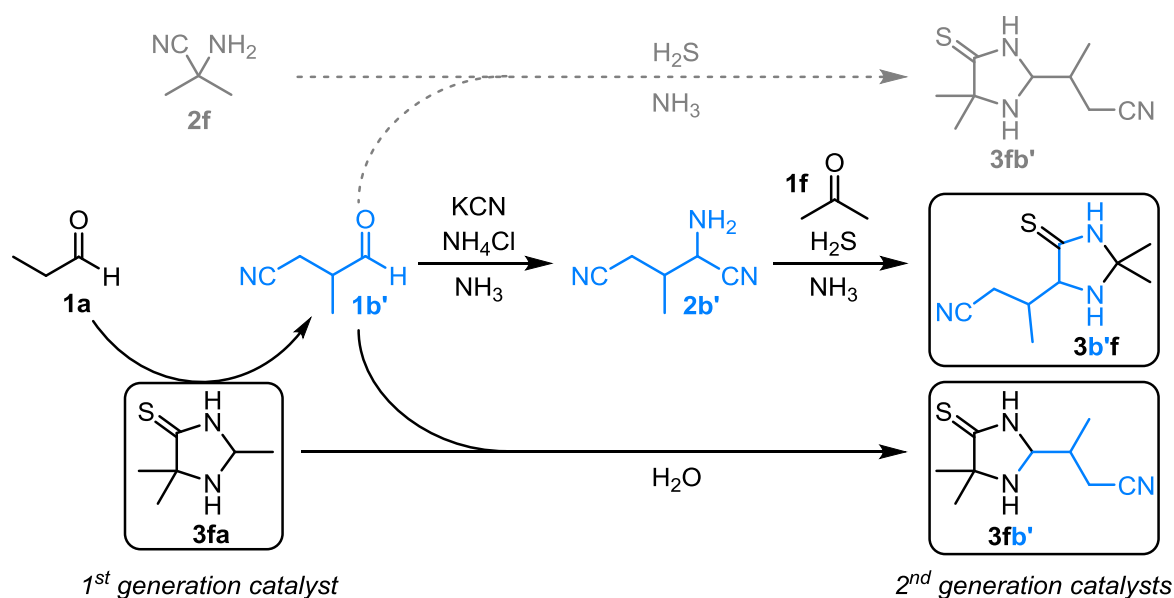
Scheme 4.14: Mechanisms for the molecular self-mutation of imidazolidine-4-thiones. A 2nd generation of catalysts is formed through incorporation of the self-functionalised aldehyde **1b'** in ring position 5 via aminonitrile **2b'** and successive ring formation or in ring position 2 by dynamic carbonyl exchange from a 1st generation catalyst.

Another variation mechanism is provided by the dynamic exchange of carbonyl building blocks at ring position 2 in water (Section 4.2.2). Providing the advantage of possible structural mutation without the need for additional reactants, ongoing adaption of the catalyst to the surroundings is feasible. To again verify this hypothesis for the formation of a 2nd generation of imidazolidine-4-thiones, **3fa** was stirred in water with the cyanomethylated aldehyde **1b'**. Satisfyingly, with this method **3fb'** was formed and successfully isolated in 2 % yield.[208]

Both pathways show that structural mutations can easily occur and are not limited to non-functionalised carbonyl compounds. Thus, the imidazolidine-4-thiones can (self-)vary to adapt to their environment or gain a new or better function. As is true for the Darwinian biological evolution, mutations can be random and do not necessarily result in improvement. Which structure prevails is a question of selection.

Selection

The selection of single imidazolidine-4-thiones **3** could be based on a preference in their formation or a superior function. In Section 4.3, the selectivity of formation was extensively discussed which revealed that individual structures are indeed favoured depending on the reaction medium. In ammonia, the incorporation of acetone prevailed with a significant selectivity for the formation of **3fa**. Remarkably, exactly this compound was the most active chiral catalyst in the α-cyanomethylation of propionaldehyde (Section 4.5). In pure water, the selectivity for acetone switched to a more uniform distribution with a low insertion of the ketone. Although the proportion of the higher active catalysts decreased in this scenario, it favoured the formation of chiral imidazolidine-4-thiones, important for the transfer of stereoinformation. Moreover, we cannot select for a function that is not there yet. Only a small number of catalytic transformations were tested so far and the primarily formed species in pure water might be the most efficient or selective for undiscovered ones. Independent of the corresponding function of selected imidazolidine-4-thiones, the potential of changing selectivity opens up the possibility of driving such a system out of equilibrium.

Concluding, a first form of evolution on the molecular level is presented (Figure 4.25).
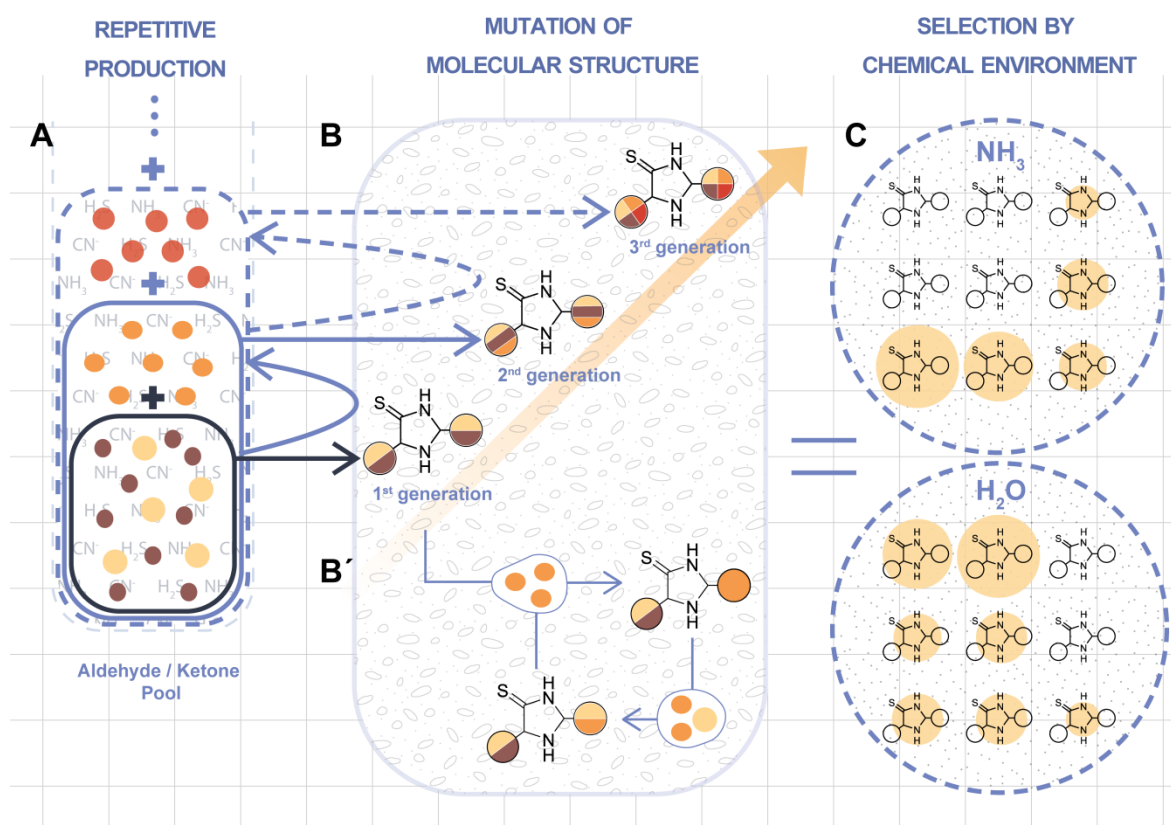
Figure 4.25: Molecular evolution of imidazolidine-4-thione organocatalysts on the early Earth. Solid arrows refer to implemented pathways towards 2nd generation organocatalysts, dashed lines represent conceivable molecular mutations to next generations. The Figure was adapted from the submitted manuscript of Closs and Trapp.[208]

Imidazolidine-4-thiones **3** can continuously form out of a prebiotically plausible feedstock that is catalytically functionalised and extended by them (A). New aldehydes and ketones provide the starting point for higher generations of catalysts (B) or can be subsequently incorporated into already existing structures (B'). These mutations enable a dynamic change in structure over time. Finally, certain species are preferred over others to allow for a selection process (C). Ongoing research on additional catalytic transformations as well as the catalytic activity of 2nd generation imidazolidine-4-thiones seems promising in extending the versatility and selectivity of applications. Especially the latter investigations could proof superior behaviour of higher generations and thus not only the capability of self-variation but self-optimisation. This molecular evolution of imidazolidine-4-thiones not only transfers the complex mechanisms of Darwinian evolution to primitive early Earth conditions but might represent a pre-existing analogue that has been replaced over millions of years by a more sophisticated system through evolutionary natural selection.

5 Conclusion and Outlook

In view of the emergence of versatile complexity from a simple feedstock on the early Earth, this thesis investigated organocatalysis as powerful tool for the origin of life. A prebiotically plausible and active organocatalyst had to be discovered that, at best, is able to change over time to adapt to its ever-evolving environment. Throughout the presented study on imidazolidine-4-thiones, all these criteria were met, culminating in a first form of evolution on the molecular level comprising the three processes of *repetitive production*, *mutation*, and *selection* (Figure 5.1).
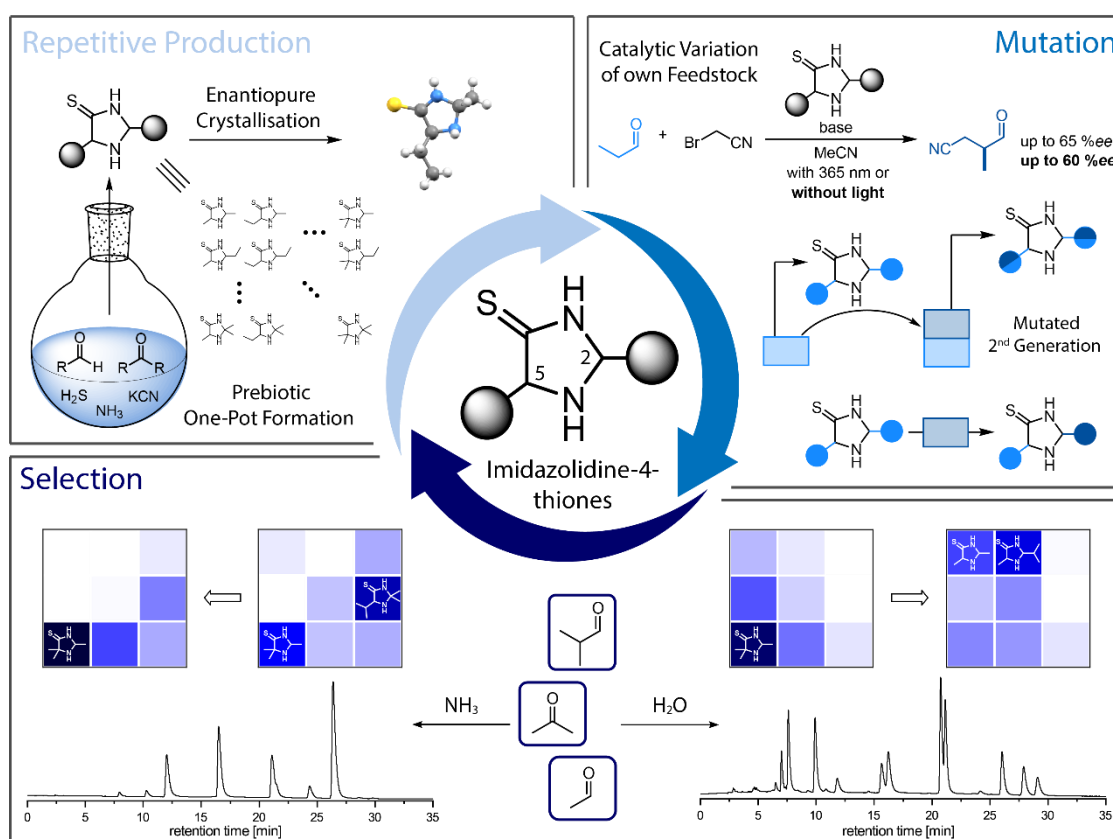
Figure 5.1: Graphical summary of the investigations on imidazolidine-4-thiones as prebiotic organocatalysts that led to a first form of molecular evolution: Robust and highly plausible self-assembly out of one-pot mixtures (*repetitive production*); Organocatalytic α-alkylation of aldehydes and incorporation of these alkylated aldehydes into the molecular structure (*mutation*); Selectivity studies with HPLC revealed distinct preferences in the formation depending on the reaction medium (*selection*).

Regarding their plausible prebiotic formation, a library of imidazolidine-4-thiones **3** was synthesised in aqueous ammonia from plausible α-aminonitriles **2**, H_2S, and carbonyl compounds **1**. In addition to ketones, prebiotically more abundant aldehydes were included as building blocks, which has previously not been possible via this pathway. To further simplify the synthetic approach to an even more realistic scenario, the formation

of imidazolidine-4-thiones **3** was realised out of a one-pot aqueous solution of a carbonyl compound, cyanide, H_2S, and ammonia in isolable amounts. Detailed analysis of the intermediates and side-products under various conditions revealed a robust self-assembly of imidazolidine-4-thiones and thus a not only plausible but rather unavoidable existence of these molecules on the early Earth (Figure 5.1, *repetitive production*). Upon crystallisation out of the formed racemic mixture, an enantiopure crystal was observed. These conglomerates are rare but widely discussed as potential source for symmetry breaking by spontaneous resolution. Finding this characteristic in an organocatalyst provides the additional benefit of transferable stereoinformation via asymmetric catalysis and thus a potential role in the emergence of a homochiral world.

To verify the catalytic activity of imidazolidine-4-thiones **3** in prebiotically plausible and relevant transformations, the α-alkylation of small aldehydes was chosen to access increasing molecule size as well as versatile functionalisation. This reaction has not been feasible under prebiotic conditions so far and also proven challenging in modern chemistry. Inspired by the procedure of MACMILLAN, who achieved alkylation by coupling enamine catalysis with photoredox activation, our group has adapted the process of cyanomethylation to prebiotically plausible conditions making use of sun irradiation. Here, propionaldehyde is converted with bromoacetonitrile in acetonitrile using alkylated pyridines found on meteorites as base and excluding the photosensitiser as well as the need for an inert atmosphere. Satisfyingly, imidazolidine-4-thiones **3** successfully catalysed this reaction, yielding the product aldehyde in up to 78 % yield and 65 %*ee* (Figure 5.1, *mutation*). By this, catalysts **3** enabled completely prebiotic conditions as well as exceeded the activity of the non-prebiotic MacMillan imidazolidinone.

Although the described process of α-cyanomethylation of propionaldehyde is plausible on a primitive Earth, it still limits the location to the presence of sun irradiation as well as alkylated pyridine bases. This thesis further extended the accessibility of this α-alkylation by discovering a purely organocatalytic approach in the dark that is not dependant on the specific bases mentioned above. Simply reacting propionaldehyde with bromoacetonitrile in the presence of a base and catalytic amounts of **3** gave the desired cyanomethylated aldehyde (Figure 5.1, *mutation*). So far, such a direct catalytic conversion with alkyl halides has not been feasible even in modern chemistry and, instead, always needed light

or additional alkyl-activating reagents. After comprehensive investigations with ¹H NMR spectroscopy and HR-MS on the course of reaction, reaction intermediates, and selective protection of potential reactive sites, a new mechanism was proposed (Figure 5.2).
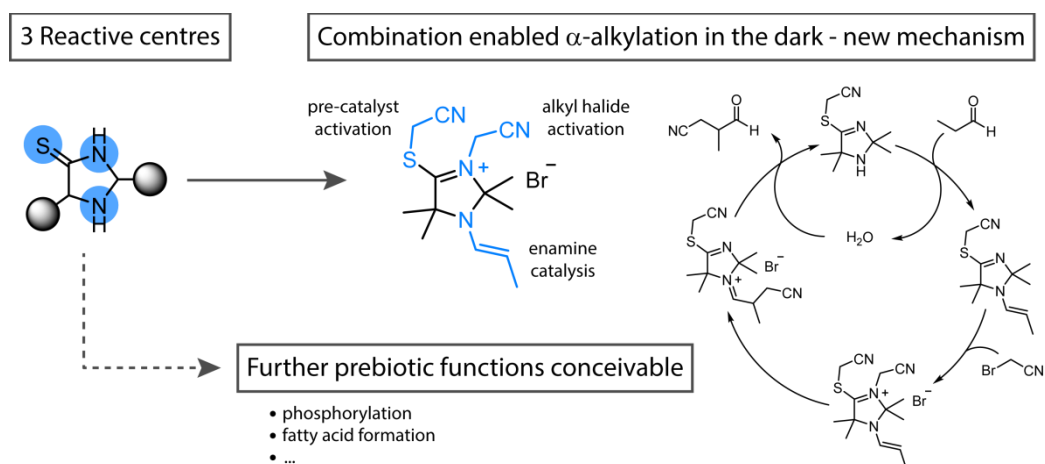
Figure 5.2: Graphical summary of the investigations on the reactivity of imidazolidine-4-thiones: Mechanistic studies on the purely organocatalytic α-alkylation of aldehydes revealed participation of all reactive centres.

In contrast to other secondary amine organocatalysts used to enable this transformation via enamine catalysis, imidazolidine-4-thiones **3** provide two additional reactive centres at the sulphur and nitrogen atom of the thioamide functional group. Here, **3** is initially alkylated at the thioamide sulphur to form the active catalyst. This *S*-cyanomethylated structure now activates the aldehyde as enamine as well as the alkyl halide as ammonium salt. While initial experiments indicated the following C-C bond forming step to occur intramolecularly, quantumchemical calculations are currently performed to further exclude the intermolecular alternative.

Further insight into the reactivity of the different reactive centres was gained by determination of the corresponding nucleophilic parameters. The nucleophilic reactivity of the thioamide sulphur turned out to be approximately one order of magnitude higher than that of the amine which supported the finding of initial *S*-cyanomethylation. This characteristic prevented amine *N*-alkylation which is often reported as critical deactivation of the catalyst in alkylation reactions. Compared to established organocatalysts, all nucleophilicities of **3** are higher than those of the MacMillan imidazolidinones but lower than those of most pyrrolidines. Thereby, the competing aldol reaction, efficiently catalysed by the latter, is not as present which leaves the aldehyde substrate for the desired α-alkylation.

With catalysing the alkylation of aldehydes, imidazolidine-4-thiones not only extended the pool of prebiotic molecules but also modified their own building blocks, thereby providing new feedstock material. Successful incorporation of the alkylated aldehyde into the imidazolidine-4-thione skeleton verified the potential of this dynamic (self-)mutation (Figure 5.1, *mutation*). As new carbonyl species become available over time through local differences, meteoritic transport, or catalytic functionalisation, the catalyst can evolve (itself) into higher generations. These changes of the molecular structure can be associated with changes in the catalytic ability and selectivity, potentially resulting in new functions. In addition, a second variation mechanism was observed that allows for ongoing mutation even in the absence of hydrogen sulphide, ammonia, and cyanide. Simply by stirring **3** with different aldehydes in water, the carbonyl moiety in ring position 2 was exchanged. Further, both ketones and aldehydes were released but only the latter were integrated which selectively guarantees the chirality of the catalyst.

Moreover, the selectivity in the formation of imidazolidine-4-thiones **3** from a realistic prebiotic pool of aldehydes and ketones **1** was extensively studied. An analytical method for the separation of aminonitriles **2** (CE), the products of the first synthesis step, and of the imidazolidine-4-thiones **3** (HPLC) was developed. Various substrate mixtures of each building block were applied in the two-step synthesis as well as the one-pot reaction to analyse the resulting ratio of products. Here, the second step of formation – the condensation of aminonitrile **2** with H_2S and aldehyde/ketone **1** – turned out to determine the selectivity. In concentrated aqueous ammonia, a significant preference for the incorporation of acetone was observed, especially in ring position 5. Notably, these favoured structural variants as well as the preferentially formed *trans*-isomers also revealed superior activity and enantioselectivity in the investigated catalysis. Transferring the formation of **3** to water revealed an opposing influence on the product distribution and thus the reaction medium as a possible mode of selection (Figure 5.1, *selection*).

The dynamic interplay of the here presented properties – highly plausible formation (*repetitive production*), (self-)variation of the molecular structure (*mutation*), selectivity for certain species (*selection*) – enabled imidazolidine-4-thiones to provide a first form of molecular evolution on the early Earth. Besides conceptually demonstrating the possibility of such a process in the pre-Darwinian world, this class of organocatalysts

represents a simple but powerful system for catalysing and assisting the emergence of complexity and homochirality. Considering the discovered potential of their multiple reactive sites and the number of prebiotic transformations that are still inaccessible or incompatible, the catalytic possibilities of imidazolidine-4-thiones in an early Earth scenario are far from exhausted. Preliminary results on their application in the Formose reaction, the much needed selective phosphorylation of nucleosides as well as the so far unfeasible formation of lipids are promising and further strengthen their prebiotic relevance. In view of an ongoing evolution, a selection of higher generation catalysts in terms of preferential formation or superior catalytic behaviour would be highly interesting. Further catalysed functionalisations of aldehydes would additionally lead to further possible mutations and thus generations of the imidazolidine-4-thiones with unpredictable prebiotic potential.

Although this thesis aimed to investigate imidazolidine-4-thiones **3** regarding their relevance on the early Earth, it did not limit their potential to this context. The discovery of their ability to catalyse the α-cyanomethylation of aldehydes without the need for additional reagents or photo-induction could also benefit modern chemistry. This simple way of catalysing the alkylation with alkyl halides has not been succeeded so far and could be optimised as well as extended to further functionalisations. Instead of restricting the catalytic activity of catalysts **3** to their amine for enamine or H-bonding catalysis, the presented (combined) potential of the thioamide could be used to improve current or access new organocatalytic transformations.

6 Experimental Section

6.1 Chemicals and Instruments

All solvents and chemicals were purchased from commercial sources (abcr GmbH, Acros Organics b.v.b.a., Sigma-Aldrich Co. LLC, Strem Chemicals Inc. and TCI Europe N.V.) and stored according to the respective instructions. Argon gas (Ar 5.0) and hydrogen sulphide gas (H_2S 5.0) were purchased from Air Liquide Deutschland GmbH. Propionaldehyde was distilled and stored under argon at -20 °C prior to the organocatalytic reaction. Isolated compounds were stored under argon at -20 °C.

NMR spectroscopy

NMR spectra were recorded on a 400 MHz Bruker Avance III HD spectrometer and a 600 MHz Varian NMR-System with a CryoProbe Prodigy. Spectra were calibrated using the residual solvent peaks. Chemical shifts δ are reported in ppm and coupling constants J in Hz. The different multiplicities are defined by s (singlet), d (doublet), t (triplet), q (quartet), sext (sextet), m (multiplet), bs (broad singlet) or by combinations of these. The assignment of all signals was realized by two-dimensional NMR spectroscopy (COSY, HSQC, HMBC). Atom numbering for NMR assignments is not based on IUPAC. Numbers separated by "," refer to an assignment of both atoms, numbers separated by "/" refer to an assignment of one of the atoms. Magnetically inequivalent hydrogen atoms of the same carbon atom are differentiated by a and b.

Mass Spectrometry

Mass spectrometric analysis was performed using a Thermo Scientific Q Exactive Plus mass spectrometer coupled to electrospray ionization (ESI) by direct injection. As injection solvent, 80:20 isopropanol:water with 0.05 % formic acid at a flow rate of 0.05 mL/min was used. The sample was dissolved in acetonitrile or distilled water and the mass spectrometer was operated in full scan measuring in positive and negative mode. The capillary temperature was at 250 °C, spray voltage at 4.2 kV (positive mode) or 3.5 kV (negative mode), sheath gas flow rate at 2 µL/min and auxiliary gas flow rate at 3 µL/min.

<u>HPLC-Analysis</u>

Analytical HPLC measurements were performed on an Agilent Series 1200 Infinity system equipped with a high-performance autosampler model HiP-ALS SL+ and a G1315D photodiode array detector (DAD) coupled to a 6120 Quadrupole LC/MS detector with atmospheric-pressure chemical ionization (APCI). The peaks were detected at 270 nm. The separation of different imidazolidine-4-thiones was performed with a 4.6 mm x 250 mm EC Nucleodur 100-5 (Macherey Nagel) at 20 °C and a flow of 1.00 mL/min. 1 µL of the sample was injected and eluted using a gradient elution of *n*-hexane and isopropanol. The analytical isomer separation was performed with a 4.6 mm x 250 mm Chiralpak IC (Cellulose tris(3,5-dichlorophenylcarbamate) immobilized on 5 µm silica-gel) at 20 °C and a flow of 1.00 mL/min. 2 µL of the sample were injected and eluted with mixtures of *n*-hexane and isopropanol.

Preparative HPLC for isomer separation was performed on an Agilent Series 1260 Infinity semi-preparative LC system with a 20 mm x 250 mm Chiralpak IC (Cellulose tris(3,5-dichlorophenylcarbamate) immobilized on 5 µm silica-gel) additionally equipped with a Chiralpak IC guard column (20 mm x 10 mm) at 20 °C and a flow of 20.0 mL/min.

<u>GC-Analysis</u>

GC analysis of the one-pot mixture of aldehyde and hydrogen sulphide in ammonia was performed with a Thermo Scientific Trace GC Ultra with split injector (15 mL/min) and a flame ionization detector at 250 °C. The instrument was coupled to an ISQ single quadrupole on electron impact (EI) mode operated at 70 eV. The temperatures of the injection, transfer interface, and ion source were set to 250 °C, 300 °C, and 200 °C, respectively. An SE-30 column (dimethylpolysiloxane, 25 m x 250 µm i.d., 250 nm film thickness) was used as stationary phase. 0.1 µL samples were injected and helium was used as the carrier gas at a constant pressure of 80 kPa. The starting temperature of 70 °C was held for 5 min before raising it with a gradient of 3 K/min until 220 °C which was again held for 5 min.

Chiral GC analysis of the α-cyanomethylation of propionaldehyde was performed with a Thermo Scientific Trace GC with split injector (30 mL/min) and a flame ionization detector at 250 °C. A fused-silica capillary coated with heptakis(2,3-di-O-methyl-6-O-TBDMS) β-cyclodextrin in PS 086 (8.5 m x 250 µm i.d., 250 nm film thickness) was used as stationary

phase. 0.1 μL samples were injected and separation was obtained at a constant temperature of 50 °C using helium as the carrier gas at a constant pressure of 150 kPa.

CE-Analysis

CE-Analysis was performed with a 3D CE ChemStation by Agilent Technologies. The experiments were performed in a bare fused silica capillary provided by MicroQuartz with a total length of 80 cm and an effective length of 71.7 cm. the samples were injected hydrodynamically by applying a pressure of 200 mbar s^{-1} and detected by contactless conductivity detection. 2 M acetic acid was used as running buffer.

Crystal Structure Analysis

X-ray crystallographic analyses were performed on a Bruker D8 Venture TXS. The data sets were recorded using Mo Kα (λ = 0.71073 Å) radiation. Intensities were corrected for Lorentz and polarization effects.

Kinetic Measurements with Stopped-Flow UV-Vis Spectroscopy

The kinetics of the reactions of imidazolidine-4-thiones **3** with benzhydrylium ions were followed by UV-Vis spectroscopy using a stopped-flow spectrophotometer system (Applied Photophysics SX.18MV-R or SX20 Stopped Flow Spectrometers; 10 mm light path). Stock solutions of **3**, benzhydrylium ions, and pyridine bases were prepared in anhydrous acetonitrile, freshly distilled over phosphorus pentoxide. The kinetic runs were initiated by first mixing equal volumes of acetonitrile solutions of the bases and the electrophiles and second mixing equal volumes of these mixtures and acetonitrile solutions of **3**. For the resulting concentrations of the reactants, the following mixing ratio has to be taken into account:

[**3**]*   [base]*   [electrophile]*

measurement :   [**3**] = 0.5 x [**3**]*
                [base] = 0.25 x [base]*
                [electrophile] = 0.25 x [electrophile]*
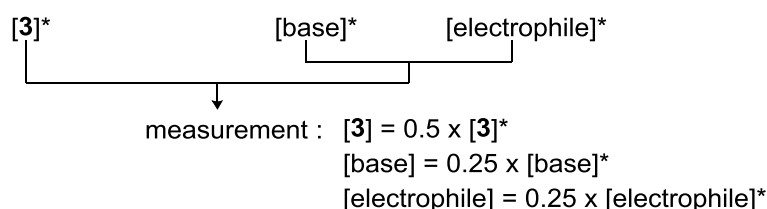
The temperature of the solutions during the kinetic studies was maintained at 20 ± 0.2 °C by using a circulating bath cryostat.

6.2 Synthetic Procedures and Characterisation of Isolated Compounds

6.2.1 α-Aminonitriles
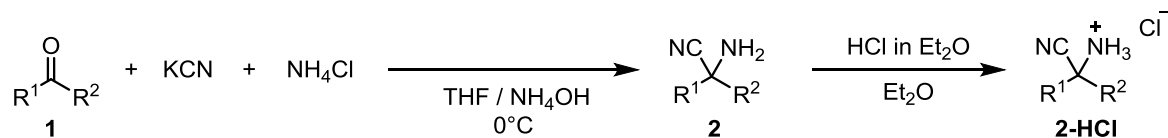
General Procedure GP-1

The respective aldehyde or ketone **1** (25 mmol, 1.0 eq.) was dissolved in a mixture of 7.5 mL tetrahydrofuran and 1.75 mL concentrated aqueous ammonia (28 – 30 %). Ammonium chloride (1.34 g, 25 mmol, 1.0 eq.) and potassium cyanide (1.63 g, 25 mmol, 1.0 eq) were added and the suspension was stirred for 1.5 h (7 h for a ketone). 7.5 g sodium sulfate and 20 mL diethyl ether were added and the mixture was stirred for 30 min (12 h for a ketone). The solution was decanted and the residue washed with 20 mL of diethyl ether. The organic phases were combined and concentrated *in vacuo*. The residual oil was dissolved in 20 mL of diethyl ether and 12.5 mL of HCl in diethyl ether (2M) were added. The precipitate was filtered off and recrystallized from acetonitrile to yield the hydrochloride salt of the amino nitrile **2-HCl** as a white solid.

1-Cyanoethan-1-aminium chloride (2a-HCl)
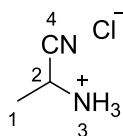
1.39 mL of acetaldehyde **1a** (1.10 g, 25.0 mmol, 1.0 eq.) were treated with **GP-1** to yield **2a-HCl** as white solid (0.78 g, 7.3 mmol, 29 %).

¹H NMR (400 MHz, DMSO-d_6) δ = 9.08 (bs, 3H, H³), 4.55 (q, J = 7.0 Hz, 1H, H²), 1.54 (d, J = 6.9 Hz, 3H, H¹).

¹³C NMR (101 MHz, DMSO-d_6) δ = 117.8 (C⁴), 36.3 (C²), 16.8 (C¹).

1-Cyanopropan-1-aminium chloride (2b-HCl)
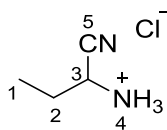
1.80 mL of propionaldehyde **1b** (1.46 g, 25.0 mmol, 1.0 eq.) were treated with **GP-1** to yield **2b-HCl** as white solid (1.46 g, 12.0 mmol, 48 %).

HRMS (EI, 70 eV) m/z: calculated for $C_4H_8N_2$ [M-HCl]$^+$: 84.0682, found: 84.0683.

^{1}H NMR (400 MHz, DMSO-d_6) δ = 9.31 (bs, 3H, H^4), 4.54 – 4.46 (m, 1H, H^3), 2.02 – 1.76 (m, 2H, H^2), 1.06 – 0.97 (m, 3H, H^1).

^{13}C NMR (101 MHz, DMSO-d_6) δ = 116.8 (C^5), 41.8 (C^3), 23.9 (C^2), 9.4 (C^1).

1-Cyanobutan-1-aminium chloride (2c-HCl)
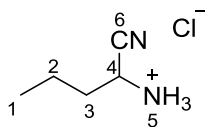
2.25 mL of butyraldehyde **1c** (1.80 g, 25.0 mmol, 1.0 eq.) were treated with **GP-1** to yield **2c-HCl** as white solid (1.21 g, 8.7 mmol, 35 %).

HRMS (EI, 70 eV) m/z: calculated for $C_5H_{10}N_2$ [M-HCl] $^+$: 98.0838, found: 98.0835.

^{1}H NMR (400 MHz, DMSO-d_6) δ = 9.13 (bs, J = 37.7 Hz, 3H, H^5), 4.54 (dd, J = 8.0, 6.8 Hz, 1H, H^4), 1.53 – 1.35 (m, 2H, H^3), 1.89 – 1.79 (m, 2H, H^2), 0.93 (td, J = 7.3, 1.1 Hz, 3H, H^1).

^{13}C NMR (101 MHz, DMSO-d_6) δ = 116.9 (C^6), 40.5 (C^4), 32.2 (C^3), 18.0 (C^2), 13.1 (C^1)

1-Cyano-2-methylpropan-1-aminium chloride (2d-HCl)
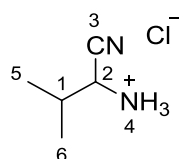
2.25 mL of isobutyraldehyde **1d** (1.80 g, 25.0 mmol, 1.0 eq.) were treated with **GP-1** to yield **2d-HCl** as white solid (1.75 g, 12.8 mmol, 51 %).

HRMS (EI, 70 eV) *m/z*: calculated for $C_5H_{10}N_2$ [M-HCl]$^+$: 98.0838, found: 98.0834.

¹H NMR (400 MHz, DMSO-d_6) δ = 9.30 (bs, 3H, H⁴), 4.52 (d, *J* = 5.5 Hz, 1H, H²), 2.36 – 2.17 (m, 1H, H¹), 1.03 (dd, *J* = 9.3, 6.8 Hz, 6H, H⁵,⁶).

¹³C NMR (101 MHz, DMSO-d_6) δ = 115.7 (C³), 46.3 (C²), 29.3 (C¹), 18.6 (C⁵/⁶), 17.1 (C⁵/⁶).

Cyano(phenyl)methanaminium chloride (2e-HCl)
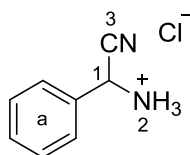
2.55 mL of benzaldehyde **1e** (2.65 g, 25.0 mmol, 1.0 eq.) were treated with **GP-1** to yield **2e-HCl** as white solid (1.86 g, 11.0 mmol, 44 %).

¹H NMR (400 MHz, DMSO-d_6) δ = 9.71 (bs, 3H, H²), 7.72 – 7.64 (m, 2H, Hᵃ), 7.57 – 7.49 (m, 3H, Hᵃ), 6.08 – 5.83 (m, 1H, H¹).

¹³C NMR (101 MHz, DMSO-d_6) δ = 130.4 (Cᵃ), 130.3 (Cᵃ), 129.3 (Cᵃ), 128.4 (Cᵃ), 116.3 (C³), 43.2 (C¹).

2-Cyanopropan-2-aminium chloride (2f-HCl)
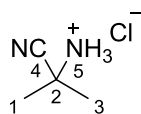
1.84 mL of acetone **1f** (1.45 g, 25.0 mmol, 1.0 eq.) were treated with **GP-1** to yield **2f-HCl** as white solid (1.59 g, 13.3 mmol, 53 %).

HRMS (EI, 70 eV) m/z: calculated für $C_4H_8N_2$ [M-HCl] $^+$: 84.0682, found: 84.0681.

^{1}H NMR (400 MHz, DMSO-d_6) δ = 9.43 (bs, 3H, H^5), 1.71 – 1.67 (m, 6H, H^{1,3}).

^{13}C NMR (101 MHz, DMSO-d_6) δ = 119.6 (C^4), 46.4 (C^2), 24.7 (C^{1,3}).

2-Cyanobutan-2-aminium chloride (2g-HCl)
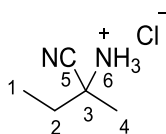
2.24 mL of butanone **1g** (1.80 g, 25.0 mmol, 1.0 eq.) were treated with **GP-1** to yield **2g-HCl** as white solid (1.95 g, 14.5 mmol, 58 %).

HRMS (EI, 70 eV) m/z: calculated für $C_5H_{10}N_2$ [M-HCl] $^+$: 98.0838, found: 98.0839.

^{1}H NMR (400 MHz, DMSO-d_6) δ = 9.44 (bs, 3H, H^6), 2.07 – 1.86 (m, 2H, H^2), 1.65 (s, 3H, H^4), 1.04 (t, J = 7.5 Hz, 3H, H^1).

^{13}C NMR (101 MHz, DMSO-d_6) δ = 118.5 (C^5), 51.0 (C^3), 30.6 (C^2), 22.4 (C^4), 8.4 (C^1).

6.2.2 Imidazolidine-4-thiones

The synthesis of imidazolidine-4-thiones **3** was oriented on the procedure of PAVENTI and EDWARD.[180] However, variations were made regarding the reaction conditions and the workup. With this protocol, also the reaction with aldehydes (R^3 / R^4 = H) was successful.
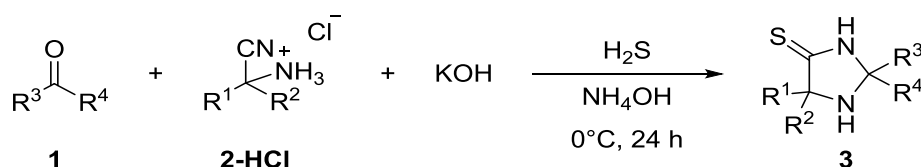
General Procedure GP-2

The hydrochloride salt of the amino nitrile **2-HCl** (2.5 mmol, 1.0 eq.) and potassium hydroxide (140 mg, 2.5 mmol, 1.0 eq) were dissolved in 4 mL of concentrated aqueous ammonia (28 – 30 %). After cooling to 0 °C, the respective aldehyde or ketone **1** (2.5 mmol, 1.0 eq.) was added and hydrogen sulphide was bubbled through the solution (3 x 17 bar). The vial was sealed and left stirring for 12 h, letting the mixture warm up to room temperature. The remaining hydrogen sulphide was purged with nitrogen at 55 °C and the suspension was then extracted with dichloromethane. The organic phases were dried over sodium sulfate and the solvent was removed *in vacuo*. Purification by flash chromatography (*n*-pentane:EtOAc, dry-load) was performed to separate other imidazolidine-4-thiones that were additionally formed as side-products (even if NMR analysis indicated the presence of a single and clean imidazolidine-4-thione, the purification step was performed to remove residual sulphur compounds that could falsify subsequent catalytic investigations).

Imidazolidine-4-thiones **3af**, **3ef**, **3fe**, **3ff**, **3fg**, **3gg**, **3ff-Me** have been characterised before[171,173,180,184,209] and we already published imidazolidine-4-thiones **3aa**, **3ab**, **3ad**, **3af**, **3ba**, **3bb**, **3bd**, **3bf**, **3da**, **3db**, **3dd**, **3df**, **3fa**, **3fb**, **3fd**, **3ff**.[194]

2,5-Dimethylimidazolidine-4-thione (3aa)
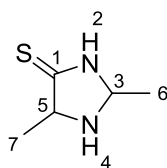
1-Cyanoethan-1-aminium chloride **2a** (266 mg, 2.50 mmol, 1.0 eq.) reacted with acetaldehyde **1a** (110 mg, 140 µL, 2.50 mmol, 1.0 eq.), potassium hydroxide and hydrogen sulphide following **GP-2**. Column chromatography (SiO$_2$, EtOAc) of the crude product yielded the title compound **3aa** (235 mg, 1.80 mmol, 72 %) as a white solid consisting of two diastereomers (1:1 ratio as determined by ^{1}H NMR).

HRMS (ESI) *m*/z: calculated for C$_5$H$_{11}$N$_2$S [M+H]$^+$: 131.0637, found: 131.0637.

Retardation factor: R$_f$ = 0.22 (EtOAc).

Diastereomer A:

^{1}H NMR (400 MHz, CDCl$_3$) δ = 8.88 (b, 1H, H^2), 4.92 (qd, *J* = 6.0, 1.2 Hz, 1H, H^3), 4.01 (qd, *J* = 6.9, 1.2 Hz, 1H, H^5), 1.43 (d, *J* = 7.0 Hz, 3H, H^7), 1.41 (d, *J* = 6.0 Hz, 3H, H^6).

^{13}C NMR (101 MHz, CDCl$_3$) δ = 207.4 (C^1), 72.7 (C^3), 66.6 (C^5), 21.3 (C^6) 19.2 (C^7).

Diastereomer B:

^{1}H NMR (400 MHz, CDCl$_3$) δ = 8.88 (b, 1H, H^2), 4.77 (qd, *J* = 5.8, 1.7 Hz, 1H, H^3), 3.88 – 3.69 (m, 1H, H^5), 1.50 (d, *J* = 6.7 Hz, 3H, H^7), 1.45 (d, *J* = 5.8 Hz, 3H, H^6).

^{13}C NMR (101 MHz, CDCl$_3$) δ = 208.1 (C^1), 72.3 (C^3), 67.2 (C^5), 20.7 (C^6), 19.2 (C^7).

2-Ethyl-5-methylimidazolidine-4-thione (3ab)
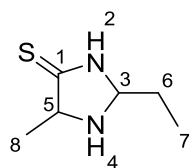
1-Cyanoethan-1-aminium chloride **2a** (266 mg, 2.50 mmol, 1.0 eq.) reacted with propionaldehyde **1b** (145 mg, 180 µL, 2.50 mmol, 1.0 eq.), potassium hydroxide and hydrogen sulphide following **GP-2**. Column chromatography (SiO$_2$, EtOAc) of the crude product yielded the title compound **3ab** (195 mg, 1.35 mmol, 54 %) as a slightly yellow solid consisting of two diastereomers (1:1 ratio as determined by ^{1}H NMR).

HRMS (ESI) *m/z*: calculated for C$_6$H$_{13}$N$_2$S [M+H]$^+$: 145.0794, found: 145.0792.

Retardation factor: R$_f$ = 0.33 (EtOAc).

Diastereomer A:

^{1}**H NMR** (400 MHz, CDCl$_3$) δ = 9.62 (b, 1H, H^2), 4.71 (td, *J* = 6.1, 1.4 Hz, 1H, H^3), 3.95 (qd, *J* = 7.0, 1.4 Hz, 1H, H^5), 1.99 (b, 1H), 1.66 (p, *J* = 7.4 Hz, 2H, H^6), 1.42 (d, *J* = 6.9 Hz, 3H, H^8), 0.99 (t, *J* = 7.5 Hz, 3H, H^7).

^{13}**C NMR** (101 MHz, CDCl$_3$) δ = 206.8 (C^1), 77.7 (C^3), 66.4 (C^5), 28.6 (C^6), 19.4 (C^8), 9.4 (C^7).

Diastereomer B:

^{1}**H NMR** (400 MHz, CDCl$_3$) δ = 9.62 (b, 1H, H^2), 4.61 (td, *J* = 5.9, 1.8 Hz, 1H, H^3), 3.79 (qd, *J* = 6.7, 1.8 Hz, 1H, H^5), 1.99 (b, 1H), 1.72 (p, *J* = 7.5 Hz, 2H, H^6), 1.47 (d, *J* = 6.7 Hz, 3H, H^8), 1.02 (t, *J* = 7.5 Hz, 3H, H^7).

^{13}**C NMR** (101 MHz, CDCl$_3$) δ = 207.4 (C^1), 78.0 (C^3), 66.8 (C^5), 28.0 (C^6), 19.2 (C^8), 9.2 (C^7).

5-Methyl-2-propylimidazolidine-4-thione (3ac)
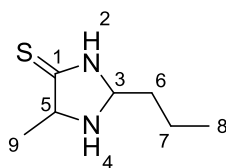
1-Cyanoethan-1-aminium chloride **2a** (266 mg, 2.50 mmol, 1.0 eq.) reacted with butyraldehyde **1c** (180 mg, 225 μL, 2.50 mmol, 1.0 eq.), potassium hydroxide and hydrogen sulphide following **GP-2**. Column chromatography (SiO$_2$, EtOAc:n-pentane 4:1) of the crude product yielded the title compound **3ac** (52.0 mg, 0.33 mmol, 12 %) as a white solid consisting of two diastereomers (1:1 ratio as determined by ^{1}H NMR).

HRMS (ESI) *m/z*: calculated for C$_7$H$_{14}$N$_2$S [M+H]$^+$: 159.0950, found: 159.0949

Retardation factor: R$_f$ = 0.41 (EtOAc:n-pentane 4:1)

Diastereomer A:

^{1}**H NMR** (599 MHz, CDCl$_3$) δ = 8.79 (s, 1H, H^2), 4.76 (td, *J* = 6.2, 1.3 Hz, 1H, H^3), 3.96 (qd, *J* = 6.9, 1.3 Hz, 1H, H^5), 1.93 (bs, 1H, H^4), 1.73 – 1.58 (m, 2H, H^6), 1.55 – 1.45 (m, 2H, H^7), 1.44 (d, *J* = 7.0 Hz, 3H, H^9), 0.99 (t, *J* = 7.4 Hz, 3H, H^8).

^{13}**C NMR** (151 MHz, CDCl$_3$) δ = 207.3 (C^1), 76.5 (C^3), 66.3 (C^5), 37.7 (C^6), 19.4 (C^9), 18.6 (C^7), 13.9 (C^8).

Diastereomer B:

^{1}**H NMR** (599 MHz, CDCl$_3$) δ = 8.79 (bs, 1H, H^2), 4.66 (td, *J* = 6.0, 1.7 Hz, 1H, H^3), 3.78 (qd, *J* = 6.8, 1.7 Hz, 1H, H^5), 1.93 (bs, 1H, H^4), 1.73 – 1.58 (m, 2H, H^6), 1.49 (d, *J* = 6.8 Hz, 3H, H^9), 1.48 – 1.44 (m, 2H, H^7), 0.97 (t, *J* = 7.4 Hz, 3H, H^8).

^{13}**C NMR** (151 MHz, CDCl$_3$) δ = 207.9 (C^1), 76.2 (C^3), 66.8 (C^5), 37.2 (C^6), 19.3 (C^9), 18.5 (C^7), 14.0 (C^8).

2-Isopropyl-5-methylimidazolidine-4-thione (3ad)
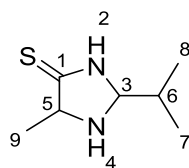
1-Cyanoethan-1-aminium chloride **2a** (266 mg, 2.50 mmol, 1.0 eq.) reacted with isobutyraldehyde **1d** (176 mg, 228 μL, 2.50 mmol, 1.0 eq.), potassium hydroxide and hydrogen sulphide following **GP-2**. Column chromatography (SiO$_2$, EtOAc) of the crude product yielded the title compound **3ad** (176 mg, 1.11 mmol, 44 %) as a yellow solid consisting of two diastereomers (1:1 ratio as determined by ^{1}H NMR).

HRMS (ESI) *m/z*: calculated for C$_7$H$_{15}$N$_2$S [M+H]$^+$: 159.0950, found: 159.0947.

Retardation factor: R$_f$ = 0.58 (EtOAc).

Diastereomer A:

^{1}**H NMR** (400 MHz, CDCl$_3$) δ = 8.88 (b, 1H, H^2), 4.53 (dd, *J* = 6.0, 1.7 Hz, 1H, H^3), 3.94 (qd, *J* = 6.9, 1.6 Hz, 1H, H^5), 1.90 (b, 1H, H^4), 1.87 – 1.76 (m, 1H, H^6), 1.44 (d, *J* = 6.9 Hz, 3H, H^9), 0.98 (dd, *J* = 6.8, 1.5 Hz, 6H, H$^{7/8}$).

^{13}**C NMR** (101 MHz, CDCl$_3$) δ = 207.3 (C^1), 81.8 (C^3), 66.7 (C^5), 33.8 (C^6), 20.0 (C^9), 17.8 (C$^{7/8}$), 17.7 (C$^{7/8}$).

Diastereomer B:

^{1}**H NMR** (400 MHz, CDCl$_3$) δ = 8.88 (b, 1H, H^2), 4.46 (dd, *J* = 6.2, 1.9 Hz, 1H, H^3), 3.82 (qd, *J* = 6.7, 1.8 Hz, 1H, H^5), 1.90 (b, 1H, H^4), 1.87 – 1.76 (m, 1H, H^6), 1.49 (d, *J* = 6.7 Hz, 3H, H^9), 1.02 (dd, *J* = 6.8, 2.3 Hz, 6H, H$^{7/8}$).

^{13}**C NMR** (101 MHz, CDCl$_3$) δ = 208.0 (C^1), 81.5 (C^3), 66.7 (C^5), 32.5 (C^6), 19.4 (C^9), 18.0 (C$^{7/8}$), 17.9 (C$^{7/8}$).

2,2,5-Trimethylimidazolidine-4-thione (3af)
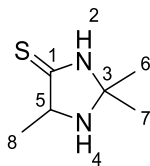
1-Cyanoethan-1-aminium chloride **2a** (266 mg, 2.50 mmol, 1.0 eq.) reacted with acetone **1f** (145 mg, 185 µL, 2.5 mmol, 1.0 eq.), potassium hydroxide and hydrogen sulphide following **GP-2**. Column chromatography (SiO$_2$, EtOAc) of the crude product yielded the title compound **3ad** (85 mg, 0.59 mmol, 24 %) as a white solid.

HRMS (ESI) *m/z*: calculated for C$_6$H$_{13}$N$_2$S [M+H]$^+$: 145.0794, found: 145.0792.

^{1}H NMR (400 MHz, CDCl$_3$) δ = 9.19 (s, 1H, H^2), 3.95 (q, *J* = 6.8 Hz, 1H, H^5), 1.87 (b, 1H, H^4), 1.52 (s, 3H, H$^{6/7}$), 1.49 (d, *J* = 6.7 Hz, 3H, H$^{6/7}$), 1.42 (s, 3H, H^8).

^{13}C NMR (101 MHz, CDCl$_3$) δ = 205.6 (C^1), 79.8 (C^3), 66.1 (C^5), 28.5 (C$^{6/7}$), 27.4 (C$^{6/7}$), 19.6 (C^8).
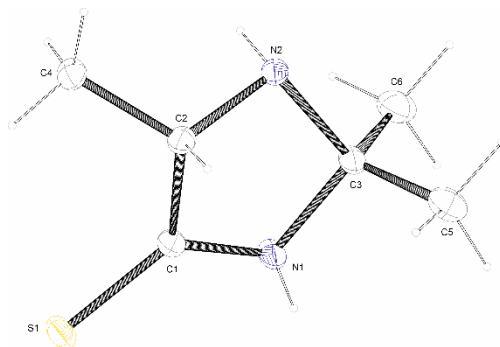
net formula	$C_6H_{12}N_2S$
M_r/g mol^{-1}	144.24
crystal size/mm	$0.070 \times 0.050 \times 0.030$
T/K	109.(2)
radiation	MoKα
diffractometer	'Bruker D8 Venture TXS'
crystal system	monoclinic
space group	'P 1 21/n 1'
a/Å	8.0207(6)
b/Å	9.6194(5)
c/Å	10.1195(6)
α/°	90
β/°	90.840(2)
γ/°	90
V/Å^3	780.68(8)
Z	4
calc. density/g cm^{-3}	1.227
μ/mm^{-1}	0.332
absorption correction	Multi-Scan
transmission factor range	0.89–0.99
refls. measured	11797
R_{int}	0.0269
mean $\sigma(I)/I$	0.0165
θ range	3.218–27.100
observed refls.	1517
x, y (weighting scheme)	0.0222, 0.4409
hydrogen refinement	mixed
Flack parameter	?
refls in refinement	1720
parameters	126
restraints	3
$R(F_{obs})$	0.0331
$R_w(F^2)$	0.0774
S	1.135
shift/error$_{max}$	0.001
max electron density/e Å^{-3}	0.264
min electron density/e Å^{-3}	−0.219

2-Ethyl-2,5-dimethylimidazolidine-4-thione (3ag)
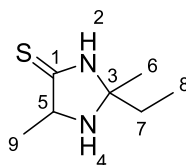
1-Cyanoethan-1-aminium chloride **2a** (266 mg, 2.50 mmol, 1.0 equiv.) reacted with butanone **1g** (176 mg, 228 μL, 2.5 mmol, 1.0 eq.), potassium hydroxide and hydrogen sulphide following **GP-2**. Column chromatography (SiO$_2$, EtOAc) of the crude product yielded the title compound **3ad** (11 mg, 0.07 mmol, 3 %) as a yellow solid consisting of two diastereomers (1:1 ratio as determined by ^{1}H NMR).

HRMS (ESI) *m/z*: calculated for C$_7$H$_{15}$N$_2$S [M+H]$^+$: 159.0950, found: 159.0945.

Diastereomer A:

^{1}**H NMR** (400 MHz, CDCl$_3$) δ = 9.00 (bs, 1H, H^2), 3.97 (q, *J* = 6.8 Hz, 1H, H^5), 1.92 – 1.60 (m, 3H, H^{4,7}), 1.49 (d, *J* = 6.8 Hz, 3H, H^9), 1.38 (s, 3H, H^6), 0.99 (t, *J* = 7.4 Hz, 3H, H^8).

^{13}**C NMR** (101 MHz, CDCl$_3$) δ = 205.9 (C^1), 82.5 (C^3), 65.8 (C^5), 33.6 (C^7), 25.5 (C^6), 19.6 (C^9), 8.3 (C^8).

Diastereomer B:

^{1}**H NMR** (400 MHz, CDCl$_3$) δ = 9.00 (bs, 1H, H^2), 3.93 (q, *J* = 6.8 Hz, 1H, H^5), 1.92 – 1.60 (m, 3H, H^{4,7}), 1.49 (d, *J* = 6.8 Hz, 3H, H^9), 1.46 (s, 3H, H^6), 0.97 (t, *J* = 7.6 Hz, 3H, H^8).

^{13}**C NMR** (101 MHz, CDCl$_3$) δ = 205.9 (C^1), 82.6 (C^3), 66.5 (C^5), 33.8 (C^7), 26.2 (C^6), 20.2 (C^9), 8.9 (C^8).

5-Ethyl-2-methylimidazolidine-4-thione (3ba)
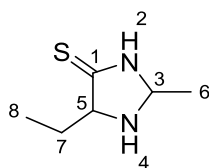
1-Cyanopropan-1-aminium chloride **2b** (302 mg, 2.50 mmol, 1.0 eq.) reacted with acetaldehyde **1a** (110 mg, 140 μL, 2.50 mmol, 1.0 eq.), potassium hydroxide and hydrogen sulphide following **GP-2**. Column chromatography (SiO$_2$, EtOAc) of the crude product yielded the title compound **3ba** (235 mg, 1.63 mmol, 65 %) as a white solid consisting of two diastereomers (6:4 ratio as determined by ^{1}H NMR).

HRMS (ESI) *m/z*: calculated for C$_6$H$_{13}$N$_2$S [M+H]$^+$: 145.0794, found: 145.0792.

Retardation factor: R_f = 0.29 (EtOAc).

Diastereomer A (major):

^{1}H NMR (400 MHz, CDCl$_3$) δ = 8.81 (b, 1H, H^2), 4.89 (qd, *J* = 5.9, 1.4 Hz, 1H, H^3), 3.87 (ddd, *J* = 8.7, 3.7, 1.4 Hz, 1H, H^5), 2.08 – 1.96 (m, 1H, H$^{7a/b}$), 1.71 (b, 1H, H^4), 1.68 – 1.55 (m, 1H, H$^{7a/b}$), 1.41 (d, *J* = 5.9 Hz, 3H, H^6), 1.04 (t, *J* = 7.4 Hz, 3H, H^8).

^{13}C NMR (101 MHz, CDCl$_3$) δ = 206.5 (C^1), 73.3 (C^3), 72.4 (C^5), 26.7 (C^7), 21.5 (C^6), 10.6 (C^8).

Diastereomer B (minor):

^{1}H NMR (400 MHz, CDCl$_3$) δ = 8.88 (b, 1H, H^2), 4.80 (qd, *J* = 5.8, 1.8 Hz, 1H, H^3), 3.67 (ddd, *J* = 8.5, 3.7, 1.7 Hz, 1H, H^5), 2.32 – 2.19 (m, 1H, H$^{7a/b}$), 1.71 (b, 1H, H^4), 1.68 – 1.55 (m, 1H, H$^{7a/b}$), 1.45 (d, *J* = 5.8 Hz, 3H, H^6), 1.04 (t, *J* = 7.5 Hz, 3H, H^8).

^{13}C NMR (101 MHz, CDCl$_3$) δ = 207.0 (C^1), 72.5 (C^5), 72.4 (C^3), 26.5 (C^7), 20.9 (C^6), 10.4 (C^8).
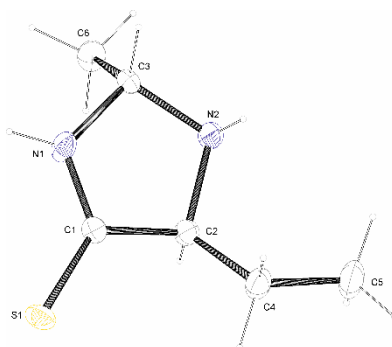
net formula	$C_6H_{12}N_2S$
M_r/g mol^{-1}	144.24
crystal size/mm	$0.090 \times 0.060 \times 0.050$
T/K	109.(2)
radiation	MoKα
diffractometer	'Bruker D8 Venture TXS'
crystal system	hexagonal
space group	'P 61'
a/Å	7.4887(2)
b/Å	7.4887(2)
c/Å	24.8643(10)
α/°	90
β/°	90
γ/°	120
V/Å^3	1207.59(8)
Z	6
calc. density/g cm^{-3}	1.190
μ/mm^{-1}	0.322
absorption correction	Multi-Scan
transmission factor range	0.93–0.98
refls. measured	13081
R_{int}	0.0376
mean $\sigma(I)/I$	0.0263
θ range	3.141–27.456
observed refls.	1775
x, y (weighting scheme)	0.0266, 0.4509
hydrogen refinement	H(C) constr, H(N) refxyz
Flack parameter	0.01(3)
refls in refinement	1850
parameters	100
restraints	1
$R(F_{obs})$	0.0305
$R_w(F^2)$	0.0713
S	1.069
shift/error$_{max}$	0.001
max electron density/e Å^{-3}	0.236
min electron density/e Å^{-3}	−0.164

2,5-Diethylimidazolidine-4-thione (3bb)
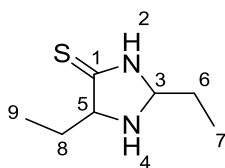
1-Cyanopropan-1-aminium chloride **2b** (302 mg, 2.50 mmol, 1.0 eq.) reacted with propionaldehyde **1b** (145 mg, 179 μL, 2.50 mmol, 1.0 eq.), potassium hydroxide and hydrogen sulphide following **GP-2**. Column chromatography (SiO$_2$, EtOAc) of the crude product yielded the title compound **3bb** (301 mg, 1.90 mmol, 76 %) as a white solid consisting of two diastereomers (5.5:4.5 ratio as determined by ^{1}H NMR).

HRMS (ESI) *m/z*: calculated for C$_7$H$_{15}$N$_2$S [M+H]$^+$: 159.0950, found: 159.0950.

Retardation factor: R$_f$ = 0.52 (EtOAc).

Diastereomer A (minor):

^{1}H NMR (599 MHz, CDCl$_3$) δ = 9.06 (b, 1H, H^2), 4.70 (td, *J* = 5.9, 1.6 Hz, 1H, H^3), 3.89 – 3.78 (m, 1H, H^5), 2.12 – 1.96 (m, 1H, H$^{8a/b}$), 1.68 – 1.57 (m, 3H, H$^{6,8a/b}$), 1.07 – 0.97 (m, 6H, H^{7,9}).

^{13}C NMR (151 MHz, CDCl$_3$) δ = 206.9 (C^1), 78.5 (C^3), 72.1 (C^5), 29.0 (C^6), 27.0 (C^8), 10.4 (C$^{7/9}$), 9.3 (C$^{7/9}$).

Diastereomer B (major):

^{1}H NMR (599 MHz, CDCl$_3$) δ = 9.06 (b, 1H, H^2), 4.65 (td, *J* = 5.9, 1.7 Hz, 1H, H^3), 3.73 – 3.67 (m, 1H, H^5), 2.30 – 2.17 (m, 1H, H$^{8a/b}$), 1.72 (p, *J* = 7.4 Hz, 2H, H^6), 1.07 – 0.97 (m, 6H, H^{7,9}).

^{13}C NMR (151 MHz, CDCl$_3$) δ = 206.9 (C^1), 77.7 (C^3), 72.1 (C^5), 28.3 (C^6), 26.7 (C^8), 10.3 (C$^{7/9}$), 9.2 (C$^{7/9}$).

5-Ethyl-2-propylimidazolidine-4-thione (3bc)
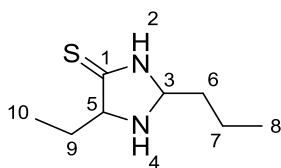
1-Cyanopropan-1-aminium chloride **2b** (302 mg, 2.50 mmol, 1.0 eq.) reacted with butyraldehyde **1c** (180 mg, 225 μL, 2.50 mmol, 1.0 eq.), potassium hydroxide and hydrogen sulphide following **GP-2**. Column chromatography (SiO$_2$, EtOAc:n-pentane 1:1) of the crude product yielded the title compound **3bc** (132 mg, 0.77 mmol, 32 %) as a white solid consisting of two diastereomers (1:1 ratio as determined by ^{1}H NMR).

Retardation factor: R$_f$ = 0.40 (EtOAc:n-pentane 1:1)

Diastereomer A:

^{1}**H NMR** (400 MHz, CDCl$_3$) δ = 8.55 (bs, 1H, H^2), 4.75 (td, J = 6.1, 1.5 Hz, 1H, H^3), 3.84 (ddd, J = 8.4, 3.8, 1.5 Hz, 1H, H^5), 2.15 (bs, 1H, H^4), 2.04 (dqd, J = 15.0, 7.5, 3.8 Hz, 1H, H$^{9a/b}$), 1.73 – 1.32 (m, 5H, H$^{6, 7, 9a/b}$), 1.11 – 0.88 (m, 6H, H$^{8, 10}$).

^{13}**C NMR** (101 MHz, CDCl$_3$) δ = 206.9, 206.5, 77.0, 76.3, 72.0, 72.0, 38.0, 37.4, 26.9, 26.6, 18.5, 14.0, 14.0, 10.5, 10.4.

Diastereomer B:

^{1}**H NMR** (400 MHz, CDCl$_3$) δ = 8.55 (bs, 1H, H^2), 4.69 (td, J = 6.0, 1.8 Hz, 1H, H^3), 3.68 (ddd, J = 8.5, 3.7, 1.7 Hz, 1H, H^5), 2.24 (dqd, J = 15.1, 7.6, 3.6 Hz, 1H, H$^{9a/b}$), 2.15 (bs, 1H, H^4), 1.73 – 1.32 (m, 5H, H$^{6, 7, 9a/b}$), 1.11 – 0.88 (m, 6H, H$^{8, 10}$).

^{13}**C NMR** (101 MHz, CDCl$_3$) δ = 206.9, 206.5, 77.0, 76.3, 72.0, 72.0, 38.0, 37.4, 26.9, 26.6, 18.5, 14.0, 14.0, 10.5, 10.4.

5-Ethyl-2-isopropylimidazolidine-4-thione (3bd)
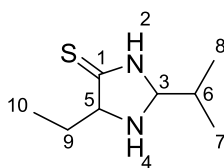
1-Cyanopropan-1-aminium chloride **2b** (302 mg, 2.50 mmol, 1.0 eq.) reacted with isobutyraldehyde **1d** (180 mg, 228 µL, 2.50 mmol, 1.0 eq.), potassium hydroxide and hydrogen sulphide following **GP-2**. Column chromatography (SiO$_2$, EtOAc : *n*-pentane 1:1) of the crude product yielded the title compound **3bd** (92.0 mg, 0.53 mmol, 20 %) as a white solid consisting of two diastereomers (6:4 ratio as determined by ^{1}H NMR).

HRMS (ESI) *m/z*: calculated for C$_8$H$_{16}$N$_2$S [M+H]$^+$: 173.1107, found: 173.1103.

Retardation factor: R$_f$ = 0.40 (EtOAc:*n*-pentane 1:1).

Diastereomer A (minor):

^{1}**H NMR** (400 MHz, CDCl$_3$) δ = 8.64 (b, 1H, H^2), 4.54 (dd, *J* = 5.7, 1.9 Hz, 1H, H^3), 3.84 (ddd, *J* = 8.0, 3.8, 1.9 Hz, 1H, H^5), 2.05 (dqd, *J* = 14.0, 7.5, 3.8 Hz, 1H, H$^{9a/b}$), 1.88 (b, 1H, H^4), 1.87-1.55 (m, 2H, H$^{6,9a/b}$), 1.08 – 0.95 (m, 9H, H^{7,8,10}).

^{13}**C NMR** (101 MHz, CDCl$_3$) δ = 206.4 (C^1), 82.2 (C^3), 72.1 (C^5), 34.0 (C^6), 27.4 (C^9), 17.7 (C$^{7/8}$), 17.7 (C$^{7/8}$), 10.2 (C^{10}).

Diastereomer B (major):

^{1}**H NMR** (400 MHz, CDCl$_3$) δ = 8.64 (b, 1H, H^2), 4.48 (dd, *J* = 6.1, 1.9 Hz, 1H, H^3), 3.73 (ddd, *J* = 8.3, 3.7, 1.9 Hz, 1H, H^5), 2.21 (dqd, *J* = 14.2, 7.6, 3.6 Hz, 1H, H$^{9a/b}$), 1.88 (b, 1H, H^4), 1.87-1.55 (m, 2H, H$^{6,9a/b}$), 1.08 – 0.95 (m, 9H, H^{7,8,10}).

^{13}**C NMR** (101 MHz, CDCl$_3$) δ = 206.9 (C^1), 81.5 (C^3), 71.8 (C^5), 32.8 (C^6), 26.8 (C^9), 17.9 (C$^{7/8}$), 17.9 (C$^{7/8}$), 10.3 (C^{10}).

5-Ethyl-2,2-dimethylimidazolidine-4-thione (3bf)
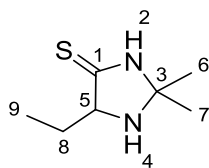
1-Cyanopropan-1-aminium chloride **2b** (302 mg, 2.50 mmol, 1.0 eq.) reacted with acetone **1f** (145 mg, 185 µL, 2.5 mmol, 1.0eq.), potassium hydroxide and hydrogen sulphide following **GP-2**. Column chromatography (SiO$_2$, EtOAc) of the crude product yielded the title compound **3bf** (111 mg, 0.70 mmol, 28 %) as a white solid.

HRMS (ESI) *m*/z: calculated for C$_7$H$_{15}$N$_2$S [M+H]$^+$: 159.0950, found: 159.0949.

Retardation factor: R_f = 0.45 (EtOAc).

^{1}H NMR (400 MHz, CDCl$_3$) δ = 9.31 (b, 1H, H^2), 3.83 (dd, *J* = 8.5, 3.7 Hz, 1H, H^5), 2.28 – 2.16 (m, 1H, H$^{8a/b}$), 1.86 (b, 1H, H^4), 1.69 – 1.55 (m, 1H, H$^{8a/b}$), 1.51 (s, 3H, H$^{6/7}$), 1.42 (s, 3H, H$^{6/7}$), 1.03 (t, *J* = 7.5 Hz, 3H, H^9).

^{13}C NMR (101 MHz, CDCl$_3$) δ = 204.5 (C^1), 80.0 (C^3), 71.4 (C^5), 28.6 (C$^{6/7}$), 27.8 (C$^{6/7}$), 26.9 (C^8), 10.4 (C^9).

2,5-Diethyl-2-methylimidazolidine-4-thione (3bg)
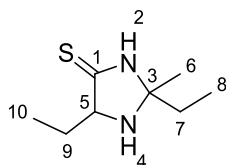
1-Cyanopropan-1-aminium chloride **2b** (302 mg, 2.50 mmol, 1.0 eq.) reacted with butanone **1g** (176 mg, 228 μL, 2.5 mmol, 1.0 eq.), potassium hydroxide and hydrogen sulphide following **GP-2**. Column chromatography (SiO$_2$, EtOAc) of the crude product yielded the title compound **3bg** (235 mg, 1.37 mmol, 55 %) as a white solid consisting of two diastereomers (ratio not determined).

HRMS (ESI) *m/z*: calculated for C$_8$H$_{16}$N$_2$S [M+H]$^+$: 173.1107, found: 173.1106.

Diastereomer A (major):

^{1}H NMR (400 MHz, CDCl$_3$) δ = 9.65 (bs, 1H, H^2), 3.85 – 3.77 (m, 1H, H^5), 2.24 – 2.08 (m, 1H, H$^{9a/b}$), 1.66 (q, *J* = 7.4 Hz, 1H, H^7), 1.70 – 1.55 (m, 2H, H$^{9a/b}$), 1.43 (s, 3H, H^6), 1.04 – 0.97 (m, 3H, H^{10}), 0.98 – 0.90 (m, 3H, H^8).

^{13}C NMR (101 MHz, CDCl$_3$) δ = 204.2 (C^1), 82.9 (C^3), 71.8 (C^5), 34.2 (C^7), 27.2 (C^9), 26.5 (C^6), 10.1 (C^{11}), 8.7 (C^8).

Diastereomer B (minor):

^{1}H NMR (400 MHz, CDCl$_3$) δ = 9.65 (bs, 1H, H^2), 3.85 – 3.77 (m, 1H, H^5), 2.24 – 2.08 (m, 1H, H$^{9a/b}$), 1.75 (q, *J* = 7.6 Hz, 1H, H^7), 1.70 – 1.55 (m, 2H, H$^{9a/b}$), 1.37 (s, 3H, H^6), 1.04 – 0.97 (m, 3H, H^{10}), 0.98 – 0.90 (m, 3H, H^8).

^{13}C NMR (101 MHz, CDCl$_3$) δ = 204.2 (C^1), 82.8 (C^3), 71.0 (C^5), 33.6 (C^7), 26.8 (C^9), 25.8 (C^6), 10.3 (C^{11}), 8.3 (C^8).

2-Methyl-5-propylimidazolidine-4-thione (3ca)
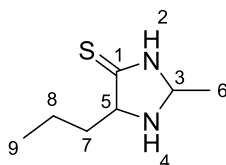
1-Cyanobutan-1-aminium chloride **2c** (337 mg, 2.50 mmol, 1.0 eq.) reacted with acetaldehyde **1a** (110 mg, 140 μL, 2.50 mmol, 1.0 eq.), potassium hydroxide and hydrogen sulphide following **GP-2**. Column chromatography (SiO$_2$, EtOAc) of the crude product yielded the title compound **3ca** (125 mg, 0.79 mmol, 32 %) as a white solid consisting of two diastereomers (5.5:4.5 ratio as determined by ^{1}H NMR).

HRMS (ESI) *m/z*: calculated for C$_7$H$_{14}$N$_2$S [M+H]$^+$: 159.0950, found: 159.0948

Retardation factor: 1. Diastereomer R$_f$ = 0.35 (EtOAc)

  2. Diastereomer R$_f$ = 0.35 (EtOAc)

Diastereomer A (minor):

^{1}**H NMR** (400 MHz, CDCl$_3$) δ = 8.83 (bs, 1H, H^2), 4.89 (q, *J* = 5.9 Hz, 1H, H^3), 3.90 (dd, *J* = 9.0, 3.5 Hz, 1H, H^5), 2.07 − 1.89 (m, 1H, H$^{7a/b}$), 1.74 (bs, 1H, H^4), 1.61 − 1.34 (m, 6H, H$^{6,7a/b,8}$), 0.98 (t, *J* = 7.2 Hz, 3H, H$^{9A/B}$), 0.96 (d, *J* = 7.4 Hz, 3H, H$^{9A/B}$).

^{13}**C NMR** (101 MHz, CDCl$_3$) δ = 206.8 (C^1), 73.2 (C^3), 71.1 (C^5), 35.6 (C^7), 21.3 (C$^{8/6}$), 19.8 (C$^{8/6}$), 14.0 (C^9).

Diastereomer B (major):

^{1}**H NMR** (400 MHz, CDCl$_3$) δ = 8.88 (bs, 1H, H^2), 4.78 (q, *J* = 5.6, 5.1 Hz, 1H, H^3), 3.75 − 3.64 (m, 1H, H^5), 2.34 − 2.15 (m, 1H, H$^{7a/b}$), 1.74 (bs, 1H, H^4), 1.61 − 1.34 (m, 6H, H$^{6,7a/b,\ 8}$), 0.98 (t, *J* = 7.2 Hz, 3H, H$^{9A/B}$), 0.96 (d, *J* = 7.4 Hz, 3H, H$^{9A/B}$).

^{13}**C NMR** (101 MHz, CDCl$_3$) δ =207.3 (C^1), 72.6 (C^3), 71.2 (C^5), 35.8 (C^7), 20.8 (C$^{8/6}$), 19.7 (C$^{8/6}$), 14.0 (C^9).
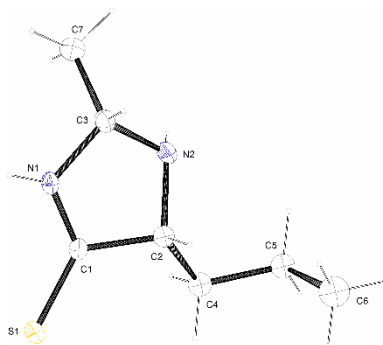
net formula	$C_7H_{14}N_2S$
M_r/g mol^{-1}	158.26
crystal size/mm	$0.100 \times 0.040 \times 0.030$
T/K	109.(2)
radiation	MoKα
diffractometer	'Bruker D8 Venture TXS'
crystal system	orthorhombic
space group	'P c a 21'
a/Å	14.4015(8)
b/Å	9.4719(5)
c/Å	13.0301(7)
α/°	90
β/°	90
γ/°	90
V/Å^3	1777.43(17)
Z	8
calc. density/g cm^{-3}	1.183
μ/mm^{-1}	0.297
absorption correction	Multi-Scan
transmission factor range	0.92–0.99
refls. measured	17843
R_{int}	0.0563
mean $\sigma(I)/I$	0.0503
θ range	3.012–27.095
observed refls.	3293
x, y (weighting scheme)	0.0235, 1.0731
hydrogen refinement	H(C) constr, H(N) refxyz
Flack parameter	0.06(5)
refls in refinement	3902
parameters	193
restraints	10
$R(F_{obs})$	0.0468
$R_w(F^2)$	0.0985
S	1.073
shift/error$_{max}$	0.001
max electron density/e Å^{-3}	0.194
min electron density/e Å^{-3}	−0.388

SADI restraint applied for N-H distances. The asymmetric unit contains two formula units, one of which is depicted above. The disorder has been described by a split model; split atoms have been refined isotropically. The main part is depicted above.

2-Ethyl-5-propylimidazolidine-4-thione (3cb)
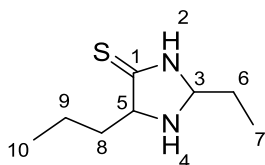
1-Cyanobutan-1-aminium chloride **2c** (337 mg, 2.50 mmol, 1.0 eq.) reacted with propionaldehyde **1b** (145 mg, 179 μL, 2.50 mmol, 1.0 eq.), potassium hydroxide and hydrogen sulphide following **GP-2**. Column chromatography (SiO$_2$, EtOAc:n-pentane 1:1) of the crude product yielded the title compound **3cb** (211 mg, 1.22 mmol, 48 %) as a white solid consisting of two diastereomers (1:1 ratio as determined by ^{1}H NMR).

HRMS (ESI) m/z: calculated for C$_8$H$_{16}$N$_2$S [M+H]$^+$: 173.1107, found: 173.1107.

Retardation factor: 1. Diastereomer R$_f$ = 0.24 (EtOAc:n-pentane 1:1)

                   2. Diastereomer R$_f$ = 0.34 (EtOAc:n-pentane 1:1)

Diastereomer A:

^{1}**H NMR** (599 MHz, CDCl$_3$) δ = 8.72 (bs, 1H, H^2), 4.70 (td, J = 5.9, 1.5 Hz, 1H, H^3), 3.87 (ddd, J = 8.7, 3.7, 1.6 Hz, 1H, H^5), 2.07 – 1.94 (m, 1H, H$^{8a/b}$), 1.77 – 1.61 (m, 3H, H$^{4,\,6}$), 1.60 – 1.35 (m, 3H, H$^{8a/b,\,9}$), 1.04 (t, J = 7.5 Hz, 3H, H$^{7A/B}$), 1.01 (t, J = 7.4 Hz, 3H, H$^{7A/B}$), 0.98 (t, J = 7.1 Hz, 3H, H$^{10A/B}$), 0.97 (t, J = 7.2 Hz, 3H, H$^{10A/B}$).

^{13}**C NMR** (151 MHz, CDCl$_3$) δ = 207.3 (C^1), 78.3 (C^3), 70.8 (C^5), 36.1 (C^8), 28.9 (C^6), 19.7 (C^9), 14.0 (C^{10}), 9.3 (C^7).

Diastereomer B:

^{1}**H NMR** (599 MHz, CDCl$_3$) δ = 8.72 (bs, 1H, H^2), 4.63 (td, J = 5.8, 1.8 Hz, 1H, H^3), 3.75 – 3.69 (m, 1H, H^5), 2.29 – 2.17 (m, 1H, H$^{8a/b}$), 1.77 – 1.61 (m, 3H, H$^{4/6}$), 1.60 – 1.35 (m, 3H, H$^{8a/b,9}$) 1.04 (t, J = 7.5 Hz, 3H, H$^{7A/B}$), 1.01 (t, J = 7.4 Hz, 3H, H$^{7A/B}$), 0.98 (t, J = 7.1 Hz, 3H, H$^{10A/B}$), 0.97 (t, J = 7.2 Hz, 3H, H$^{10A/B}$).

^{13}**C NMR** (151 MHz, CDCl$_3$) δ = 206.9 (C^1), 77.7 (C^3), 70.8 (C^5), 36.1 (C^8), 28.3 (C^6), 19.7 (C^9), 14.0 (C^{10}), 9.2 (C^7).

2,5-Dipropylimidazolidine-4-thione (3cc)
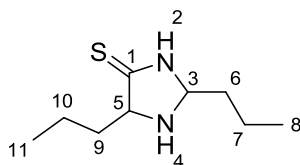
1-Cyanobutan-1-aminium chloride **2c** (336 mg, 2.50 mmol, 1.0 eq.) reacted with butyraldehyde **1c** (180 mg, 225 µL, 2.50 mmol, 1.0 eq.), potassium hydroxide and hydrogen sulphide following **GP-2**. Column chromatography (SiO$_2$, EtOAc:*n*-pentane 1:1) of the crude product yielded the title compound **3cc** (196 mg, 1.05 mmol, 44 %) as a white solid consisting of two diastereomers (6:4 ratio as determined by ^{1}H NMR).

Retardation factor: 1. Diastereomer R$_f$ = 0.57 (EtOAc:*n*-pentane 1:1)

2. Diastereomer R$_f$ = 0.65 (EtOAc:*n*-pentane 1:1)

Diastereomer A (major):

^{1}H NMR (400 MHz, CDCl$_3$) δ = 8.67 (bs, 1H, H^2), 4.74 (td, *J* = 6.1, 1.5 Hz, 1H, H^3), 3.86 (ddd, *J* = 8.8, 3.6, 1.5 Hz, 1H, H^3), 2.31 – 1.92 (m, 1H, H$^{9a/b}$), 1.71 – 1.58 (m, 3H, H^{4,6}), 1.58 – 1.30 (m, 5H, H$^{7,9a/b, 10}$), 1.05 – 0.87 (m, 6H, H$^{8, 11}$).

^{13}C NMR (101 MHz, CDCl$_3$) δ = 206.9 (C^1), 76.9 (C^3), 70.7 (C^5), 37.9, 36.0 (C^{10}), 19.7 (C$^{7/10}$), 18.5 (C$^{7/10}$), 14.0 (C$^{8/11}$), 14.0(C$^{8/11}$).

Diastereomer B (minor):

^{1}H NMR (400 MHz, CDCl$_3$) δ = 8.52 (bs, 1H, H^2), 4.67 (td, *J* = 6.0, 1.8 Hz, 1H, H^3), 3.74 – 3.64 (m, 1H, H^5), 2.31 – 1.92 (m, 1H, H$^{10a/b}$), 1.71 – 1.58 (m, 3H, H^{4,6}), 1.58 – 1.30 (m, 5H, H$^{7,9a/b,10}$), 1.05 – 0.87 (m, 6H, H^{8,11}).

^{13}C NMR (101 MHz, CDCl$_3$) δ = 207.3 (C^1), 76.3 (C^3), 70.8 (C^5), 37.4 (C^6), 36.0 (C^9), 19.7 (C$^{7/10}$), 18.5 (C$^{7/10}$), 14.0 (C$^{8/11}$), 14.0 (C$^{8/11}$).

2-Isopropyl-5-propylimidazolidine-4-thione (3cd)
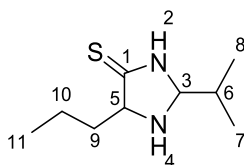
1-Cyanobutan-1-aminium chloride **2c** (337 mg, 2.50 mmol, 1.0 eq.) reacted with isobutyraldehyde **1d** (180 mg, 228 μL, 2.50 mmol, 1.0 eq.), potassium hydroxide and hydrogen sulphide following **GP-2**. Column chromatography (SiO$_2$, EtOAc:n-pentane 1:1) of the crude product yielded the title compound **3cd** (103 mg, 0.55 mmol, 24 %) as a white solid consisting of two diastereomers (6:4 ratio as determined by ^{1}H NMR).

HRMS (ESI) m/z: calculated for C$_9$H$_{18}$N$_2$S [M+H]$^+$: 187.1263, found: 187.1259.

Retardation factor: 1. Diastereomer R$_f$ = 0.52 (EtOAc:n-pentane 1:1)

2. Diastereomer R$_f$ = 0.60 (EtOAc:n-pentane 1:1)

Diastereomer A (major):

^{1}H NMR (400 MHz, CDCl$_3$) δ = 8.13 (bs, 1H, H^2), 4.46 (dd, J = 6.4, 1.9 Hz, 1H, H^3), 3.78 – 3.71 (m, 1H, H^5), 2.28 – 2.17 (m, 1H, H$^{9a/b}$), 1.86 – 1.74 (m, 2H, H$^{4,\,9a/b}$), 1.62 – 1.37 (m, 3H, H$^{6,\,10}$), 1.04 – 0.94 (m, 9H, H$^{7,\,8,\,11}$).

^{13}C NMR (101 MHz, CDCl$_3$) δ = 207.6 (C^1), 81.5 (C^3), 70.6 (C^5), 36.2 (C^6), 32.8 (C^9), 19.6 (C^{10}), 18.0 (C$^{7/8}$), 18.0 (C$^{7/8}$), 14.1 (C^{11}).

Diastereomer B (minor):

^{1}H NMR (400 MHz, CDCl$_3$) δ = 8.13 (bs, 1H, H^2), 4.52 (dd, J = 5.9, 1.8 Hz, 1H, H^3), 3.89 – 3.83 (m, 1H, H^5), 2.11 – 1.94 (m, 1H, H$^{9a/b}$), 1.86 – 1.74 (m, 2H, H$^{4,\,9a/b}$), 1.62 – 1.37 (m, 3H, H$^{6,\,10}$), 1.04 – 0.94 (m, 9H, H$^{7,\,8,\,11}$).

^{13}C NMR (101 MHz, CDCl$_3$) δ = 207.2 (C^1), 82.0 (C^3), 70.8 (C^5), 36.5 (C^6), 33.9 (C^9), 19.5 (C^{10}), 17.7 (C$^{7/8}$), 17.7 (C$^{7/8}$), 14.0 (C^{11}).

2,2-Dimethyl-5-propylimidazolidine-4-thione (3cf)
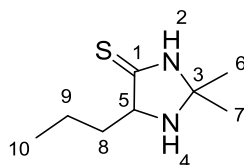
1-Cyanobutan-1-aminium chloride **2c** (337 mg, 2.50 mmol, 1.0 eq.) reacted with acetone **1f** (145 mg, 185 μL, 2.5 mmol, 1.0eq.), potassium hydroxide and hydrogen sulphide following **GP-2**. Column chromatography (SiO$_2$, EtOAc) of the crude product yielded the title compound **3cf** (161 mg, 0.93 mmol, 37 %) as a white solid.

HRMS (ESI) *m/z*: calculated for C$_8$H$_{16}$N$_2$S [M+H]$^+$: 173.1107, found: 173.1107.

^{1}H NMR (400 MHz, CDCl$_3$) δ = 9.31 (b, 1H, H^2), 3.83 (dd, *J* = 8.5, 3.7 Hz, 1H, H^5), 2.28 – 2.16 (m, 1H, H$^{8a/b}$), 1.86 (b, 1H, H^4), 1.69 – 1.55 (m, 1H, H$^{8a/b}$), 1.51 (s, 3H, H$^{6/7}$), 1.42 (s, 3H, H$^{6/7}$), 1.03 (t, *J* = 7.5 Hz, 3H, H^9).

^{13}C NMR (101 MHz, CDCl$_3$) δ = 204.5 (C^1), 80.0 (C^3), 71.4 (C^5), 28.6 (C$^{6/7}$), 27.8 (C$^{6/7}$), 26.9 (C^8), 10.4 (C^9).
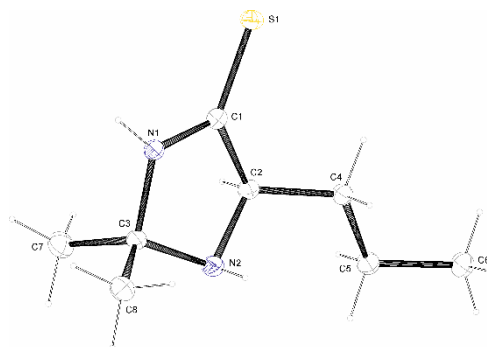
net formula	$C_8H_{16}N_2S$
M_r/g mol^{-1}	172.29
crystal size/mm	$0.100 \times 0.040 \times 0.030$
T/K	110.(2)
radiation	MoKα
diffractometer	'Bruker D8 Venture TXS'
crystal system	triclinic
space group	'P -1'
a/Å	7.2056(4)
b/Å	7.5204(4)
c/Å	9.6334(5)
α/°	71.686(2)
β/°	82.890(2)
γ/°	88.970(2)
V/Å^3	491.65(5)
Z	2
calc. density/g cm^{-3}	1.164
μ/mm^{-1}	0.274
absorption correction	Multi-Scan
transmission factor range	0.87–0.99
refls. measured	5007
R_{int}	0.0222
mean $\sigma(I)/I$	0.0299
θ range	2.849–26.363
observed refls.	1711
x, y (weighting scheme)	0.0247, 0.2740
hydrogen refinement	mixed
Flack parameter	?
refls in refinement	1979
parameters	130
restraints	8
$R(F_{obs})$	0.0354
$R_w(F^2)$	0.0835
S	1.090
shift/error$_{max}$	0.001
max electron density/e Å^{-3}	0.352
min electron density/e Å^{-3}	−0.242

2-Ethyl-2-methyl-5-propylimidazolidine-4-thione (3cg)
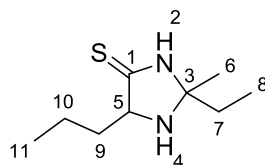
1-Cyanobutan-1-aminium chloride **2c** (337 mg, 2.50 mmol, 1.0 eq.) reacted with butanone **1g** (176 mg, 228 μL, 2.5 mmol, 1.0 eq.), potassium hydroxide and hydrogen sulphide following **GP-2**. Column chromatography (SiO$_2$, EtOAc) of the crude product yielded the title compound **3bg** (327 mg, 1.76 mmol, 70 %) as a white solid consisting of two diastereomers (ratio not determined).

HRMS (ESI) *m/z*: calculated for C$_9$H$_{18}$N$_2$S [M+H]$^+$: 187.1263, found: 187.1257.

Diastereomer A (major):

^{1}H NMR (400 MHz, CDCl$_3$) δ = 8.23 (bs, 1H, H^2), 3.95 – 3.80 (m, 1H, H^5), 1.28 – 2.16 (m, 1H, H$^{9a/b}$), 1.83 – 1.72 (m, 2H, H^7), 1.62 – 1.42 (m, 1H, H$^{9a/b,\ 10}$), 1.40 (s, 3H, H^6), 1.03 – 0.92 (m, 6H, H^{8,11}).

^{13}C NMR (101 MHz, CDCl$_3$) δ = 205.3 (C^1), 82.7 (C^3), 69.8 (C^5), 36.4 (C^9), 33.7 (C^7), 25.7 (C^6), 19.7 (C^{10}), 14.1 (C^{11}), 8.4 (C^8).

Diastereomer B (minor):

^{1}H NMR (400 MHz, CDCl$_3$) δ = 8.23 (bs, 1H, H^2), 3.95 – 3.80 (m, 1H, H^5), 1.28 – 2.16 (m, 1H, H$^{9a/b}$), 1.69 (q, *J* = 7.9 Hz, 2H, H^7), 1.62 – 1.42 (m, 1H, H$^{9a/b,\ 10}$), 1.46 (s, 3H, H^6), 1.03 – 0.92 (m, 6H, H^{8,11}).

^{13}C NMR (101 MHz, CDCl$_3$) δ = 205.4 (C^1), 82.8 (C^3), 70.6 (C^5), 36.8 (C^9), 34.2 (C^7), 26.5 (C^6), 19.6 (C^{10}), 14.0 (C^{11}), 8.8 (C^8).

5-Isopropyl-2-methylimidazolidine-4-thione (3da)
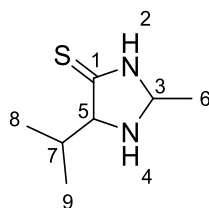
1-Cyano-2-methylpropan-1-aminium chloride **2d** (337 mg, 2.50 mmol, 1.0 eq.) reacted with acetaldehyde **1a** (110 mg, 140 µL, 2.50 mmol, 1.0 eq.), potassium hydroxide and hydrogen sulphide following **GP-2**. Column chromatography (SiO$_2$, EtOAc) of the crude product yielded the title compound **3da** (201 mg, 1.27 mmol, 51 %) as a white solid consisting of two diastereomers (1:1 ratio as determined by ^{1}H NMR).

HRMS (ESI) *m/z*: calculated for C$_7$H$_{15}$N$_2$S [M+H]$^+$: 159.0950, found: 159.0948.

Retardation factor: 1. Diastereomer R$_f$ = 0.39 (EtOAc)

2. Diastereomer R$_f$ = 0.48 (EtOAc).

Diastereomer A:

^{1}H NMR (400 MHz, CDCl$_3$) δ = 8.95 (b, 1H, H^2), 4.84 (qd, *J* = 5.9, 2.0 Hz, 1H, H^3), 3.93 (dd, *J* = 2.9, 2.0 Hz, 1H, H^5), 2.45 (heptd, *J* = 6.9, 2.9 Hz, 1H, H^7), 1.87 (b, 1H, H^4), 1.41 (d, *J* = 5.8 Hz, 3H, H^6), 1.07 (d, *J* = 7.0 Hz, 3H, H$^{8/9}$), 0.87 (d, *J* = 6.6 Hz, 3H, H$^{8/9}$).

^{13}C NMR (101 MHz, CDCl$_3$) δ = 205.6 (C^1), 76.3 (C^5), 74.6 (C^3), 32.2 (C^7), 22.2 (C^6), 20.6 (C$^{8/9}$), 15.6 (C$^{8/9}$).

Diastereomer B:

^{1}H NMR (400 MHz, CDCl$_3$) δ = 8.95 (b, 1H, H^2), 4.84 (qd, *J* = 5.9, 2.0 Hz, 1H, H^3), 3.76 (t, *J* = 2.5 Hz, 1H, H^5), 2.63 (heptd, *J* = 7.0, 2.9 Hz, 1H, H^7), 1.87 (b, 1H, H^4), 1.44 (d, *J* = 5.8 Hz, 3H, H^6), 1.08 (d, *J* = 7.0 Hz, 3H, H$^{8/9}$), 0.87 (d, *J* = 6.6 Hz, 3H, H$^{8/9}$).

^{13}C NMR (101 MHz, CDCl$_3$) δ = 206.1 (C^1), 76.1 (C^5), 72.4 (C^3), 29.4 (C^7), 21.12 (C^6), 20.55 (C$^{8/9}$), 14.91 (C$^{8/9}$).

2-Ethyl-5-isopropylimidazolidine-4-thione (3db)
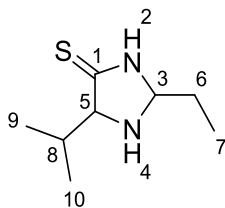
1-Cyanoethan-1-aminium chloride **2d** (266 mg, 2.50 mmol, 1.0 eq.) reacted with propionaldehyde **1b** (145 mg, 179 µL, 2.50 mmol, 1.0 eq.), potassium hydroxide and hydrogen sulphide following **GP-2**. Column chromatography (SiO$_2$, EtOAc) of the crude product yielded the title compound **3db** (235 mg, 1.80 mmol, 72 %) as a white solid consisting of two diastereomers (6:4 ratio as determined by ^{1}H NMR).

HRMS (ESI) *m/z*: calculated for C$_8$H$_{17}$N$_2$S [M+H]$^+$: 173.1107, found: 173.1104.

Retardation factor: 1. Diastereomer R$_f$ = 0.32 (EtOAc:*n*-pentane 1:1)

2. Diastereomer R$_f$ = 0.41 (EtOAc:*n*-pentane 1:1).

Diastereomer A (major):

^{1}H NMR (400 MHz, CDCl$_3$) δ = 8.57 (b, 1H, H^2), 4.71 – 4.64 (m, 1H, H^3), 3.85 – 3.74 (m, 1H, H^5), 2.63 (heptd, *J* = 7.0, 2.9 Hz, 1H, H^8), 1.86 (b, 1H, H^4), 1.76 – 1.64 (m, 2H, H^6), 1.10 – 0.97 (m, 6H, H$^{9,\,10}$), 0.87 (d, J = 6.8 Hz, 3H, H^7).

^{13}C NMR (101 MHz, CDCl$_3$) δ = 206.2 (C^1), 77.3 (C^3), 75.6 (C^5), 29.7 (C^8), 28.4 (C^6), 20.6 (C$^{9/10}$), 15.0 (C^7), 9.1 (C$^{9/10}$).

Diastereomer B (minor):

^{1}H NMR (400 MHz, CDCl$_3$) δ = 8.57 (b, 1H, H^2), 4.71 – 4.64 (m, 1H, H^3), 3.93 – 3.89 (m, 1H, H^5), 2.48 (heptd, *J* = 6.8, 2.9 Hz, 1H, H^8), 1.86 (b, 1H, H^4), 1.76 – 1.64 (m, 2H, H^6), 1.10 – 0.97 (m, 6H, H$^{9,\,10}$), 0.86 (d, *J* = 6.8 Hz, 3H, H^7).

^{13}C NMR (101 MHz, CDCl$_3$) δ = 205.8 (C^1), 79.4 (C^3), 75.9 (C^5), 32.3 (C^8), 29.6 (C^6), 20.5 (C$^{9/10}$), 15.4 (C^7), 9.1 (C$^{9/10}$).

5-Isopropyl-2-propylimidazolidine-4-thione (3dc)
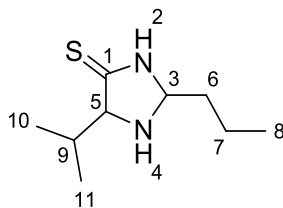
1-Cyano-2-methylpropan-1-aminium chloride **2d** (337 mg, 2.50 mmol, 1.0 eq.) reacted with butyraldehyde **1c** (180 mg, 225 μL, 2.50 mmol, 1.0 eq.), potassium hydroxide and hydrogen sulphide following **GP-2**. Column chromatography (SiO$_2$, EtOAc:*n*-pentane 1:1) of the crude product yielded the title compound **3dc** (211 mg, 1.13 mmol, 48 %) as a white solid consisting of two diastereomers (1:1 ratio as determined by ^{1}H NMR).

Retardation factor: 1. Diastereomer R$_f$ = 0.69 (EtOAc:*n*-pentane 1:1)

2. Diastereomer R$_f$ = 0.69 (EtOAc:*n*-pentane 1:1)

Diastereomer A:

^{1}**H NMR** (400 MHz, CDCl$_3$) δ = 8.95 (bs, 1H, H^2), 4.81 – 4.64 (m, 1H, H^3), 3.95 – 3.86 (m, 1H, H^5), 2.53 – 2.40 (m, 1H, H^9), 1.82 (bs, 1H, H^4), 1.72 – 1.58 (m, 2H, H$^{6/7}$), 1.53 – 1.38 (m, 2H, H$^{6/7}$), 1.12 – 0.78 (m, 9H, H$^{8, 10, 11}$).

Diastereomer B:

^{1}**H NMR** (400 MHz, CDCl$_3$) δ = 8.95 (bs, 1H, H^2), 4.81 – 4.64 (m, 1H, H^3), 3.78 – 3.75 (m, 1H, H^5), 2.62 (heptd, *J* = 7.8, 7.2, 3.3 Hz, 1H, H^9), 1.82 (bs, 1H, H^4), 1.72 – 1.58 (m, 2H, H$^{6/7}$), 1.53 – 1.38 (m, 2H, H$^{6/7}$), 1.12 – 0.78 (m, 9H, H$^{8, 10, 11}$).

2,5-Diisopropylimidazolidine-4-thione (3dd)
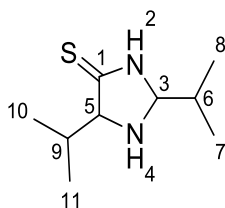
1-Cyano-2-methylpropan-1-aminium chloride **2d** (336 mg, 2.50 mmol, 1.0 eq.) reacted with isobutyraldehyde **1d** (180 mg, 228 µL, 2.50 mmol, 1.0 eq.), potassium hydroxide and hydrogen sulphide following **GP-2**. Column chromatography (SiO$_2$, EtOAc:n-pentane 1:9) of the crude product yielded the title compound **3dd** (165 mg, 0.89 mmol, 32 %) as a white solid consisting of two diastereomers (7.5:2.5 ratio as determined by ^{1}H NMR).

HRMS (ESI) m/z: calculated for C$_9$H$_{18}$N$_2$S [M+H]$^+$: 187.1263, found: 187.1261.

Retardation factor: 1. Diastereomer R$_f$ = 0.26 (EtOAc:n-pentane 1:4)

2. Diastereomer R$_f$ = 0.35 (EtOAc:n-pentane 1:4).

Diastereomer A (major):

^{1}H NMR (599 MHz, CDCl$_3$) δ = 9.36 (b, 1H, H^2), 4.49 (dd, J = 5.8, 2.3 Hz, 1H, H^3), 3.80 – 3.77 (m, 1H, H^5), 2.60 (heptd, J = 7.0, 2.8 Hz, 1H, H^9), 2.06 – 1.67 (m, 2H, H^{4,6}), 1.06 (d, J = 7.1 Hz, 3H, H$^{10/11}$), 1.00 (d, J = 6.9 Hz, 3H, H$^{7/8}$), 1.00 (d, J = 6.9 Hz, 3H, H$^{7/8}$), 0.85 (d, J = 6.8 Hz, 3H, H$^{10/11}$).

^{13}C NMR (151 MHz, CDCl$_3$) δ = 205.6 (C^1), 81.4 (C^3), 75.4 (C^5), 32.8 (C^6), 29.9 (C^9), 20.5 (C$^{10/11}$), 17.8 (C$^{7/8}$), 17.8 (C$^{7/8}$), 15.0 (C$^{10/11}$).

Diastereomer B (minor):

^{1}H NMR (599 MHz, CDCl$_3$) δ = 9.38 (b, 1H, H^2), 4.54 (dd, J = 5.3, 2.5 Hz, 1H, H^3), 3.91 – 3.87 (m, 1H, H^5), 2.46 (heptd, J = 6.9, 2.5 Hz, 1H, H^9), 2.06 – 1.70 (m, 2H, H^{4,6}), 1.04 (d, J = 7.0 Hz, 3H, H$^{10/11}$), 0.98 – 0.94 (m, 6H, H$^{7/8}$), 0.84 (d, J = 6.8 Hz, 3H, H$^{10/11}$).

^{13}C NMR (151 MHz, CDCl$_3$) δ = 205.1 (C^1), 83.3 (C^3), 76.1 (C^5), 34.2 (C^6), 32.2 (C^9), 20.4 (C$^{10/11}$), 17.5 (C$^{7/8}$), 17.4 (C$^{7/8}$), 15.2 (C$^{10/11}$).

2,2-Dimethyl-5-(propan-2-yl)imidazolidine-4-thione (3df)
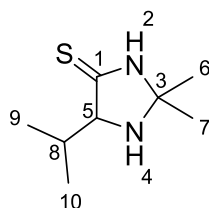
1-Cyano-2-methylpropan-1-aminium chloride **2d** (336 mg, 2.50 mmol, 1.0 eq.) reacted with acetone **1f** (145 mg, 185 μL, 2.5 mmol, 1.0eq.), potassium hydroxide and hydrogen sulphide following **GP-2**. Column chromatography (SiO$_2$, EtOAc) of the crude product yielded the title compound **3df** (185 mg, 1.07 mmol, 43 %) as a white solid.

HRMS (ESI) *m/z*: calculated for C$_8$H$_{17}$N$_2$S [M+H]$^+$: 173.1107, found: 173.1104.

Retardation factor: R$_f$ = 0.46 (EtOAc:*n*-pentane 7:3).

^{1}H NMR (400 MHz, CDCl$_3$) δ = 9.61 (b, 1H, H^2), 3.91 (d, *J* = 2.9 Hz, 1H, H^5), 2.60 (heptd, *J* = 7.0, 2.9 Hz, 1H, H^8), 1.86 (b, 1H, H^4), 1.50 (s, 3H, H$^{6/7}$), 1.42 (s, 3H, H$^{6/7}$), 1.06 (d, *J* = 7.1 Hz, 3H, H^9), 0.85 (d, *J* = 6.9 Hz, 3H, H^{10}).

^{13}C NMR (101 MHz, CDCl$_3$) δ = 203.5 (C^1), 79.9 (C^3), 75.0 (C^5), 29.7 (C^8), 28.4 (C^{6,7}), 20.5 (C$^{9/10}$), 14.9 (C$^{9/10}$).

2-Ethyl-5-isopropyl-2-methylimidazolidine-4-thione (3dg)
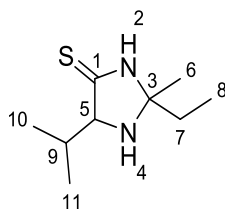
1-Cyano-2-methylpropan-1-aminium chloride **2d** (336 mg, 2.50 mmol, 1.0 eq.) reacted with butanone **1g** (176 mg, 228 µL, 2.5 mmol, 1.0 eq.), potassium hydroxide and hydrogen sulphide following **GP-2**. Column chromatography (SiO$_2$, EtOAc) of the crude product yielded the title compound **3dg** (281 mg, 1.63 mmol, 65 %) as a white solid consisting of two diastereomers (ratio not determined by ^{1}H NMR).

HRMS (ESI) *m/z*: calculated for C$_9$H$_{18}$N$_2$S [M+H]$^+$: 187.1263, found: 187.1261.

Diastereomer A (major):

^{1}H NMR (400 MHz, CDCl$_3$) δ = 8.73 (bs, 1H, H^2), 3.92 (d, *J* = 2.9 Hz, 1H, H^5), 2.70 – 2.55 (m, 1H, H^9), 1.84 – 1.71 (m, 2H, H^7), 1.39 (s, 3H, H^6), 1.09 (d, *J* = 7.1 Hz, 2H, H$^{10/11}$), 1.00 (t, *J* = 7.5 Hz, 3H, H^8), 0.88 (d, *J* = 6.8 Hz, 3H, H$^{10/11}$).

^{13}C NMR (101 MHz, CDCl$_3$) δ = 204.2 (C^1), 82.1 (C^3), 74.4 (C^5), 33.5 (C^7), 29.8 (C^9), 26.1 (C^6), 20.5 (C$^{10/11}$), 15.0 (C$^{10/11}$), 8.3 (C^8).

Diastereomer B (minor):

^{1}H NMR (400 MHz, CDCl$_3$) δ = 8.73 (bs, 1H, H^2), 5.29 (s, 1H, H^5), 2.70 – 2.55 (m, 1H, H^9), 1.84 – 1.71 (m, 2H, H^7), 1.45 (s, 3H, H^6), 1.06 (d, *J* = 7.1 Hz, 2H, H$^{10/11}$), 0.96 (t, *J* = 7.5 Hz, 3H, H^8), 0.87 (d, *J* = 6.8 Hz, 3H, H$^{10/11}$).

^{13}C NMR (101 MHz, CDCl$_3$) δ = 204.2 (C^1), 82.4 (C^3), 75.6 (C^5), 34.9 (C^7), 30.2 (C^9), 26.4 (C^6), 20.4 (C$^{10/11}$), 14.8 (C$^{10/11}$), 8.6 (C^8).

2,2-Dimethyl-5-phenylimidazolidine-4-thione (3ef)
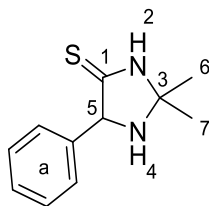
Cyano(phenyl)methanaminium chloride **2e** (422 mg, 2.50 mmol, 1.0 eq.) reacted with acetone **1f** (145 mg, 185 μL, 2.5 mmol, 1.0eq.), potassium hydroxide and hydrogen sulphide following **GP-2**. Column chromatography (SiO$_2$, EtOAc) of the crude product yielded the title compound **3dg** (430 mg, 2.08 mmol, 83 %) as a white solid.

HRMS (ESI) *m/z*: calculated for C$_{11}$H$_{15}$N$_2$S [M+H]$^+$: 207.0950, found: 207.0948.

^{1}H NMR (400 MHz, CDCl$_3$) δ = 9.73 (bs, 1H, H^2), 7.48 – 7.30 (m, 5H, H^a), 5.03 (s, 1H, H^5), 1.57 (s, 3H, H$^{6/7}$), 1.51 (s, 3H, H$^{6/7}$).

^{13}C NMR (101 MHz, CDCl$_3$) δ = 202.9 (C^1), 139.1 (C^a), 129.0 (C^a), 128.7 (C^a), 128.5 (C^a), 80.5 (C^3), 74.8 (C^5), 28.8 (C$^{6/7}$), 28.3 (C$^{6/7}$).

2-Ethyl-2-methyl-5-phenylimidazolidine-4-thione (3eg)
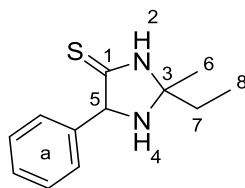
Cyano(phenyl)methanaminium chloride **2e** (422 mg, 2.50 mmol, 1.0 eq.) reacted with butanone **1g** (176 mg, 228 μL, 2.5 mmol, 1.0 eq.), potassium hydroxide and hydrogen sulphide following **GP-2**. Column chromatography (SiO$_2$, EtOAc) of the crude product yielded the title compound **3eg** (236 mg, 1.07 mmol, 43 %) as a white solid consisting of two diastereomers (4.5:5.5 ratio as determined by ^{1}H NMR).

HRMS (ESI) *m/z*: calculated for C$_{12}$H$_{17}$N$_2$S [M+H]$^+$: 221.1107, found: 221.1100.

Diastereomer A (minor):

^{1}H NMR (400 MHz, CDCl$_3$) δ = 9.25 (bs, 1H, H^2), 7.50 – 7.32 (m, 5H, H^a), 5.04 (s, 1H, H^5), 1.88 – 1.72 (m, 2H, H^7), 1.48 (s, 3H, H^6), 1.04 (t, *J* = 7.5 Hz, 3H, H^8).

^{13}C NMR (101 MHz, CDCl$_3$) δ = 203.4 (C^1), 139.2 (C^a), 129.0 (C^a), 128.7 (C^a), 128.6 (C^a), 83.0 (C^3), 74.4 (C^5), 33.7 (C^7), 26.3 (C^6), 8.5 (C^8).

Diastereomer B (major):

^{1}H NMR (400 MHz, CDCl$_3$) δ = 9.25 (bs, 1H, H^2), 7.50 – 7.32 (m, 5H, H^a), 5.00 (s, 1H, H^5), 1.88 – 1.72 (m, 2H, H^7), 1.54 (s, 3H, H^6), 1.03 (t, *J* = 7.4 Hz, 3H, H^8).

^{13}C NMR (101 MHz, CDCl$_3$) δ = 203.4 (C^1), 139.7 (C^a), 129.0 (C^a), 128.7 (C^a), 128.4 (C^a), 83.3 (C^3), 75.4 (C^5), 34.8 (C^7), 26.8 (C^6), 8.8 (C^8).

2,5,5-Trimethylimidazolidine-4-thione (3fa)
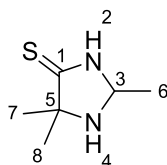
2-Cyanopropan-2-aminium chloride **2f** (302 mg, 2.50 mmol, 1.0 equiv.) reacted with acetaldehyde **1a** (110 mg, 140 μL, 2.50 mmol, 1.0 equiv.), potassium hydroxide and hydrogen sulphide following **GP-2**. Column chromatography (SiO$_2$, EtOAc) of the crude product yielded the title compound **3fa** (212 mg, 1.47 mmol, 59 %) as a white solid.

HRMS (ESI) *m/z*: calculated for C$_6$H$_{13}$N$_2$S [M+H]$^+$: 145.0794, found: 145.0792.

Retardation factor: R$_f$ = 0.19 (EtOAc).

^{1}H NMR (400 MHz, CDCl$_3$) δ = 8.99 (b, 1H, H^2), 4.77 (q, *J* = 5.8 Hz, 1H, H^3), 1.83 (b, 1H, H^4) 1.48 (s, 3H, H$^{7/8}$), 1.44 (d, *J* = 5.8 Hz, 3H, H^6), 1.33 (s, 3H, H$^{7/8}$).

^{13}C NMR (101 MHz, CDCl$_3$) δ = 211.4 (C^1), 71.1 (C^5), 70.3 (C^3), 27.7 (C$^{7/8}$), 25.6 (C$^{7/8}$), 20.7 (C^6).

2-Ethyl-5,5-dimethylimidazolidine-4-thione (3fb)
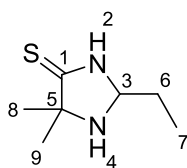
2-Cyanopropan-2-aminium chloride **2f** (302 mg, 2.50 mmol, 1.0 equiv.) reacted with propionaldehyde **1b** (146 mg, 180 μL, 2.50 mmol, 1.0 equiv.), potassium hydroxide and hydrogen sulphide following **GP2** and yielded the title compound **3fb** (196 mg, 1.24 mmol, 50 %) as a white solid.

HRMS (ESI) *m/z*: calculated for $C_7H_{15}N_2S$ [M+H]$^+$: 159.0950, found: 159.0948.

Retardation factor: $R_f = 0.46$ (EtOAc).

^{1}H NMR (400 MHz, CDCl$_3$) δ = 8.70 (b, 1H, H^2), 4.61 (t, *J* = 6.0 Hz, 1H, H^3), 1.90 (b, 1H, H^4), 1.78 – 1.67 (m, 2H, H^6), 1.48 (s, 3H, H$^{8/9}$), 1.35 (s, 3H, H$^{8/9}$), 1.04 (t, *J* = 7.5 Hz, 3H, H^7).

^{13}C NMR (101 MHz, CDCl$_3$) δ = 211.4 (C^1), 75.4 (C^3), 70.7 (C^5), 28.1 (C$^{8/9}$), 27.9 (C$^{8/9}$), 26.0 (C^6), 9.3 (C^7).
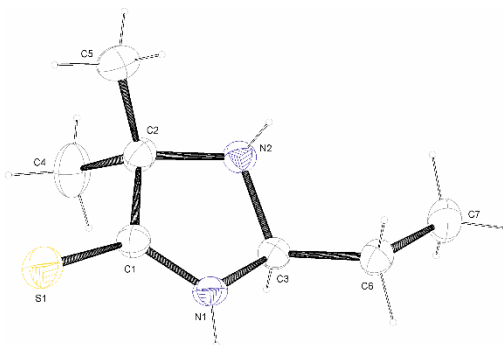
net formula	$C_7H_{14}N_2S$
M_r/g mol^{-1}	158.26
crystal size/mm	$0.090 \times 0.060 \times 0.050$
T/K	296.(2)
radiation	MoKα
diffractometer	'Bruker D8Quest'
crystal system	trigonal
space group	'P 32'
a/Å	7.8432(2)
b/Å	7.8432(2)
c/Å	12.8096(3)
α/°	90
β/°	90
γ/°	120
V/Å^3	682.42(4)
Z	3
calc. density/g cm^{-3}	1.155
μ/mm^{-1}	0.290
absorption correction	Multi-Scan
transmission factor range	0.94–0.99
refls. measured	13262
R_{int}	0.0325
mean $\sigma(I)/I$	0.0194
θ range	2.999–26.351
observed refls.	1807
x, y (weighting scheme)	0.0324, 0.0264
hydrogen refinement	H(C) constr, H(N) restr
Flack parameter	−0.29(3)
refls in refinement	1864
parameters	103
restraints	2
$R(F_{obs})$	0.0239
$R_w(F^2)$	0.0580
S	1.056
shift/error$_{max}$	0.001
max electron density/e Å^{-3}	0.087
min electron density/e Å^{-3}	−0.115

SADI applied for H(N). Refined as a 2-component merohedral twin pretending Laue clas - 3 m 1.

5,5-Dimethyl-2-propylimidazolidine-4-thione (3fc)
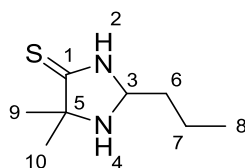
2-Cyanopropan-2-aminium chloride **2f** (302 mg, 2.50 mmol, 1.0 equiv.) reacted with butyraldehyde **1c** (180 mg, 225 μL, 2.50 mmol, 1.0 eq.), potassium hydroxide and hydrogen sulphide following **GP-2** and yielded the title compound **3fc** (134 mg, 0.78 mmol, 31 %) as a white solid.

HRMS (ESI) *m/z*: calculated for $C_8H_{17}N_2S$ [M+H]$^+$: 173.1107, found: 173.1106.

^{1}H NMR (400 MHz, CDCl$_3$) δ = 8.68 (bs, 1H, H^2), 4.65 (t, *J* = 6.1 Hz, 1H, H^3), 1.71 – 1.61 (m, 2H, H^6), 1.53 – 1.41 (m, 6H, H^7), 1.47 (s, 3H, H$^{9/10}$), 1.34 (s, 3H, H$^{9/10}$), 0.99 (t, *J* = 7.3 Hz, 3H, H^8).

2-Isopropyl-5,5-dimethylimidazolidine-4-thione (3fd)
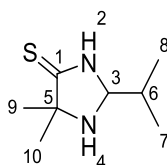
2-Cyanopropan-2-aminium chloride **2f** (302 mg, 2.50 mmol, 1.0 equiv.) reacted with isobutyraldehyde **1d** (180 mg, 228 μL, 2.50 mmol, 1.0 equiv.), potassium hydroxide and hydrogen sulphide following **GP-2**. Column chromatography (SiO$_2$, EtOAc:*n*-pentane 2:3) of the crude product yielded the title compound **3fd** (68.0 mg, 0.39 mmol, 16 %) as a white solid.

HRMS (ESI) *m/z*: calculated for $C_8H_{16}N_2S$ [M+H]$^+$: 173.1107, found: 173.1107.

Retardation factor: R$_f$ = 0.32 (EtOAc:*n*-pentane 2:3).

^{1}H NMR (400 MHz, CDCl$_3$) δ = 8.30 (b, 1H, H^2), 4.43 (d, *J* = 6.4 Hz, 1H, H^3), 1.91 – 1.73 (m, 1H, H^6), 1.67 (b, 1H, H^4), 1.48 (s, 3H, H$^{9/10}$), 1.37 (s, 3H, H$^{9/10}$), 1.03 (d, *J* = 6.8 Hz, 6H, H^{7,8}).

^{13}C NMR (101 MHz, CDCl$_3$) δ =79.3 (C^3), 70.7 (C^5), 32.6 (C^6), 27.9 (C$^{9/10}$), 26.3 (C$^{9/10}$), 18.1 (C$^{7/8}$), 18.0 (C$^{7/8}$).

2,2,5,5-Tetramethylimidazolidine-4-thione (3ff)
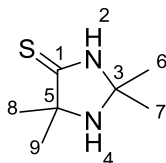
2-Cyanopropan-2-aminium chloride **2f** (302 mg, 2.50 mmol, 1.0 eq.) reacted with acetone (145 mg, 185 µL, 2.5 mmol, 1.0 eq.), potassium hydroxide and hydrogen sulphide following **GP-2**. Column chromatography (SiO$_2$, EtOAc:*n*-pentane 2:3) of the crude product yielded the title compound **3fd** (196 mg, 1.24 mmol, 50 %) as a white solid.

HRMS (ESI) *m*/z: calculated for C$_7$H$_{15}$N$_2$S [M+H]$^+$: 159.0950, found: 159.0946.

Retardation factor: R$_f$ = 0.40 (EtOAc).

^{1}H NMR (400 MHz, CDCl$_3$) δ = 8.82 (b, 1H, H^2), 1.90 (b, 1H, H^4), 1.50 (s, 6H, H$^{6,7/8,9}$), 1.48 (s, 6H, H$^{6,7/8,9}$).

^{13}C NMR (101 MHz, CDCl$_3$) δ = 208.7 (C^1), 78.4 (C^3), 71.16 (C^5), 30.25 (C^{6,7,8,9}).
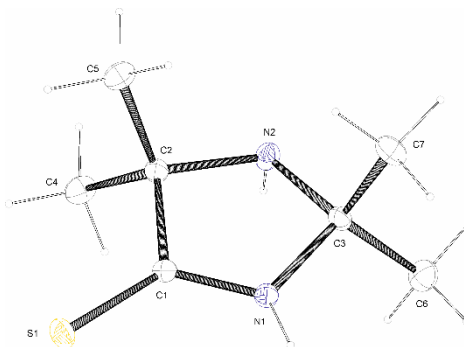
net formula	$C_7H_{14}N_2S$
M_r/g mol^{-1}	158.26
crystal size/mm	$0.474 \times 0.411 \times 0.295$
T/K	143(2)
radiation	MoKα
diffractometer	'Oxford XCalibur'
crystal system	orthorhombic
space group	'P n a 21'
a/Å	10.1458(5)
b/Å	8.7981(4)
c/Å	9.7260(6)
α/°	90
β/°	90
γ/°	90
V/Å^3	868.18(8)
Z	4
calc. density/g cm^{-3}	1.211
μ/mm^{-1}	0.304
absorption correction	multi-scan
transmission factor range	0.93263–1.00000
refls. measured	5473
R_{int}	0.0294
mean $\sigma(I)/I$	0.0358
θ range	4.531–27.466
observed refls.	1792
x, y (weighting scheme)	0.0554, 0.0539
hydrogen refinement	H(C) constr, H(N) refall
Flack parameter	0.32(13)
refls in refinement	1915
parameters	104
restraints	1
$R(F_{obs})$	0.0351
$R_w(F^2)$	0.0912
S	1.038
shift/error$_{max}$	0.001
max electron density/e Å^{-3}	0.351
min electron density/e Å^{-3}	−0.202

5-Ethyl-2,5-dimethylimidazolidine-4-thione (3ga)
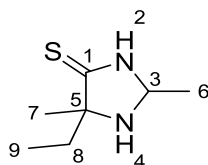
2-Cyanobutan-2-aminium chloride **2g** (337 mg, 2.50 mmol, 1.0 eq.) reacted with acetaldehyde **1a** (180 mg, 140 μL, 2.50 mmol, 1.0 eq.), potassium hydroxide and hydrogen sulphide following **GP-2**. Column chromatography (SiO$_2$, EtOAc) of the crude product yielded the title compound **3ga** (315 mg, 1.99 mmol, 80 %) as a white solid consisting of two diastereomers (1:1 ratio as determined by ^{1}H NMR).

HRMS (ESI) *m/z*: calculated for C$_7$H$_{14}$N$_2$S [M+H]$^+$: 159.0950, found: 159.0949.

Retardation factor: 1. Diastereomer R$_f$ = 0.36 (EtOAc)

2. Diastereomer R$_f$ = 0.47 (EtOAc)

Diastereomer A:

^{1}**H NMR** (400 MHz, CDCl$_3$) δ = 8.94 (bs, 1H, H^2), 4.79 (q, *J* = 5.7 Hz, 1H, H^3), 1.84 (m, 1H, H^4), 1.76 – 1.59 (m, 2H, H^8), 1.48 – 1.41 (m, 3H, H^6), 1.30 (s, 3H, H^7), 0.97 (t, *J* = 7.5 Hz, 3H, H^9).

^{13}**C NMR** (101 MHz, CDCl$_3$) δ = 210.7(C^1), 74.3 (C^5), 70.3 (C^3), 32.2 (C^8), 24.5 (C^7), 20.8 (C^6), 8.6 (C^9).

Diastereomer B:

^{1}**H NMR** (400 MHz, CDCl$_3$) δ = 8.94 (bs, 1H, H^2), 4.75 (q, *J* = 5.7 Hz, 1H, H^3), 2.00 – 1.74 (m, 2H, H^8), 1.84 (bs, 1H, H^4), 1.48 – 1.41 (m, 3H, H^6), 1.42 (s, 3H, H^7), 0.95 (t, *J* = 7.5 Hz, 3H, H^9).

^{13}**C NMR** (101 MHz, CDCl$_3$) δ = 210.7 (C^1), 74.2 (C^5), 71.2 (C^3), 31.9 (C^8), 26.4 (C^7), 21.7 (C^6), 8.2 (C^9).

5-Ethyl-5-methyl-2-propylimidazolidine-4-thione (3gb)
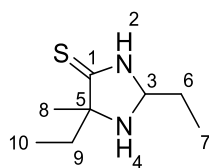
2-Cyanobutan-2-aminium chloride **2g** (337 mg, 2.50 mmol, 1.0 eq.) reacted with propionaldehyde **1b** (146 mg, 180 μL, 2.50 mmol, 1.0 eq.), potassium hydroxide and hydrogen sulphide following **GP-2**. Column chromatography (SiO$_2$, EtOAc:n-pentane 1:3) of the crude product yielded the title compound **3gb** (23.0 mg, 0.12 mmol, 4 %) as a white solid.

HRMS (ESI) m/z: calculated for C$_8$H$_{17}$N$_2$S [M+H]$^+$: 173.1107, found: 173.1106.

Retardation factor: R_f = 0.40 (EtOAc:n-pentane 1:3)

^{1}H NMR (400 MHz, CDCl$_3$) δ = 9.34 (bs, 1H, H^2), 4.66 (t, J = 5.9 Hz, 1H, H^3), 1.98 – 1.71 (m, 3H), 1.71 – 1.57 (m, 2H), 1.55 – 1.37 (m, 4H), 1.29 (s, 3H, H^9), 1.04 – 0.88 (m, 6H$^{8/11}$).

2,5-Diethyl-2,5-dimethylimidazolidin-4-thion (3gg)
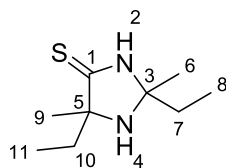
2-Cyanobutan-2-aminium chloride **2g** (337 mg, 2.50 mmol, 1.0 eq.) reacted with isobutyraldehyde **1g** (176 mg, 228 μL, 2.5 mmol, 1.0 eq.), potassium hydroxide and hydrogen sulphide following **GP-2**. Column chromatography (SiO$_2$, EtOAc:*n*-pentane 1:3) of the crude product yielded the title compound **3gg** (331.6 mg, 1.78 mmol, 71 %) as a white solid consisting of two diastereomers (ratio was not determined).

HRMS (ESI) *m/z*: calculated for C$_9$H$_{18}$N$_2$S [M+H]$^+$: 187.1263, found: 187.1258.

Diastereomer A:

^{1}H NMR (400 MHz, CDCl$_3$) δ = 9.12 (bs, 1H, H^2), 1.83 – 1.73 (m, 2H, H^{10}), 1.73 – 1.65 (m, 2H, H^7), 1.44 (s, 3H, H^6), 1.43 (s, 3H, H^7), 1.01 – 0.91 (m, 6H, H^{8,11}).

^{13}C NMR (101 MHz, CDCl$_3$) δ = 207.9 (C^1), 81.1 (C^3), 73.8 (C^5), 35.3 (C^7), 33.9 (C^{10}), 28.9 (C^9), 28.1 (C^6), 8.7 (C^8), 8.5 C^{11}).

Diastereomer B:

^{1}H NMR (400 MHz, CDCl$_3$) δ = 9.12 (bs, 1H, H^2), 1.83 – 1.73 (m, 2H, H^{10}), 1.73 – 1.65 (m, 2H, H^7), 1.41 (s, 3H, H^6), 1.41 (s, 3H, H^7), 1.01 – 0.91 (m, 6H, H^{8,11}).

^{13}C NMR (101 MHz, CDCl$_3$) δ = 207.9 (C^1), 81.2 (C^3), 74.0 (C^5), 35.8 (C^7), 34.2 (C^{10}), 28.6 (C^9), 27.5 (C^6), 8.8 (C^8), 8.5 (C^{11}).

6.2.3 Intermediates and Side-products

2,4,6-Triethyl-1,3,5-dithiazinane (4b)

For pure isolation of **4b**, a one-pot procedure without the addition of potassium cyanide was performed, that resembled the synthesis of KAWAI et al.[196]
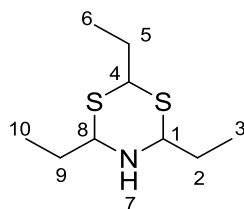
Propionaldehyde **1b** (179 μL, 2.5 mmol, 3.0 eq.) was dissolved in 4.0 mL concentrated aqueous ammonia at 0 °C. Hydrogen sulphide was bubbled through the solution (2 x 17 bar), the vial was sealed and left stirring for 20 h, thereby letting the temperature increase to room temperature. The remaining hydrogen sulphide was purged with nitrogen at 55 °C and the mixture was extracted with diethyl ether. The combined organic phases were washed with hot water, dried over sodium sulfate and concentrated *in vacuo*. Without further purification the title compound **4b** was yielded as colourless liquid (75 mg, 0.37 mmol, 44 %).

HRMS (ESI) *m/z*: calculated for $C_9H_{20}NS_2$ [M+H]$^+$: 206.1032, found: 206.1030.

¹H NMR (400 MHz, CDCl$_3$) δ = 4.27 (t, *J* = 6.5 Hz, 1H, H^4), 4.01 (dt, *J* = 12.1, 6.4 Hz, 2H, H^{1,8}), 1.89 − 1.81 (m, 2H, H^5), 1.81 − 1.72 (m, 4H, H^{2,9}), 1.57 (b, 1H, H^7), 1.11 (t, *J* = 7.4 Hz, 3H, H^6), 1.06 (t, *J* = 7.5 Hz, 6H, H^{3,10}).

¹³C NMR (101 MHz, CDCl$_3$) δ = 68.0 (C^{1,8}), 51.9 (C^4), 30.5 (C^{2,9}), 30.2 (C^5), 10.9 (C^6), 10.5 (C^{3,10}).

2-((1-Cyanopropyl)amino)butanethioamide (13b)
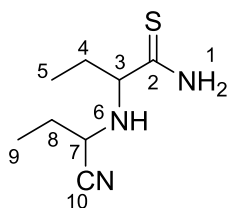
Potassium cyanide (163 mg, 2.5 mmol, 1.0 eq.), ammonium chloride (134 mg, 2.5 mmol, 1.0 eq.), and propionaldehyde **1b** (180 μL, 2.5 mmol, 1.0 eq.) were dissolved in 4.0 mL water at 0 °C. Hydrogen sulphide was bubbled through the solution (3 x 17 bar) and the vial was sealed and left stirring for 5 days. The precipitate was filtered and washed with H_2O. Column chromatography (SiO$_2$, 2:1 *n*-pentane:EtOAc) of the crude product yielded the title compound **13b** (7 mg, 0.04 mmol, 3 %) as a white solid.

HRMS (ESI) *m/z*: calculated for $C_8H_{16}N_3S$ [M+H]$^+$: 186.1059, found: 186.1058.

Retardation factor: R_f = 0.53 (1:1 *n*-pentane:EtOAc).

¹H NMR (400 MHz, acetone-d_6) δ = 8.92 (b, 1H, H^{1a}), 8.81 (s, 1H, H^{1b}), 3.65 (dd, *J* = 7.0, 5.5 Hz, 1H, H^7), 3.45 (t, *J* = 7.0 Hz, 1H, H^3), 1.88 – 1.75 (m, 3H, H$^{4, 8a}$), 1.68 (dq, *J* = 13.9, 7.2 Hz, 1H, H^{8b}), 1.08 (t, *J* = 7.4 Hz, 3H, H^5), 0.98 (t, *J* = 7.5 Hz, 3H, H^9).

¹³C NMR (101 MHz, acetone-d_6) δ = 212.9 (C^2), 120.9 (C^{10}), 69.8 (C^7), 51.4 (C^3), 27.6 (C^4), 10.6 (C^5), 10.4 (C^9). C^8 masked by the acetone peak.

2,2'-Azanediyldibutanethioamide (14b)
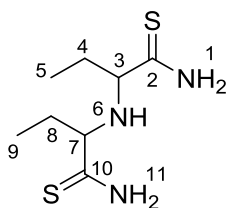
Potassium cyanide (163 mg, 2.5 mmol, 1.0 eq.), ammonium chloride (134 mg, 2.5 mmol, 1.0 eq.), and propionaldehyde **1b** (180 μL, 2.5 mmol, 1.0 eq.) were dissolved in 4.0 mL water at 0 °C. Hydrogen sulphide was bubbled through the solution (3 x 17 bar) and the vial was sealed and left stirring for 5 days. The precipitate was filtered and washed with H_2O. Column chromatography (SiO$_2$, 2:1 *n*-pentane:EtOAc) of the crude product yielded the title compound **14b** (57 mg, 0.36 mmol, 29 %) as a white solid.

HRMS (ESI) *m/z*: calculated for $C_8H_{17}N_3S_2$ [M+H]$^+$: 220.0937, found: 220.0933.

Retardation factor: R$_f$ = 0.21 (1:1 *n*-pentane:EtOAc).

¹H NMR (400 MHz, DMSO-*d*$_6$) δ = 9.78 – 9.67 (m, 2H, H^{1,11}), 9.19 – 9.09 (m, 2H, H^{1,11}), 3.08 (q, *J* = 6.3 Hz, 2H, H^{3,7}), 1.61 – 1.46 (m, 4H, H^{4,8}), 0.85 (t, *J* = 7.5 Hz, 6H, H^{5,9}).

¹³C NMR (101 MHz, DMSO-*d*$_6$) δ = 209.7 (C^{2,10}), 67.8 (C^{3,7}), 29.0 (C^{4,8}), 10.3 (C^{5,9}).

6.2.4 Derivatives of Imidazolidine-4-thiones

1,2,2,5,5-pentamethylimidazolidine-4-thione (3ff-*N1*-Me)
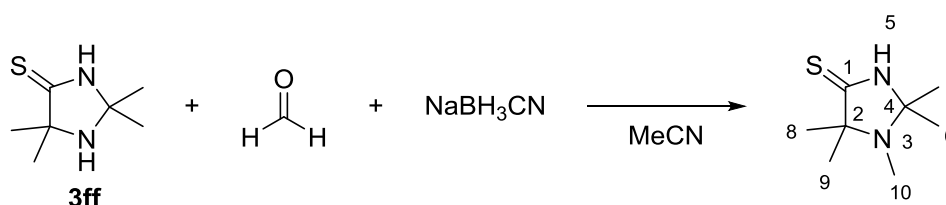
3ff (79 mg, 0.50 mmol, 1.0 eq.) and sodium cyanoborohydride (47 mg, 1.6 mmol, 1.5 eq.) were dissolved in 2 mL acetonitrile and 56 µL (23 mg, 0.75 mmol, 1.5 eq.) formaldehyde solution (37 %) was added. The pH was adjusted to neutral with a few drops of concentrated acetic acid and the solution was stirred for 1.5 h. Water was added and the mixture was extracted with dichloromethane. The organic phases were dried over sodium sulfate and the solvent was removed *in vacuo*. Column chromatography (SiO$_2$, isohexane:EtOAc 4:1) of the crude product yielded the title compound **3ff-*N1*-Me** (35 mg, 0.20 mmol, 40 %) as colourless solid.

As side-reaction, additional hydroxymethylation at the thioamide nitrogen occurred and the retention factors of the corresponding product and **3ff-*N1*-Me** were very similar. To isolate **3ff-*N1*-Me** from the combined fractions, preparative HPLC at 20 °C and a flow of 20 mL/min *n*-hexane:isopropanol 99:1 was used (Nucleodur 100-5, 21 mm x 250 mm, Macherey Nagel).

HRMS (ESI) *m/z*: calculated for C$_8$H$_{17}$N$_2$S [M+H]$^+$: 173.1107, found: 173.1108.

¹H NMR (400 MHz, CD$_3$CN) δ 8.94 (bs, 1H, H^5), 2.32 (s, 3H, H^{10}), 1.32 (s, 6H, H^{6,7}), 1.26 (s, 6H, H^{8,9}).

¹³C NMR (101 MHz, CD$_3$CN) δ 207.4 (C^1), 80.1 (C^4), 72.2 (C^2), 27.9 (C^{10}), 26.2 (C$^{6/7/8/9}$), 26.1 (C$^{6/7/8/9}$).

Note: Methylation at the amine was confirmed by the obtained crystal structure and can also be verified by the present H^5-Signal, as well as clear coupling in the HMBC spectrum: H^{10} couples with both C^2 and C^4 and not with C^1.
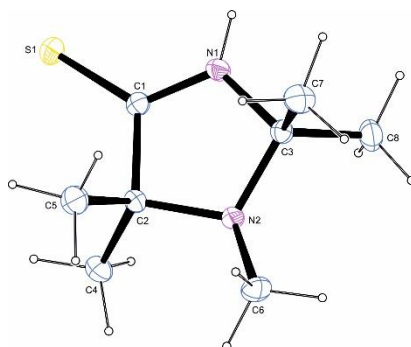
net formula	$C_8H_{16}N_2S$
M_r/g mol^{-1}	172.29
crystal size/mm	$0.070 \times 0.050 \times 0.030$
T/K	173.(2)
radiation	MoKα
diffractometer	'Bruker D8 Venture TXS'
crystal system	monoclinic
space group	'P 1 21/c 1'
a/Å	10.7020(15)
b/Å	8.2529(10)
c/Å	11.4916(14)
α/°	90
β/°	109.411(4)
γ/°	90
V/Å^3	957.3(2)
Z	4
calc. density/g cm^{-3}	1.195
μ/mm^{-1}	0.281
absorption correction	Multi-Scan
transmission factor range	0.94–0.99
refls. measured	16359
R_{int}	0.0426
mean $\sigma(I)/I$	0.0273
θ range	3.102–27.481
observed refls.	1957
x, y (weighting scheme)	0.0380, 0.5396
hydrogen refinement	mixed
Flack parameter	?
refls in refinement	2191
parameters	109
restraints	0
$R(F_{obs})$	0.0364
$R_w(F^2)$	0.0958
S	1.070
shift/error$_{max}$	0.001
max electron density/e Å^{-3}	0.475
min electron density/e Å^{-3}	−0.233

2-((2,2,5,5-tetramethyl-2,5-dihydro-1H-imidazol-4-yl)thio)acetonitrile (3ff-CN)
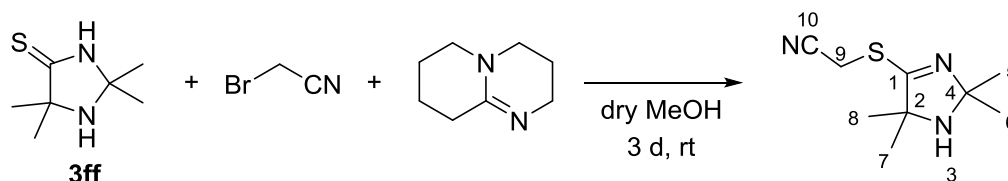
3ff (317 mg, 2.0 mmol, 1.0 eq.) was dissolved in 8 mL dry methanol under an argon atmosphere. 271 μL 1,8-diazabicyclo[5.4.0]undec-7-ene (276 mg, 2.0 mmol, 1.0 eq.) and 140 μL bromoacetonitrile (240 mg, 2.0 mmol, 1.0 eq.) were added and the mixture was stirred at room temperature for 3 d. The solvent was removed *in vacuo* and the crude product was purified with column chromatography (DCM:MeOH 20:1) to yield the title compound **3ff-CN** (395 mg, 2.0 mmol, quant.) as colourless solid.

HRMS (ESI) *m/z*: calculated for $C_9H_{16}N_3S$ [M+H]$^+$: 198.1059, found: 198.1059.

Retardation factor: R_f = 0.31 (20:1 DCM:MeOH).

¹H NMR (400 MHz, CD$_3$CN) δ 3.85 (s, 2H, H^9), 1.34 (s, 6H, H^{5,6}), 1.28 (s, 6H, H^{7,8}).

¹³C NMR (101 MHz, CD$_3$CN) δ 172.3 (C^1), 118.0 (C^{10}), 90.0 (C^4), 71.0 (C^2), 30.9 (C^{5,6}), 29.0 (C^{7,8}), 17.3 (C^9).

Note: Alkylation at the thioamide sulphur can be verified by the clear coupling in the HMBC spectrum (H^9 only couples with C^1) as well as a significant upfield shift of the C^1 signal in the ¹³C spectrum.

4-(benzylthio)-2,2,5,5-tetramethyl-2,5-dihydro-1H-imidazole (3ff-Bz)
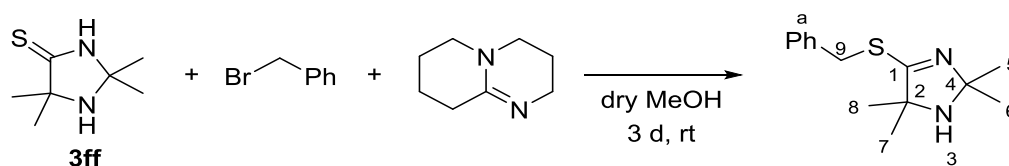
3ff (127 mg, 0.80 mmol, 1.0 eq.) was dissolved in 3 mL dry methanol under an argon atmosphere. 119 µL 1,8-diazabicyclo[5.4.0]undec-7-ene (122 mg, 0.80 mmol, 1.0 eq.) and 95 µL benzylbromide (137 mg, 0.80 mmol, 1.0 eq.) were added and the mixture was stirred at room temperature for 3 d. The solvent was removed *in vacuo* and the crude product was purified with column chromatography (isohexane:EtOAc 1:1) to yield the title compound **3ff-Bz** (132 mg, 0.53 mmol, 66 %) as colourless solid.

HRMS (ESI) *m/z*: calculated for $C_{14}H_{21}N_2S$ [M+H]$^+$: 249.1420, found: 249.1418.

Retardation factor: R_f = 0.15 (1:1 isohexane:EtOAc).

^{1}H NMR (400 MHz, CDCl$_3$) δ = 7.41 − 7.21 (m, 5H, H^a), 4.27 (s, 2H, H^9), 1.44 (s, 6H, H^{5,6}), 1.33 (s, 6H, H^{7,8}).

^{13}C NMR (101 MHz, CDCl$_3$) δ = 174.5 (C^1), 137.2 (C^a), 129.2 (C^a), 128.7 (C^a), 127.5 (C^a), 89.0 (C^4), 70.7 (C^2), 35.8 (C^9), 30.8 (C^{5,6}), 29.0 (C^{7,8}).

Note: Alkylation at the thioamide sulphur can be verified by the clear coupling in the HMBC spectrum (H^9 only couples with C^1) as well as a significant upfield shift of the C^1 signal in the ^{13}C spectrum.

4-(benzylthio)-2,5,5-trimethyl-2,5-dihydro-1H-imidazole (3fa-Bz)
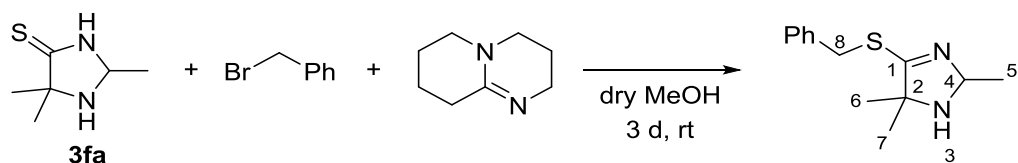
3fa (115 mg, 0.80 mmol, 1.0 eq.) was dissolved in 3 mL dry methanol under an argon atmosphere. 239 μL 1,8-diazabicyclo[5.4.0]undec-7-ene (244 mg, 1.60 mmol, 2.0 eq.) and 95 μL benzylbromide (137 mg, 0.80 mmol, 1.0 eq.) were added and the mixture was stirred at room temperature for 3 d. The solvent was removed *in vacuo* and the crude product was purified with column chromatography (isohexane:EtOAc 1:1) to yield the title compound **3fa-Bz** (147 mg, 0.63 mmol, 79 %) as colourless solid.

HRMS (ESI) *m/z*: calculated for $C_{13}H_{19}N_2S$ [M+H]$^+$: 235.1263, found: 235.1263.

Retardation factor: R_f = 0.14 (1:1 isohexane:EtOAc).

^{1}H NMR (400 MHz, CDCl$_3$) δ = 7.41 – 7.26 (m, 5H, H^a), 4.85 (q, *J* = 6.1 Hz, 1H, H^4), 4.27 (d, *J* = 1.9 Hz, 2H, H^8), 1.46 (d, *J* = 6.2 Hz, 3H, H^5), 1.35 (s, 6H, H$^{6/7}$), 1.24 (s, 6H, H$^{6/7}$).

^{13}C NMR (101 MHz, CDCl$_3$) δ = 178.2 (C^1), 137.0 (C^a), 129.1 (C^a), 128.7 (C^a), 127.5 (C^a), 82.1 (C^4), 70.3 (C^2), 36.0 (C^8), 26.8 (C$^{7/8}$), 25.4 (C^{7,8}), 22.4 (C^5).

Note: Alkylation at the thioamide sulphur can be verified by the clear coupling in the HMBC spectrum (H^8 only couples with C^1) as well as a significant upfield shift of the C^1 signal in the ^{13}C spectrum.

6.2.5 Second generation compounds

3-Methyl-4-oxobutanenitrile (1b')

To gain maximum yield for the isolation, **1b'** was synthesized via the organocatalytic photoredox approach developed by E. FUKS and catalysed with **3ff**.[194]
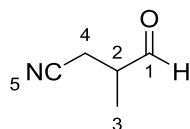
Freshly distilled propionaldehyde **1b'** (1.79 mL, 25 mmol, 5.0 eq.), bromoacetonitrile (349 µL, 5.0 mmol, 1.0 eq.), 2,6-lutidine (1.16 mL, 10 mmol, 2.0 eq.) and 2,2,5,5-tetramethylimidazolidine-4-thione **3dd** (158 mg, 1.0 mmol, 0.2 eq.) were dissolved in 2.0 mL DMSO in a flat bottom vial. The sample was stirred and irradiated overnight by a Roschwege Star-UV365-01-00-00 emitter (365 nm) placed below. The reaction mixture was quenched with water and 2 M HCl and extracted with diethyl ether. The combined organic phases were dried over $MgSO_4$, filtered and concentrated by evaporation in the nitrogen stream. The title compound was isolated as slightly yellow oil (220 mg, 2.3 mmol, 46 %) using column chromatography (SiO_2, 4:1 n-pentane:Et_2O).

Retardation factor: R_f = 0.15 (3:2 n-pentane:Et_2O).

^{1}H NMR (400 MHz, $CDCl_3$) δ = 9.65 (s, 1H, H^1), 2.78 (m, 1H, H^2), 2.67 (dd, J = 16.9 Hz, 5.5 Hz, 1H, H$^{4a/b}$), 2.46 (dd, J = 16.9 Hz, 7.6 Hz, 1H, H$^{4a/b}$), 1.37 (d, J = 7.5 Hz, 3H, H^3).

^{13}C NMR (101 MHz, $CDCl_3$) δ = 200.0 (C^1), 117.8 (C^5), 42.8 (C^2), 18.0 (C^4), 13.4 (C^3).

^{1}H NMR (400 MHz, CD_3CN) δ = 9.58 (s, 1H, H^1), 2.85 – 2.75 (m, 1H, H^2), 2.63 (dd, J = 17.0 Hz, 6.1 Hz, 1H, H$^{4a/b}$), 2.53 (dd, J = 17.1 Hz, 6.5 Hz, 1H, H$^{4a/b}$), 1.25 (d, J = 7.5 Hz, 3H, H^3).

^{13}C NMR (101 MHz, CD_3CN) δ = 202.6 (C^1), 119.4 (C^5), 43.1 (C^2), 18.1 (C^4), 13.1 (C^3).

4-Hydroxy-3-methylbutanenitrile

For *ee*-value determination of the α-cyanomethylation of propionaldehyde **1b** in acetonitrile without light, the crude catalysis mixture was directly reduced with NaBH$_4$ to yield the corresponding alcohol, following the procedure of E. FUKS.[194]
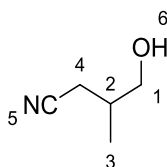
Acetonitrile was evaporated in the nitrogen stream at room temperature and the residual oil was re-dissolved in 1 mL of CH$_2$Cl$_2$ and cooled to -78 °C. An excess of NaBH$_4$ was added and the reaction was stirred for 2 h. The reaction mixture was quenched with water and extracted with CH$_2$Cl$_2$. The solvent was evaporated in the nitrogen stream and the crude was purified by column chromatography (SiO$_2$, *n*-pentane:Et$_2$O 2:1).

Retardation factor: R$_f$ = 0.05 (*n*-pentane:Et$_2$O 2:1)

^{1}H NMR (400 MHz, CDCl$_3$) δ = 1.08 (d, *J* = 6.9 Hz, 3H, H^3), 1.76 (bs, 1H, H^6), 2.11-2.00 (m, 1H, H^2), 2.39 (dd, *J* = 16.7 Hz, *J* = 7.0 Hz, 1H, H^4), 2.50 (dd, *J* = 16.8 Hz, *J* = 5.5 Hz, 1H, H^4), 3.50 (dd, *J* = 10.7 Hz, *J* = 7.5 Hz, 1H, H^1), 3.66 (dd, *J* = 10.7 Hz, *J* = 4.9 Hz, 1H, H^1).

^{13}C NMR (101 MHz, CDCl$_3$) δ = 16.0 (C^3), 21.1 (C^1), 33.1 (C^2), 66.0 (C^4), 118.9 (C^5).

1,3-Dicyano-2-methylpropan-1-aminium chloride (2b')
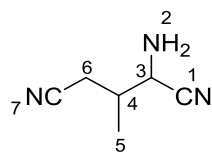
3-Methyl-4-oxobutanenitrile **1b'** (198 mg, 2.0 mmol, 1.0 eq.) was treated with **GP-1** except for the final precipitation as hydrochloride salt. **2b'** was obtained as colourless liquid.

HRMS (ESI) *m/z*: calculated for $C_6H_{10}N_3$ [M+H]$^+$: 124.0869, found: 124.0870.

Diastereomer A:

¹H NMR (400 MHz, DMSO-d_6) δ = 6.77 (d, *J* = 6.0 Hz, 2H, H^2), 4.42 − 4.35 (m, 1H, H^3), 2.74-2.61 (m, 2H, H^6), 2.25 − 2.10 (m, 1H, H^4), 1.08 (d, *J* = 6.9 Hz, 3H, H^5).

¹³C NMR (101 MHz, DMSO-d_6) δ = 119.9 (C^1), 119.1 (C^7), 63.5 (C^3), 34.7 (C^4), 19.5 (C^6), 14.8 (C^5).

Diastereomer B:

¹H NMR (400 MHz, DMSO-d_6) δ = 6.72 (d, *J* = 5.5 Hz, 2H, H^2), 4.61 − 4.56 (m, 1H, H^3), 2.74-2.61 (m, 1H, H$^{6a/b}$), 2.57 − 2.43 (m, 1H, H$^{6a/b}$), 2.25 − 2.10 (m, 1H, H^4), 1.09 (d, *J* = 6.8 Hz, 3H, H^5).

¹³C NMR (101 MHz, DMSO-d_6) δ = 119.6 (C^1), 118.8 (C^7), 62.8 (C^3), 34.3 (C^4), 19.3 (C^6), 14.2 (C^5).

3-(2,2-Dimethyl-5-thioxoimidazolidin-4-yl)butanenitrile (3b'f)
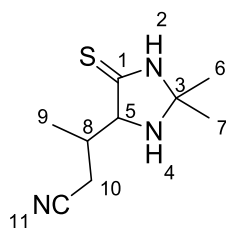
1,3-Dicyano-2-methylpropan-1-aminium chloride **2b'** (399 mg, 2.50 mmol, 1.0 eq.) reacted with acetone (185 µL, 2.5 mmol, 1.0 eq.), potassium hydroxide and hydrogen sulphide following **GP-2**. Column chromatography (SiO$_2$, 1:1 *n*-pentane:EtOAc) of the crude product yielded the title compound **3b'f** (17 mg, 0.08 mmol, 3 %) as a white solid.

HRMS (ESI) *m/z*: calculated for C$_9$H$_{16}$N$_3$S [M+H]$^+$: 198.1059, found: 198.1056.

Retardation factor: R$_f$ = 0.61 (1:1 *n*-pentane:EtOAc).

^{1}H NMR (400 MHz, CDCl$_3$) δ = 9.00 (s, 1H, H^2), 4.15 (d, *J* = 3.3 Hz, 1H, H^5), 2.78 (sextd, *J* = 7.0, 3.2 Hz, 1H, H^8), 2.50 (dd, *J* = 7.4, 1.7 Hz, 2H, H^{10}), 1.94 (bs, 1H, H^4), 1.50 – 1.46 (m, 3H, H^{6,7}), 1.04 (d, *J* = 6.8 Hz, 3H, H^9).

^{13}C NMR (101 MHz, CDCl$_3$) δ = 201.1 (C^1), 118.7 (C^{11}), 80.0 (C^3), 72.1 (C^5), 33.1 (C^8), 29.4 (C$^{6/7}$), 28.8 (C$^{6/7}$), 22.6 (C^{10}), 13.3 (C^9).

3-(4,4-Dimethyl-5-thioxoimidazolidin-2-yl)butanenitrile (3fb')
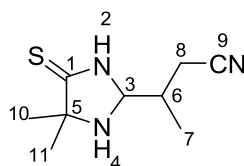
2,5,5-Trimethylimidazolidine-4-thione **3fa** (101 mg, 0.7 mmol, 1.0 eq.) was dissolved in 5.0 mL distilled water. 3-Methyl-4-oxobutanenitrile **1b'** (136 mg, 1.4 mmol, 2.0 eq.) was added and the mixture was stirred for 12 h. The solution was extracted with dichloromethane, the combined organic phases were dried over sodium sulfate, filtered and concentrated *in vacuo*. Column chromatography (SiO$_2$, 1:1 isohexane:EtOAc) of the crude product yielded the title compound (3 mg, 15 µmol, 2 %) as a white solid.

HRMS (ESI) *m/z*: calculated for C$_9$H$_{16}$N$_3$S [M+H]$^+$: 198.1059, found: 198.1060.

Retardation factor: R$_f$ = 0.24 (1:1 isohexane:EtOAc).

Diastereomer A:

¹H NMR (400 MHz, CDCl$_3$) δ = 9.03 (b, 1H, H^2), 4.80 (d, *J* = 4.8 Hz, 1H, H^3), 2.56 (dd, *J* = 16.9, 5.7 Hz, 1H, H^{8a}), 2.36 (dd, *J* = 16.9, 7.6 Hz, 1H, H^{8b}), 2.14 - 2.05 (m, 1H, H^6), 1.45 (s, 3H, H$^{10/11}$), 1.40 (s, 3H, H$^{10/11}$), 1.17 (d, *J* = 7.0 Hz, 3H, H^7).

¹³C NMR (101 MHz, CDCl$_3$) δ = 211.2 (C^1), 118.2 (C^9), 76.3 (C^3), 70.4 (C^5), 35.2 (C^6), 28.9 (C$^{10/11}$), 27.9 (C$^{10/11}$), 20.1 (C^8), 14.7 (C^7).

Diastereomer B:

¹H NMR (400 MHz, CDCl$_3$) δ = 8.95 (b, 1H, H^2), 4.60 (d, *J* = 7.1 Hz, 1H, H^3), 2.52 (dd, *J* = 6.0, 4.7 Hz, 2H, H^{8a,b}), 2.05 - 1.96 (m, 1H, H^6), 1.90 (b, 1H, H^4), 1.43 (s, 3H, H$^{10/11}$), 1.41 (s, 3H, H$^{10/11}$), 1.20 (d, *J* = 6.8 Hz, 3H, H^7).

¹³C NMR (101 MHz, CDCl$_3$) δ = 211.2 (C^1), 118.2 (C^9), 77.1 (C^3), 70.4 (C^5), 36.2 (C^6), 29.5 (C$^{10/11}$), 27.9 (C$^{10/11}$), 20.4 (C^8), 15.8 (C^7).

6.3 One-Pot-Synthesis

6.3.1 Reaction of Carbonyl with Hydrogen Sulphide in Ammonia
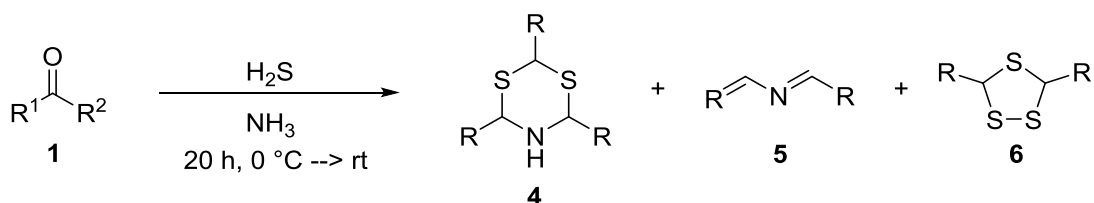
The carbonyl **1** (1 mmol) or a mixture thereof (1 mmol each) was dissolved in 1.5 mL concentrated aqueous ammonia (28 – 30 %) and hydrogen sulphide was bubbled through the solution (1 x 17 bar) at 0 °C. The mixture was stirred for 20 h, thereby letting the temperature increase to room temperature. The solution was extracted with diethyl ether and the organic phases were dried over sodium sulfate. The crude mixture was directly analysed by GC-MS on an SE-30 column (25 m, 250 µm i.d., 250 nm film thickness) starting at 70 °C (5 min), followed by 3K/min to 220 °C (5 min) with a pressure of 80 kPa.
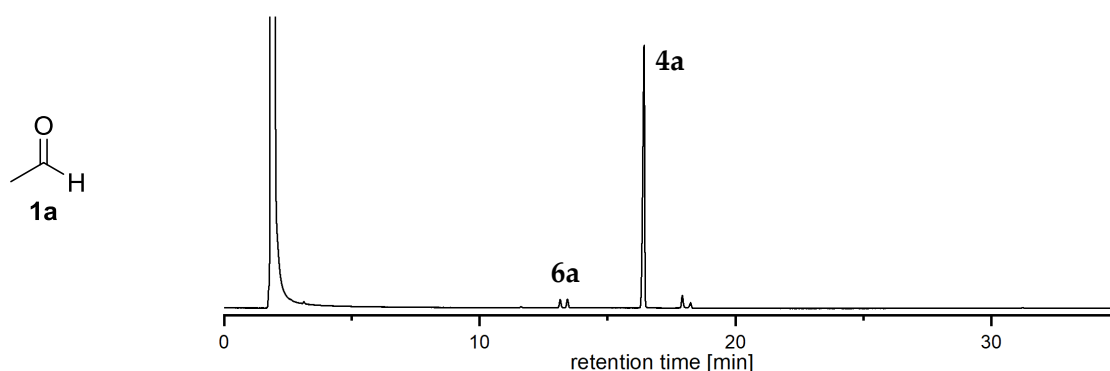
Figure 6.1: GC-chromatogram of the reaction of **1a** with H₂S in concentrated aqueous ammonia after 20 h.
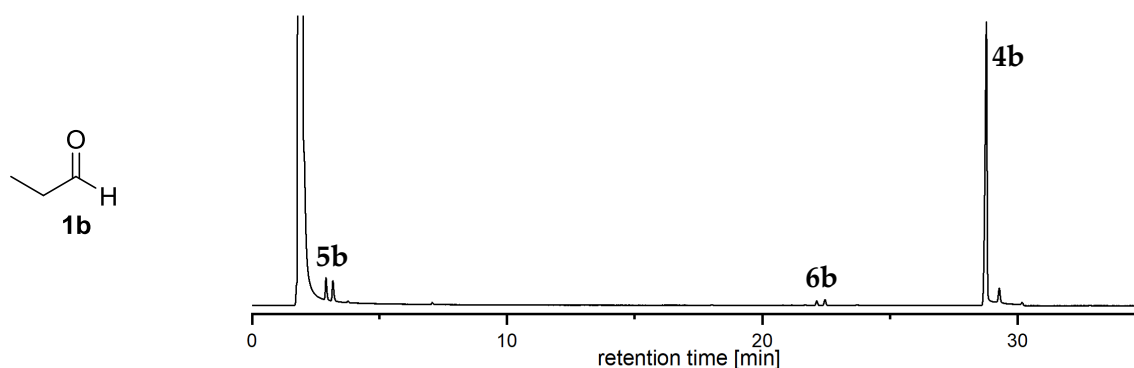
Figure 6.2: GC-chromatogram of the reaction of **1b** with H₂S in concentrated aqueous ammonia after 20 h.
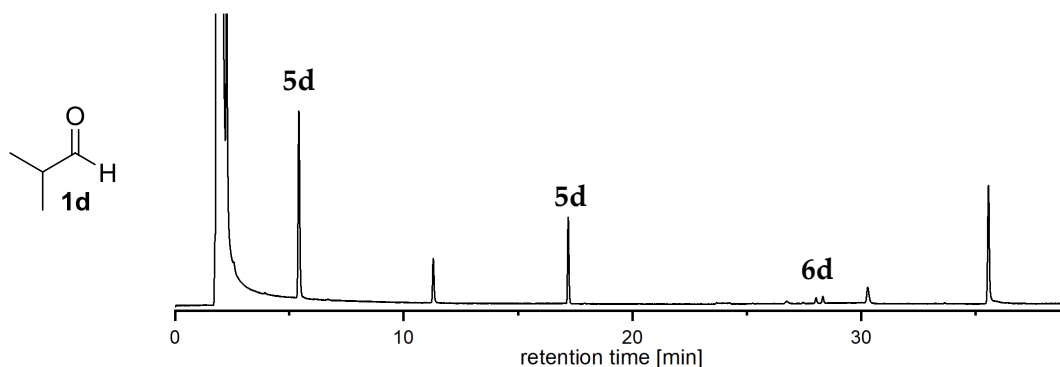
Figure 6.3: GC-chromatogram of the reaction of **1d** with H₂S in concentrated aqueous ammonia after 20 h.
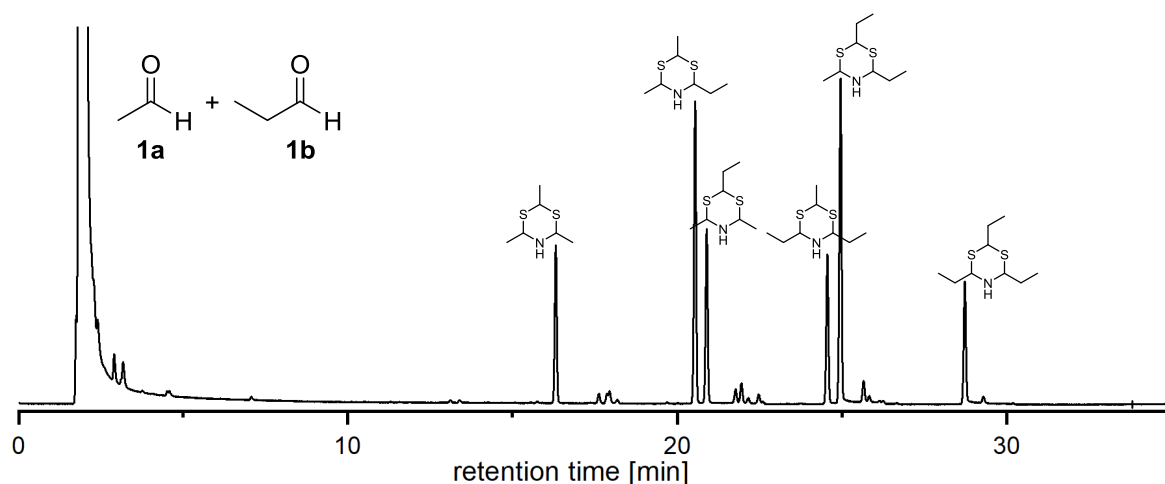
Figure 6.4: GC-chromatogram of the reaction of a mixture of **1a** and **1b** with H₂S in concentrated aqueous ammonia after 20 h. Exact peak assignment of the six differently substituted dithiazinanes was possible due to characteristic MS-fragmentation.

For the reaction with propionaldehyde **1b**, 1 µL samples were taken directly after H₂S addition as well as after 1 h and 2 h, diluted in 1 mL acetonitrile and analysed by Orbitrap-MS.
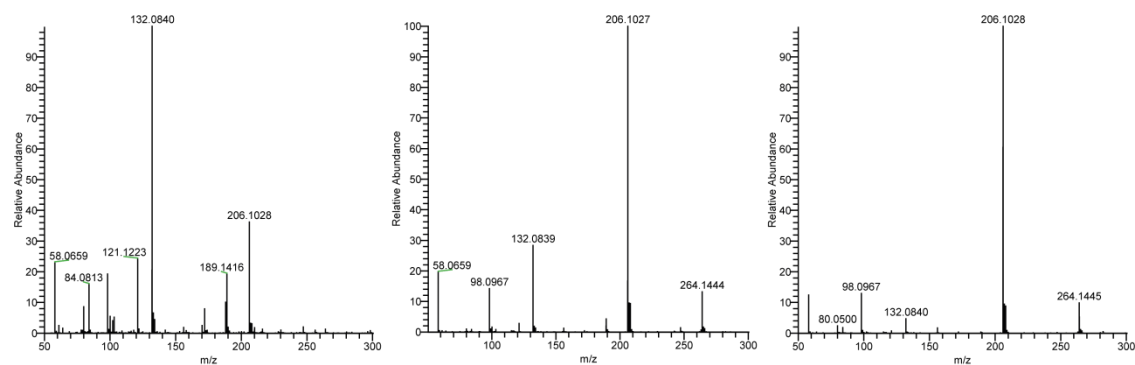
Figure 6.5. One-pot reaction of propionaldehyde 1b with NH₄Cl and H₂S. High resolution mass spectra of the reaction in concentrated aqueous ammonia. Samples were taken directly after mixing the reactants as well as after 1 h and 2 h and diluted with acetonitrile before the measurement.

6.3.2 One-Pot reaction in water and ammonia

1b : R^1 = Et, R^2 = H
1f : R^1 = Me, R^2 = Me
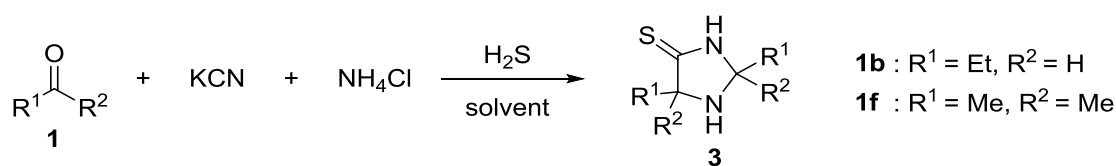
Potassium cyanide (81 mg, 1.25 mmol, 1.0 eq.) and ammonium chloride (67 mg, 1.25 mmol, 1.0 eq.) were dissolved in 2 mL of the respective solvent (concentrated aqueous ammonia or water). After cooling to 0 °C, propionaldehyde **1b** (90 µL, 1.25 mmol, 1.0 eq.) or acetone **1f** (93 µL, 1.25 mmol, 1.0 eq.) was added and hydrogen sulphide was bubbled through the solution (1 x 17 bar). The vial was sealed and left stirring, thereby letting the temperature of the mixture increase to room temperature. 1 µL samples were taken over the course of the reaction after 30 min, 2 h, 4 h, 24 h, and 48 h, diluted in 1 mL acetonitrile and directly analyzed with Orbitrap-MS. The observed *m/z* values were assigned to intermediates or plausible side-products of the investigated reaction.

For the reactions with **1b**, imidazolidine-4-thione **3bb** was isolated after 24 h to compare the respective yields. The remaining hydrogen sulphide was purged with nitrogen at 55 °C, the solution was extracted with dichloromethane and the combined organic phases were dried over sodium sulfate, filtered and concentrated *in vacuo*. Column chromatography (SiO₂, 1:1 isohexane:EtOAc) of the crude product yielded the title compound **3bb** as a white solid (for all analytical data see Section 6.2.2).

Solvent:	water (pH 8.0)	ammonia (pH 10.5)	two-step synthesis[194]
Yield **3bb**:	18.3 mg, 0.11 mmol, 19 %	6.4 mg, 0.04 mmol, 6 %	149.9 mg, 0.95 mmol, 76 %

One-pot procedure of propionaldehyde **1b**
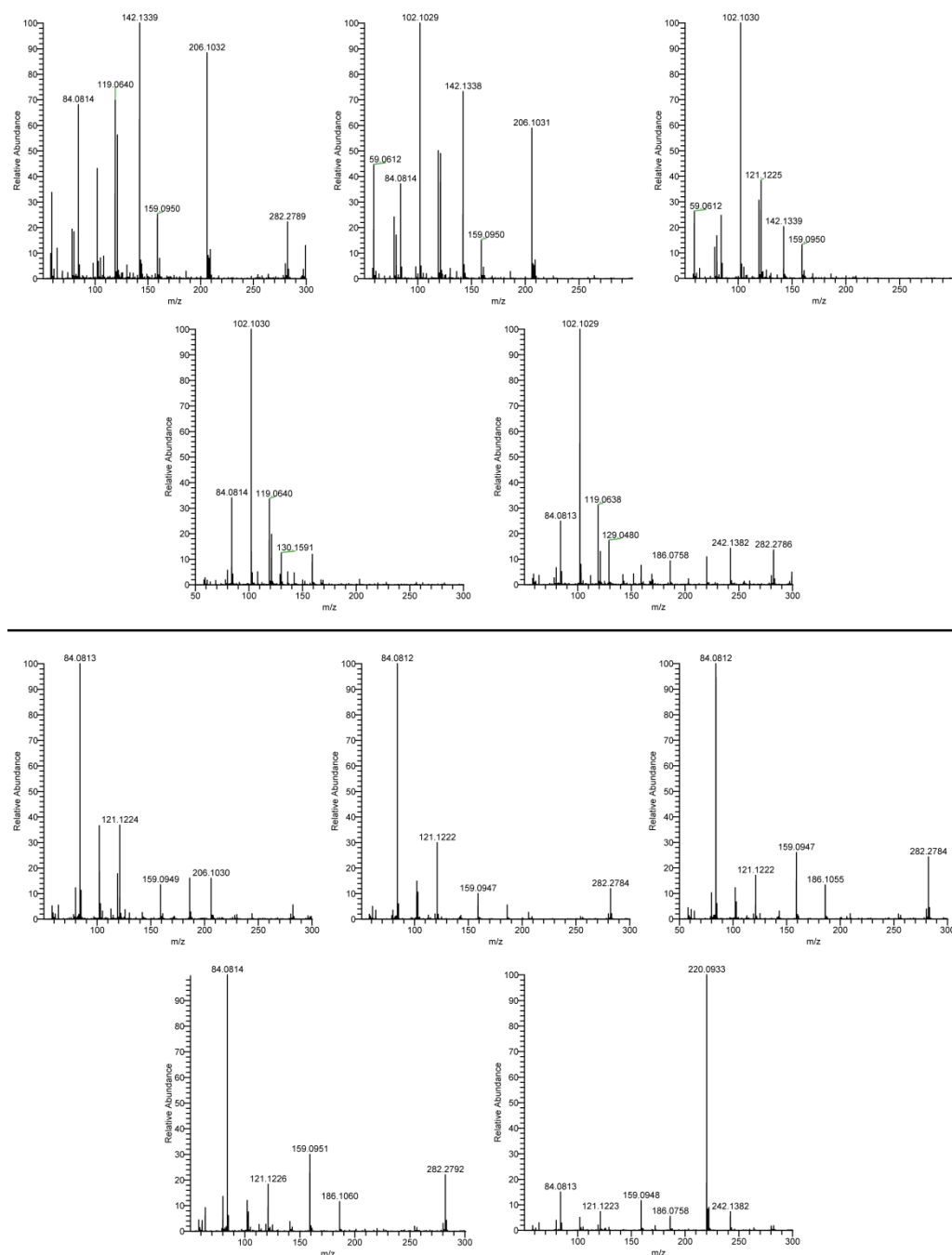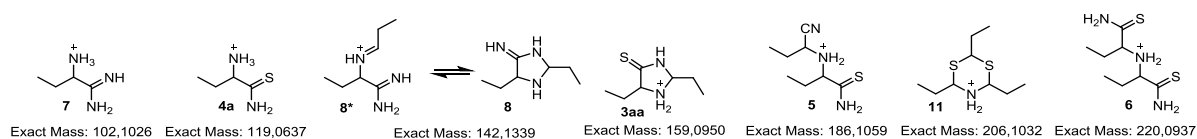
Figure 6.6: One-pot reaction of propionaldehyde 1b with KCN, NH₄Cl and H₂S. Molecules detected in the mass spectra (top) as well as high resolution mass spectra of the reaction in concentrated aqueous ammonia (middle) and water (bottom). Samples were taken after 30 min, 2 h, 4 h, 24 h, and 48 h and diluted with acetonitrile before the measurement.

One-pot procedure of acetone **1f**

Exact Mass: 116.1070   Exact Mass: 142.1339   Exact Mass: 159.0950   Exact Mass: 186.1059
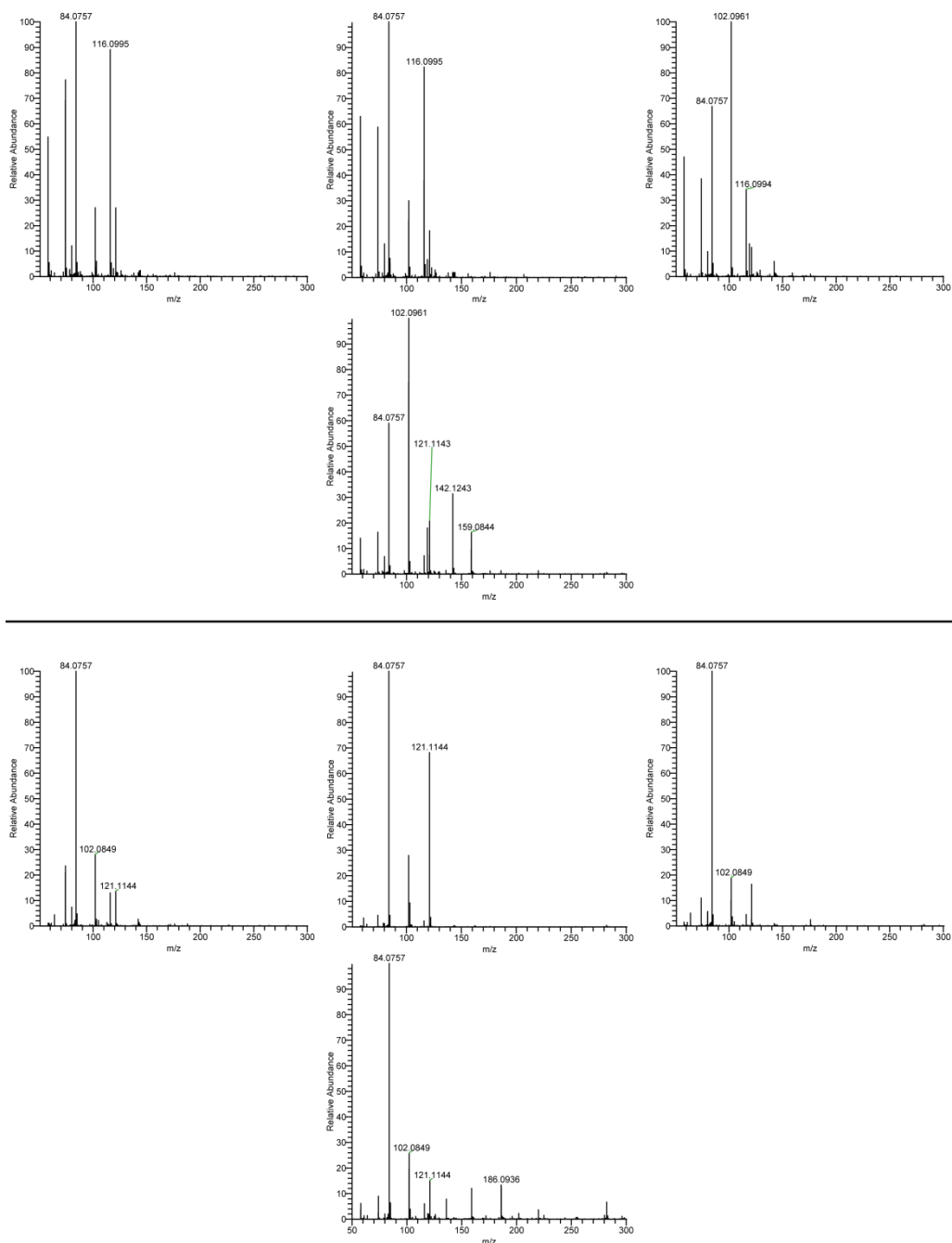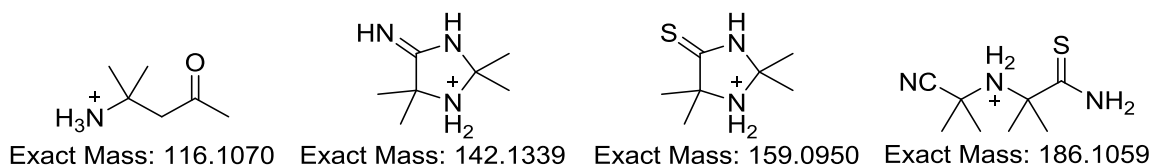
Figure 6.7: One-pot reaction of acetone 1f with KCN, NH₄Cl and H₂S. Molecules detected in the mass spectra (top) as well as high resolution mass spectra of the reaction in concentrated aqueous ammonia (middle) and water (bottom). Samples were taken after 30 min, 2 h, 4 h, and 24 h and diluted with acetonitrile before the measurement.

6.4 Dynamic Carbonyl Exchange

Side-chain exchange with a mixture of reactants
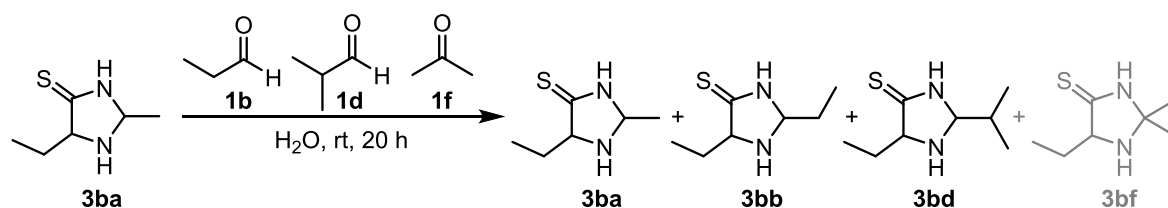
5-Ethyl-2-methylimidazolidine-4-thione **3ba** (14.4 mg, 100 µmol, 1.0 equiv.) was dissolved in 1.0 mL distilled water (pH 7.5). Propionaldehyde **1b** (7.4 µL, 100 µmol, 1.0 equiv.), isobutyraldehyde **1d** (9.1 µL, 100 µmol, 1.0 equiv.) and acetone **1f** (7.4 µL, 100 µmol, 1.0 equiv.) were added and the mixture was stirred for 20 h. The solution was extracted with dichloromethane, the combined organic phases were dried over sodium sulfate, filtered and concentrated *in vacuo*. The resulting mixture was directly analysed with NMR spectroscopy.
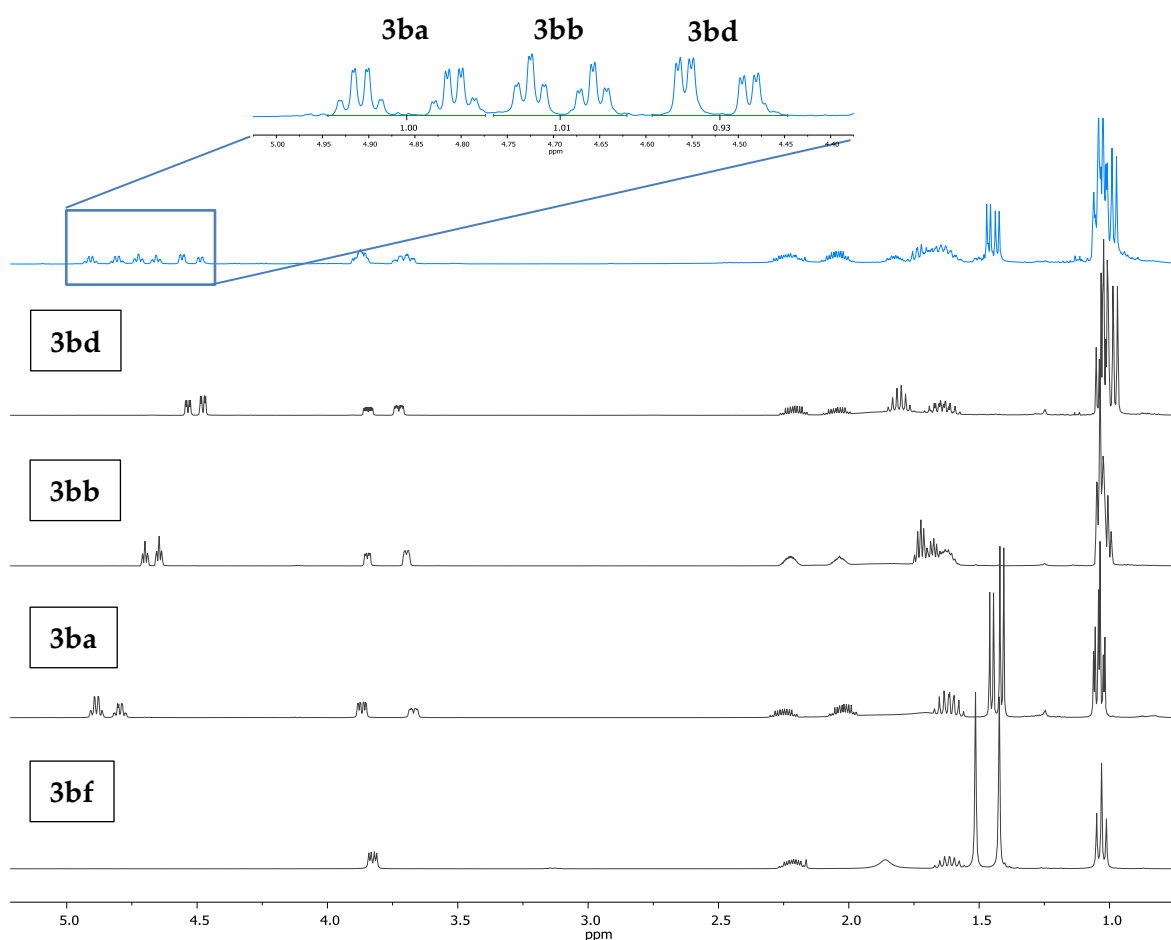
Figure 6.8: ^{1}H NMR spectra of imidazolidine-4-thiones **3ba**, **3bb**, and **3bd** formed from a mixture of **3ba**, propionaldehyde **1b**, isobutyraldehyde **1d**, and acetone **1f** in water (blue, top). Enlarged area illustrates the ratio of products (1:1:1). Reference spectra of imidazolidine-4-thiones are shown below in black.

Side-chain exchange dependence on pH-value

The reaction was repeated in water of different pH values, adjusted with 2 M NaOH. Above a pH value of 10, no exchange of the second carbonyl moiety was observed.
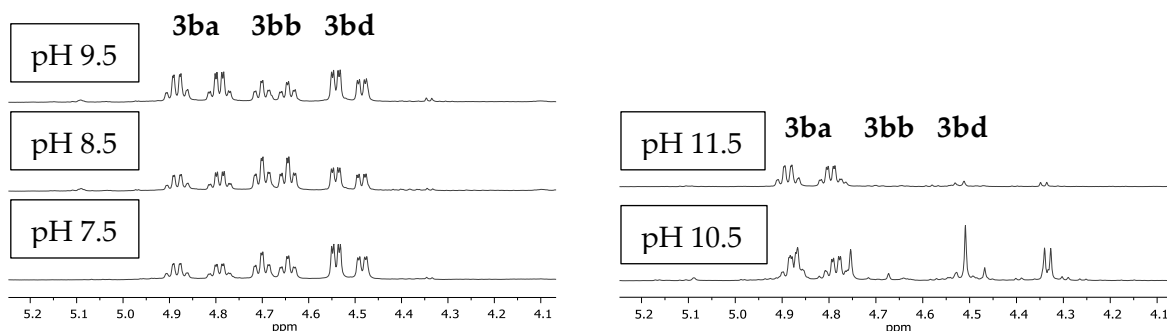
Figure 6.9: Excerpts of the ^{1}H NMR spectra of imidazolidine-4-thiones **3ba**, **3bb**, and **3bd** formed from a mixture of **3ba**, propionaldehyde **1b**, isobutyraldehyde **1d**, and acetone **1f** at different pH values.

No side-chain exchange with acetone

To verify that acetone is not incorporated into the imidazolidine-4-thione skeleton by dynamic exchange, it was added solely and thus as only possible reaction partner. No significant incorporation was detected.
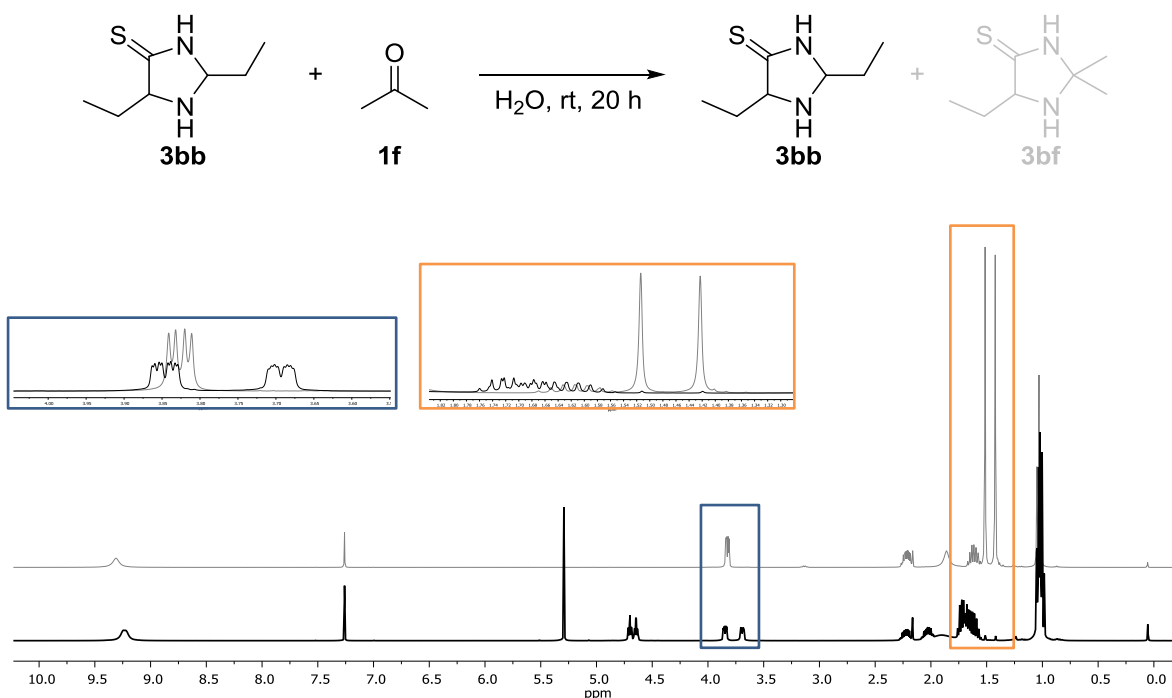
Figure 6.10: ^{1}H NMR spectra of the mixture of **3bb** with acetone **1f** in water (black, bottom) and reference spectra of **3bf** (gray, top). Enlarged areas illustrate only slight formation of **3bf**.

Side-chain exchange dependence on reactant equivalents

To further examine the amount of exchange based on the present ratio of reactants, the previously used 1:1 ratio of aldehyde **1** to imidazolidine-4-thione **3** was extended to 2:1 and 5:1. The observed exchange reflected the used ratio of the reactants.
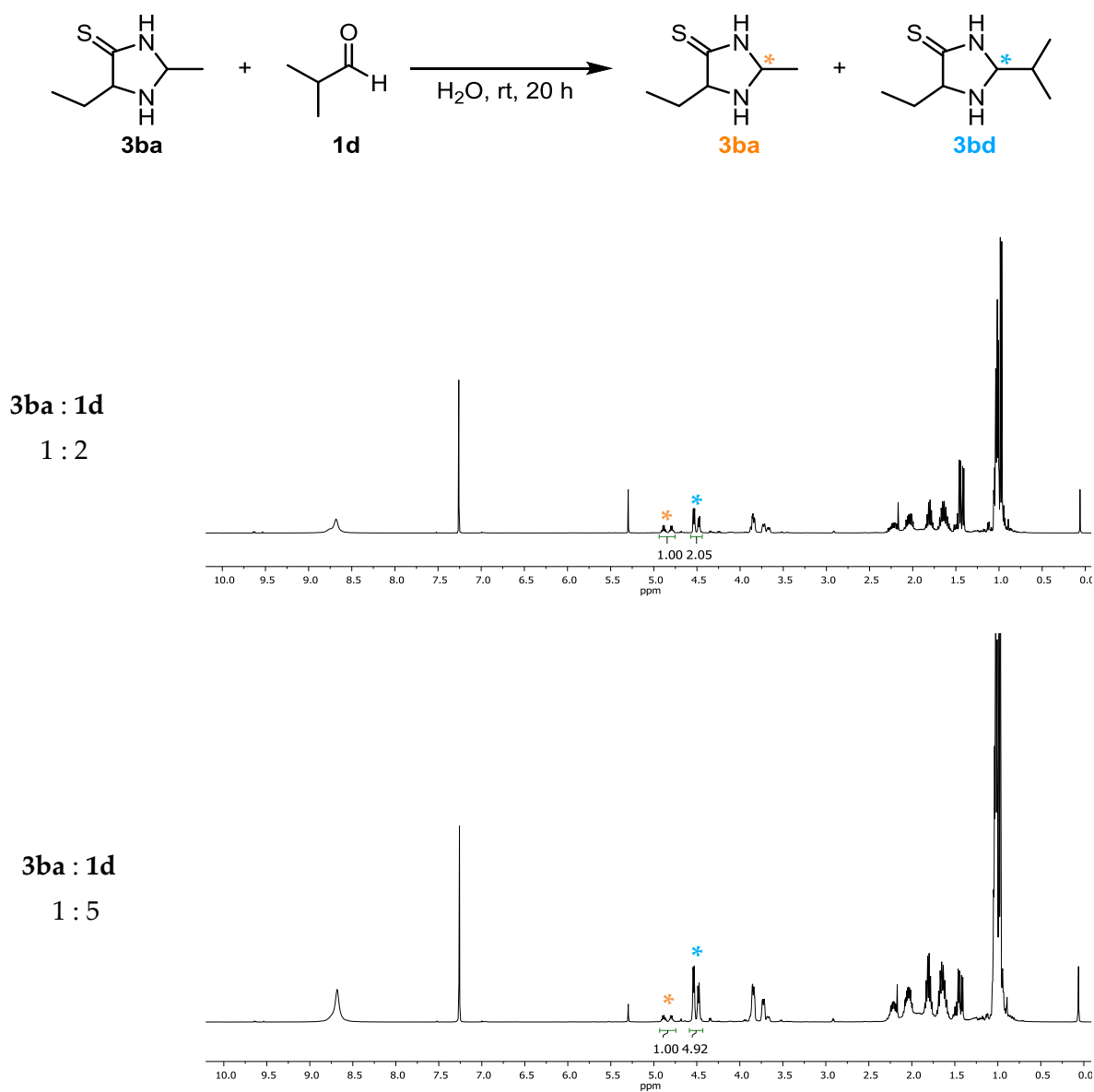
Figure 6.11: ^{1}H NMR spectra of imidazolidine-4-thiones **3ba** and **3bd** formed from a mixture of **3ba** and isobutyraldehyde **1d** in a ratio of 1:2 (top) and 1:5 (bottom). Highlighted signals were used for integration and refer to the characteristic proton of ring position 2.

6.5 Selectivity Studies

6.5.1 Aminonitrile formation
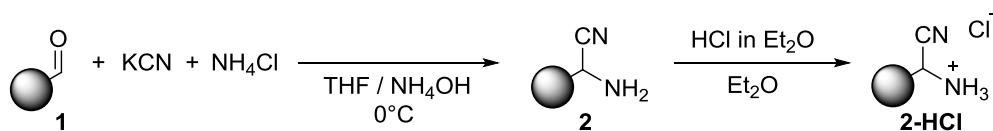
A mixture of aldehydes and/or ketones **1** (5 mmol each) was dissolved in a mixture of 4.5 mL tetrahydrofuran and 1.05 mL concentrated aqueous ammonia (28 – 30 %) at 0 °C. Ammonium chloride (mmol: 0.5 x total mmol **1**) and potassium cyanide (mmol: 0.5 x total mmol **1**) were added and the suspension was stirred for 1.5 h. 4.5 g sodium sulfate and 12 mL diethyl ether were added and the mixture was stirred for 30 min. The solution was decanted and the residue washed with 20 mL of diethyl ether. The organic phases were combined and concentrated *in vacuo*. The residual oil was dissolved in 12 mL of diethyl ether and 7 mL of HCl in diethyl ether (2 M) were added. The precipitate was filtered off and recrystallised from acetonitrile. This mixture was directly analysed with ^{1}H NMR. In addition, 7.0 mg were dissolved in 5 mL of bidistilled water and 100 μL thereof were diluted with 400 μL bidistilled water and analysed with CE.
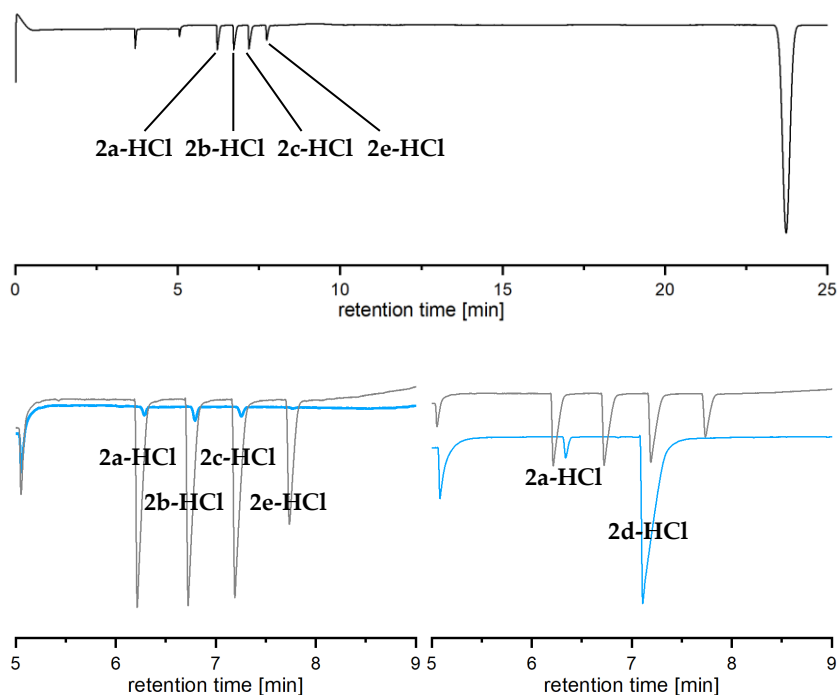
Figure 6.12: CE electropherograms of the HCl-salts of α-aminonitriles **2** separated with 2 M acetic acid as elution buffer. Top: reference mixture of **2a-HCl**, **2b-HCl**, **2c-HCl**, and **2e-HCl**. Bottom left: products formed from a mixture of acetaldehyde **1a**, propionaldehyde **1b**, butyraldehyde **1c**, and benzaldehyde **1e** (blue). Bottom right: products formed from a mixture of acetaldehyde **1a**, isobutyraldehyde **1d**, and acetone **1f** (not detected) (blue). In grey the reference electropherogram is superimposed.

6.5.2 Imidazolidine-4-thione Formation

One aminonitrile, several carbonyl compounds

Each aminonitrile **2a-g** (0.5 mmol) was reacted with a mixture of aldehydes **1a-e** (0.5 mmol each) and a mixture of aldehydes and ketones **1a-g** (0.5 mmol each) in 1 mL of concentrated aqueous ammonia according to **GP-2**. The crude mixture was dissolved in 0.3 mL isopropanol and 2.7 mL *n*-hexane and analysed with HPLC-MS.

Table 6.1: Relative proportion of imidazolidine-4-thiones determined by HPLC peak integration. Mixtures of carbonyl compounds without (upper line) and with ketones **1f** and **1g** (bottom line) were applied.

	Reaction with:						
	1a	**1b**	**1c**	**1d**	**1e**	**1f**	**1g**
2a	14 %	15 %	37%	30%	4%	-	-
	13 %	17 %	12%	19%	4%	12%	23%
2b	8 %	23 %	30%	34%	5%	-	-
	19 %	14 %	7%	13%	5%	14%	28%
2c	19 %	23 %	25%	25%	8%	-	-
	11 %	12 %	5%	10%	5%	21%	36%
2d	44 %	29 %	15%	11%	1%	-	-
	14 %	7 %	4%	6%	1%	26%	42%
2e	35 %	26 %	19 %	20 %	0 %	-	-
	10 %	18 %	14 %	21 %	0 %	13 %	26 %
2f	65 %	19 %	6%	6%	4%	-	-
	35 %	17 %	8%	11%	6%	12%	11%
2g	56 %	27 %	8%	6%	3%	-	-
	31 %	32 %	13%	4%	8%	3%	9%
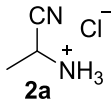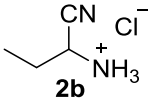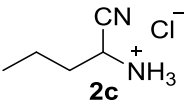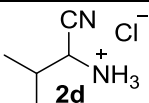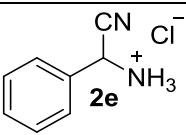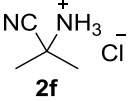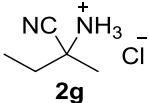
One carbonyl compound, several aminonitriles

Propionaldehyde **1a** (0.25 mmol) or acetone **1f** (0.25 mmol) were reacted with a mixture of aminonitriles **2a,b,d** (0.25 mmol each) and a mixture of aminonitriles **2a,b,d,f** (0.25 mmol each) in 1 mL of concentrated aqueous ammonia according to **GP-2**. The crude mixture was dissolved in 0.3 mL isopropanol and 2.7 mL hexane and analysed with HPLC-MS.

Table 6.2: Relative proportion of imidazolidine-4-thiones determined by HPLC peak integration. Aminonitrile mixtures without (upper line) and with **2f** (bottom line) were applied. [a] formed due to degradation of **2f** to **1f**. [b] combined proportion of **3bf** and **3ff** due to peak overlap.

	3aa	3ba	3da	3fa	3af	3bf	3df	3ff
O ‖ (1a) H	13 %	33 %	54 %	-				
	9 %	9 %	13 %	28 %	13 %[a]	10 %[a]	18 %[a]	
O ‖ (1f)					21 %	32 %	47 %	-
					25 %	41 %[b]	34 %	41 %[b]

Two-Step

A mixture of aldehydes and/or ketones **1** (20 mmol each) were reacted with ammonium chloride (10 mmol) and potassium cyanide (10 mmol) in 6.0 mL tetrahydrofuran and 1.4 mL concentrated aqueous ammonia (28 – 30 %) according to **GP-1** without subsequent precipitation as HCl salts. After 1.5 h, 6.0 g sodium sulfate and 16 mL diethyl ether were added and the mixture was stirred for 30 min. The solution was decanted and the residue washed with 20 mL of diethyl ether. The organic phases were combined and concentrated *in vacuo*. 50 mg of this crude mixture (0.625 mmol each if an equal product distribution with quantitative yield would have formed) were reacted with the same mixture of aldehydes and/or ketones **1** (1.25 mmol each) according to **GP-2**. The crude mixture was dissolved in 0.4 mL isopropanol and 3.6 mL hexane and analysed with HPLC-MS.

One-Pot Formation

Time dependent imidazolidine-4-thione formation
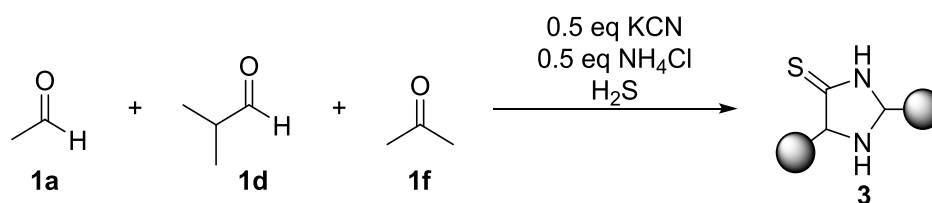
Ammonium chloride (1 mmol, 0.5 eq) and potassium cyanide (1 mmol, 0.5 eq) were dissolved in 2.0 mL of the respective solvent. Propionaldehyde **1b** (2 mmol, 1.0 eq), isobutyraldehyde **1d** (2 mmol, 1.0 eq), and acetone **1f** (2 mmol, 1.0 eq) were added and hydrogen sulphide (2 x 17 bar) was bubbled through the solution at 0 °C. At certain time periods 1 L samples were taken and dissolved in a mixture of 0.1 mL isopropanol and 0.9 mL hexane and analysed with HPLC-MS.
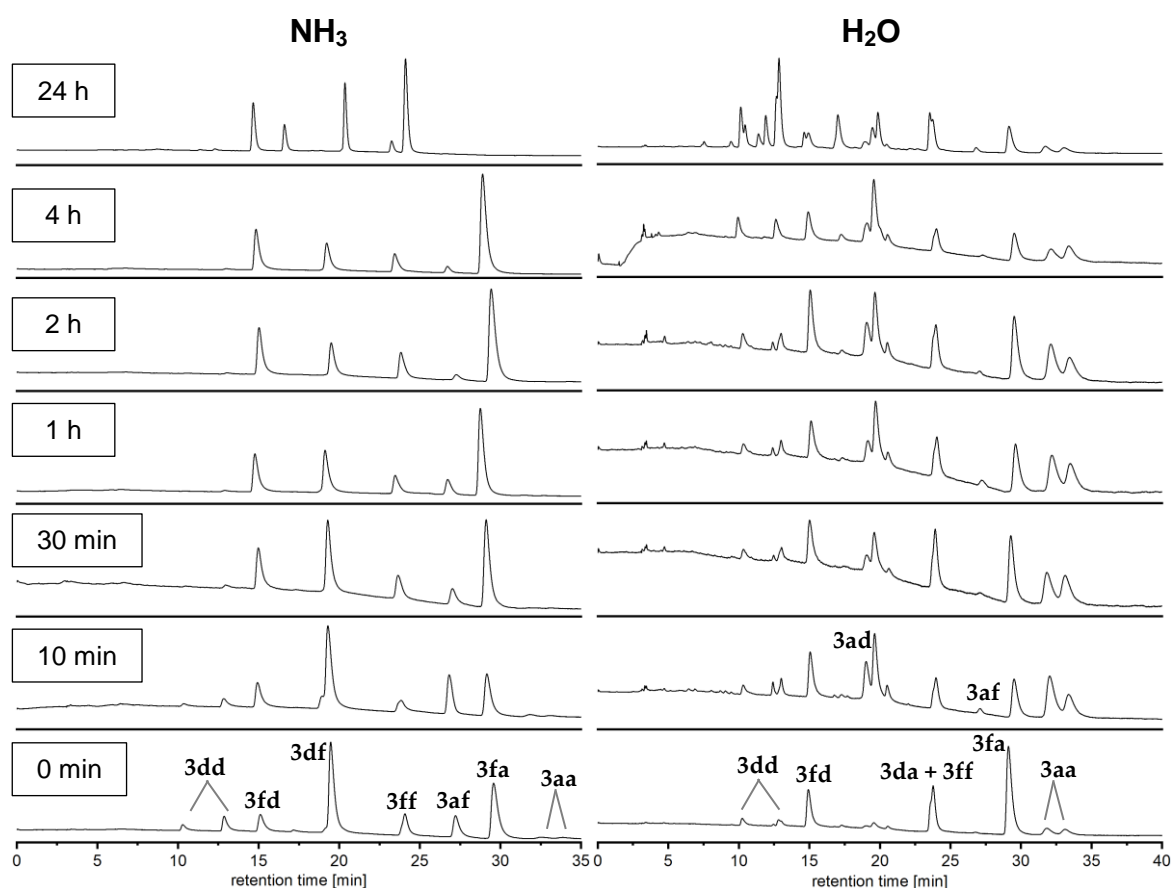
Figure 6.13: HPLC separation of imidazolidine-4-thiones formed from a one-pot mixture of acetaldehyde **1a**, isobutyraldehyde **1d**, and acetone **1f** in concentrated aqueous ammonia (left) and water (right) after certain reaction times. Product species are assigned in the chromatogram at the bottom. Separation was performed on a 4.6 mm x 250 mm EC Nucleodur 100-5 with gradient elution of *n*-hexane (A)/isopropanol (B): A/B 99/1 → 95/5 (10 min) → 90/10 (15 min) → 60/40 (25 min). The deviating retention times in the 24 h measurement in ammonia (left) are due to a new column, but structures could be confirmed with associated MS spectra.

162

Table 6.3: Relative peak integration of HPLC chromatograms presented in Figures S14 and S15. Formation of imidazolidine-4-thiones 3 from a one-pot mixture of acetaldehyde 1b, isobutyraldehyde 1c, and acetone 1d in water or ammonia at certain reaction times.

	Catalyst [%]	Time [min]						
		0	10	30	60	120	240	1440
H₂O	**3bb**	7.9	32.2	30.0	32.3	25.3	20.7	12.4
	3bc	2.6	27.2	14.4	21.1	22.8	31.5	14.5
	3bd	0.0	1.2	0.7	1.6	0.6	0.7	2.3
	3cb	18.8	5.8	13.2	9.0	9.0	6.6	23.3
	3cc	5.2	4.9	5.2	5.0	5.9	12.8	19.0
	3cd	0.0	0.0	0.0	0.0	0.0	0.0	0.0
	3db	46.9	13.1	21.5	17.2	19.1	13.2	18.7
	3dc	15.5	12.6	12.0	10.8	14.4	11.4	6.8
	3dd	3.0	3.0	3.0	3.0	3.0	3.0	3.0
NH₃	**3bb**	2.5	3.0	0.0	0.8	0.0	0.0	0.0
	3bc	0.0	0.0	0.0	0.0	0.0	0.0	0.0
	3bd	9.2	15.4	6.8	7.0	2.6	2.4	4.5
	3cb	0.0	0.0	0.0	0.0	0.0	0.0	0.0
	3cc	6.8	4.9	1.7	0.9	0.0	0.7	1.0
	3cd	38.0	39.7	27.8	20.6	14.1	14.0	10.2
	3db	27.9	19.0	37.5	43.0	50.9	53.3	40.7
	3dc	6.8	11.5	16.6	18.6	20.4	20.4	20.0
	3dd	8.9	6.5	9.6	9.1	12.0	9.2	23.6

6.6 Organocatalytic α-alkylation without light

The experimental data of the corresponding photoredox α-alkylation is published[194] and can be found in the doctoral thesis of E. FUKS.[201]
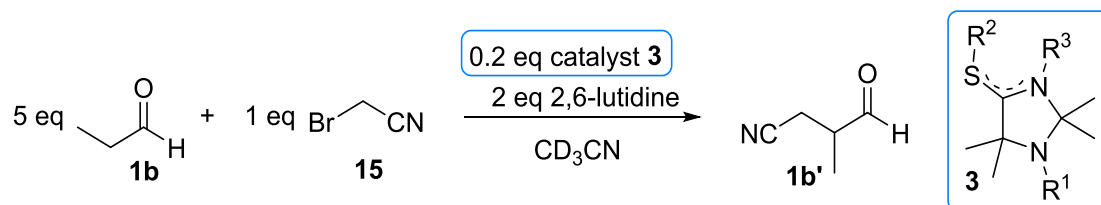
The imidazolidine-4-thione (derivative) **3** (0.12 mmol, 0.2 eq.) was dissolved in 0.3 mL deuterated acetonitrile. Bromoacetonitrile **15** (42 μL, 0.60 mmol, 1.0 eq.), 2,6-lutidine (140 μL, 1.20 mmol, 2.0 eq.), and propionaldehyde **1b** (215 μL, 3.0 mmol, 5.0 eq.) were added and the mixture was stirred under the respective conditions. Samples were taken after 3 h and 24 h and directly analysed with NMR spectrometry. The yield was determined by comparing the product aldehyde signal to the aromatic signal of mesitylene (15 μL) as internal standard.

¹H NMR analysis
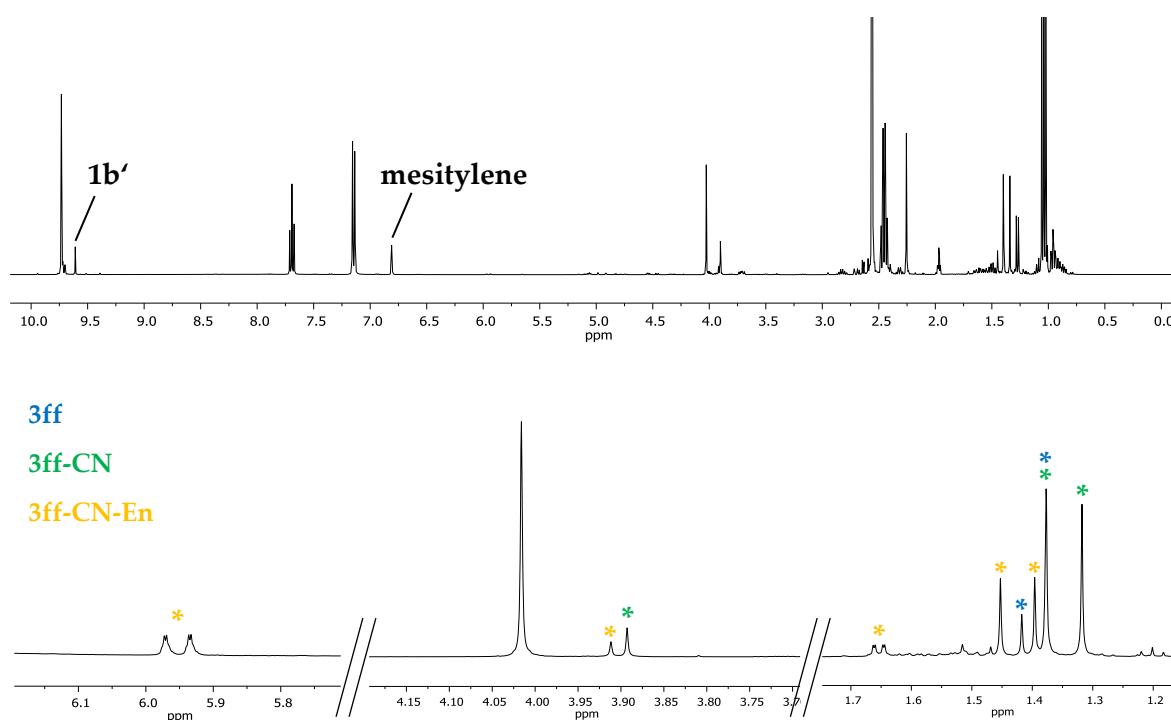
Figure 6.14: Exemplary ¹H NMR spectra of the cyanomethylation of **1b** with **15**, catalysed by **3ff**. Top: full ¹H NMR spectrum after 3 h to illustrate yield determination. Bottom: merged excerpts of the ¹H-NMR spectrum after 30 min to illustrate the corresponding peaks of all imidazolidine-4-thione derivatives.

The structure of **3ff-CN** was verified by isolation of the compound (see Section 6.2.4). It also formed when reacting **3ff** with bromoacetonitrile **15** and 2,6-lutidine in acetonitrile without the addition of propionaldehyde **1b**.

The structure of the enamine **3ff-CN-En** only formed when reacting **3ff** with both propionaldehyde **1b** and bromoacetonitrile **15** or **3ff-CN** with propionaldehyde **1b**. The structure was verified by 2D NMR spectra.
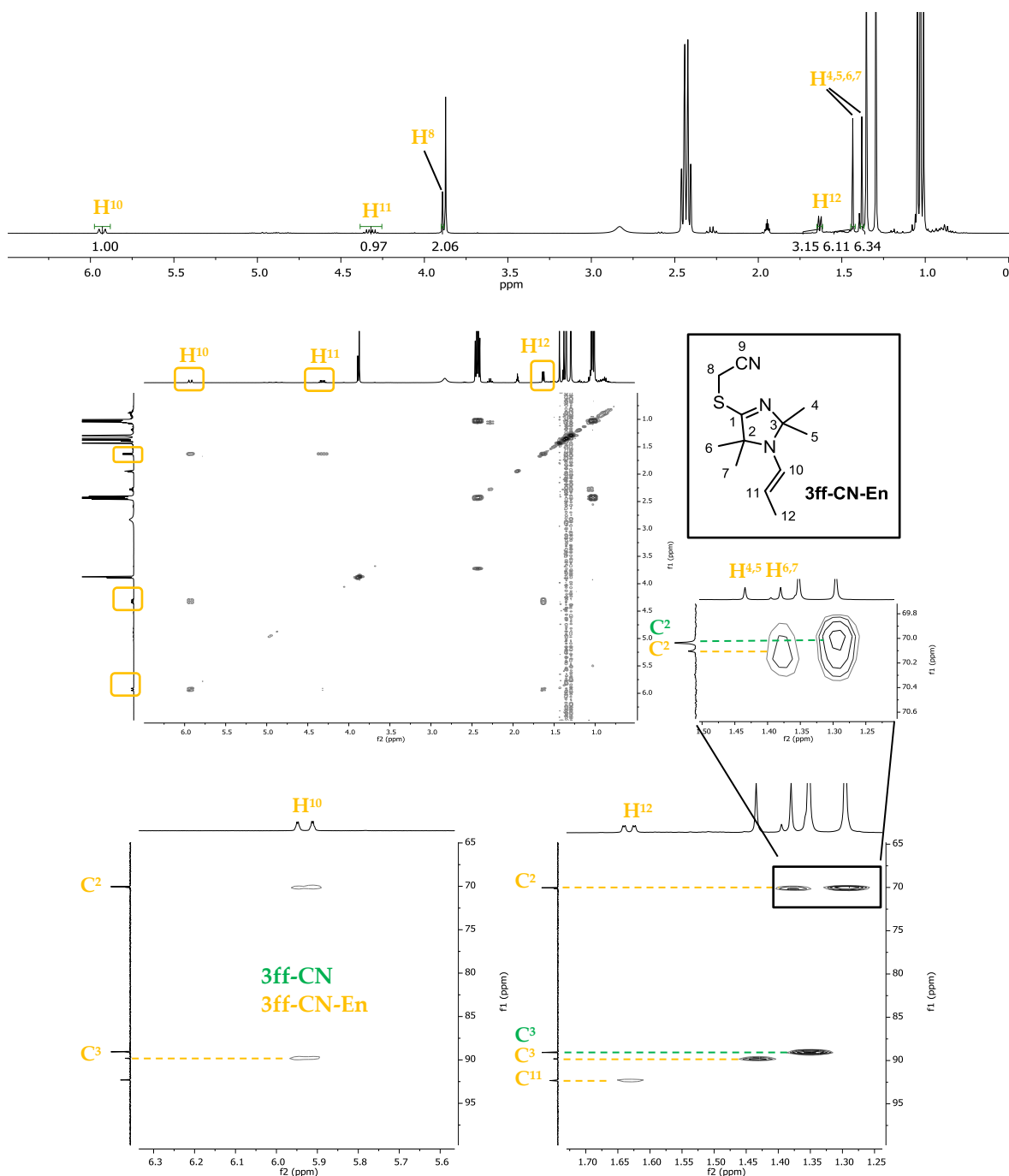
Figure 6.15: Verification of the structure of **3ff-CN-En** with NMR analysis of a mixture of **3ff-CN** and **1b**. Top: integrated ^{1}H NMR spectrum. Bottom: COSY and HMBC spectra with assigned carbon and hydrogen peaks.

Screening of imidazolidine-4-thiones (derivatives) and reaction conditions

Table 6.4: Different catalysts and reaction conditions for the organocatalytic alkylation of propionaldehyde at 40 °C. Yield refers to the product yield after 3 h, determined by comparison to mesitylene as internal standard.

Entry	Catalyst	R^1	R^2	R^3	Conditions	Yield
1	**3ff**	H	-	H	365 nm	76 %
2					40 °C	25 %
3					40 °C, dark glass	24 %
4					40 °C, aluminium foil	25 %
5					room temperature	10 %
6					365 nm, 0 °C	75 %
7	-	-	-	-	40 °C	-
8	**3ff-*N1*-Me**	Me	-	H	40 °C, dark glass	-
9	**3ff-*N3*-Me**	H	-	Me	40 °C, dark glass	-
10[a]	**3ff-CN** + 2,6-lutidine-HCl	H	CH_2CN	-	40 °C, dark glass	-
11	**3ff-Bz**	H	CH_2Ph	-	40 °C, dark glass	35 %
12 (8 + 9)[b]	**3ff-*N1*-Me** + **3ff-*N3*-Me**	Me H	- -	H Me	40 °C, dark glass	-
13	**3ff**	H	-	H	40 °C, dark glass, K_2CO_3 as base	9 %
14	**3fa**	H	-	H	40 °C, dark glass	13 %
15	**3af**	H	-	H	40 °C, dark glass	-
16	**3dd**	H	-	H	40 °C, dark glass	-

Reaction monitoring

For reaction monitoring, the catalysis was performed directly in an NMR tube and ¹H NMR spectra were recorded every ten minutes for 20 h with the NMR spectrometer operated at 40 °C.

Asymmetric catalysis

To apply enantiopure imidazolidine-4-thiones as catalysts, the enantiomers were separated with preparative chiral HPLC. The purity of the obtained enantiomers was checked with analytical HPLC as shown in the following chromatograms and the assignment was possible if absolute stereochemistry was confirmed via crystallisation.
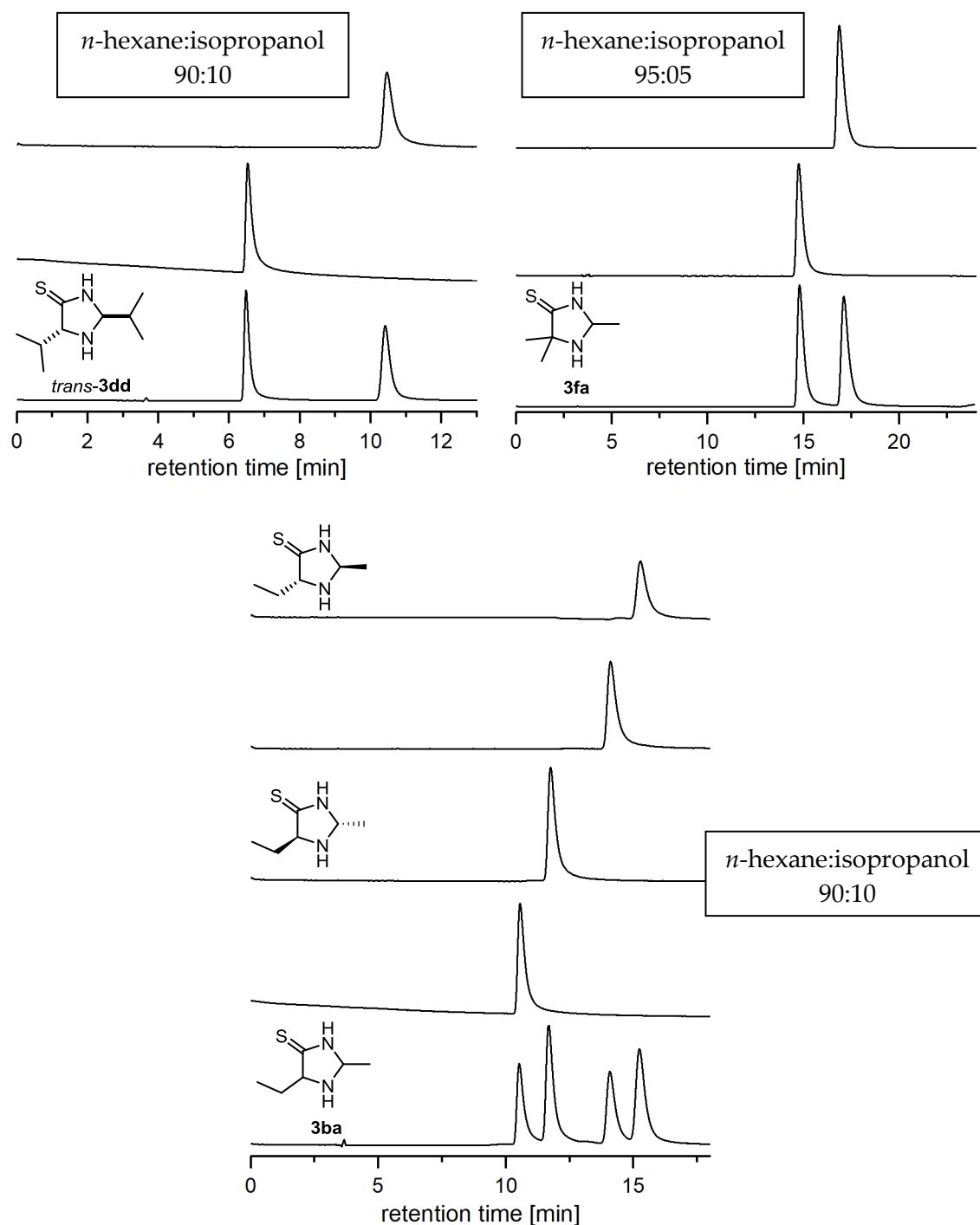
Figure 6.16: Chiral HPLC separation of **3** on a Chiralpak IC (Cellulose tris(3,5-dichlorophenylcarbamate) immobilized on 5 μm silica-gel) eluted with *n*-hexane/isopropanol at 20 °C and a flow of 1.00 mL/min. The bottom chromatogram refers to the racemic mixture and the upper chromatograms to the separated enantiomers. The used ratio of solvents used for the separation is given for each molecule.

167

For the *ee*-value determination, the crude reaction product was directly reduced with NaBH$_4$ after 6 h. Acetonitrile was evaporated in the nitrogen stream at room temperature and the residual oil was redissolved in 1 mL of CH$_2$Cl$_2$ and cooled to -78 °C. An excess of NaBH$_4$ was added and the reaction was stirred for 2 h. The reaction mixture was quenched with water and extracted with CH$_2$Cl$_2$. The solvent was evaporated in the nitrogen stream and the crude was purified by column chromatography (SiO$_2$, pentane/Et$_2$O 2:1). The resulting enantiomers were separated by GC on an SE-30 column (Heptakis(2,3-di-O-methyl-6-O-TBDMS) β-cyclodextrin in PS 086 (8.5 m, 50 °C, 150 kPa).
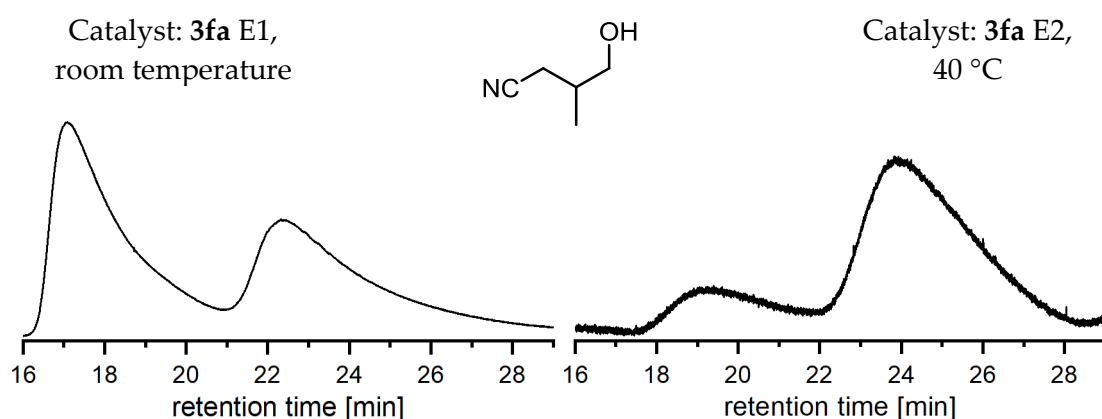
Figure 6.17: GC separation of the corresponding alcohol of the cyanomethylated propionaldehyde **1b'** formed in the reaction catalysed by **3fa**. Left: reaction with enantiomer 1 (15 min in Figure 6.16) at 40 °C. Right: reaction with enantiomer 2 (17.5 min in Figure 6.16) at room temperature.

6.7 Nucleophilicity

Product Study
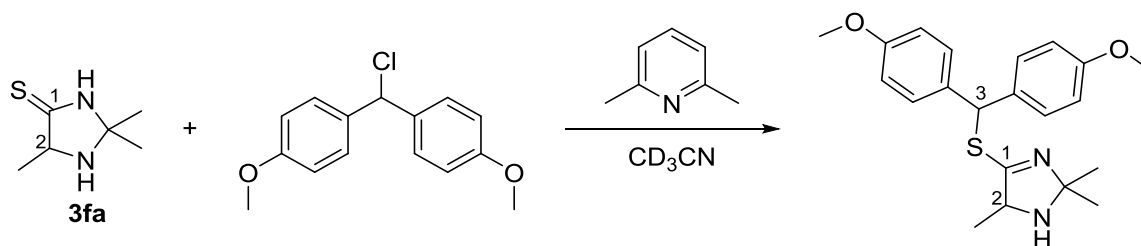
The benzhydrylium chloride (7.6 mg, 29 µmol, 1.0 eq) was dissolved in 0.5 mL of deuterated acetonitrile in an NMR tube (Figure 6.18, grey ^{1}H NMR spectra). 2,6-Lutidine (17 µL, 145 µmol, 5.0 eq) and **3fa** (8.4 mg, 58 µmol, 2.0 eq) were added which resulted in immediate discolouration (Figure 6.18, black ^{1}H NMR spectra).
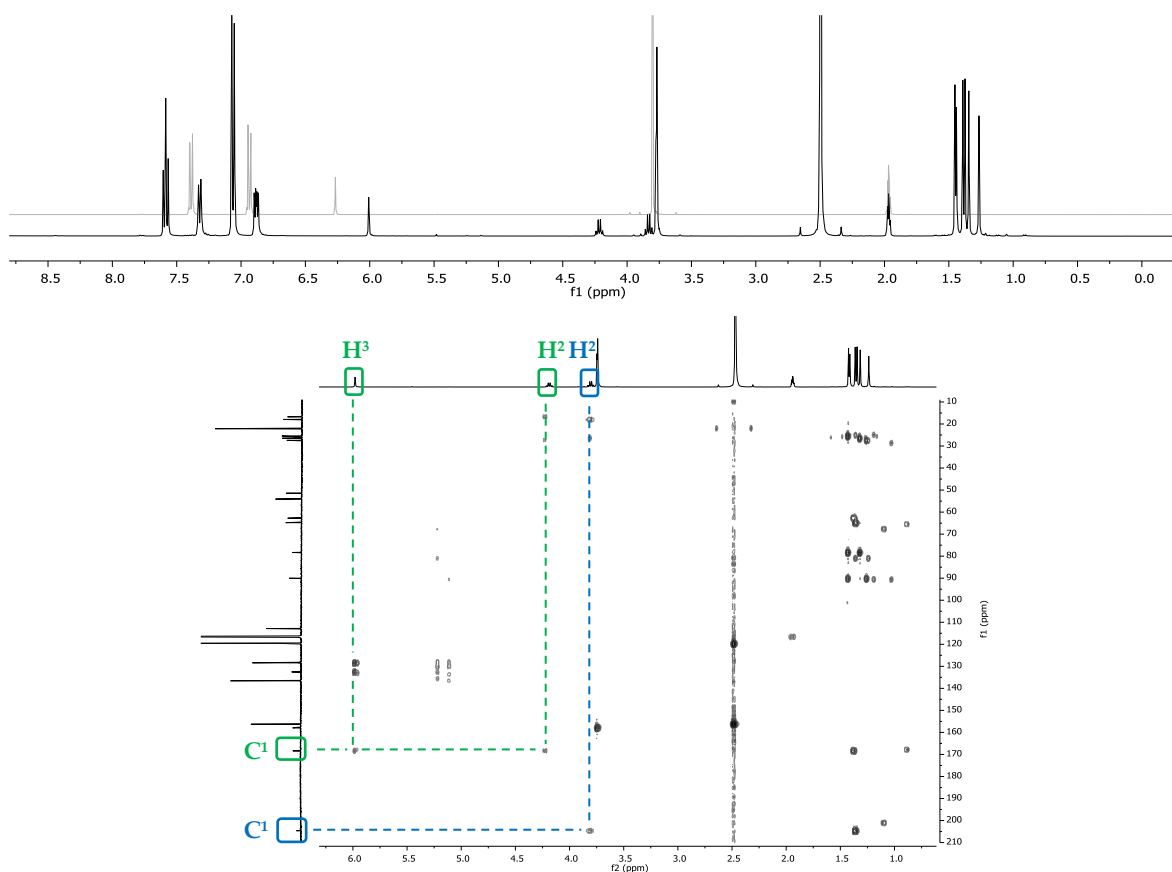
Figure 6.18: In-situ NMR analysis of the reaction of **3fa** with a benzhydrylium chloride. Top: ^{1}H NMR spectrum of the reaction mixture (black) with the reference spectrum of the benzhydrylium substrate superimposed (grey). Bottom: HMBC spectrum of the reaction mixture with characteristic peaks of **3fa** (blue) and the product (green) highlighted.

Note: Nucleophilic attack from the thioamide sulphur can also be verified by the significant upfield shift of the C^1 signal of the product in the ^{13}C spectrum.

Kinetics
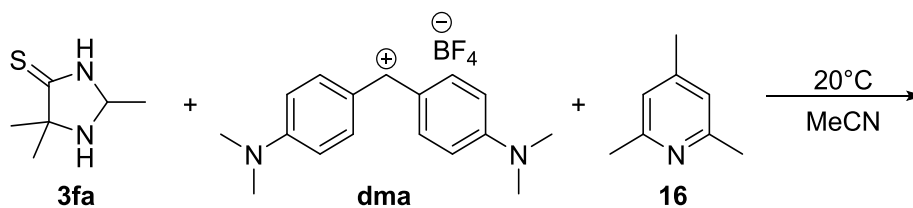
Table 6.5: Kinetics of the reaction of **3fa** with **dma** and **16** (2.6 mM). Detection at 605 nm.

[**3fa**] / M	[**dma**] / M	$k_{obs\,/\,s}^{-1}$
1.02×10^{-4}		1.04
1.53×10^{-4}		1.24
2.04×10^{-4}	7.94×10^{-6}	1.47
2.55×10^{-4}		1.67
3.06×10^{-4}		1.88

$k_{obs} = 4.14 \times 10^3\,[\mathbf{3fa}] + 0.62$

$R^2 = 0.9996$
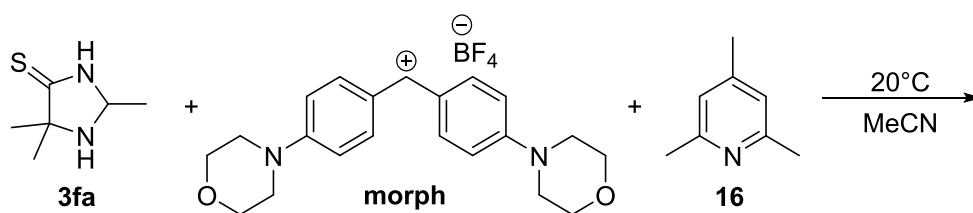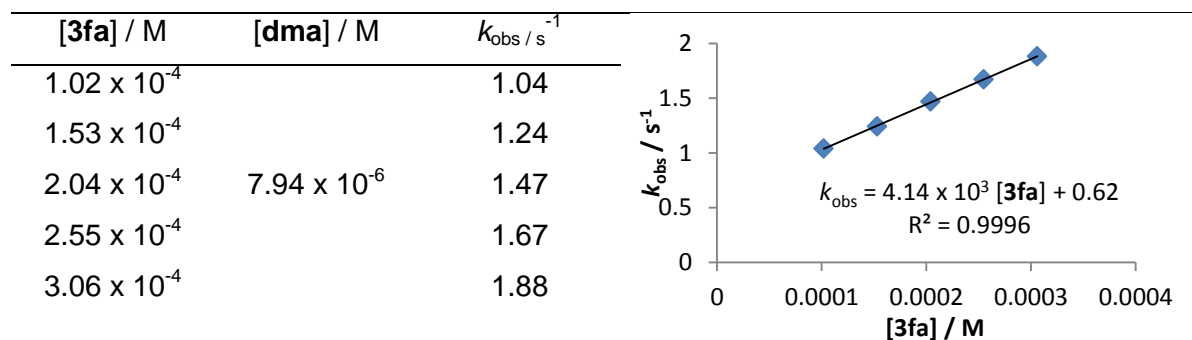
Table 6.6: Kinetics of the reaction of **3fa** with **morph** and **16** (1.2 mM). Detection at 612 nm.

[**3fa**] / M	[**morph**] / M	$k_{obs\,/\,s}^{-1}$
1.02×10^{-4}		3.36
1.53×10^{-4}		4.72
2.04×10^{-4}	8.84×10^{-6}	6.35
2.55×10^{-4}		8.05
3.06×10^{-4}		9.52

$k_{obs} = 3.07 \times 10^4\,[\mathbf{3fa}] + 0.14$

$R^2 = 0.9987$

3fa   +   mfa   +   16 $\xrightarrow{\text{20°C} \atop \text{MeCN}}$
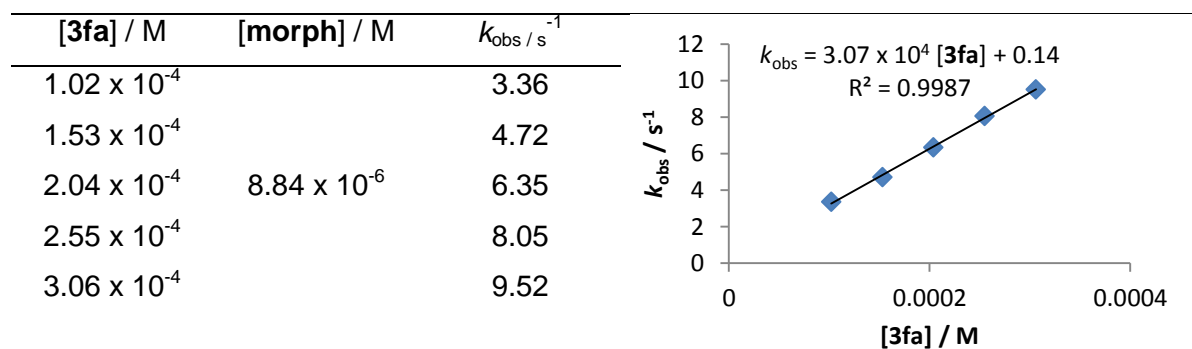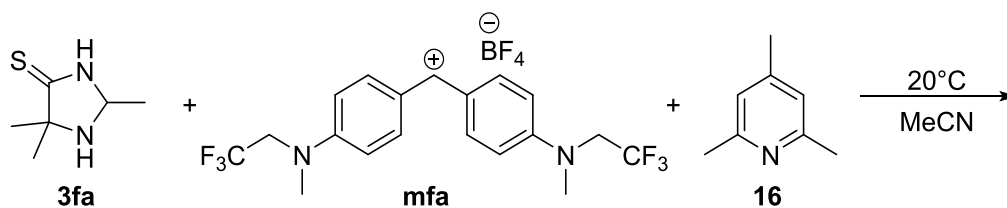
Table 6.7: Kinetics of the reaction of **3fa** with **mfa** and **16** (2.1 mM). Detection at 586 nm.

[3fa] / M	[mfa] / M	$k_{obs / s}^{-1}$
1.11×10^{-4}		6.24×10^{1}
1.66×10^{-4}		1.00×10^{2}
2.22×10^{-4}	9.45×10^{-6}	1.38×10^{2}
2.77×10^{-4}		1.70×10^{2}
3.33×10^{-4}		2.07×10^{2}
3.88×10^{-4}		2.43×10^{2}

$k_{obs} = 6.46 \times 10^5 \, [\textbf{3fa}] - 7.72$
$R^2 = 0.9995$

3fa   +   pfa   +   17 $\xrightarrow{\text{20°C} \atop \text{MeCN}}$
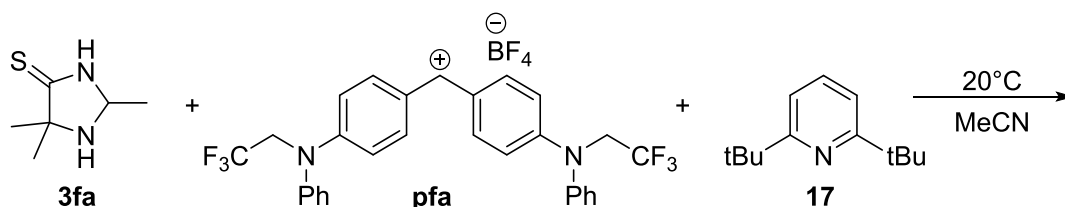
Table 6.8: Kinetics of the reaction of **3fa** with **pfa** and **17** (1.4 mM). Detection at 592 nm.

[3fa] / M	[pfa] / M	$k_{obs / s}^{-1}$
8.86×10^{-5}		6.51×10^{1}
1.18×10^{-4}		1.20×10^{2}
1.48×10^{-4}	9.00×10^{-6}	1.55×10^{2}
1.77×10^{-4}		2.10×10^{2}
2.07×10^{-4}		2.63×10^{2}
2.36×10^{-4}		3.17×10^{2}

$k_{obs} = 1.69 \times 10^6 - 85.7$
$R^2 = 0.9963$

Table 6.9: Determination of s_N and N for **3fa** in acetonitrile.

electrophile	E	k_2 / M^{-1} s^{-1}
dma	-7.02	4.14×10^3
morph	-5.53	3.07×10^4
mfa	-3.85	6.46×10^5
pfa	-3.14	1.69×10^6
$s_N = 0.69$	$N = 12.17$	

$\log k_2 = 0.69 \, E + 8.40$
$R^2 = 0.996$
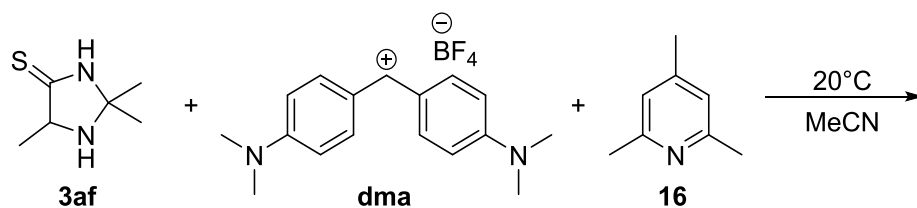
Table 6.10: Kinetics of the reaction of **3af** with **dma** and **16** (10.4 mM). Detection at 605 nm.

[3af] / M	[dma] / M	k_{obs} / s^{-1}	
1.73×10^{-4}		1.43	
2.60×10^{-4}		1.87	
3.47×10^{-4}	9.70×10^{-6}	2.20	
4.33×10^{-4}		2.57	
5.20×10^{-4}		2.73	

$k_{obs} = 3.81 \times 10^3$ [3af] + 0.84
$R^2 = 0.9797$
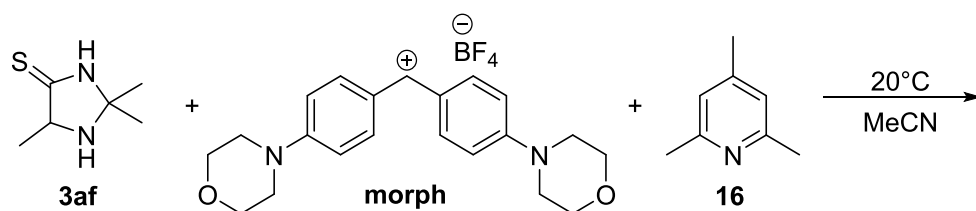
Table 6.11: Kinetics of the reaction of **3af** with **morph** and **16** (1.7 mM). Detection at 612 nm.

[3af] / M	[morph] / M	k_{obs} / s^{-1}	
1.73×10^{-4}		5.86	
2.60×10^{-4}		9.40	
3.47×10^{-4}	9.43×10^{-6}	1.27×10^1	
4.33×10^{-4}		1.51×10^1	
5.20×10^{-4}		1.81×10^1	

$k_{obs} = 3.49 \times 10^4$ [3af] + 0.14
$R^2 = 0.9963$

172
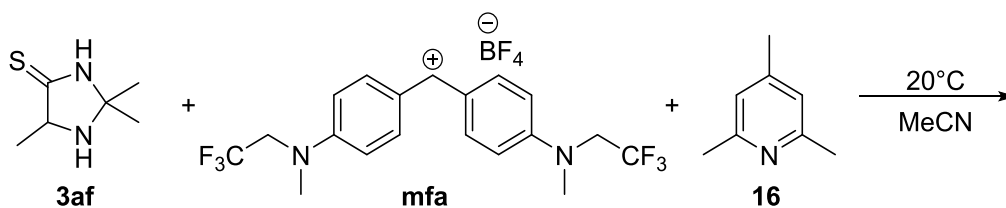
Table 6.12: Kinetics of the reaction of **3af** with **mfa** and **16** (1.9 mM). Detection at 586 nm.

[3af] / M	[mfa] / M	k_{obs} / s^{-1}
1.25 x 10^{-4}		5.85 x 10^{1}
1.87 x 10^{-4}		9.13 x 10^{1}
2.50 x 10^{-4}	9.56 x 10^{-6}	1.23 x 10^{2}
3.12 x 10^{-4}		1.54 x 10^{2}
3.74 x 10^{-4}		1.89 x 10^{2}

$k_{obs} = 5.17 \times 10^5\ [\textbf{3af}] - 6.04$
$R^2 = 0.9995$

Table 6.13: Determination of s_N and N for **3af** in acetonitrile.

electrophile	E	k_2 / M^{-1} s^{-1}
dma	-7.02	3.81 x 10^{3}
morph	-5.53	3.49 x 10^{4}
mfa	-3.85	5.17 x 10^{5}

$s_N = 0.67$ $\quad$ $N = 12.39$

$\log k_2 = 0.67\ E + 8.29$
$R^2 = 0.9995$

173
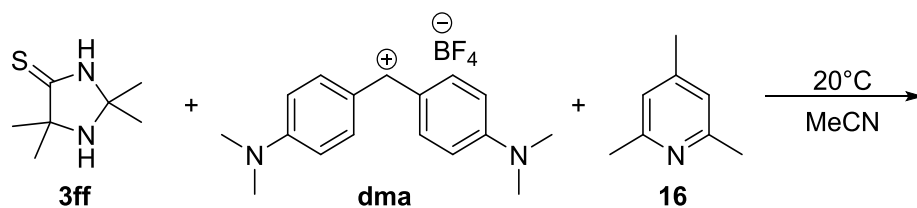
Table 6.14: Kinetics of the reaction of **3ff** with **dma** and **16** (10.4 mM). Detection at 605 nm.

[3ff] / M	[dma] / M	k_{obs} / s^{-1}
2.16 x 10^{-4}		1.28
3.24 x 10^{-4}		1.47
4.32 x 10^{-4}	9.70 x 10^{-6}	1.71
5.40 x 10^{-4}		1.93
6.48 x 10^{-4}		2.12

$k_{obs} = 1.98 \times 10^3 \, \mathbf{[3ff]} + 0.85$
$R^2 = 0.9984$
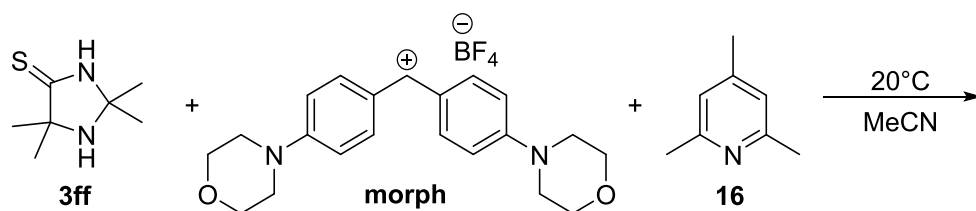
Table 6.15: Kinetics of the reaction of **3ff** with **morph** and **16** (1.7 mM). Detection at 612 nm.

[3ff] / M	[morph] / M	k_{obs} / s^{-1}
2.16 x 10^{-4}		7.57
3.24 x 10^{-4}		1.07 x 10^1
4.32 x 10^{-4}	9.43 x 10^{-6}	1.46 x 10^1
5.40 x 10^{-4}		1.81 x 10^1

$k_{obs} = 3.27 \times 10^4 \, \mathbf{[3ff]} + 0.36$
$R^2 = 0.9983$
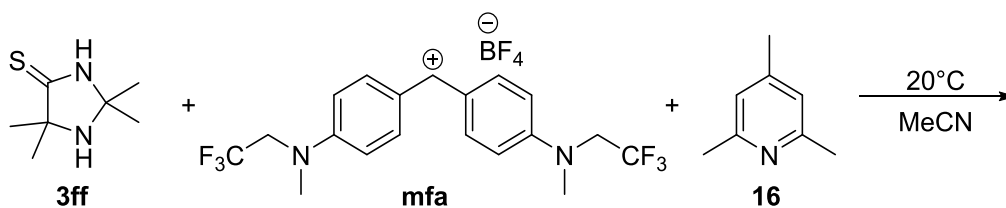
Table 6.16: Kinetics of the reaction of **3ff** with **mfa** and **16** (1.9 mM). Detection at 586 nm.

[3af] / M	[mfa] / M	$k_{obs / s}^{-1}$
1.26×10^{-4}		7.37×10^{1}
1.90×10^{-4}		1.22×10^{2}
2.53×10^{-4}	9.56×10^{-6}	1.23×10^{2}
3.16×10^{-4}		1.54×10^{2}
3.79×10^{-4}		1.89×10^{2}

$k_{obs} = 7.33 \times 10^5 \text{ [3ff]} - 17.69$
$R^2 = 0.9992$

Table 6.17: Determination of s_N and N for **3ff** in acetonitrile.

electrophile	E	k_2 / M^{-1} s^{-1}
dma	-7.02	1.98×10^{3}
morph	-5.53	3.27×10^{4}
mfa	-3.85	7.33×10^{5}
$s_N = 0.81$	$N = 11.11$	

$\log k_2 = 0.81 \, E + 8.99$
$R^2 = 1$
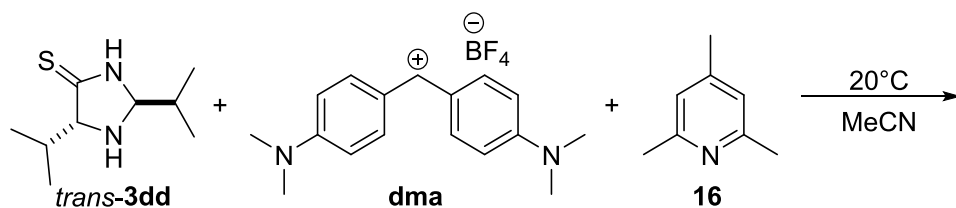
Table 6.18: Kinetics of the reaction of *trans*-**3dd** with **dma** and **16** (10.4 mM). Detection at 605 nm.

[*trans*-**3dd**] / M	[**dma**] / M	$k_{obs / s}^{-1}$
1.69 x 10^{-4}		0.59
2.53 x 10^{-4}		0.72
3.37 x 10^{-4}	9.70 x 10^{-6}	0.88
4.21 x 10^{-4}		1.03

$k_{obs} = 1.76 \times 10^3 \, [\text{*trans*-}\mathbf{3dd}] + 0.29$
$R^2 = 0.9984$
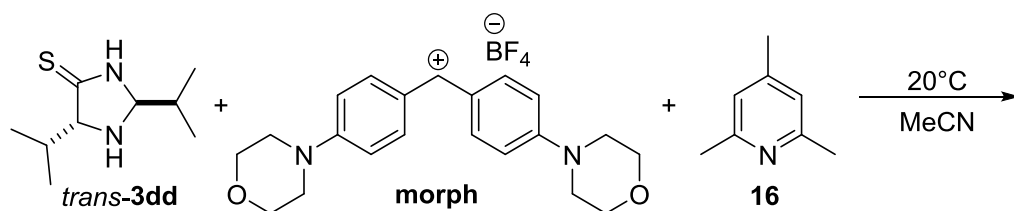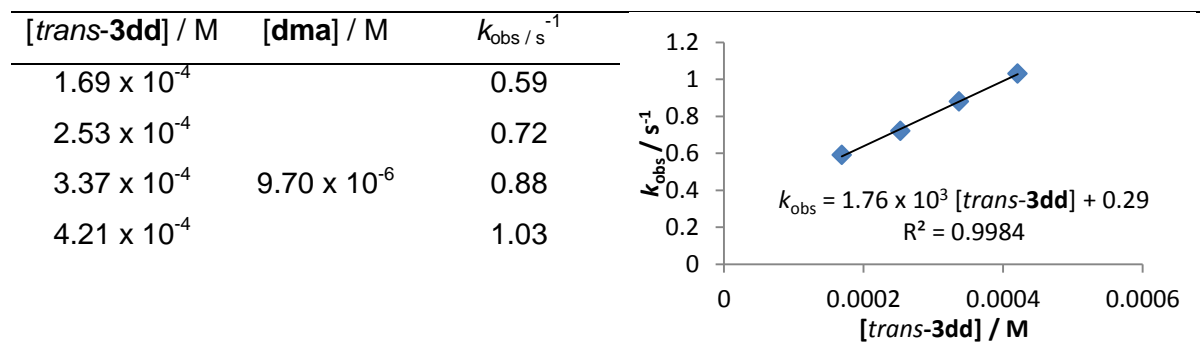
Table 6.19: Kinetics of the reaction of *trans*-**3dd** with **morph** and **16** (1.7 mM). Detection at 612 nm.

[*trans*-**3dd**] / M	[**morph**] / M	$k_{obs / s}^{-1}$
1.69 x 10^{-4}		3.82
2.53 x 10^{-4}		6.25
3.37 x 10^{-4}	1.06 x 10^{-5}	8.26
4.21 x 10^{-4}		10.43

$k_{obs} = 2.60 \times 10^4 \, [\text{*trans*-}\mathbf{3dd}] - 0.48$
$R^2 = 0.9986$
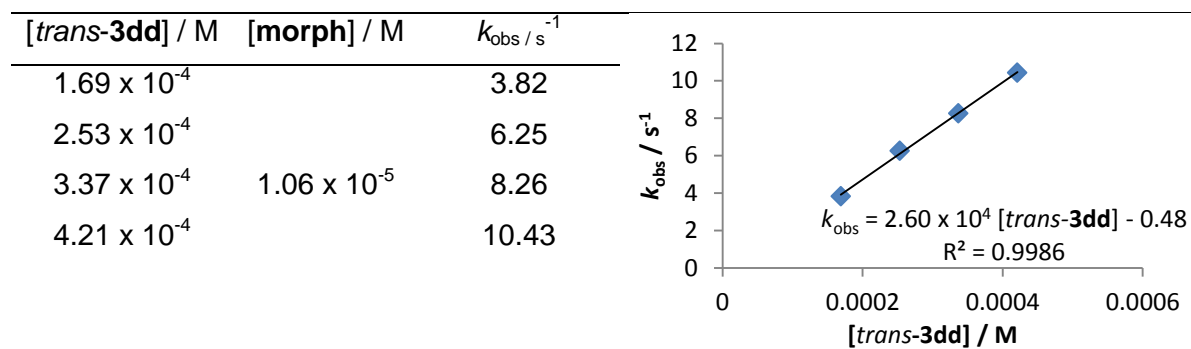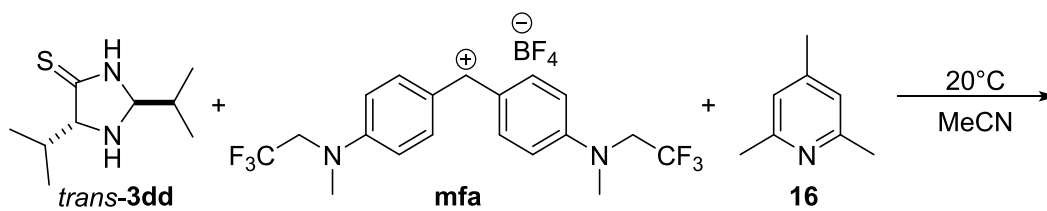
Table 6.20: Kinetics of the reaction of *trans*-**3dd** with **mfa** and **16** (1.9 mM). Detection at 586 nm.

[*trans*-**3dd**] / M	[**mfa**] / M	k_{obs} / s^{-1}
1.15 x 10^{-4}		5.41 x 10^{1}
1.72 x 10^{-4}		8.61 x 10^{1}
2.30 x 10^{-4}	8.82 x 10^{-6}	1.17 x 10^{2}
2.87 x 10^{-4}		1.49 x 10^{2}
3.45 x 10^{-4}		1.81 x 10^{2}

$k_{obs} = 5.49 \times 10^5 \, [\textit{trans}\text{-}\mathbf{3dd}] - 8.77$
$R^2 = 1$

Table 6.21: Determination of s_N and N for *trans*-**3dd** in acetonitrile.

electrophile	E	k_2 / M^{-1} s^{-1}
dma	-7.02	1.76 x 10^{3}
morph	-5.53	2.60 x 10^{4}
mfa	-3.85	5.49 x 10^{5}

$s_N = 0.79 \qquad N = 11.10$

$\log k_2 = 0.79 \, E + 8.77$
$R^2 = 1$
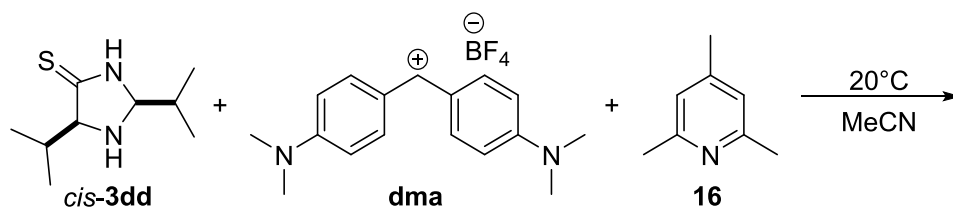
Table 6.22: Kinetics of the reaction of *cis*-**3dd** with **dma** and **16** (10.4 mM). Detection at 605 nm.

[*cis*-**3dd**] / M	[**dma**] / M	$k_{obs / s}^{-1}$
1.62 x 10^{-4}		0.59
2.43 x 10^{-4}		0.72
3.24 x 10^{-4}	9.70 x 10^{-6}	0.82
4.05 x 10^{-4}		0.93
4.86 x 10^{-4}		1.03

$k_{obs} = 1.35 \times 10^3 \, [\textit{cis-}\textbf{3dd}] + 0.38$
$R^2 = 0.9977$

Table 6.23: Kinetics of the reaction of *cis*-**3dd** with **morph** and **16** (1.7 mM). Detection at 612 nm.

[*cis*-**3dd**] / M	[**morph**] / M	$k_{obs / s}^{-1}$
1.62 x 10^{-4}		3.24
2.43 x 10^{-4}		5.34
3.24 x 10^{-4}	1.06 x 10^{-5}	7.20
4.05 x 10^{-4}		9.43
4.86 x 10^{-4}		10.94

$k_{obs} = 2.41 \times 10^4 \, [\textit{cis-}\textbf{3dd}] - 0.57$
$R^2 = 0.9971$

Table 6.24: Kinetics of the reaction of *cis*-3dd with **mfa** and **16** (1.9 mM). Detection at 586 nm.

[*cis*-3dd] / M	[mfa] / M	$k_{obs / s}^{-1}$
1.18×10^{-4}		4.58×10^1
1.77×10^{-4}		6.94×10^1
2.36×10^{-4}	8.82×10^{-6}	9.66×10^1
2.95×10^{-4}		1.24×10^2
3.54×10^{-4}		1.49×10^2

$k_{obs} = 4.43 \times 10^5$ [*cis*-3dd] - 7.52
$R^2 = 0.9995$

Table 6.25: Determination of s_N and N for *cis*-3dd in acetonitrile.

electrophile	E	k_2 / M^{-1} s^{-1}
dma	-7.02	1.35×10^3
morph	-5.53	2.41×10^4
mfa	-3.85	4.43×10^5

$s_N = 0.79$ $N = 11.04$

$\log k_2 = 0.79\, E + 8.72$
$R^2 = 0.999$
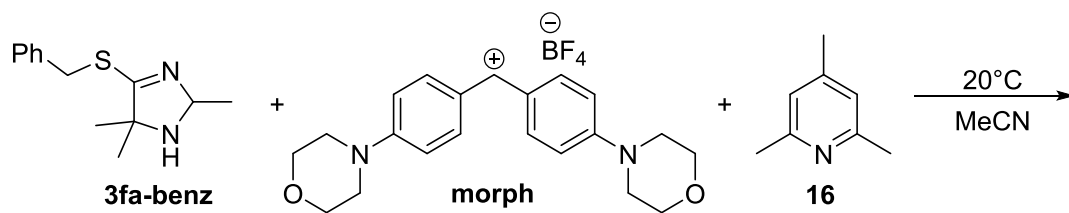
Table 6.26: Kinetics of the reaction of **3fa-Bz** with **morph** and **16** (1.1 mM). Detection at 612 nm.

[3fa-benz] / M	[morph] / M	$k_{obs\,/\,s}^{-1}$
2.59 x 10^{-4}		0.41
3.89 x 10^{-4}		0.69
5.18 x 10^{-4}	9.43 x 10^{-6}	0.94
6.48 x 10^{-4}		1.19
7.78 x 10^{-4}		1.46

$k_{obs} = 2.00 \times 10^3$ **[3fa-Bz]** - 0.10
$R^2 = 0.9996$
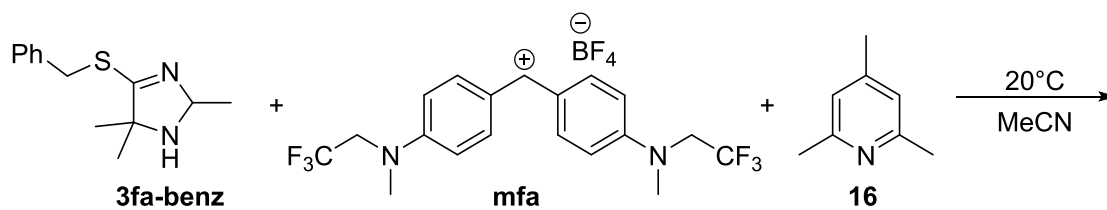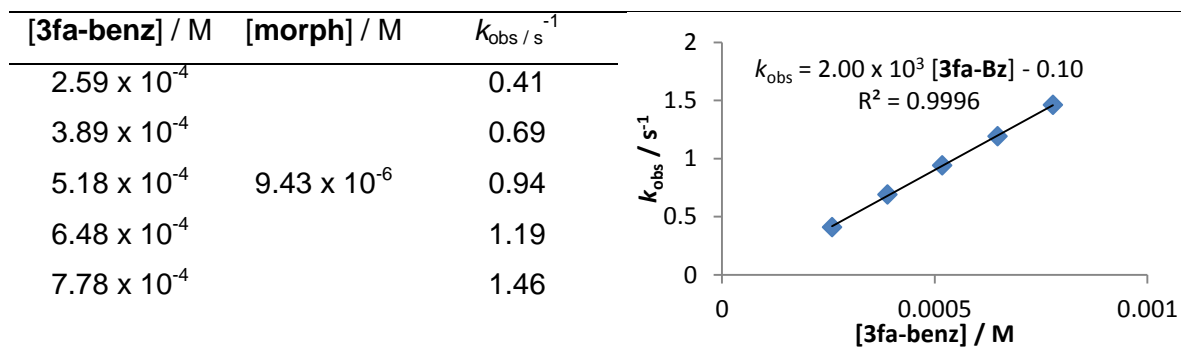
Table 6.27: Kinetics of the reaction of **3fa-Bz** with **mfa** and **16** (1.9 mM). Detection at 586 nm.

[3fa-benz] / M	[mfa] / M	$k_{obs\,/\,s}^{-1}$
1.36 x 10^{-4}		3.55
1.81 x 10^{-4}		5.00
2.27 x 10^{-4}	9.19 x 10^{-6}	6.50
2.72 x 10^{-4}		7.97
3.17 x 10^{-4}		9.79

$k_{obs} = 3.41 \times 10^4$ **[3fa-Bz]** - 1.17
$R^2 = 0.9978$
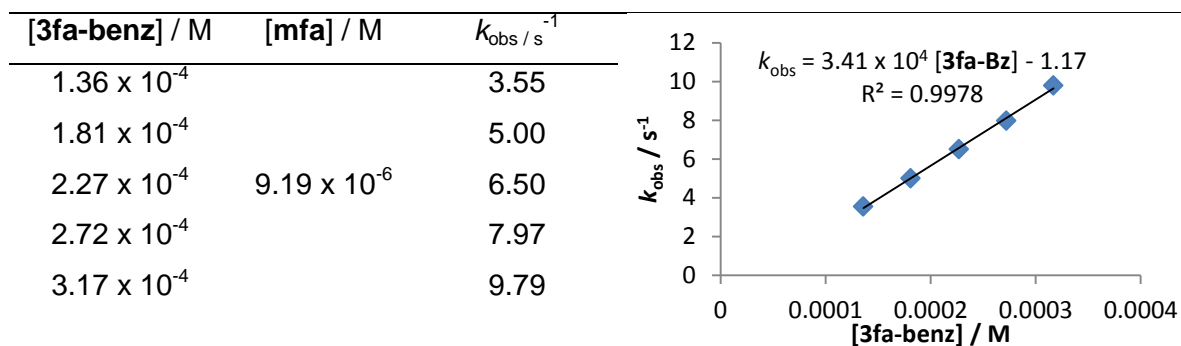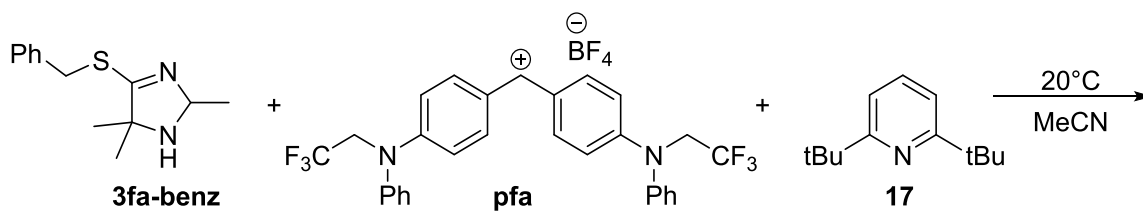
Table 6.28: Kinetics of the reaction of **3fa-Bz** with **pfa** and **17** (1.4 mM). Detection at 592 nm.

[3fa-benz] / M	[pfa] / M	k_{obs} / s^{-1}
1.36×10^{-4}		3.55
1.81×10^{-4}		5.00
2.27×10^{-4}	9.50×10^{-6}	6.50
2.72×10^{-4}		7.97
3.17×10^{-4}		9.79

$k_{obs} = 1.34 \times 10^5$ [**3fa-Bz**] - 1.36
$R^2 = 0.9999$

Table 6.29: Determination of s_N and N for **3fa-Bz** in acetonitrile.

electrophile	E	k_2 / M^{-1} s^{-1}
morph	-5.53	2.00×10^3
mfa	-3.85	3.41×10^4
pfa	-3.14	1.34×10^5

$s_N = 0.78$ $N = 9.73$

$\log k_2 = 0.78\ E + 7.59$
$R^2 = 0.999$

7 Bibliography

[1]   A. Eschenmoser, *Tetrahedron* **2007**, *63*, 12821-12844.

[2]   N. H. Sleep, K. Zahnle, P. S. Neuhoff, *Proc. Natl. Acad. Sci. U.S.A.* **2001**, *98*, 3666-3672.

[3]   S. J. Mojzsis, G. Arrhenius, K. D. McKeegan, T. M. Harrison, A. P. Nutman, C. R. L. Friend, *Nature* **1996**, *384*, 55-59.

[4]   J. W. Schopf, *Science* **1993**, *260*, 640-646.

[5]   S. A. Wilde, J. W. Valley, W. H. Peck, C. M. Graham, *Nature* **2001**, *409*, 175-178.

[6]   T. Owen, R. D. Cess, V. Ramanathan, *Nature* **1979**, *277*, 640-642.

[7]   H. S. Jones, *Sci. Prog.* **1950**, *38*, 417-429.

[8]   P. H. Abelson, *Proc. Natl. Acad. Sci. U.S.A.* **1966**, *55*, 1365-1372.

[9]   N. H. Sleep, *Cold Spring Harb. Perspect. Biol.* **2010**, *2*.

[10]   S. L. Miller, H. C. Urey, *Science* **1959**, *130*, 245-251.

[11]   G. Schlesinger, S. L. Miller, *J. Mol. Evol.* **1983**, *19*, 376-382.

[12]   Y. L. Yung, J. P. Pinto, *Nature* **1978**, *273*, 730-732.

[13]   C. Sagan, C. Chyba, *Science* **1997**, *276*, 1217-1221.

[14]   L. Schaefer, B. Fegley, *Icarus* **2007**, *186*, 462-483.

[15]   K. Zahnle, L. Schaefer, B. Fegley, *Cold Spring Harb. Perspect. Biol.* **2010**, *2*.

[16]   S. Pizzarello, G. W. Cooper, G. J. Flynn, in *Meteorites and the Early Solar System II*, The University of Arizona Press, **2006**, pp. 625-651.

[17]   M. P. Callahan, K. E. Smith, H. J. Cleaves, J. Ruzicka, J. C. Stern, D. P. Glavin, C. H. House, J. P. Dworkin, *Proc. Natl. Acad. Sci. U.S.A.* **2011**, *108*, 13995-13998.

[18]   J. Oró, J. Gibert, H. Lichtenstein, S. Wikstrom, D. A. Flory, *Nature* **1971**, *230*, 105-106.

[19]   S. Pizzarello, *Orig. Life Evol. Biosph.* **2004**, *34*, 25-34.

[20]   A. P. C. Mann, D. A. Williams, *Nature* **1980**, *283*, 721-725.

[21]   B. Burcar, M. Pasek, M. Gull, B. J. Cafferty, F. Velasco, N. V. Hud, C. Menor-Salván, *Angew. Chem. Int. Ed.* **2016**, *55*, 13249-13253.

[22]   J. W. Morse, F. T. Mackenzie, *Aquat. Geochem.* **1998**, *4*, 301-319.

[23]   W. Martin, J. Baross, D. Kelley, M. J. Russell, *Nat. Rev. Microbiol.* **2008**, *6*, 805-814.

[24]   J. A. Baross, S. E. Hoffman, *Orig. Life Evol. Biosph.* **1985**, *15*, 327-345.

[25]   Deborah S. Kelley, a. John A. Baross, J. R. Delaney, *Annu. Rev. Earth Planet. Sci.* **2002**, *30*, 385-491.

[26]   D. S. Kelley, J. A. Karson, G. L. Früh-Green, D. R. Yoerger, T. M. Shank, D. A. Butterfield, J. M. Hayes, M. O. Schrenk, E. J. Olson, G. Proskurowski, M. Jakuba, A. Bradley, B. Larson, K. Ludwig, D. Glickson, K. Buckman, A. S. Bradley, W. J. Brazelton, K. Roe, M. J. Elend, A. Delacour, S. M. Bernasconi, M. D. Lilley, J. A. Baross, R. E. Summons, S. P. Sylva, *Science* **2005**, *307*, 1428-1434.

[27]   G. Proskurowski, M. D. Lilley, J. S. Seewald, G. L. Früh-Green, E. J. Olson, J. E. Lupton, S. P. Sylva, D. S. Kelley, *Science* **2008**, *319*, 604-607.

[28]   J. P. Ferris, *Orig. Life Evol. Biosph.* **1992**, *22*, 109-134.

[29]   B. Fegley, R. G. Prinn, H. Hartman, G. H. Watkins, *Nature* **1986**, *319*, 305-308.

[30]   C. Chyba, C. Sagan, *Nature* **1992**, *355*, 125-132.

[31]   K. Kurosawa, S. Sugita, K. Ishibashi, S. Hasegawa, Y. Sekine, N. O. Ogawa, T. Kadono, S. Ohno, N. Ohkouchi, Y. Nagaoka, T. Matsui, *Orig. Life Evol. Biosph.* **2013**, *43*, 221-245.

[32]   J. P. Ferris, W. J. Hagan, *Tetrahedron* **1984**, *40*, 1093-1120.

[33]   J. D. Sutherland, *Angew. Chem. Int. Ed.* **2016**, *55*, 104-121.

[34] J. C. Aponte, D. Whitaker, M. W. Powner, J. E. Elsila, J. P. Dworkin, *ACS Earth Space Chem.* **2019**, *3*, 463-472.

[35] G. A. Jungclaus, G. U. Yuen, C. B. Moore, J. G. Lawless, *Meteoritics* **1976**, *11*, 231-237.

[36] P. de Marcellus, C. Meinert, I. Myrgorodska, L. Nahon, T. Buhse, L. L. S. d'Hendecourt, U. J. Meierhenrich, *Proc. Natl. Acad. Sci. U.S.A.* **2015**, *112*, 965-970.

[37] M. H. Engel, S. A. Macko, *Nature* **1997**, *389*, 265-268.

[38] K. Kvenvolden, J. Lawless, K. Pering, E. Peterson, J. Flores, C. Ponnamperuma, I. R. Kaplan, C. Moore, *Nature* **1970**, *228*, 923-926.

[39] S. Epstein, R. V. Krishnamurthy, J. R. Cronin, S. Pizzarello, G. U. Yuen, *Nature* **1987**, *326*, 477-479.

[40] S. Miyakawa, H. Yamanashi, K. Kobayashi, H. J. Cleaves, S. L. Miller, *Proc. Natl. Acad. Sci. U.S.A.* **2002**, *99*, 14628-14631.

[41] S. L. Miller, *J. Am. Chem. Soc.* **1955**, *77*, 2351-2361.

[42] S. L. Miller, *Science* **1953**, *117*, 528-529.

[43] R. J. C. Hennet, N. G. Holm, M. H. Engel, *Naturwissenschaften* **1992**, *79*, 361-365.

[44] A. Strecker, *Liebigs Ann.* **1850**, *75*, 27-45.

[45] J. Oró, S. S. Kamat, *Nature* **1961**, *190*, 442-443.

[46] R. E. Moser, A. R. Claggett, C. N. Matthews, *Tetrahedron Lett.* **1968**, *9*, 1599-1603.

[47] J. P. Ferris, P. C. Joshi, E. H. Edelson, J. G. Lawless, *J. Mol. Evol.* **1978**, *11*, 293-311.

[48] J. Hulshof, C. Ponnamperuma, *Orig. Life* **1976**, *7*, 197-224.

[49] H. Sawai, R. Lohrmann, L. E. Orgel, *J. Mol. Evol.* **1975**, *6*, 165-184.

[50] A. L. Weber, J. M. Caroon, J. T. Warden, R. M. Lemmon, M. Calvin, *BioSystems* **1977**, *8*, 277-286.

[51] M. G. Schwendinger, B. M. Rode, *Anal. Sci.* **1989**, *5*, 411-414.

[52] J. P. Ferris, A. R. Hill, R. Liu, L. E. Orgel, *Nature* **1996**, *381*, 59-61.

[53] K. Kawamura, H. Takeya, T. Kushibe, *Adv. Space Res.* **2009**, *44*, 267-275.

[54] P. Canavelli, S. Islam, M. W. Powner, *Nature* **2019**, *571*, 546-549.

[55] M. G. Schwendinger, R. Tattler, S. Saetia, K. R. Liedl, R. T. Kroemer, B. M. Rode, *Inorg. Chim. Acta* **1995**, *228*, 207-214.

[56] B. M. Rode, M. G. Schwendinger, *Orig. Life Evol. Biosph.* **1990**, *20*, 401-410.

[57] A. Butlerow, *Liebigs Ann. Chem.* **1861**, *120*, 295-298.

[58] D. J. Ritson, J. D. Sutherland, *Angew. Chem. Int. Ed.* **2013**, *52*, 5845-5847.

[59] M. Ferus, F. Pietrucci, A. M. Saitta, A. Knížek, P. Kubelík, O. Ivanek, V. Shestivska, S. Civiš, *Proc. Natl. Acad. Sci. U.S.A.* **2017**, *114*, 4306-4311.

[60] J. P. Ferris, R. A. Sanchez, L. E. Orgel, *J. Mol. Biol.* **1968**, *33*, 693-704.

[61] R. A. Sanchez, J. P. Ferbis, L. E. Orgel, *J. Mol. Biol.* **1967**, *30*, 223-253.

[62] M. P. Robertson, S. L. Miller, *Nature* **1995**, *375*, 772-774.

[63] M. W. Powner, B. Gerland, J. D. Sutherland, *Nature* **2009**, *459*, 239-242.

[64] S. Islam, D.-K. Bučar, M. W. Powner, *Nat. Chem.* **2017**, *9*, 584-589.

[65] S. Stairs, A. Nikmal, D.-K. Bučar, S.-L. Zheng, J. W. Szostak, M. W. Powner, *Nat. Commun.* **2017**, *8*, 15270.

[66] S. Becker, I. Thoma, A. Deutsch, T. Gehrke, P. Mayer, H. Zipse, T. Carell, *Science* **2016**, *352*, 833-836.

[67] J. S. Teichert, F. M. Kruse, O. Trapp, *Angew. Chem. Int. Ed.* **2019**, *58*, 9944-9947.

[68] C. Gibard, S. Bhowmik, M. Karki, E.-K. Kim, R. Krishnamurthy, *Nat. Chem.* **2018**, *10*, 212-217.

[69] M. Frenkel-Pinter, M. Samanta, G. Ashkenasy, L. J. Leman, *Chem. Rev.* **2020**, *120*, 4707-4765.

[70] S. Islam, M. W. Powner, *Chem* **2017**, *2*, 470-501.

[71] B. H. Patel, C. Percivalle, D. J. Ritson, C. D. Duffy, J. D. Sutherland, *Nat. Chem.* **2015**, *7*, 301-307.

[72] A. P. Johnson, H. J. Cleaves, J. P. Dworkin, D. P. Glavin, A. Lazcano, J. L. Bada, *Science* **2008**, *322*, 404-404.

[73] K. Harada, S. W. Fox, *Nature* **1964**, *201*, 335-336.

[74] W. Groth, H. von Weyssenhoff, *Naturwissenschaften* **1957**, *44*, 510-511.

[75] C. Huber, F. Kraus, M. Hanzlik, W. Eisenreich, G. Wächtershäuser, *Chem. Eur. J.* **2012**, *18*, 2063-2080.

[76] T. Z. Jia, K. Chandru, Y. Hongo, R. Afrin, T. Usui, K. Myojo, H. J. Cleaves, *Proc. Natl. Acad. Sci. U.S.A.* **2019**, *116*, 15830-15835.

[77] S.-S. Yu, R. Krishnamurthy, F. M. Fernández, N. V. Hud, F. J. Schork, M. A. Grover, *Phys. Chem. Chem. Phys.* **2016**, *18*, 28441-28450.

[78] J. G. Forsythe, S.-S. Yu, I. Mamajanov, M. A. Grover, R. Krishnamurthy, F. M. Fernández, N. V. Hud, *Angew. Chem. Int. Ed.* **2015**, *54*, 9871-9875.

[79] G. Wald, *Ann. N.Y. Acad. Sci.* **1957**, *69*, 352-368.

[80] W. A. Bonner, *Orig. Life Evol. Biosph.* **1991**, *21*, 407-420.

[81] J. R. Cronin, S. Pizzarello, *Science* **1997**, *275*, 951-955.

[82] S. Pizzarello, *Acc. Chem. Res.* **2006**, *39*, 231-237.

[83] M. Levine, C. S. Kenesky, D. Mazori, R. Breslow, *Org. Lett.* **2008**, *10*, 2433-2436.

[84] R. Breslow, M. Levine, Z.-L. Cheng, *Orig. Life Evol. Biosph.* **2009**, *40*, 11.

[85] G. E. Tranter, *Nature* **1985**, *318*, 172-173.

[86] R. Zanasi, P. Lazzeretti, A. Ligabue, A. Soncini, *Phys. Rev. E* **1999**, *59*, 3382-3385.

[87] M. Quack, *Angew. Chem. Int. Ed.* **2002**, *41*, 4618-4630.

[88] G. E. Tranter, *BioSystems* **1987**, *20*, 37-48.

[89] S. F. Mason, G. E. Tranter, *Proc. R. Soc. Lond. A. Math. Phys. Sci.* **1985**, *397*, 45-65.

[90] H. Buschmann, R. Thede, D. Heller, *Angew. Chem. Int. Ed.* **2000**, *39*, 4033-4036.

[91] W. Kuhn, E. Braun, *Naturwissenschaften* **1929**, *17*, 227-228.

[92] C. Meinert, S. V. Hoffmann, P. Cassam-Chenaï, A. C. Evans, C. Giri, L. Nahon, U. J. Meierhenrich, *Angew. Chem. Int. Ed.* **2014**, *53*, 210-214.

[93] U. J. Meierhenrich, L. Nahon, C. Alcaraz, J. H. Bredehöft, S. V. Hoffmann, B. Barbier, A. Brack, *Angew. Chem. Int. Ed.* **2005**, *44*, 5630-5634.

[94] E. Rubenstein, W. A. Bonner, H. P. Noyes, G. S. Brown, *Nature* **1983**, *306*, 118-118.

[95] J. Bailey, *Orig. Life Evol. Biosph.* **2001**, *31*, 167-183.

[96] A. Collet, M. J. Brienne, J. Jacques, *Chem. Rev.* **1980**, *80*, 215-230.

[97] C. Viedma, *Orig. Life Evol. Biosph.* **2001**, *31*, 501-509.

[98] L. Pasteur, *Ann. Chim. Phys.* **1848**, *24*, 442-459.

[99] A. V. Tarasevych, A. E. Sorochinsky, V. P. Kukhar, J.-C. Guillemin, *Orig. Life Evol. Biosph.* **2013**, *43*, 129-135.

[100] J. Jacques, A. Collet, S. H. Wilen, *Enantiomers, racemates, and resolutions*, Wiley, **1981**.

[101] D. G. Blackmond, *Philos. Trans. R. Soc. Lond. B. Biol. Sci.* **2011**, *366*, 2878-2884.

[102] F. C. Frank, *Biochim. Biophys. Acta* **1953**, *11*, 459-463.

[103] C. Puchot, O. Samuel, E. Dunach, S. Zhao, C. Agami, H. B. Kagan, *J. Am. Chem. Soc.* **1986**, *108*, 2353-2357.

[104] K. Soai, T. Shibata, H. Morioka, K. Choji, *Nature* **1995**, *378*, 767-768.

[105] I. Sato, H. Urabe, S. Ishiguro, T. Shibata, K. Soai, *Angew. Chem. Int. Ed.* **2003**, *42*, 315-317.

[106] T. Kawasaki, Y. Matsumura, T. Tsutsumi, K. Suzuki, M. Ito, K. Soai, *Science* **2009**, *324*, 492-495.

[107] T. Kawasaki, K. Suzuki, K. Hatase, M. Otsuka, H. Koshima, K. Soai, *Chem. Commun.* **2006**, 1869-1871.

[108] K. Soai, S. Osanai, K. Kadowaki, S. Yonekubo, T. Shibata, I. Sato, *J. Am. Chem. Soc.* **1999**, *121*, 11235-11236.

[109] T. Shibata, J. Yamamoto, N. Matsumoto, S. Yonekubo, S. Osanai, K. Soai, *J. Am. Chem. Soc.* **1998**, *120*, 12157-12158.

[110] M. Mauksch, S. B. Tsogoeva, I. M. Martynova, S. Wei, *Angew. Chem. Int. Ed.* **2007**, *46*, 393-396.

[111] D. K. Kondepudi, R. J. Kaufman, N. Singh, *Science* **1990**, *250*, 975-976.

[112] J. M. McBride, R. L. Carter, *Angew. Chem. Int. Ed.* **1991**, *30*, 293-295.

[113] C. Viedma, *Phys. Rev. Lett.* **2005**, *94*, 065504.

[114] C. Viedma, J. E. Ortiz, T. d. Torres, T. Izumi, D. G. Blackmond, *J. Am. Chem. Soc.* **2008**, *130*, 15274-15275.

[115] W. L. Noorduin, T. Izumi, A. Millemaggi, M. Leeman, H. Meekes, W. J. P. Van Enckevort, R. M. Kellogg, B. Kaptein, E. Vlieg, D. G. Blackmond, *J. Am. Chem. Soc.* **2008**, *130*, 1158-1159.

[116] H. J. Morowitz, *J. Theor. Biol.* **1969**, *25*, 491-494.

[117] J. Huang, L. Yu, *J. Am. Chem. Soc.* **2006**, *128*, 1873-1878.

[118] M. Klussmann, H. Iwamura, S. P. Mathew, D. H. Wells, U. Pandya, A. Armstrong, D. G. Blackmond, *Nature* **2006**, *441*, 621-623.

[119] R. Breslow, M. S. Levine, *Proc. Natl. Acad. Sci. U.S.A.* **2006**, *103*, 12979-12980.

[120] R. Breslow, Z.-L. Cheng, *Proc. Natl. Acad. Sci. U.S.A.* **2009**, *106*, 9144-9146.

[121] R. Breslow, Z.-L. Cheng, *Proc. Natl. Acad. Sci. U.S.A.* **2010**, *107*, 5723-5725.

[122] J. F. Kerridge, M. S. Matthews, *Meteorites and the Early Solar System*, University of Arizona Press, **1988**.

[123] E. T. Peltzer, J. L. Bada, *Nature* **1978**, *272*, 443-444.

[124] R. Breslow, M. S. Levine, *Tetrahedron Lett.* **2006**, *47*, 1809-1812.

[125] J. E. Hein, D. G. Blackmond, *Acc. Chem. Res.* **2012**, *45*, 2045-2054.

[126] J. E. Hein, E. Tse, D. G. Blackmond, *Nat. Chem.* **2011**, *3*, 704-706.

[127] J. von Liebig, *Liebigs Ann.* **1860**, *113*, 246-247.

[128] Z. G. Hajos, D. R. Parrish, *J. Org. Chem.* **1974**, *39*, 1615-1621.

[129] U. Eder, G. Sauer, R. Wiechert, *Angew. Chem. Int. Ed.* **1971**, *10*, 496-497.

[130] F. Hoffmann-La Roche & Co. AG, DE2102623 (29.07.1971).

[131] Schering AG, DE2014757 (07.10.1971).

[132] B. List, *Chem. Rev.* **2007**, *107*, 5413-5415.

[133] A. Erkkilä, I. Majander, P. M. Pihko, *Chem. Rev.* **2007**, *107*, 5416-5470.

[134] S. Mukherjee, J. W. Yang, S. Hoffmann, B. List, *Chem. Rev.* **2007**, *107*, 5471-5569.

[135] D. Enders, O. Niemeier, A. Henseler, *Chem. Rev.* **2007**, *107*, 5606-5655.

[136] I. Atodiresei, I. Schiffers, C. Bolm, *Chem. Rev.* **2007**, *107*, 5683-5712.

[137] A. G. Doyle, E. N. Jacobsen, *Chem. Rev.* **2007**, *107*, 5713-5743.

[138] T. Akiyama, *Chem. Rev.* **2007**, *107*, 5744-5758.

[139] E. A. C. Davie, S. M. Mennen, Y. Xu, S. J. Miller, *Chem. Rev.* **2007**, *107*, 5759-5812.

[140] M. P. van der Helm, B. Klemm, R. Eelkema, *Nat. Rev. Chem.* **2019**, *3*, 491-508.

[141] A. B. Northrup, I. K. Mangion, F. Hettche, D. W. C. MacMillan, *Angew. Chem. Int. Ed.* **2004**, *43*, 2152-2154.

[142] A. B. Northrup, D. W. C. MacMillan, *Science* **2004**, *305*, 1752-1755.

[143] S. Pizzarello, A. L. Weber, *Science* **2004**, *303*, 1151-1151.

[144] S. W. Fox, C. R. Windsor, *Science* **1970**, *170*, 984-986.

[145] G. M. Muñoz Caro, U. J. Meierhenrich, W. A. Schutte, B. Barbier, A. Arcones Segovia, H. Rosenbauer, W. H. P. Thiemann, A. Brack, J. M. Greenberg, *Nature* **2002**, *416*, 403-406.

[146] K. Plankensteiner, H. Reiner, B. M. Rode, *Mol. Divers.* **2006**, *10*, 3-7.

[147] A. L. Weber, S. Pizzarello, *Proc. Natl. Acad. Sci. U.S.A.* **2006**, *103*, 12713-12717.

[148] L. Burroughs, P. A. Clarke, H. Forintos, J. A. R. Gilks, C. J. Hayes, M. E. Vale, W. Wade, M. Zbytniewski, *Org. Biomol. Chem.* **2012**, *10*, 1565-1570.

[149] L. Burroughs, M. E. Vale, J. A. R. Gilks, H. Forintos, C. J. Hayes, P. A. Clarke, *Chem. Commun.* **2010**, *46*, 4776-4778.

[150] R. Breslow, V. Ramalingam, C. Appayee, *Orig. Life Evol. Biosph.* **2013**, *43*, 323-329.

[151] G. Stork, A. Brizzolara, H. Landesman, J. Szmuszkovicz, R. Terrell, *J. Am. Chem. Soc.* **1963**, *85*, 207-222.

[152] N. Vignola, B. List, *J. Am. Chem. Soc.* **2004**, *126*, 450-451.

[153] D. A. Nicewicz, D. W. C. MacMillan, *Science* **2008**, *322*, 77-80.

[154] D. A. Nagib, M. E. Scott, D. W. C. MacMillan, *J. Am. Chem. Soc.* **2009**, *131*, 10875-10877.

[155] E. R. Welin, A. A. Warkentin, J. C. Conrad, D. W. C. MacMillan, *Angew. Chem. Int. Ed.* **2015**, *54*, 9668-9672.

[156] H.-W. Shih, M. N. Vander Wal, R. L. Grange, D. W. C. MacMillan, *J. Am. Chem. Soc.* **2010**, *132*, 13600-13603.

[157] A. Gualandi, M. Marchini, L. Mengozzi, M. Natali, M. Lucarini, P. Ceroni, P. G. Cozzi, *ACS Catal.* **2015**, *5*, 5927-5931.

[158] M. Cherevatskaya, M. Neumann, S. Füldner, C. Harlander, S. Kümmel, S. Dankesreiter, A. Pfitzner, K. Zeitler, B. König, *Angew. Chem. Int. Ed.* **2012**, *51*, 4062-4066.

[159] P. Riente, A. Matas Adams, J. Albero, E. Palomares, M. A. Pericàs, *Angew. Chem. Int. Ed.* **2014**, *53*, 9613-9616.

[160] M. Neumann, S. Füldner, B. König, K. Zeitler, *Angew. Chem. Int. Ed.* **2011**, *50*, 951-954.

[161] E. Arceo, A. Bahamonde, G. Bergonzini, P. Melchiorre, *Chem. Sci.* **2014**, *5*, 2438-2442.

[162] E. Arceo, I. D. Jurberg, A. Álvarez-Fernández, P. Melchiorre, *Nat. Chem.* **2013**, *5*, 750-756.

[163] M. Silvi, E. Arceo, I. D. Jurberg, C. Cassani, P. Melchiorre, *J. Am. Chem. Soc.* **2015**, *137*, 6120-6123.

[164] R. R. Shaikh, A. Mazzanti, M. Petrini, G. Bartoli, P. Melchiorre, *Angew. Chem. Int. Ed.* **2008**, *47*, 8707-8710.

[165] R. Ballini, A. Palmieri, M. Petrini, R. R. Shaikh, *Adv. Synth. Catal.* **2008**, *350*, 129-134.

[166] P. G. Cozzi, F. Benfatti, L. Zoli, *Angew. Chem. Int. Ed.* **2009**, *48*, 1313-1316.

[167] A. R. Brown, W.-H. Kuo, E. N. Jacobsen, *J. Am. Chem. Soc.* **2010**, *132*, 9286-9288.

[168] E. Gómez-Bengoa, A. Landa, A. Lizarraga, A. Mielgo, M. Oiarbide, C. Palomo, *Chem. Sci.* **2011**, *2*, 353-357.

[169] E. Gatewood, T. B. Johnson, *J. Am. Chem. Soc.* **1928**, *50*, 1422-1427.

[170] A. H. Cook, I. Heilbron, A. P. Mahadevan, *J. Chem. Soc.* **1949**, 1061-1064.

[171] F. Asinger, W. Schäfer, H. Meisel, H. Kersten, A. Saus, *Monatsh. Chem.* **1967**, *98*, 338-352.

[172] H. T. Bucherer, V. A. Lieb, *J. Prakt. Chem.* **1934**, *141*, 5-43.

[173] J. D. Christian, *J. Org. Chem.* **1957**, *22*, 396-399.

[174] H. T. Bucherer, W. Brandt, H. Barsch, *J. Prakt. Chem.* **1934**, *140*, 129-171.

[175] Monsanto Chemicals, US2842553A (08.07.1958).

[176] X. Liang, J. Fan, F. Shi, W. Su, *Tetrahedron Lett.* **2010**, *51*, 2505-2507.

[177] G. Nováková, P. Drabina, B. Frumarová, M. Sedlák, *Adv. Synth. Catal.* **2016**, *358*, 2541-2552.

[178] F. Asinger, W. Schäfer, H. Kersten, H. Meisel, A. Saus, *Monatsh. Chem.* **1967**, *98*, 1832-1842.

[179] F. Asinger, W. Schäfer, H. Kersten, A. Saus, *Monatsh. Chem.* **1967**, *98*, 1843-1851.

[180] M. Paventi, J. T. Edward, *Can. J. Chem.* **1987**, *65*, 282-289.

[181] G. Nováková, P. Drabina, J. Svoboda, M. Sedlák, *Tetrahedron: Asymmetry* **2017**, *28*, 791-796.

[182] D. F. Bushey, F. C. Hoover, *J. Org. Chem.* **1980**, *45*, 4198-4206.

[183] Rohm and Haas Company, EP1229023A1 (07.08.2002).

[184] F. Asinger, K. Hentschel, A. Saus, *Monatsh. Chem.* **1976**, *107*, 35-41.

[185] Ciba-Geigy Corporation, US3956310 (11.05.1976).

[186] Rohm and Haas Company, EP1413577A1 (28.04.2004).

[187] W. E. Stewart, T. H. Siddall, *Chem. Rev.* **1970**, *70*, 517-551.

[188] K. B. Wiberg, P. R. Rablen, *J. Am. Chem. Soc.* **1995**, *117*, 2201-2209.

[189] X. Liang, N. Li, X. Chen, W. Su, *RSC Adv.* **2014**, *4*, 44039-44042.

[190] X. Liang, S. Li, W. Su, *Tetrahedron Lett.* **2012**, *53*, 289-291.

[191] D. P. Summers, S. Chang, *Nature* **1993**, *365*, 630-633.

[192] K. R. Olson, K. D. Straub, *Physiology* **2016**, *31*, 60-72.

[193] P. D. Clark, N. I. Dowling, M. Huang, *J. Mol. Evol.* **1998**, *47*, 127-132.

[194] A. C. Closs, E. Fuks, M. Bechtel, O. Trapp, *Chem. Eur. J.* **2020**, *26*, 10702-10706.

[195] C. K. Shu, B. D. Mookherjee, H. A. Bondarovich, M. L. Hagedorn, *J. Agric. Food. Chem.* **1985**, *33*, 130-132.

[196] T. Kawai, M. Irie, M. Sakaguchi, *J. Agric. Food. Chem.* **1985**, *33*, 393-397.

[197] D. Kutlán, P. Presits, I. Molnár-Perl, *J. Chromatogr. A* **2002**, *949*, 235-248.

[198] H. D. Flack, *Helv. Chim. Acta* **2003**, *86*, 905-921.

[199] H. D. Flack, *Acta Cryst. A* **1983**, *39*, 876-881.

[200] N. F. W. Ligterink, M. Kama, *A&A* **2018**, *614*, A112.

[201] E. Hagelskamp, Doctoral thesis, Ludwig Maximilian University Munich **2020**.

[202] P. G. Stoks, A. W. Schwartz, *Geochim. Cosmochim. Acta* **1982**, *46*, 309-315.

[203] Z. Martins, *Life* **2018**, *8*, 28.

[204] T. Schnitzer, H. Wennemers, *J. Org. Chem.* **2020**, *85*, 7633-7640.

[205] F. An, B. Maji, E. Min, A. R. Ofial, H. Mayr, *J. Am. Chem. Soc.* **2020**, *142*, 1526-1547.

[206] H. Mayr, T. Bug, M. F. Gotta, N. Hering, B. Irrgang, B. Janker, B. Kempf, R. Loos, A. R. Ofial, G. Remennikov, H. Schimmel, *J. Am. Chem. Soc.* **2001**, *123*, 9500-9512.

[207] http://www.cup.lmu.de/oc/mayr/DBintro.html (03.06.2021).

[208] A. C. Closs, O. Trapp, *submitted manuscript*.

[209] F. Asinger, H. Offermanns, P. Müller, H. Andree, *Monatsh. Chem.* **1968**, *99*, 2059-2071.

Danksagung

An dieser Stelle möchte ich mich bei all den Menschen bedanken, die mich während meiner Promotion begleitet und einen Teil zu dieser Arbeit beigetragen haben.

Allen voran danke ich meinem Doktorvater *Prof. Oliver Trapp* für die Möglichkeit, dieses Thema unter seiner Leitung bearbeiten zu dürfen. Vielmehr jedoch für sein Vertrauen in die selbstständige Arbeit, die dennoch jederzeit auf seine Unterstützung, Ideen und Kreativität zurückgreifen konnte. Seine begeisternde und positive Art schätzte ich sehr und ließ Rückschläge schnell vergessen.

Bei *Prof. Paul Knochel* möchte ich mich herzlichst für die Übernahme des Zweitgutachtens bedanken, sowie bei *Dr. Armin Ofial*, *Prof. Franz Bracher*, *Prof. Konstantin Karaghiosoff* und *Prof. Philip Tinnefeld* für die Teilnahme an meiner Prüfungskommission.

Dr. Armin Ofial und *Dr. Feng An* danke ich zudem für die technische Unterstützung sowie hilfreichen und produktiven Gespräche zu Reaktivitäten, Kinetik und Nukleophilie.

Weiterhin danke ich allen Mitarbeitern der Ludwig-Maximilians-Universität München, insbesondere den Analytik-Abteilungen und den Angestellten unseres Arbeitskreises, die den Forschungsbetrieb erst ermöglichen.

Ein großer Dank geht an meine Forschungspraktikanten *Max* und *Doreen*, die mit viel Einsatz diese Arbeit vorangetrieben haben. *Max* danke ich darüber hinaus, wie auch *Marian*, für den anschließenden Austausch, die Ideen und Diskussionen über die Welt der Imidazolidine-4-thione. Ich wünsche euch damit weiterhin viel Erfolg und Freude.

Ich bedanke mich außerdem bei *Laura* und *Flo* für das sehr sorgfältige und aufwendige Korrekturlesen.

Vor allem möchte ich dem gesamten Arbeitskreis für die tolle gemeinsame Zeit danken, die weit über den Laboralltag hinausging und mich viele Freunde reicher machte.
Danke an F3.017 – *Fabi*, *Max*, *Jenny*, *Flo*, und *Nathalie* – für das (kommentarlose) Ertragen des Schwefelgeruchs und die grandiose freundschaftliche Atmosphäre, die mich, trotz Rausschmeißermusik in den letzten Wochen, jeden Tag mit Freude in die Uni gehen ließ. Besonders möchte ich mich dabei bei *Fabi* bedanken, für dein offenes Ohr, deine

Lockerheit, den Spaß, die Unternehmungen und die perfekte Mischung aus Unterstützung und Ablenkung, die immer zur rechten Zeit zur Stelle war. Ich hoffe, sie bleibt mir noch weiter erhalten! Ebenfalls Danke an die Ottolenghi-Runde – *M²*, *Flo*, *Jenny*, *Simone*, *Lena* – für die vorzüglichen Freitage und Mittwoche, die Ausweitung zu Sushi und Sekt und vielleicht irgendwann nach London. Danke *Elina* für die schöne Zusammenarbeit sowie *Maren* für die gemeinsamen Konferenzen. Ein besonderer Dank gilt *Laura*, für deine zahlreichen, ehrlichen Ratschläge, deinen Ansporn sowie deine tägliche Anteilnahme, auf die ich mich immer verlassen konnte.

Mein größter Dank geht an *Max*. Danke für dein herausforderndes Hinterfragen, stets begleitet von motivierendem Zuspruch und einer bedingungslosen Unterstützung, die du trotz Entfernung, Arbeitsstress und meiner Widerrede aufbringst.

Schließlich danke ich meinem *Papa* für sein unermüdliches Interesse an (meiner) Chemie, meinem Bruder *Otto* für sein grafisches Auge und seine Illustrator Skills sowie meiner gesamten Familie und meinen Freunden, die mit unvergesslichen Abenden, Erlebnissen und Reisen für den nötigen Ausgleich gesorgt haben.